Non-Eutectic Mixture Organocatalysts (NEMOs): a Step Towards High Temperature Polymerizations

A manuscript submitted to the

Universidad del País Vasco (UPV/EHU)
Donostia-San Sebastián – España

and

Université de Mons
Mons – Belgium

For the degree of

DOCTOR IN SCIENCES

Presented by

Andere Basterretxea Gorostiza

Under the supervision of

Dr. Haritz Sardon (UPV/EHU)

Dr. Olivier Coulembier (UMONS)

Donostia, July 2019

Summary

Organocatalysts have proved to be an efficient and profitable alternative to their organometallic analogues in many different polymerization processes and nowadays represent an invaluable tool in polymer chemistry. A key reason for transitioning to organocatalysts is not only their ability to be effectively removed from resultant products, but also their potential to form hydrogen bonding interaction that may play a unique role to exquisitely control the catalytic activity and selectivity of the polymerization process.

While some of these organocatalysts have been largely implemented in research laboratories, the use of organocatalyst in industrial bulk polymerization processes is still scarce. This is probably related with the poor thermal stability of organic acids and bases at temperatures (150-250 °C) that would be practical for polymerization and as such hinders their utilization at industrial scale. The degradation of the catalyst during the reaction results in several drawbacks such as the coloration of the final product, the promotion of undesirable reactions or low reaction yields. This work addresses some of the challenges arising from the use of organocatalyst at high temperatures through the use of non-stoichiometric acid-base mixture catalysts described here as Non-Eutectic Mixtures Organocatalysts (NEMOs).

To provide context to this, **Chapter 1** offers an introduction to the synthesis and characterization of these organic acid-base mixtures highlighting the recent literature which described their formation and use in chain growth and step-growth polymerizations as well as in polymer recycling by depolymerization. Afterwards, such concept of acid-base organocatalysts for high temperature polymerizations was applied in the following chapters.

Chapter 2 approached a versatile polymerization at high temperature as is the synthesis of aliphatic polyethers by self-condensation. Different mixtures of a common acid, methanesulfonic acid (MSA) and a common base, 1,5,7-Triazabicyclo[4.4.0]dec-5-ene (TBD) were characterized and the Non-Eutectic Mixture Organocatalys (NEMOs) with excess in MSA demonstrated to be highly efficient as catalysts in the synthesis of poly(oxyalkylene)s by self-condensation in bulk conditions. This synthesis route resulted in a series of aliphatic poly(oxyalkylene)s with different number of methylene units in the chain. In addition, the recyclability of the NEMO was also demonstrated.

In order to expand the scope of the use of the NEMO, in Chapter 3 and 4 the polymerization process was implemented in the synthesis of copolyethers. Chapter 3, report a series of polyoxyalkylene copolyethers obtained by copolymerization of 1,6-hexanediol and 1,12-dodecanediol which were able to crystallize in the entire composition range and displayed an isomorphic behavior, behavior which is considered not very common in random copolymers. On the other hand, in Chapter 4 fully bio-based copolyethers were prepared by the self condensation of 1,6-hexanediol and 1,4-cyclohexanedimethanol. This approach proved to be a simple and sustainable route to synthesize fully bio-based copolyethers ranging from amorphous to semicrystalline by varying the ratio of the comonomers. Also the isomer content of the comonomer 1,4-cyclohexanedimethanol exhibited an influence on the thermal properties of the copolymers.

Moving to another prevalent high temperature polymerization, the Ring-Opening Polymerization (ROP) of L-lactide in bulk was studied in Chapter 5. For that different acid-base mixtures based on MSA and 4-dimethylaminopyridine (DMAP) were characterized and explored in the ROP of L-lactide in bulk. The stoichiometric mixture (1:1) and the NEMO (2:1) showed extraordinary thermal resistance and particular effectively for the catalysis of ROP. In particular, the NEMO MSA:DMAP 2:1 exceptionally resisted up to 250°C showing also good stereocontrol of the reaction up

to 180°C, being this contribution as far as we know, the first one reporting stereocontrolled ROP of L-lactide in bulk conditions.

To finish, **Chapter 6** holds the conclusions of the contributions achieved here in the use of organic acid-base mixtures as resistant and efficient catalyst of the synthesis of valuable polymers such as polyethers and polyesters. In addition, a perspective on the implementation of these organocatalyst in industrial processes is given, revealing that although there is still way ahead, there is no doubt that further progresses must continue in this field in order to enable the design of even faster, selective, cost-effective and thermally stable organocatalysts.

Resumen

Los organocatalizadores han demostrado ser una alternativa eficiente y rentable a sus análogos organometálicos en muchos procesos de polimerización y hoy en día representan una herramienta invaluable en química de polímeros. Una de las razones clave para la transición a los organocatalizadores no es solo su capacidad para ser eliminados de manera efectiva de los productos resultantes, sino también su potencial en la formación de interacciones de enlaces de hidrógeno que puede desempeñar un papel único para controlar de manera exquisita la actividad catalítica y la selectividad de un proceso de polimerización.

Si bien algunos de estos organocatalizadores se han implementado en gran medida en laboratorios de investigación, el uso de organocatalizadores en procesos industriales de polimerización llevados a cabo en masa es aún escaso. Probablemente esto esté relacionado con la generalmente pobre estabilidad térmica de dichos ácidos y bases orgánicos a temperaturas altas (150-250 °C) que son prácticas para la polimerización complicando así su uso a escala industrial. La degradación del catalizador durante la reacción da como resultado varios inconvenientes, tales como la coloración del producto final, la promoción de reacciones secundarios o bajos rendimientos de reacción. Este trabajo aborda algunos de los desafíos planteados por el uso de organocatalizadores a altas temperaturas a través del uso de catalizadores formados por mezclas no estequiométricas de ácidos y bases descritas aquí como organocatalizadores de mezclas no eutécticas (NEMO).

Para proporcionar contexto a esto, el **Capítulo 1** ofrece una introducción a la síntesis y caracterización de estas mezclas ácido-base destacando la literatura reciente que describe su preparación y uso en polimerizaciones de crecimiento de cadena, polimerizaciones de crecimiento por etapas, y en procesos de despolimerización.

Posteriormente, dicho concepto de emplear organocatalizadores ácido-base en polimerizaciones a alta temperatura se aplicó en los siguientes capítulos.

El **Capítulo 2** abordó una polimerización versátil a alta temperatura, como lo es la síntesis de poliéteres alifáticos por autocondensación. Se caracterizaron diferentes mezclas de un ácido común, ácido methanesulfónico (MSA) y una base común, 1,5,7-triazabicilo(4.4.0)dec-5-eno (TBD) y la mezcla no eutéctica (NEMO) con exceso en MSA demostró ser altamente eficiente como catalizadores en la síntesis de poliéteres preparados por autocondensación. Esta ruta de síntesis dió como resultado una serie de poli(oxialquileno)s alifáticos con diferente número de unidades de metileno en la cadena. Además, también se demostró la reciclabilidad y reutilización del catalizador NEMO.

Para ampliar el alcance del uso del NEMO, en el **Capítulo 3 y 4** el proceso de polimerización previamente reportado se implementó en la síntesis de copoliéteres. El **Capítulo 3,** informa sobre una serie de copoliéteres obtenidos por copolimerización de 1,6-hexanodiol y 1,12-dodecanodiol. Los copoliéteres mostraron cristalización en todo el rango de composición y mostraron un comportamiento isomórfico, comportamiento que no se considera muy común en copolímeros aleatorios. Por otro lado, en el **Capítulo 4,** se prepararon copoliéteres de base biológica mediante autocondensación de 1,6-hexanodiol y 1,4-ciclohexanodimetanol. Este enfoque demostró ser una ruta simple y sostenible para sintetizar copoliéteres de base biológica que varían de amorfos a semicristalinos variando la proporción de los comonómeros. También se observó que el contenido de isómeros del comonómero 1,4-ciclohexanodimetanol influye considerablemenete en las propiedades térmicas de los copolímeros.

Pasando a otra polimerización de alta temperatura, en el **Capítulo 5** se estudió la polimerización de apertura de anillo de la L-lactida en masa. Para ello, se

caracterizaron y exploraron diferentes mezclas ácido-base basadas en MSA y 4-dimethilaminopiridina (DMAP) como catalizadores. La mezcla estequiométrica (1:1) y el NEMO (2:1) mostraron una resistencia térmica extraordinaria y particularmente efectiva para la catálisis de dicha polimerización. En particular, el NEMO MSA: DMAP 2:1 resistió excepcionalmente hasta 250°C, mostrando también un buen estereocontrol de la reacción hasta 180°C, siendo esta contribución, por lo que sabemos, la primera que informa de una polimerización de apertura de anillo de L-lactida estereocontrolada en masa a alta temperatura.

Para finalizar, el **Capítulo 6** contiene las conclusiones de las contribuciones logradas en este trabajo en el uso de mezclas de ácido-base como catalizadores resistentes y eficientes en la síntesis de polímeros valiosos como poliéteres y poliésteres. Además, se ofrece una perspectiva sobre la implementación de estos organocatalizadores en procesos industriales, lo que revela que, aunque todavía hay mucho camino por delante, no hay duda de que los avances en este campo deben de continuar en esta linea para permitir el diseño aún más rápido y selectivo de organocatalizadores rentables y térmicamente estables.

Table of content

CHAPTER 1. Introduction

CHAPTER 2. Polyether synthesis by bulk self-condensation of diols catalyzed by a Non-Eutectic Mixture Organocatalysts

CHAPTER 3. Isomorphic polyoxyalkylene copolyethers

obtained by copolymerization of 1,6-hexanediol and 1,12-dodecanediol

CHAPTER 4. Synthesis and Characterization of Fully Bio-

based Poly(oxyhexamethylene-co-1,4-cyclohexanedimethanol) copolyethers

CHAPTER 5. Bulk Ring-Opening Polymerization (ROP) of

L-lactide catalyzed by a NEMO

List of abbreviations

A	Acetic acid
BA	Benzoic acid
BnOH	Benzyl alcohol
CDCl3	Deuterated chloroform
CHDO	1,4-Cyclohexanedimethanol
CLO	ε-Caprolactone
CR	Creatinine
Đ	Dispersity
DBU	1,8-Diazabicyclo[5.4.0]undec-7-ene
DFT	Density functional theory
DMAP	4-Dimethylaminopyridine
DMSO	Dimethyl sulfoxide
DSC	Differential scanning calorimetry
FT-IR	Fourier Transform Infrared Spectroscopy
G	Glycolic acid
GC	Gas chromatography
HDO	1,6-Hexanediol
HOTf	Triflic acid
LLA	L-lactide
mol. %	Molar percentage
MSA	Methanesulfonic acid
Mn	Number-average molar mass
NaOH	Sodium hydroxide
NEMO	Non-Eutectic Mixture Organocatalyst

NMR	Nuclear Magnetic Resonance
PEG	Polyethyeleglycol
PET	Poly(ethylene terephthalate)
PLLA	Poly(L-lactide)
PPG	Polypropyleneglycol
PTMG	Polytetramethylenglycol
RI	Refractive index
ROP	Ring-opening polymerization
RT	Room temperature
Sac	Saccharine
SEC	Size exclusion chromatography
TBD	1,5,7-Triazabicyclo[4.4.0]dec-5-ene
TFA	Trifluoro acetic acid
T_g	Glass transition temperature
TGA	Thermogravimetric analyses
T_m	Melting temperature
TMC	Trimethylene carbonate
TU	Thiourea
UV-vis	Ultraviolet/visible
VL	δ-valerolactone
WAXS	Wide Angle X-RAY Scattering
wt. %	Weight percentage

Thesis Map

2.1 Characterization of the acid base organocatalysts based on MSA and TBD

2.2 Catalytic activity testing and optimization

2. Polyether Synthesis by Bulk Self-Condensation of Diols

2.3 Synthesis of aliphatic polyethers with different number of methylene units

4.1 Synthesis and characterization of Poly(oxyhexamethylene-co-1,4-cyclohexanedimethanol) copolyethers

1. Introdu
Acid -Ba
mixtur
Organoca

4.2 Thermal characterization of Poly(oxyhexamethylene-co-1,4-cyclohexanedimethanol) copolyethers

4. Synthesis and Characterization of Fully Bio-based Copolyethers

4.3 Influence of CHDM cis-trans isomeric configuration on the thermal properties.

MAP

3.1 Synthesis and characterization of poly(oxyhexamethylene-co-oxydodecamethylene) copolyethers

3. Synthesis of Isomorphic polyoxyalkylene copolyethers
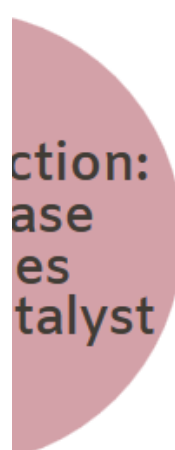
3.2 Thermal Characterization of poly(oxyhexamethylene-co-oxydodecamethylene) copolyethers

3.2 Expanding the scope of the polymerization to terpolymer synthesis

ction:
ase
es
talyst

5.1 Characterization of the acid base organocatalysts based on MSA and DMAP

5.2 Catalyst evaluation in the Ring Opening Polymerization of L-lactide in bulk.

5. Bulk Ring Opening Polymerization (ROP) of L-lactide

5.3 Step towards high temperarute polymerization of L-lactide

5.4 Expanding the scope of the polymerization process

Chapter 1

Introduction

1.1 Moving towards sustainable polymerizations

Sustainability is considered as one of the most extended challenges facing polymer science nowadays.[1,2] Figure 1.1 represents the three pillars of a sustainable development which could be also applied to polymer science. These three pillars should reinforce each other in order to move to a more sustainable system.
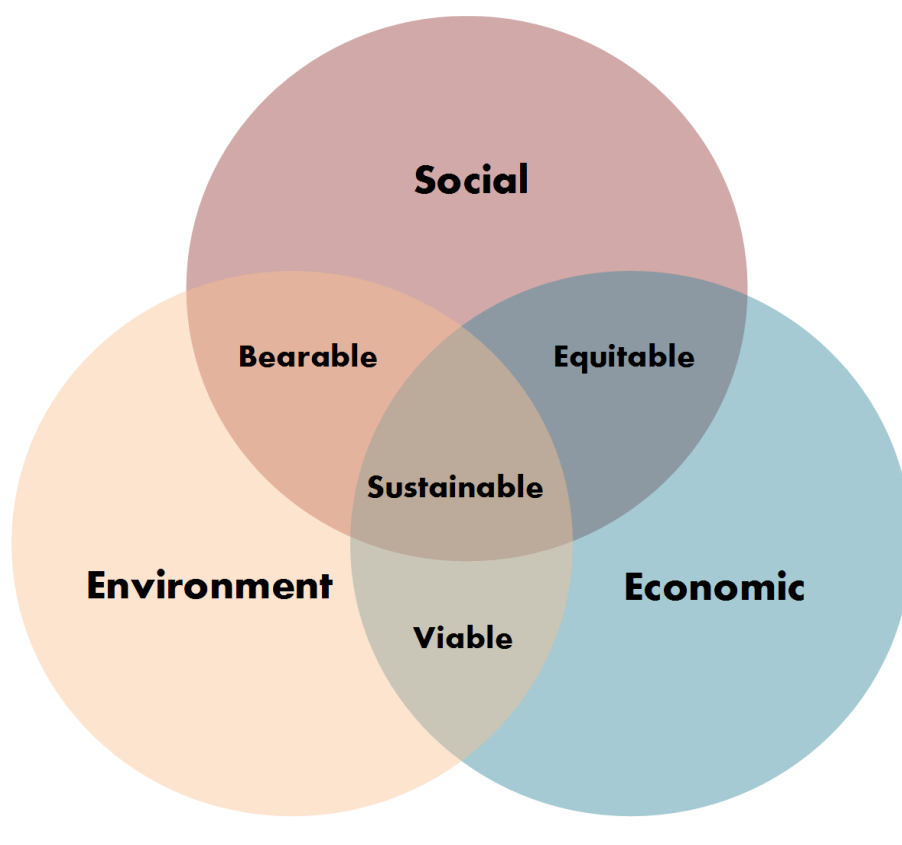
Figure 1.1. Sustainable development vector diagram.

Considering the pillar of the environmental protection, during the last years new legislations have been indroduced with stricter procedures which focus their attention in industrial processes, characteristics of the products used, and the quantity of wastes

and emissions generated. Consequently, industrial synthesis system has set up three general objectives which are summarized as follows:[2]

- Reducing the generation of polluting chemicals in chemical processes.

- Reducing the use of hazardous chemicals in chemical processes.

- Reducing the use of scarce raw materials and non-renewable.

The pressure to fulfill these objectives, reduce energy consumption and conserve natural resources is continously increasing. The "ideal" synthetic process is the one that produces useful compounds in high yield with high levels of selectivity in an economic, energy-saving, environmentally benign, and sustainable way. Up to now, these objectives are partially achieved by using metallic-based catalysts. However the use of metallic-based catalysts entails a high environmental and economic cost – some widely used metals risk complete disappearance in the next 100 years (e.g. zinc or silver), while others will be seriously threatened in the future if their consumption continues to increase. In addition, in most of the cases due to their coordination abilities, the metallic-based catalyst remains in the products and complicate the recyclability of the polymer.

All these general concerns introduce and provide the context for the present work, which taking all previously mentioned into consideration, focus on the use of **acid-base mixture organocatalysts in high temperature polymerizations** as an alternative to metallic-based catalysts to move towards more sustainable polymerizations.

1.2 Acid-Base Mixture Organocatalysts: a step towards hight temperature polymerizations

Organocatalysis has become nowadays a very popular and powerful tool in polymerization reactions. Since the pioneering work of Hedrick and Waymouth about the metal-free ring-opening polymerization of lactide, the use of organocatalysis provide a precise alterative to their organometallic analogues in the majority of polymerizations including chain growth, step-growth, stereoselective, controlled radical or ring-opening metathesis polymerizations.[3–12] In addition, organocatalysis is expected to play an important role in the future of plastics circular economy based on depolymerization reactions or chemical recycling processes as well as in the development of additive manufacturing of polymers.[13–15] The main attribute of organocatalysts as compared with organometallic catalysts resides in its versatility, high selectivity and possibility of purification or recovery of the catalyst from the final polymer. However, typical organic compounds need high catalyst loading and demonstrate poor thermal stability that leads to the degradation of the catalyst during high temperature processes. These two reasons have limited the industrial implementation of organocatalyzed (de)-polymerizations.[16,17]

Nowadays, the average temperature production range of industrially relevant polymers such as polyesters (PET, PLLA), polyamides, polycarbonates or polyurethanes is in between 150 and 300 °C.[18] Albeit nucleophilic and basic organocatalysts together with strong sulfonic-based acids have demonstrated excellent catalytic activity in multiple polymerization processes, when used at high temperatures their low boiling points and the lack of thermal stability limits their performance and generate undesirable side reactions.[19]
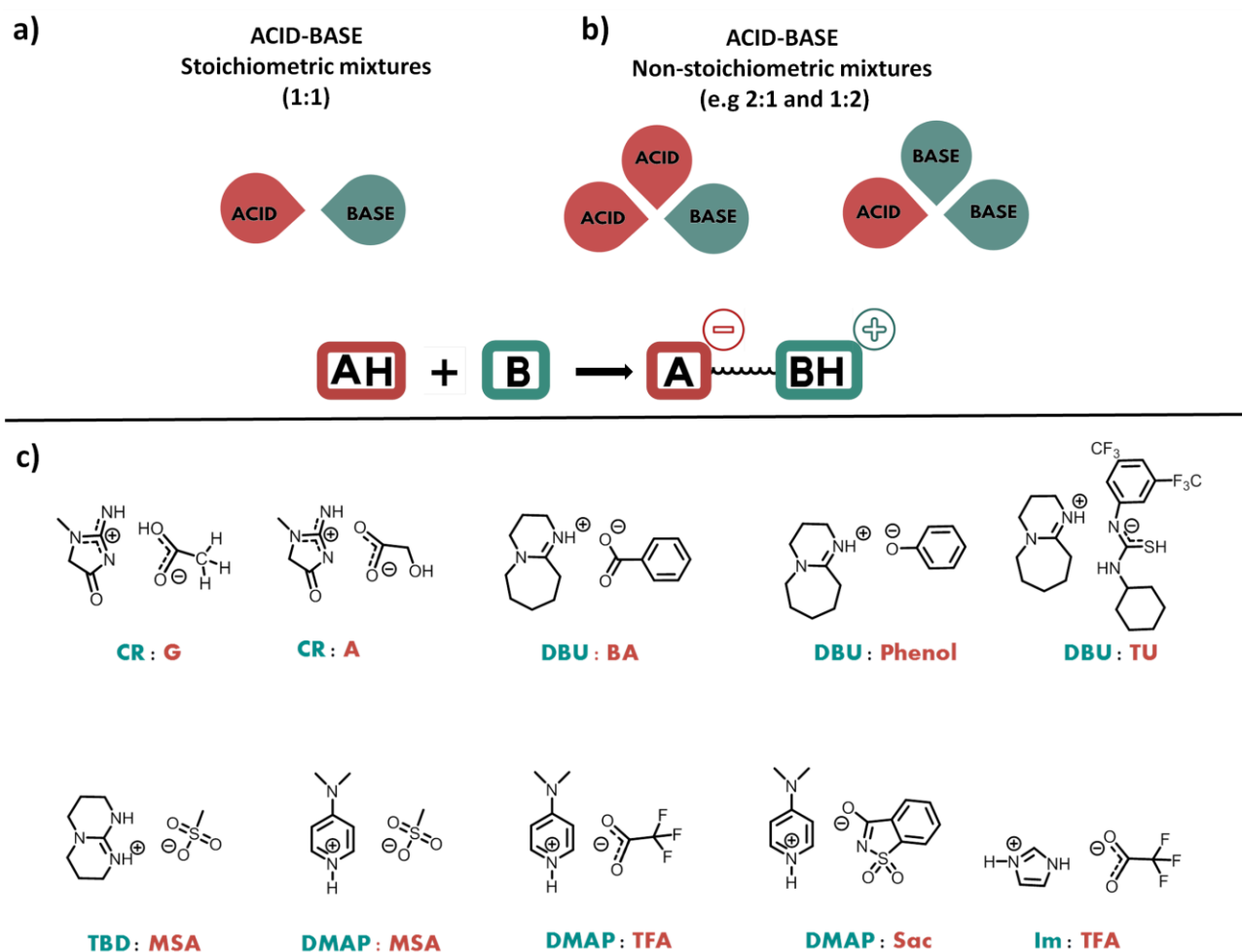
Figure 1.2 Graphical representation of the proton transfer reaction between an acid and a base and the formation of (a) stoichiometric (salts or protic ionic liquid)s and (b) non-stoichiometric mixture organocatalysts (NEMO) and (c) chemical examples of some acid-base ionic organocatalysts.

In this chapter, we summarize the results presented in the literature in the use of a family of thermally stable organocatalysts based on ionic compounds composed of physical mixtures of organic acids and bases. These catalysts have successfully been used in industrially relevant conditions, requiring high temperatures, both in chain growth and step-growth polymerizations of polyesters, polyesteramides or polyethers.[17,20–22] Moreover, the chapter will also address the recent efforts in the use of these acid-base mixtures in polymer recycling by chemical depolymerization which

has nowadays raised significant attention from an economic and environmental perspective.[13] We intend to keep the scope of this work as narrow as possible and it will be solely based on acid-base mixtures prepared by physical interaction (proton transfer reaction) not covering the extensive literature based on frustrated ion pairs, ionic liquids or acidic ionic liquids as catalyst for polymerizations.[23,24]

One of the major reasons to focus on this type of ionic organocatalysts prepared from acid-base mixtures is that their synthesis is a very simple and scalable process. As shown in Figure 1.2 a, when a Brönsted acid is mixed with a Brönsted base, a proton transfer reaction occurs between the acid (proton donor) and the base (proton acceptor) resulting in an ionic compound.[24] While in some cases this ionic complex emerges as a salt which can be purified by recrystallization, in other cases an ionic liquid could be formed. These ionic complexes are widely known as protic ionic salts and protic ionic liquids (PILs), respectively. The driving force for the proton transfer reaction is the pK_a difference between a given acid and a given base.

In order to form a stable ionic complex, the pK_a difference between the acid and the base has to be sufficiently high (higher than 4 in aqueous solution and greater in neat).[25] It is worth to remark that this process is dynamic and reversible. The synthesis of these compounds can be carried out in solution, bulk or even in solid state.[26] Interestingly, a remarkable aspect is that the proton transfer reaction not only occurs in stoichiometric mixtures but also in non-stoichiometric ones (Figure 1.2 b).

In the latter, the ionic interactions between the non-stoichiometric components also occur resulting in complexes with excess of one of the components.[27] Some of these non-stoichiometric mixtures have been described as Deep-Eutectic Solvents (DES) or more recently as Non-Eutectic Mixture Organocatalysts (NEMO).[20,27,28]

Thus, Figure 1.2 c shows the chemical structures of some ionic organocatalysts prepared by mixing acids and bases. Examples include imidazolium base compounds, thiourea (TU), strong bases such as 1,5,7-triazabicyclodec-5-ene (TBD), 4-dimethylaminopyridine (DMAP) and 1,8-diazabicyclo[5.4.0]undec-7-ene (DBU), strong acids such as methanesulfonic acid (MSA) and trifluoro acetic acid (TFA), benzoic acid (BA) and some bio-inspired acid and base compounds such as creatinine (CR), saccharine (Sac), glycolic acid (G) and acetic acid (A).

In light of this, these acid-base mixtures can act as bifunctional catalysts or as an organocatalysts with an acidic or basic ionic nature based on their stoichiometry. Different techniques can be used to provide evidences about the formation of these hydrogen-bonded ionic compounds. NMR spectroscopy, FTIR spectroscopy and ionic conductivity analysis provides relevant data of the molecular interactions within these acid-base mixtures.[20,28] Furthermore, quantum chemical calculations have also helped to gain insight about the interactions between the acid and the base and to get better insight into the molecular structures.

It is not surprising that the large variety of acid and bases together with the possibility to tune the acid or base character of the mixtures by playing with the stoichiometry give access to a wide range of catalytic compounds. In spite of the initial benefit of ionic compounds as alternative solvents to volatile organic compounds (VOCs) to carry out organic and polymerization reactions, in this chapter we will emphasize the possibility of using acid-base mixtures not as solvents but as catalyst for (de)polymerizations.
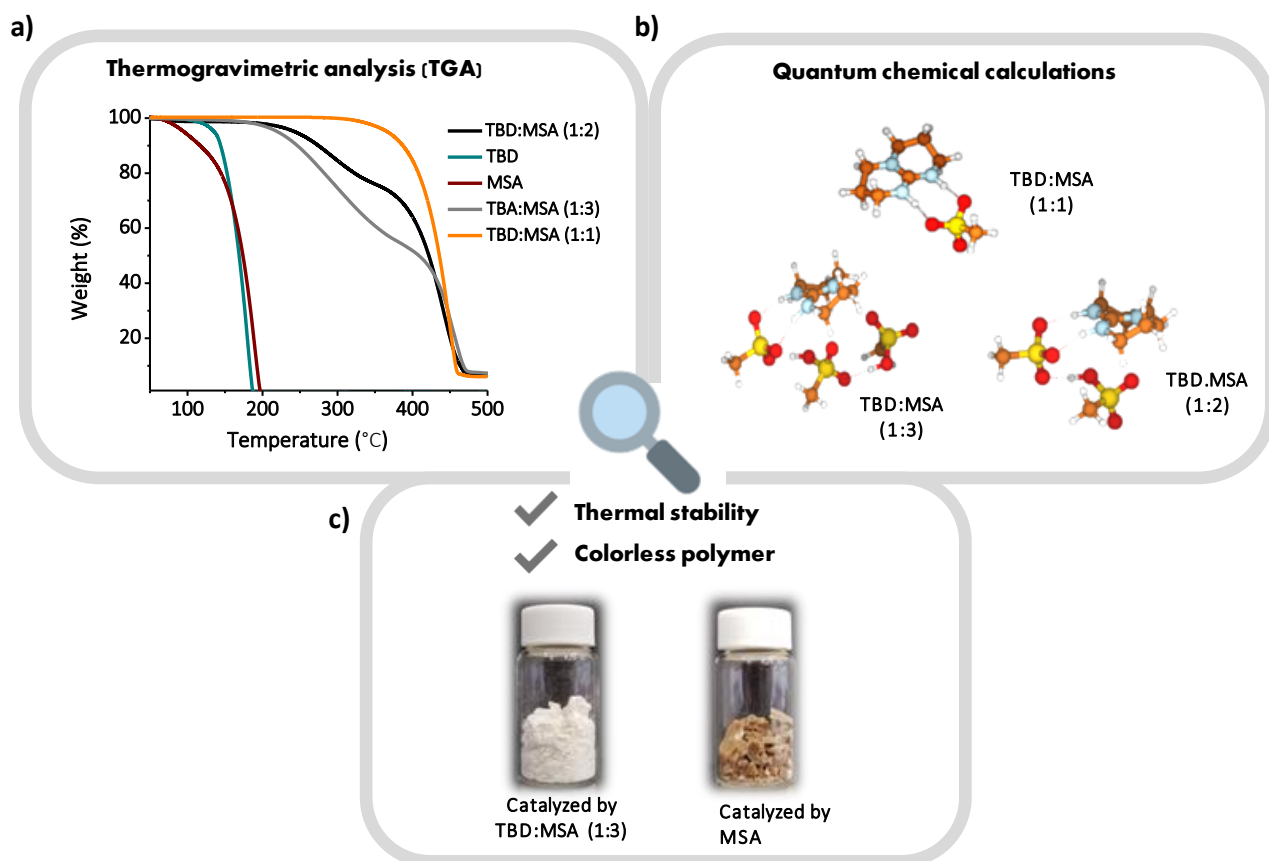
Figure 1.3. a) Thermogravimetric analysis (TGA) of different stoichiometric and non-stoichiometric mixtures of 1,5,7-triazabicyclodec-5-ene (TBD) and methanesulfonic acid (MSA), b) quantum chemical calculated molecular structures of the different mixtures and c) images of the poly(oxyalkylene) samples synthesized with the NEMO TBD:MSA and MSA only.

The potential of these ionic compounds to be used as organocatalyts is governed from their functionality (acid-base excess), ionic nature and hydrogen bonding ability. As an example, Figure 1.3 shows the particular case of acid-base organocatalysts formed by stoichiometric and non-stoichiometric mixtures of methanesulfonic acid (MSA) and 1,5,7-triazabicyclodec-5-ene (TBD) which was firstly studied by Del Monte et al. for the ROP of ε-caprolactone.[27] Hence, it was demonstrated the good catalytic performance of different NEMOs based on TBD:MSA mixtures in mild conditions. However, they did not exploit one of the most intriguing property of these stoichiometric and non-stoichiometric mixtures which is related with their sensational thermal stability much

higher than the individual compounds as shown in Figure 1.3 a. Whereas the acid and the base have a degradation temperature or boiling point close to 150 °C the ionic mixtures in some cases resist temperatures up to 400 °C.[20,22] This thermal stability opens a window of opportunities for this catalyst family to be used in polymerizations reactions that take place between 150 and 300 °C. To shed some light in how the ionic interactions between the constituents of the mixture which dictates such thermal stability, DFT calculations can be performed. Thereby, the Figure 1.3 b shows the ionic optimized structures for stoichiometric and non-stoichiometric mixtures of TBD and MSA. Regarding these structures, the mixture containing TBD:MSA (1:2), apart from showing the proton transfer from MSA to TBD, it shows the ability of forming strong hydrogen bonding interaction between the two MSA molecules supporting the observations done by ^{1}H NMR and justifying the excellent thermal stability of the non-stoichiometric mixtures.[20] Another indicator of thermal stability is the final color of the polymer. Owing to the commercial application of the polymers, the absence of any coloration of the material is a critical factor when considering high temperature polymerizations. As it can be observed in the Figure 1.3 c, the NEMO 1:3 employed in a polymerization process at 200 °C gave as a result colorless poly(oxyalkylene), while when using the acid MSA as individual catalyst under the same conditions brownish polymer was obtained, indicating the benefit of the acid-base mixtures in the reported temperature polymerization.[20]

1.3 Covering high temperature polymerizations

As mentioned in the introduction, industrially relevant polymers such as PET, PLA, polyamides or polyurethanes are synthesized in bulk polymerizations at elevated temperatures. Due to the commercial interest of these materials together with the collective purpose of moving towards more sustainable systems, in the last years several efforts have been focused on the implementation of the thermally stable organocatalysts in high temperature polymerizations.[1]

Such efforts are summarized in the next paragraphs covering three different examples where these acid-base mixtures have shown to potentially replace organometallic catalysts including a) the Ring-Opening Polymerizations (ROP), b) step-growth polymerizations and c) chemical depolymerizations. Figure 1.4 summarized all reviewed studies and the catalyst used in each case.
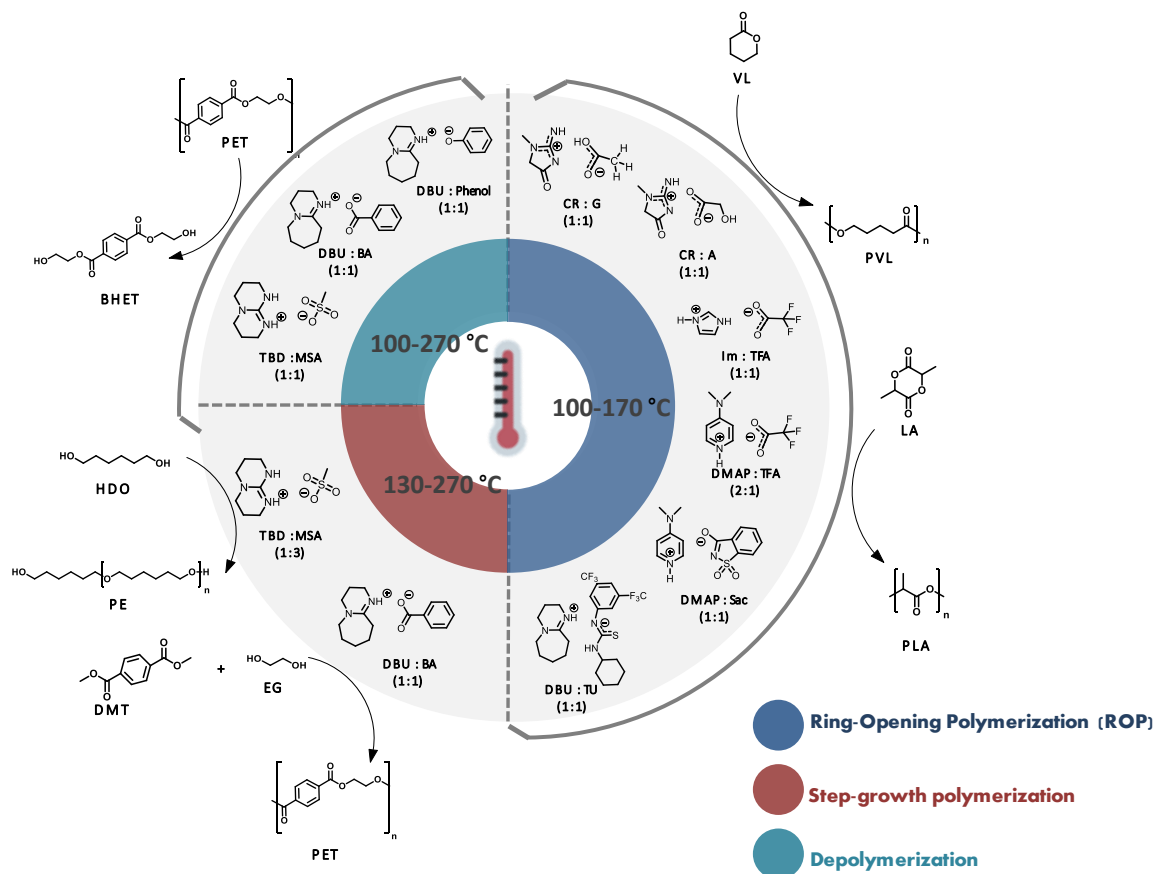
Figure 1.4. Graphical representation of the acid-base mixtures used as catalysts of high temperature polymerizations.

1.3.1 Ring-Opening Polymerizations

One of the first examples about the use of organic acid-base mixtures in industrially relevant conditions was related with the ROP of cyclic esters. Despite the numerous advantages that the use of organic catalysts provides to their metal-based analogues in mild conditions, the use of organocatalysts at high temperatures or mimicking industrial polymerization conditions remains underexplored, relative to more traditional metal-based polymerizations.[7,16,29] A prevalent example in this area is the ROP of L-lactide (LLA). Albeit poly(L-lactide) (PLLA) is one of the most consumed biobased material in the world, and one of the materials with greater potential to replace petroleum-based systems especially in packaging applications, the actual

industrial production of PLLA requires the use of organometallic catalysts such as SnOct$_2$. Given that the use of tin catalysts is increasingly restricted, more benign alternatives are needed and organocatalysis may play an important role only if they could overcome the limitations associated with their poor thermal stability.

Up to now, beyond the pure organic acids and bases, acid-base ionic compounds have appeared to be one of the most promising ones owing to their outstanding thermal stability.[16,30,31] Regarding the literature, the first acid-base mixture organocatalyst reported on the bulk ROP of LLA was the stoichiometric mixture of creatinine and glycolic acid 1:1 (CR:G), and creatinine and acetic acid 1:1 (CR:A).[32] Zhao et al. used these two complexes as both initiator and catalyst of the bulk ROP of LLA at 130 °C and 110 °C. Good control over the polymerization was obtained and polymers with M_n up to 15 kg mol^{-1} and narrow dispersities were obtained within about four days. However, racemization reactions of PLLA were observed and temperatures above 130 °C were not tested. A different catalytic system composed of imidazole-based salt formed by the mixture of imidazole and trifluoro acetic acid 1:1 (Im:TFA) was described by Coulembier et al.[33] Im:TFA combined with benzyl alcohol formed an stable system up to 170 °C able to catalyze the ROP of LLA at 140 °C. After 3.7 h almost 85% of monomer conversion was obtained for a theoretical DP of 70 and low level of transesterification was observed by MALDI-TOF analysis. Despite its good thermal stability and efficiency, the authors observed lack of end-group fidelity.

Besides the use of acid-base mixtures based on imidazolium, pyridine-based acid-base mixtures also have been explored for the ROP of LA. As reported by Hedrick and Waymouth, DMAP showed excellent capabilities to catalyze the ROP of lactide.[3] However, due to its high activity and poor thermal stability, DMAP promoted transesterification and/or epimerization reactions on the PLA backbone, especially at elevated temperatures. Recent studies have overcome the strong activity of the DMAP

and its lack of thermal stability by forming ionic complexes with organic acids.[21,33–36] Hence, the group of Peruch explored different NEMO formed by mixing 2 equivalents of DMAP and 1 equivalent of different acids for the ROP of LLA at 100 °C.[34] From all the catalysts evaluated, the combination of DMAP and triflic acid (DMAP:HOTf) displayed an outstanding catalytic activity able to produce PLLA with M_n of 14 kg mol^{-1} in 1 h. The reaction rates were quite competitive and no transesterification reactions were observed at monomer conversions up to 80% by MALDI-TOF. However, when increasing the temperature to 130 °C significant racemization reactions were observed. Despite the loose of control at elevated temperature, both the thermal stability and the catalytic activity of the NEMO DMAP:HOTf (2:1) proved to be more controlled when compared to DMAP as individual catalyst. Following the same concept, a recent study used DMAP and saccharin system 1:1 (DMAP:Sac) as catalyst for the ROP of L-lactide (LLA) and δ-valerolactone (VL) in bulk at 140 °C.[21] They firstly combined three commercial pyridines including DMAP, PPY, and pyridine with a stoichiometric ratio of saccharine. They observed that DMAP:Sac ionic mixture was the most efficient salt in the ROP of LA. Thus, using a benzyl alcohol (BnOH) as an initiator they achieved relatively high molecular weights (M_n = 14.3 kg mol^{-1}) and narrow dispersities within 11 h. Albeit the system successfully demonstrated its versatility at 140 °C with good polymerization control, only low-medium molecular weights were attempted.

Another system that has raised interest for performing ROPs is the recently discovered new family of organocatalysts derived from thioureas and amines which exhibited high functional group tolerance and extraordinary selectivity for the ROP.[37–46] Waymouth et al. reported that the deprotonation of ureas generates a class of versatile catalysts that are simultaneously fast and selective for the controlled ROP of different cyclic monomer families including esters, carbonates and phosphoesters.[37] Using this

concept, they were able to obtain high molecular weight polymers within minutes with low dispersities. Computational studies indicate a bifunctional catalytic mechanism where the catalyst is able to simultaneously activate the carbonyl and the alcohol, and they found that using different bases with (thio)urea catalyst they were able to tune the reactivity balancing the acidity of the acid-base mixture.[41] Kiesewetter extended the employment of these catalysts at elevated temperatures and they found that properly selecting the acid-base mixture based on (thio)urea the ROP of cyclic esters could be performed even at 110 °C without suffering any catalyst degradation.[44] Alltogether, these works suggested that the dual character of the (thio)urea/base organocatalyst is highly beneficial to get a better control of the ROP in comparison to single organocatalysts.

To finish with the research related with system based on thioureas and amines, the group of Zi Chen Li further exploited their use for the controlled ROP of ester amides. They found that the acid-base mixture based on TU:DBU give rise to a good control of the polymerization achieving high-molecular weight and low dispersities in comparison to DBU as individual catalyst.[45] Moreover the group of Guo showed that using an acid-base non-stoichiometric mixture based on 7-methyl-1,5,7-triazabicyclo[4.4.0]dec-5-ene (MTBD) and Brønsted acid trifluoromethanesulfonic acid (TFA) the living/controlled ROP of TMC could be performed to afford well-defined PTMC with narrow molecular weight distributions (M_w/ M_n ~ 1.1). Despite these promising advances, these ionic organocatalysts have not been employed at industrially relevant temperatures (150 °C - 300 °C) and only stoichiometric mixtures have been investigated.[47]

1.3.2 Step-growth Polymerizations

Apart from chain growth polymerization methods such as ROP for synthesizing polyesters, some commercially available polyesters such as PET are produced via step-growth polymerization such as polycondensation. It is well accepted that most of polycondensation processes demand specific conditions such as high conversion, absence of side reactions, stoichiometry of functional groups or efficient removal of condensates to favor the reaction equilibrium and obtain high molar masses.[48,49] Most of those condensates are relatively low boiling point molecules and therefore high temperatures and high pressures are generally required to achieve high molecular weights. These harsh polymerization conditions may represent one of the reasons why the research carried out in the organocatalyzed step-growth polymerizations is much less explored than in chain growth polymerizations. However, over the past few years organocatalyzed step-growth polymerization processes have gained more and more attention from the polymer community together with the expansion of acid-base mixture organocatalysts.[4]

One of the first example about the use of acid-base mixtures for step-growth polymerizations was described by Flores et al. in the synthesis of PET at 250 °C.[17] Based on the pioneering work of Hedrick about the preparation of acid base conjugates for the ROP of lactide, they demonstrated the great potential of 1,8-diazabicyclo[5.4.0]undec-7-ene and benzoic acid 1:1 (DBU:BA) to promote the step-growth polymerization of of PET from dimethyl therephatlate (DMT) and ethylene glycol (EG) in bulk.[17,50] Kinetic studies revealed that the catalytic activity of the protic ionic salt DBU:BA was competitive in comparison to the conventional organometallic catalysts (TiBut) employed in PET synthesis. Using 5 mol % of DBU:BA ionic salt colorless PET with molar mass up to M_n 10.7 kg mol^{-1} was obtained. Albeit, these molar masses remain relatively low in comparison with commercial PET, the protic

ionic salt were found to be much more efficient and stable than the pure organic precursors being still considered a potential alternative to the organometallic analogue. The authors found that this catalyst could be also used to make copolymers based on PET. [51] Similarly, Jehanno et al. found that using 5 mol % of TBD:MSA stoichiometric mixture they were able to obtain PET with molecular weights up to 12 kg.mol^{-1} and similar thermal properties to the virgin PET by the self-condensation of bis(2-hydroxyethyl) terephthalate (BHET)

1.3.3 Depolymerization processes

Aside from the investigations of thermally stable catalyst in polymerization reactions, advances in the use of these acid-base mixtures in polymer recycling by chemical depolymerization have been also reported. The inability to recycle nearly all the current polymeric materials after the end of their useful life has created severe worldwide environmental consequences. Therefore there is a need to design thermally stable catalyst that allows the chemical depolymerization of plastics at industrial scales. In chemical depolymerization processes harsh conditions such as high temperature and pressure are also required to enhance the efficiency of the process because polymers such as PET have been particularly designed to be resistant to degradations. Despite the benefit of organometallic catalysts in terms of thermal stability they are challenging to separate from the crude product. Thereby, the use of the thermally stable acid-base organocatalyst is increasingly exploited in organocatalytic depolymerization.

Thus, acid-base salts such as DBU:BA, DBU:Phenol and TBD:MSA have been investigated in the chemical recycling of PET. DBU-based salts including DBU: BA and DBU:phenol (1:1) demonstrated to be more stable than DBU alone in PET depolymerization process.[52] Similarly, the TBD:MSA at the stoichiometric ratio 1:1 not

only demonstrated extraordinary thermal stability in the glycolysis of PET comparing to TBD and MSA as individual catalysts, but also it showed simultaneously excellent catalytic activity and selectivity.[22] This catalyst allowed to recover 90% of BHET with high purity through simple crystallization in water in only 2h at 180 °C. In addition, the catalyst was recycled up to 6 times without losing any catalytic activity.

1.4 Objectives of the thesis

Having underlined in the present chapter the recent advances on the use of acid-base mixture organocatalysts at high temperature polymerizations, this work will be focused on the design of novel acid-base mixture organocatalysts that will be used on the synthesis of valuable polymers including polyethers and polyesters.

Herein, the work can be divided into two major parts that contain both the optimization and characterization of the acid-base mixture organocatalyst and its use in the synthesis of polyethers by self-condensation (**Chapers 2, 3 and 4**), and polyesters by Ring-Opening Polymerization (ROP) (**Chapter 5**).

In order to develop an efficient organocatalytic process at high temperature, **Chapter 2** will depict the synthesis and characterization of a thermally stable acid-base mixture organocatalyst with the aim of employing it in the self-condensation of aliphatic diols in bulk conditions. Stoichiometric and non-stoichiometric ratios of the organic acid MSA and the base TBD are mixed to yield protic ionic salts and Non-Eutectic mixture Organocatalysts (NEMOs).

They are subsequently tested in the self-condensation of 1,6-hexanediol to evaluate their efficiency as catalyst. The reaction is optimized and the most efficient NEMO

(MSA:TBD 3:1) is subsequently employed in the synthesis of different semicrystalline aliphatic polyethers with different methylene units in the repetitive chain. The scope of the synthesis approach is expanded to the synthesis of aliphatic polyethers and crosslinked polyethers.

In **Chapter 3** the synthesis and the thermal behavior of aliphatic random copolyethers is investigated in the aim of broaden the properties of the materials as well as to expand the scope of the NEMO organocatalyst. Copolyethers derived from a medium chain aliphatic diol (1,6-hexanediol) and a long chain aliphatic diol (1,12-dodecanediol) are synthetized choosing the previously described polymerization conditions. A remarkable and unusual thermal behavior is described for all the copolyethers which shown to have isomorphic behavior.

In **Chapter 4**, with the aim of brings to the synthetic approach an added sustainable profit, the use of free petroleum-based materials is considered and 1,6-hexanediol and 1,4-cyclohexanediometanol bio-based monomers are copolymerized resulting in fully bio-based copolyethers. The thermal properties of these copolyethers are also determined and show a good tunability potential ranging from low T_g containing semicrystalline to amorphous materials which can have the potential to be used as elastomers or as thermoadhesives in the polyurethane industry.

Going upon the second part of the thesis, in **Chapter 5** we overcome one of the long-standing challenged in organocatalysis: the bulk Ring-Opening Polymerization (ROP) of L-lactide.

In this last chapter, another acid-base mixture organocatalyst is explored. Stoichiometric and non-stoichiometric mixtures of MSA and DMAP are characterized

and employed in the ROP of L-lactide in bulk conditions. The thermal stability of the two systems and their efficiency is studied yielding PLA owing different characteristics.

To finish, the results and the most relevant conclusions in regard to the gains and the challenges considered in this work and in the respective field will be commented.
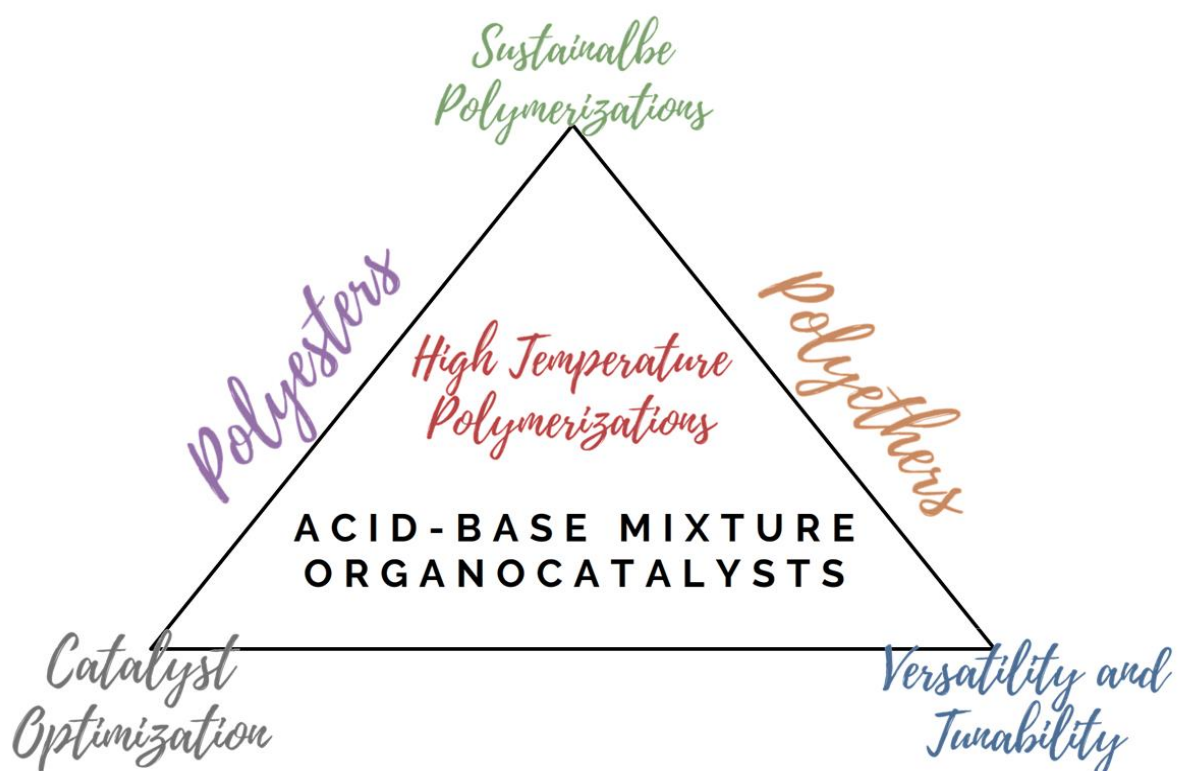

Figure 1.5. Key words of the thesis.

1.5. References

(1) Sheldon, R. A. Metrics of Green Chemistry and Sustainability: Past, Present, and Future. *ACS Sustain. Chem. Eng.* **2018**, *6* (1), 32–48. https://doi.org/10.1021/acssuschemeng.7b03505.

(2) Liang, Y.; Li, L.; Scott, R. A.; Kiick, K. L. 50th Anniversary Perspective: Polymeric Biomaterials: Diverse Functions Enabled by Advances in Macromolecular

Chemistry. *Macromolecules* **2017**, *50* (2), 483–502. https://doi.org/10.1021/acs.macromol.6b02389.

(3) Nederberg, F.; Connor, E. F.; Möller, M.; Glauser, T.; Hedrick, J. L. New Paradigms for Organic Catalysts: The First Organocatalytic Living Polymerization. *Angew. Chem. Int. Ed.* **2001**, *40* (14), 2712–2715. https://doi.org/10.1002/1521-3773(20010716)40:14<2712::AID-ANIE2712>3.0.CO;2-Z.

(4) Bossion, A.; Heifferon, K. V.; Meabe, L.; Zivic, N.; Taton, D.; Hedrick, J. L.; Long, T. E.; Sardon, H. Opportunities for Organocatalysis in Polymer Synthesis via Step-Growth Methods. *Prog. Polym. Sci.* **2019**, *90*, 164–210. https://doi.org/10.1016/j.progpolymsci.2018.11.003.

(5) Kiesewetter, M. K.; Shin, E. J.; Hedrick, J. L.; Waymouth, R. M. Organocatalysis: Opportunities and Challenges for Polymer Synthesis. *Macromolecules* **2010**, *43* (5), 2093–2107. https://doi.org/10.1021/ma9025948.

(6) Sardon, H.; Pascual, A.; Mecerreyes, D.; Taton, D.; Cramail, H.; Hedrick, J. L. Synthesis of Polyurethanes Using Organocatalysis: A Perspective. *Macromolecules* **2015**, *48* (10), 3153–3165. https://doi.org/10.1021/acs.macromol.5b00384.

(7) Dove, A. P. Organic Catalysis for Ring-Opening Polymerization. *ACS Macro Lett.* **2012**, *1* (12), 1409–1412. https://doi.org/10.1021/mz3005956.

(8) Fèvre, M.; Pinaud, J.; Gnanou, Y.; Vignolle, J.; Taton, D. N-Heterocyclic Carbenes (NHCs) as Organocatalysts and Structural Components in Metal-Free Polymer Synthesis. *Chem. Soc. Rev.* **2013**, *42* (5), 2142–2172. https://doi.org/10.1039/C2CS35383K.

(9) Khalil, A.; Cammas-Marion, S.; Coulembier, O. Organocatalysis Applied to the Ring-Opening Polymerization of β-Lactones: A Brief Overview. *J. Polym. Sci. Part Polym. Chem.* **2019**, *57* (6), 657–672. https://doi.org/10.1002/pola.29322.

(10) Kamber, N. E.; Jeong, W.; Waymouth, R. M.; Pratt, R. C.; Lohmeijer, B. G. G.; Hedrick, J. L. Organocatalytic Ring-Opening Polymerization. *Chem. Rev.* **2007**, *107* (12), 5813–5840. https://doi.org/10.1021/cr068415b.

(11) Zhu, N.; Liu, Y.; Liu, J.; Ling, J.; Hu, X.; Huang, W.; Feng, W.; Guo, K. Organocatalyzed Chemoselective Ring-Opening Polymerizations. *Sci. Rep.* **2018**, *8* (1), 3734. https://doi.org/10.1038/s41598-018-22171-6.

(12) Dove, A.; Sardon, H.; Naumann, S. *Organic Catalysis for Polymerisation*; Royal Society of Chemistry, 2018.

(13) Jehanno, C.; Pérez-Madrigal, M. M.; Demarteau, J.; Sardon, H.; Dove, A. P. Organocatalysis for Depolymerisation. *Polym. Chem.* **2018**, *10* (2), 172–186. https://doi.org/10.1039/C8PY01284A.

(14) Theriot, J. C.; McCarthy, B. G.; Lim, C.-H.; Miyake, G. M. Organocatalyzed Atom Transfer Radical Polymerization: Perspectives on Catalyst Design and Performance. *Macromol. Rapid Commun.* **2017**, *38* (13), 1700040. https://doi.org/10.1002/marc.201700040.

(15) Zivic, N.; Kuroishi, P. K.; Dumur, F.; Gigmes, D.; Dove, A. P.; Sardon, H. Recent Advances and Challenges in the Design of Organic Photoacid and Photobase Generators for Polymerizations. *Angew. Chem. Int. Ed. 0* (0). https://doi.org/10.1002/anie.201810118.

(16) Mezzasalma, L.; Dove, A. P.; Coulembier, O. Organocatalytic Ring-Opening Polymerization of L-Lactide in Bulk: A Long Standing Challenge. *Eur. Polym. J.* **2017**, *95*, 628–634. https://doi.org/10.1016/j.eurpolymj.2017.05.013.

(17) Flores, I.; Demarteau, J.; Müller, A. J.; Etxeberria, A.; Irusta, L.; Bergman, F.; Koning, C.; Sardon, H. Screening of Different Organocatalysts for the Sustainable Synthesis of PET. *Eur. Polym. J.* **2018**, *104*, 170–176. https://doi.org/10.1016/j.eurpolymj.2018.04.040.

(18) Lim, L.-T.; Auras, R.; Rubino, M. Processing Technologies for Poly(lactic Acid). *Prog. Polym. Sci.* **2008**, *33* (8), 820–852. https://doi.org/10.1016/j.progpolymsci.2008.05.004.

(19) Zhang, X.; Fevre, M.; Jones, G. O.; Waymouth, R. M. Catalysis as an Enabling Science for Sustainable Polymers. *Chem. Rev.* **2018**, *118* (2), 839–885. https://doi.org/10.1021/acs.chemrev.7b00329.

(20) Basterretxea, A.; Gabirondo, E.; Jehanno, C.; Zhu, H.; Flores, I.; Müller, A. J.; Etxeberria, A.; Mecerreyes, D.; Coulembier, O.; Sardon, H. Polyether Synthesis by Bulk Self-Condensation of Diols Catalyzed by Non-Eutectic Acid–Base Organocatalysts. *ACS Sustain. Chem. Eng.* **2019**, *7* (4), 4103–4111. https://doi.org/10.1021/acssuschemeng.8b05609.

(21) Wei, F.; Zhu, H.; Li, Z.; Wang, H.; Zhu, Y.; Zhang, L.; Yao, Z.; Luo, Z.; Zhang, C.; Guo, K. Food Sweetener Saccharin in Binary Organocatalyst for Bulk Ring-Opening Polymerization of Lactide. *Adv. Synth. Catal.* **2019**, *361* (6), 1335–1347. https://doi.org/10.1002/adsc.201801319.

(22) Jehanno, C.; Flores, I.; Dove, A. P.; Müller, A. J.; Ruipérez, F.; Sardon, H. Organocatalysed Depolymerisation of PET in a Fully Sustainable Cycle Using Thermally Stable Protic Ionic Salt. *Green Chem.* **2018**, *20* (6), 1205–1212. https://doi.org/10.1039/C7GC03396F.

(23) Hong, M.; Chen, J.; Chen, E. Y.-X. Polymerization of Polar Monomers Mediated by Main-Group Lewis Acid–Base Pairs. *Chem. Rev.* **2018**, *118* (20), 10551–10616. https://doi.org/10.1021/acs.chemrev.8b00352.

(24) Greaves, T. L.; Drummond, C. J. Protic Ionic Liquids: Evolving Structure–Property Relationships and Expanding Applications. *Chem. Rev.* **2015**, *115* (20), 11379–11448. https://doi.org/10.1021/acs.chemrev.5b00158.

(25) MacFarlane, D. R.; Kar, M.; Pringle, J. M. *Fundamentals of Ionic Liquids: From Chemistry to Applications*; John Wiley & Sons, 2017.

(26) Burrell, G. L.; Burgar, I. M.; Separovic, F.; Dunlop, N. F. Preparation of Protic Ionic Liquids with Minimal Water Content and 15N NMR Study of Proton Transfer. *Phys. Chem. Chem. Phys.* **2010**, *12* (7), 1571–1577. https://doi.org/10.1039/B921432A.

(27) del Monte, F.; Carriazo, D.; Serrano, M. C.; Gutiérrez, M. C.; Ferrer, M. L. Deep Eutectic Solvents in Polymerizations: A Greener Alternative to Conventional Syntheses. *ChemSusChem* **2014**, *7* (4), 999–1009. https://doi.org/10.1002/cssc.201300864.

(28) Jehanno, C.; Flores, I.; Dove, A. P.; Muller, A.; Ruipérez, F.; Sardon, H. Organocatalysed Depolymerisation of PET in a Fully Sustainable Cycle Using Thermally Stable Protic Ionic Salt. *Green Chem.* **2018**. https://doi.org/10.1039/C7GC03396F.

(29) Sanchez-Sanchez, A.; Rivilla, I.; Agirre, M.; Basterretxea, A.; Etxeberria, A.; Veloso, A.; Sardon, H.; Mecerreyes, D.; Cossío, F. P. Enantioselective Ring-Opening Polymerization of Rac-Lactide Dictated by Densely Substituted Amino Acids. *J. Am. Chem. Soc.* **2017**, *139* (13), 4805–4814. https://doi.org/10.1021/jacs.6b13080.

(30) Thomas, C.; Bibal, B. Hydrogen-Bonding Organocatalysts for Ring-Opening Polymerization. *Green Chem.* **2014**, *16* (4), 1687–1699. https://doi.org/10.1039/C3GC41806E.

(31) Coady, D. J.; Fukushima, K.; Horn, H. W.; Rice, J. E.; Hedrick, J. L. Catalytic Insights into Acid/Base Conjugates: Highly Selective Bifunctional Catalysts for the Ring-Opening Polymerization of Lactide. *Chem. Commun.* **2011**, *47* (11), 3105–3107. https://doi.org/10.1039/C0CC03987J.

(32) Li, H.; Zhang, S.; Jiao, J.; Jiao, Z.; Kong, L.; Xu, J.; Li, J.; Zuo, J.; Zhao, X. Controlled Synthesis of Polylactides Using Biogenic Creatinine Carboxylate Initiators. *Biomacromolecules* **2009**, *10* (5), 1311–1314. https://doi.org/10.1021/bm801479p.

(33) Coulembier, O.; Josse, T.; Guillerm, B.; Gerbaux, P.; Dubois, P. An Imidazole-Based Organocatalyst Designed for Bulk Polymerization of Lactide Isomers: Inspiration from Nature. *Chem. Commun.* **2012**, *48* (95), 11695–11697. https://doi.org/10.1039/C2CC37061A.

(34) Kadota, J.; Pavlović, D.; Hirano, H.; Okada, A.; Agari, Y.; Bibal, B.; Deffieux, A.; Peruch, F. Controlled Bulk Polymerization of L-Lactide and Lactones by Dual Activation with Organo-Catalytic Systems. *RSC Adv.* **2014**, *4* (28), 14725–14732. https://doi.org/10.1039/C4RA01239A.

(35) Kadota, J.; Pavlović, D.; Desvergne, J.-P.; Bibal, B.; Peruch, F.; Deffieux, A. Ring-Opening Polymerization of L-Lactide Catalyzed by an Organocatalytic System Combining Acidic and Basic Sites. *Macromolecules* **2010**, *43* (21), 8874–8879. https://doi.org/10.1021/ma101688d.

(36) Guillerm, B.; Lemaur, V.; Ernould, B.; Cornil, J.; Lazzaroni, R.; Gohy, J.-F.; Dubois, P.; Coulembier, O. A One-Pot Two-Step Efficient Metal-Free Process for the Generation of PEO-B-PCL-B-PLA Amphiphilic Triblock Copolymers. *RSC Adv.* **2014**, *4* (20), 10028–10038. https://doi.org/10.1039/C3RA47204C.

(37) Lin, B.; Waymouth, R. M. Urea Anions: Simple, Fast, and Selective Catalysts for Ring-Opening Polymerizations. *J. Am. Chem. Soc.* **2017**, *139* (4), 1645–1652. https://doi.org/10.1021/jacs.6b11864.

(38) Zhang, X.; Jones, G. O.; Hedrick, J. L.; Waymouth, R. M. Fast and Selective Ring-Opening Polymerizations by Alkoxides and Thioureas. *Nat. Chem.* **2016**, *8* (11), 1047–1053. https://doi.org/10.1038/nchem.2574.

(39) Pothupitiya, J. U.; Hewawasam, R. S.; Kiesewetter, M. K. Urea and Thiourea H-Bond Donating Catalysts for Ring-Opening Polymerization: Mechanistic Insights via (Non)linear Free Energy Relationships. *Macromolecules* **2018**, *51* (8), 3203–3211. https://doi.org/10.1021/acs.macromol.8b00321.

(40) Pothupitiya, J. U.; Dharmaratne, N. U.; Jouaneh, T. M. M.; Fastnacht, K. V.; Coderre, D. N.; Kiesewetter, M. K. H-Bonding Organocatalysts for the Living, Solvent-Free Ring-Opening Polymerization of Lactones: Toward an All-Lactones, All-Conditions Approach. *Macromolecules* **2017**, *50* (22), 8948–8954. https://doi.org/10.1021/acs.macromol.7b01991.

(41) Lin, B.; Waymouth, R. M. Organic Ring-Opening Polymerization Catalysts: Reactivity Control by Balancing Acidity. *Macromolecules* **2018**, *51* (8), 2932–2938. https://doi.org/10.1021/acs.macromol.8b00540.

(42) Pratt, R. C.; Lohmeijer, B. G. G.; Long, D. A.; Lundberg, P. N. P.; Dove, A. P.; Li, H.; Wade, C. G.; Waymouth, R. M.; Hedrick, J. L. Exploration, Optimization, and Application of Supramolecular Thiourea–Amine Catalysts for the Synthesis of Lactide (Co)polymers. *Macromolecules* **2006**, *39* (23), 7863–7871. https://doi.org/10.1021/ma061607o.

(43) Dharmaratne, N. U.; Pothupitiya, J. U.; Kiesewetter, M. K. The Mechanistic Duality of (Thio)urea Organocatalysts for Ring-Opening Polymerization. *Org. Biomol. Chem.* **2019**, *17* (13), 3305–3313. https://doi.org/10.1039/C8OB03174F.

(44) Coderre, D. N.; Fastnacht, K. V.; Wright, T. J.; Dharmaratne, N. U.; Kiesewetter, M. K. H-Bonding Organocatalysts for Ring-Opening Polymerization at Elevated Temperatures. *Macromolecules* **2018**, *51* (24), 10121–10126. https://doi.org/10.1021/acs.macromol.8b02219.

(45) Shi, C.-X.; Guo, Y.-T.; Wu, Y.-H.; Li, Z.-Y.; Wang, Y.-Z.; Du, F.-S.; Li, Z.-C. Synthesis and Controlled Organobase-Catalyzed Ring-Opening Polymerization of Morpholine-2,5-Dione Derivatives and Monomer Recovery by Acid-Catalyzed Degradation of the Polymers. *Macromolecules* **2019**. https://doi.org/10.1021/acs.macromol.8b02498.

(46) Dove, A. P.; Pratt, R. C.; Lohmeijer, B. G. G.; Waymouth, R. M.; Hedrick, J. L. Thiourea-Based Bifunctional Organocatalysis: Supramolecular Recognition for

Living Polymerization. *J. Am. Chem. Soc.* **2005**, *127* (40), 13798–13799. https://doi.org/10.1021/ja0543346.

(47) Wang, X.; Cui, S.; Li, Z.; Kan, S.; Zhang, Q.; Zhao, C.; Wu, H.; Liu, J.; Wu, W.; Guo, K. A Base–conjugate-Acid Pair for Living/Controlled Ring-Opening Polymerization of Trimethylene Carbonate through Hydrogen-Bonding Bifunctional Synergistic Catalysis. *Polym. Chem.* **2014**, *5* (20), 6051–6059. https://doi.org/10.1039/C4PY00773E.

(48) Long, T. E.; Turner, S. R. STEP-GROWTH POLYMERIZATION. In *Applied Polymer Science: 21st Century*; Craver, C. D., Carraher, C. E., Eds.; Pergamon: Oxford, 2000; pp 979–997. https://doi.org/10.1016/B978-008043417-9/50047-7.

(49) Zhang, M.; June, S. M.; Long, T. E.; Kong, J. Principles of Step-Growth Polymerization (Polycondensation and Polyaddition). In *Reference Module in Materials Science and Materials Engineering*; Elsevier, 2016. https://doi.org/10.1016/B978-0-12-803581-8.01410-7.

(50) Coady, D. J.; Fukushima, K.; Horn, H. W.; Rice, J. E.; Hedrick, J. L. Catalytic Insights into Acid/Base Conjugates: Highly Selective Bifunctional Catalysts for the Ring-Opening Polymerization of Lactide. *Chem. Commun.* **2011**, *47* (11), 3105–3107. https://doi.org/10.1039/C0CC03987J.

(51) Flores, I.; Etxeberria, A.; Irusta, L.; Calafel, I.; Vega, J. F.; Martínez-Salazar, J.; Sardon, H.; Müller, A. J. PET-Ran-PLA Partially Degradable Random Copolymers Prepared by Organocatalysis: Effect of Poly(l-Lactic Acid) Incorporation on Crystallization and Morphology. *ACS Sustain. Chem. Eng.* **2019**, *7* (9), 8647–8659. https://doi.org/10.1021/acssuschemeng.9b00443.

(52) Fukushima, K.; Lecuyer, J. M.; Wei, D. S.; Horn, H. W.; Jones, G. O.; Al-Megren, H. A.; Alabdulrahman, A. M.; Alsewailem, F. D.; McNeil, M. A.; Rice, J. E.; et al. Advanced Chemical Recycling of Poly(ethylene Terephthalate) through

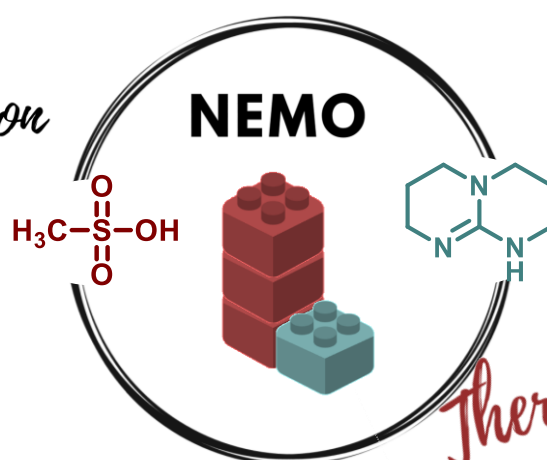Organocatalytic   Aminolysis.   *Polym.   Chem.*   **2013**,   *4*   (5),   1610–1616. https://doi.org/10.1039/C2PY20793A.
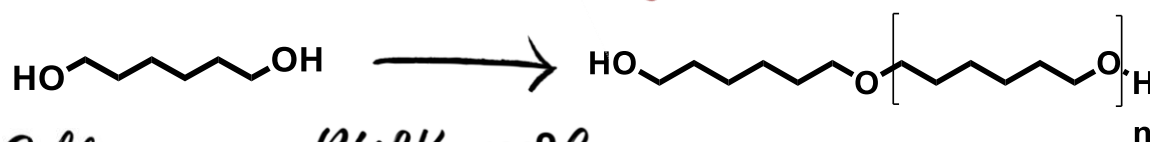
Chapter 2

Graphical abstract

1. Catalyst characterization

NEMO

$H_3C-\overset{\displaystyle O}{\underset{\displaystyle O}{S}}-OH$

Thermal stability

HO ⌢⌢ OH $\longrightarrow$ HO ⌢⌢⌢ O ⌊ ⌢⌢⌢ O ⌋$_n$ H

2. Self-condensation of aliphatic diols

BULK 200°C

Chapter 2. Polyether synthesis by bulk self-condensation of diols catalyzed by a Non-Eutectic acid-base Mixture Organocatalysts (NEMO)

2.1. Introduction

Ethers or oxyalkylenes, also named polyethers, are chemical compounds that contain R-O-R' bond, where R and R' comprise any alkyl or aryl moieties. Since their first synthesis by Wurtz in the1860s, polyethers have become an important polymer family due to their versatile syntheses, thermal and chemical stabilities, and multiple applications.[1,2]
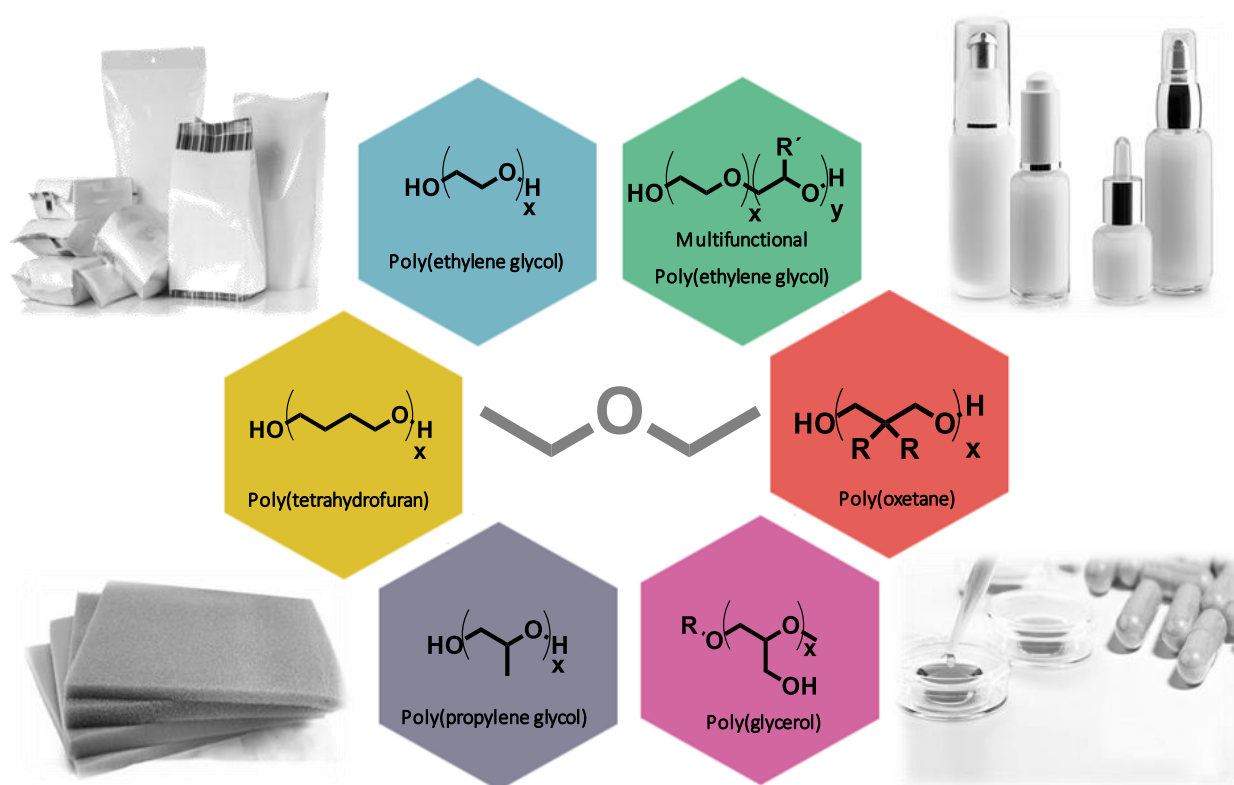
Figure 2.1. Comodity polyethers highly used in applications such as cosmetics, packaging, biomedicine or polyurethanes foams.

Polyethers such as as polyethyleneglycol (PEO or PEG), polypropyleneglycol (PPG) or polytetramethyleneglycol (PTMG) are nowadays used in many different applications ranging from surfactants, automotive industry, batteries, food and cosmetic industry, nanomedicine or as soft segments in polyurethane chemistry.[1,3–5] These polyethers are mainly produced by ring-opening polymerization of the corresponding cyclic ethers, such as oxiranes, oxetanes or tetrahydrofuran.[6–8] However, using the aforementioned method, larger size polyethers (containing 6 or more methylene units) cannot be obtained because of the extreme stability of the cyclic ethers. In contrast to short polyethers, long chain polyethers own superior properties in flexibility and hydrolytic stability and also exhibit better mechanical strength and low glass transition temperature (T_g). Their production is achieved by polycondensation using the Williamson ether synthesis.[9] In this case, the ether linkage is generated by a nucleophilic substitution of an alkoxide on an alkylating reagent (typically a halogenated alkane). Although this method is highly efficient, halogen such as chloride is generated as side product during the polymerization which may generate hydrochloric acid and detracts from the sustainable production of these polymers. Very recently, Meier et al. prepared polyethers by the reduction of polyesters in the presence of tetramethyldisiloxane and $GaBr_3$ catalyst in a more sustainable process, but this process requires the previous preparation of the analogous polyester.[10]

An old but under explored route to produce polyethers is the acid catalyzed self-condensation of alcohols resulting in an ether bond. Alcohols generally need to be activated, and typically acid catalysts are employed. The reaction proceeds in three-steps: the first one consists in the protonation of the alcohol group, forming its conjugated acid that is a better leaving group. This facilitates the second step, where nucleophilic attack of another alcohol onto the adjacent carbon via a S_N2 mechanism takes place. Finally, ether is formed via subsequent deprotonation (Figure 2.2).[11]

In the 1950s, Rhoad and Flory pioneered the self condensation of 1,10-decanediol in the presence of sulfamic or sulfuric acids at elevated temperature (300 °C) in bulk polymerization conditions.[12]
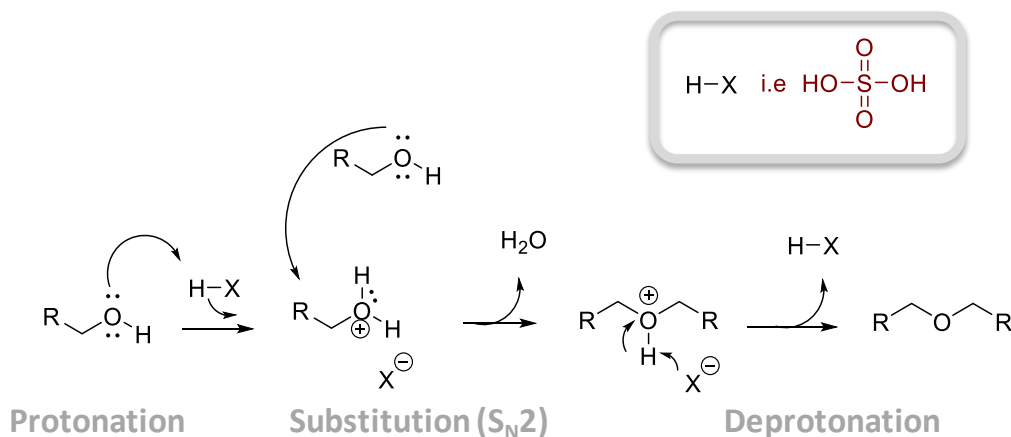

Figure 2.2. General mechanism for the condensation of alcohols in the presence of an acid as catalyst.[11]

Almost twenty years later, Kobayashi et al., used the same method to synthesize linear poly(oxyalkylene)s in the presence of H_2SO_4 and $(C_2H_5)_2O \bullet BF_3$.[13] Since this reaction is reversible, care has to be taken when ethers are used under strong acidic conditions.

Albeit the self-condensation processes in bulk is a simple and environmental friendly polymerization method, it presents a setback; since some acids are highly volatile and they can be decomposed during the polymerization process due to the harsh employed conditions. In 2011, Fradet et al. minimized these drawbacks using Brønsted Acid Ionic Liquids as solvent and catalysts which allowed the reactions to be carried out at lower temperatures (130 °C).[14] Brønsted Acid Ionic Liquids combine the catalytic activity of Brønsted Acid with the high thermal stability and low vapor pressure of ionic liquids. However, the ones employed by Fradet have elevated price and the side reactions occurring during the polymerization limited their potential.

A cost-effective alternative to Brønsted Acid Ionic liquids are Protic Ionic Liquids/Salts which can be prepared through the simple proton transfer from a Brønsted acid to a Brønsted base. These protic ionic compounds have been shown to be suitable alternatives to classic organometallic catalysts. They smartly combine the excellent catalytic ability of organocatalysts with the thermal stability of ionic liquids, resisting degradation up to > 400 °C.[15] Thus, Flores et al. demonstrated that the Protic Ionic Salt 1,8-diazabicyclo[5.4.0]undec-7-ene: benzoic acid (DBU:BA) was a competitive catalyst for PET synthesis showing a good stability and catalytic activity even at elevated temperatures up to > 250 °C.[16,17] Similarly, equimolar mixtures of 1,5,7-triazabicyclo[4.4.0]dec-5-ene (TBD) and methanesulfonic acid (MSA) proved to be an efficient and extremely thermally stable catalyst in the depolymerization of PET being even able to be recycled several times.[15] One of the key features of protic ionic compounds is their ability to form stable complexes even using non-equimolar mixtures by H-bonding interaction between the acid and base preparing the non-eutectic acid base mixtures. Taking advantage of this unique characteristic, Del monte et al. prepared different non-equimolar mixtures of methanesulfonic acid (MSA) and the 1,5,7-triazabicyclo[4.4.0]dec-5-ene (TBD) for the ring-opening polymerization (ROP) of ε-caprolactone.[18]

In this chapter, we benefited from the versatility and easy synthesis of acid base mixtures for investigating the melt self condensation of polyethers by self-condensation of diols. First, different equimolar and non-equimolar mixtures of MSA and TBD were prepared leading to protic ionic salt (1:1 mixture) and different Non-Eutectic Mixture Organocatalysts (NEMOs) which were characterized extensively. This catalytic system was investigated as it has shown some potential to work at elevated temperatures without suffering any degradation. The protic ionic salt and the NEMOs

were used in a second step for investigating the polyetherification of 1,6-hexanediol. We found that some NEMOs were highly efficient for the polymerization process and also thermally stable, which allowed the recovery and the subsequent recycling of the catalyst. This synthetic strategy was extended to seven other long chain diols which yielded semicrystalline aliphatic polyethers whose crystalline structure was also determined. To finish, we expanded the frontiers of this work by copolymerizing different long chain diols and functionality resulting in both linear and crosslinked copolyethers.

2.2. Results and discussion

2.2.1. Characterization of the acid base organocatalysts based on MSA and TBD

First, MSA and TBD mixtures at in different molar ratios such as 3:1, 2:1 and 1:1 (respectively) were prepared by simple mixing at 90 °C for 30 minutes until obtaining a transparent and homogeneous organocatalyst (Figure 2.3). In order to confirm the formation of the acid base organocatalysts the resulting mixtures were characterized by ^{1}H NMR spectroscopy in DMSO, while their thermal degradation was investigated with TGA.[15,18]
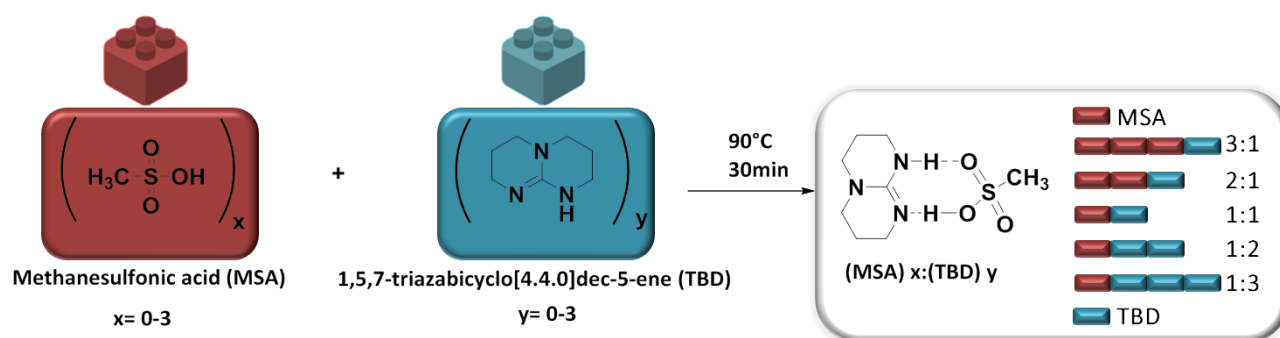
Figure 2.3. Scheme of the synthesis of the protic ionic compound (1:1) and the Non-Eutectic Mixute Organocatalysts (NEMOs).

The recorded spectra for pure TBD and MSA show the characteristic N-H proton signal of TBD at δ = 5.81 ppm and signal of MSA acid at δ = 14.16 ppm. In contrast, for the (1:1) mixture, these two signals disappear and a new one integrating for 2 protons appears at δ = 7.71 ppm, which demonstrates the formation of the Non-Eutectic Mixture Organocatalys (NEMO) by a proton transfer from MSA to TBD (Figure 2.4).
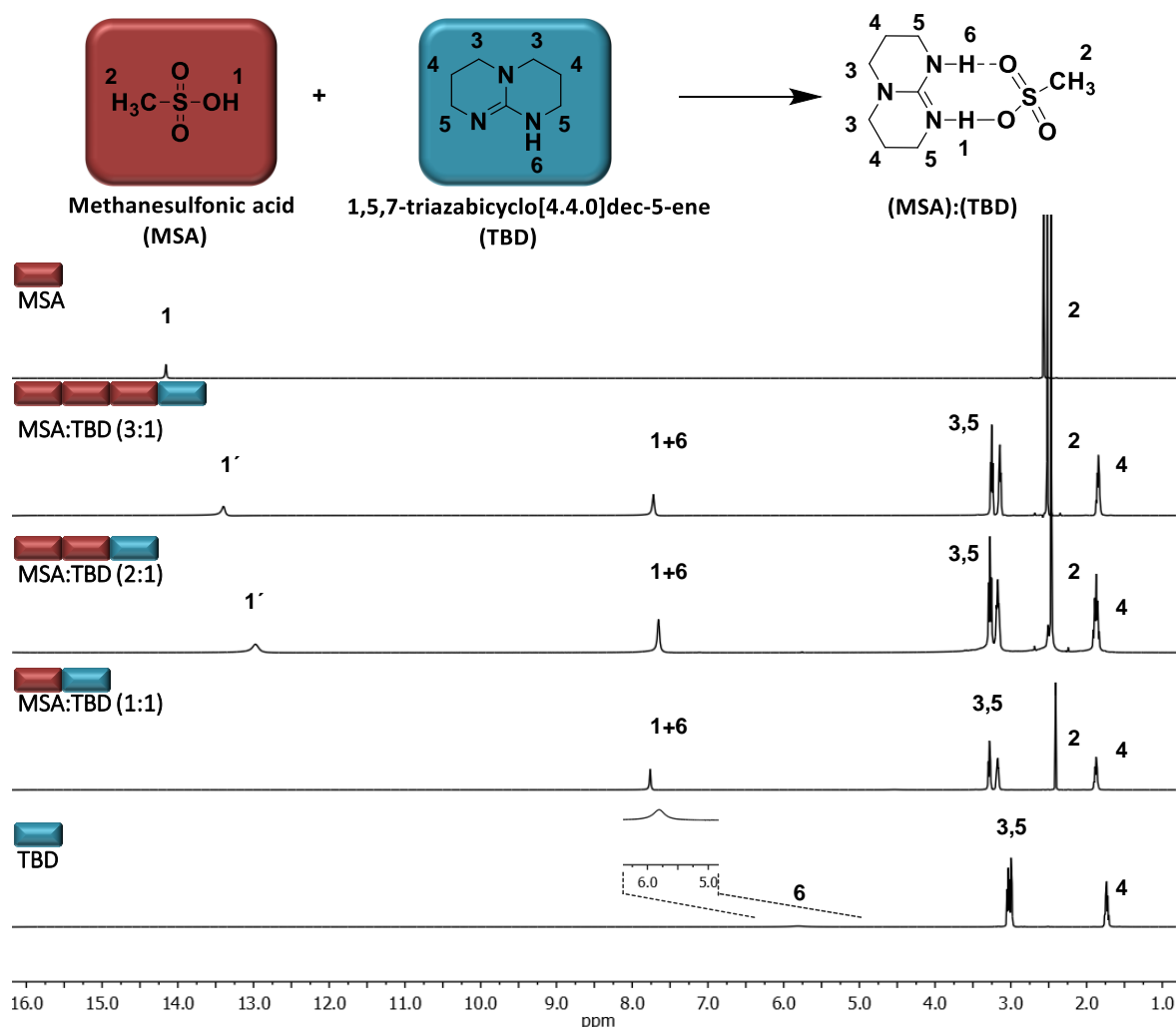

Figure 2.4.^{1}H NMR spectroscopy in DMSO of the different MSA:TBD stoichiometric and non-stoichiometric mixtures.

In the case of non-equimolar mixtures together with this band at 7.71 ppm we found the peak of the acid proton which was shifted to lower values (13.0 ppm and 13.5

ppm for the 2:1 and 3:1 mixtures, respectively). The appearance of this chemical shift in the ^{1}H NMR spectra of the mixtures as compared to those of the pure components confirms also the presence of H-bond complexes between non-equimolar mixtures of MSA and TBD (Figure 2.4).

To further understand the complex structures of the non-equimolar mixtures, the variable temperature ^{1}H NMR spectra of the 3:1 mixture were measured in its dry state (without DMSO solvent), and results are shown in Figure 2.5. At -10 °C, two peaks which were attributed to the acid proton of MSA (left side) and the N-H of the TBD (right side) can be clearly distinguished. The integrations of both peaks are roughly identical, suggesting that in this 3:1 mixture, one third of the MSA acid protons transferred to the TBD, forming a [TBD]$^+$[MSA]$^-$ complex. Whereas the remaining two thirds of MSA acid protons remain with the MSA molecules in the mixture.

Furthermore, an increase of temperature from -10 to 100 °C leads to a significant line broadening at first, then a gradual merging of both lines into a single broad line, and finally a narrowing of the single line.
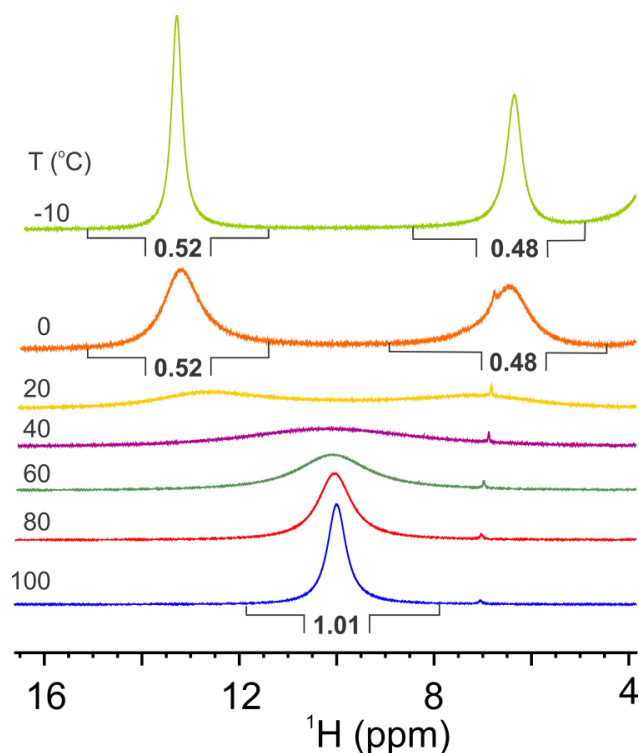
Figure 2.5. Varied temperature ^{1}H spectra of the labile proton region of the MSA:TBD 3:1 pure sample. The integrals were normalized by the area of the methyl group of the MSA (at around 2.0 ppm).

These variation of the proton line widths and positions with temperature is a typical feature and consequence of chemical exchange process between two proton spieces, and has been observed in many ionic liquids and other systems.[19,20] It is worth mentioning that, at 40 °C and above, the two proton peaks merged into a single peak, indicating that the proton exchange is fast enough to average out the environmental differences and the acid so that the N-H protons are equivalent.
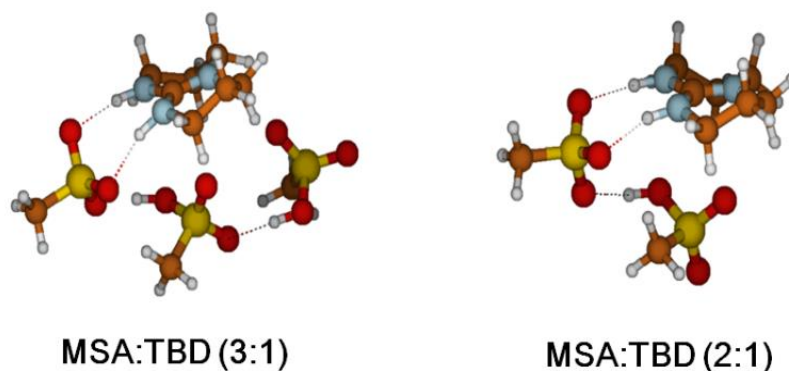
Figure 2.6. Calculated structures of MSA:TBD (2:1) and (3:1).

In order to get better insights into the molecular structures of MSA:TBD (2:1) and (3:1), both complexes have been investigated by means of quantum chemical calculations using ωB97XD/6-311++G(2df,2p) method and the resulting stable complexes are presented in Figure 2.6. Through these calculations, we found that in the case of a 2:1 complex, not only does one of the acidic proton of MSA_1 completely transfer to the basic nitrogen of TBD, thereby forming a hydrogen bond between the N-H moiety of TBD and one of the oxygen atoms of the sulfonyl group of MSA_1, but also that the acidic proton of MSA_2 forms a hydrogen bond with the sulfonyl group of MSA_1. These observations support the chemical shift of 1' (corresponding to the acidic proton of MSA) in the ^1H NMR spectra and occurs thanks to the dual character (nucleophilic & electrophilic) of organic acids.[21] Similar results were obtained for the 3:1 non-eutectic acid base complex, as MSA_3 is also joined to the complex through the transfer of its acidic proton to MSA_2. To further confirm the complex formation, the thermal-degradation profiles were studied by TGA (Figure 2.7).
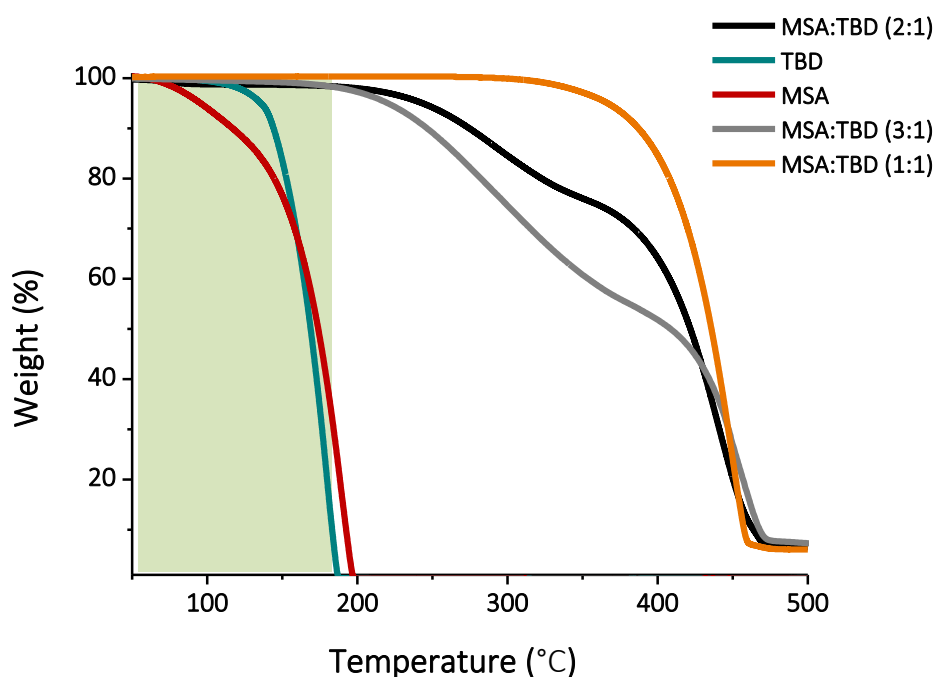
Figure 2.7. Thermogravimetric analysis of methanesulfonic acid (MSA), 1,5,7-triazabicyclo[4.4.0]dec-5-ene (TBD) and the acid base mixtures (3:1 , 2:1 and 1:1).

While TBD and MSA present a relatively low degradation temperature, with 50 % of the mass lost before 180 °C for both molecules (T50% = 170 °C for TBD and T50% = 174 °C for MSA), samples (2:1) and (3:1) show a two-step degradation profile at higher temperatures. A first deterioration of the catalysts start beyond 200°C, loosing 25 % of weight for (2:1) and 45 % for (3:1). Those losses could correspond to the releasing of one and two molecules of MSA for (2:1) and (3:1), respectively. Therefore, the second degradation event corresponds to the already reported decomposition of MSA:TBD (1:1) with T50% = 438 °C (Figure S3-S5).[15] These results revealed that the mixtures (3:1 and 2:1) were better resisting to temperature than MSA or TBD as individual components, which is in good agreement with the high dissociation energies encountered using DFT calculations of the Non-Eutectic Mixture Organocatalyst (NEMO) (Figure S3-S5). Finally, the TGA also represensent the particularly stable 1: 1 mixture which resists up to 300°C whithout any lose of weight.

2.2.2. Catalytic activity testing and optimization of the self-condensation temperature using 1,6-hexanediol

The different MSA:TBD organocatalysts were tested in the polyetherification of 1,6-hexanediol using 0.05 equiv. of organocatalyst at 180 °C under solvent free conditions (Figure 2.8, Table 2.1). The polymerizations were monitored using ^{1}H NMR, by the diagnostic disappearance of 1,6-hexanediol hydroxyl methylene protons (red signal at δ 3.65 ppm, adjacent to the alcohol) and their subsequent reappearance at δ 3.33 ppm due to ether formation (grey signal) (Figure 2.9).
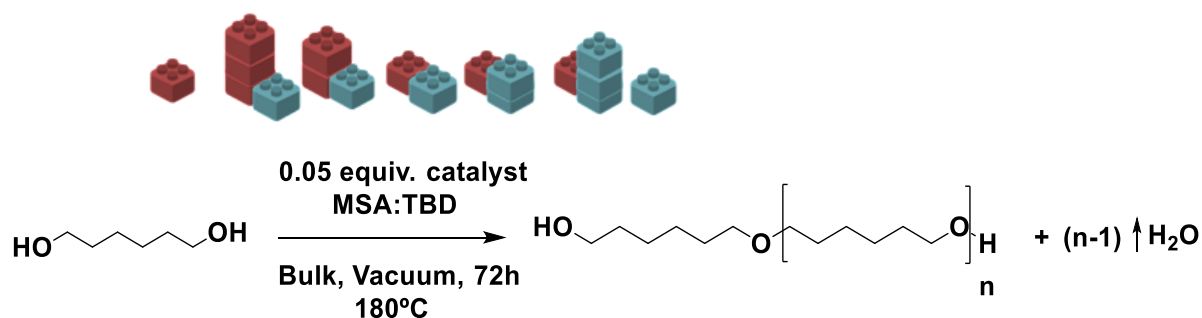
Figure 2.8. General scheme of the self-condensation reaction of 1,6-hexanediol catalyzed using different catalysts.
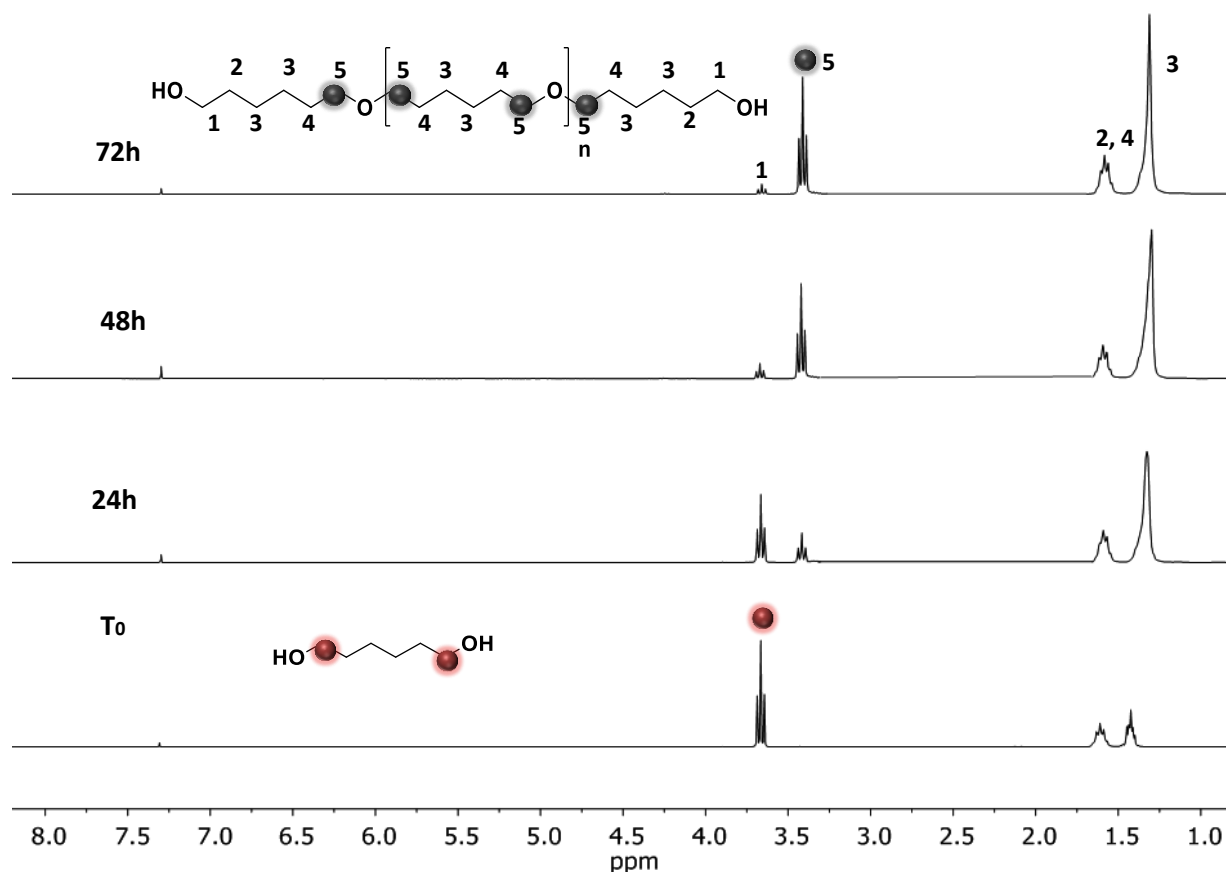
Figure 2.9. ^{1}H NMR spectra of the reaction medium during the course of the reaction. The proton signals distinguished with red and grey dots were used for the calculation of the monomer conversion.

As the molecular weights were relatively low, they were determined by NMR in order to compare all the samples as some of the samples were out of the detection limit of the SEC equipment. To do so, the polyether was end-capped with phenyl isocyanate not only to identify better the end-groups and to determine the molecular weight by NMR but also to confirm the presence of linear structures. As expected, the methylene protons adjacent to the capped alcohol shifted to higher ppm values ensuring the presence of alcohol end groups while no overlapping with internal ether groups are observed facilitating the molecular weight measurements (Figure S2.6).

The reaction was found to be dramatically catalyst dependent as it is observed in the Figure 2.10.
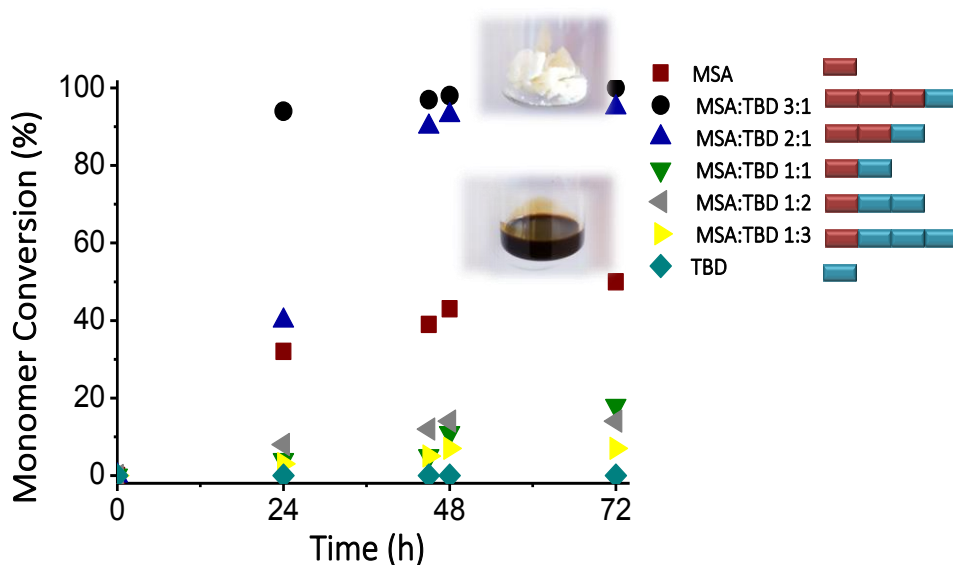

Figure 2.10. Monomer conversion values (%) at 24, 48 and 72h of reaction using different ratios of MSA:TBD as catalysts.

As expected, when pristine TBD alone was used no monomer conversion was observed (entry 1, Table 2.1). Meanwhile, when using pure MSA as catalyst the monomer conversion was 46 mol. % after 72 h (entry 2). This result confirms the catalytic activity of organic acids to mediate the self-condensation of alcohols. Nevertheless, in the presence of MSA the polymerization turned brownish. We believe that the harsh conditions required for the polymerization reaction leads to degradation of the MSA catalyst thereby preventing its catalytic action as was demonstrated by Jehanno et al. in a similar study.[15] Conversely, the NEMOs containing excess MSA (2:1 and 3:1) showed very efficient catalytic activity and monomer conversions above 95% were obtained resulting in polyether of 5,200 g mol^{-1} and 4,500 g mol^{-1} respectively (entries 3 and 4).

Table 2.1. Screened data of the optimization of the polyetherification of 1,6-hexanediol using different MSA:TBD catalytic mixtures at different temperatures.

Entry	MSA (equiv.)	TBD (equiv.)	Monomer/catalyst	Temperature/ °C	Mon. Conv (%)72h [a]	M_n (g mol^{-1})[a]	Yield.(%)[b]
1	-	1	1/0.05	180	0	-	--
2	1	-	1/0.05	180	50	900	29
3	3	1	1/0.05	180	97	5200	43
4	2	1	1/0.05	180	95	4500	39
5	1	1	1/0.05	180	18	--	--
6	1	2	1/0.05	180	14	--	--
7	1	3	1/0.05	180	7	--	--
8	3	1	1/0.05	130	80	1300	58
9	3	1	1/0.05	150	86	2400	61
10	3	1	1/0.05	*130-180	98	7000	73
11	3	1	1/0.05	**130-180-200	98	11300	84
12	3	1	1/0.05(recycled)	**130-180-200	97	10200	76

[a] Determined by ^{1}H NMR spectroscopy. [b] Isolated yield. *130 °C (24h) and 180 °C (48h) ** 130 °C (24h), 180 °C (24h) and 200 °C (24h).

Surprisingly, the obtained polymers were completely colorless suggesting that these two catalysts were not degraded during the polymerization process. In order to confirm the importance of acid excess in the polymerization two control experiments were run with excess of TBD (MSA:TBD ratios 1:2 & 1:3, respectively) (entry 6 and 7). We observed much lower monomer conversion (less than 20%) as such a reaction is known to be acid catalyzed.

In order to achieve high molecular weights, the influence of the temperature on the polymerization reaction was investigated. After screening different polymerization temperatures (entries 3, 8 and 9), we found that the highest molecular weights were obtained via polymerizing the 1,6-hexanediol at 180 °C (M_n = 5200 g mol^{-1}). While using lower temperatures i.e. 150 °C and 130°C, the attained molecular weights were substantially lower (2,400 and 1,300 g mol^{-1}, respectively). Nevertheless, we found that when running the polymerization at 180 °C the associated yield was lower in comparison to 150 °C and 130 °C due to the approach the boiling point of the monomer at the early hours of the polymerization process. In order to avoid monomer evaporation while polymerization was occurring, the polymerization was undertaken in various steps, mimicking the strategy used in other polycondensation processes such as PET or polycarbonates.[3] Thus the same reaction was carried out first at 130 °C for 24 h, after which the temperature was raised to 180 °C for 48 h. In this particular case, besides not observing any monomer evaporation during polymerization a higher molecular weight polyether (7,000 g mol^{-1}) was obtained (entry 10).

A further polymerization step at 200 °C for 24 h (entry 11) revealed an increase of the molar mass of the final polyether (11,300 g mol^{-1}) while maintaining high polymerization yields. Herein, the gradual increase of the temperature from 130 °C to 200 °C enables us to avoid the losses of monomer achieving higher yields and molecular weights (Figure 2.11). Further increase of temperature and time did not significantly alter the molecular weights or the polymerization yields.
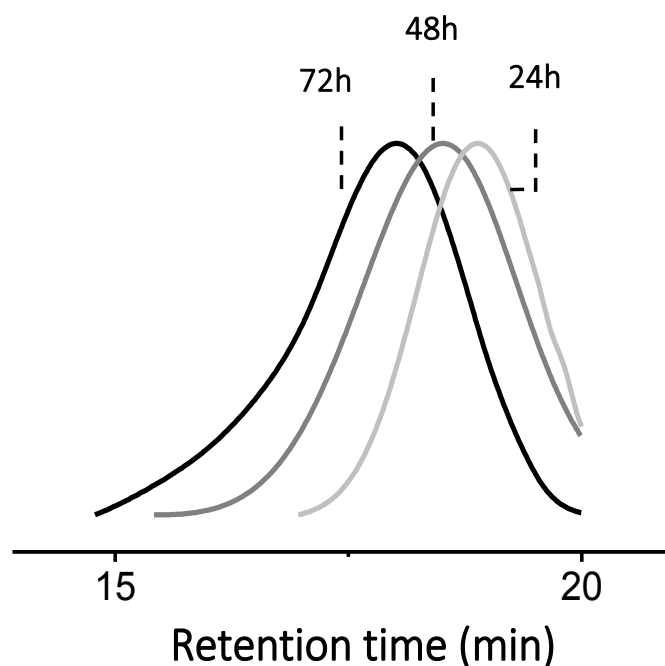
Figure 2.11. SEC chromatograms recorded after 24h, 48h and 72h.

After screening several polymerization conditions, it was found that the best results in terms of molecular weight and conversions were obtained via a multi-step polymerization process (the first one at 130 °C for 24h, a second one at 180 °C for 24 h and a third one at 200 °C for 24 h) in the presence of 5 mol % of MSA:TBD (3:1) catalyst. In order to make the process even more sustainable, we intended to recycle the organocatalyst from the polymer and re-used it in another polymerization. The catalyst was recovered near quantitatively from the polymer mixture during the purification process (90 %). To recover the catalyst, the polymer-catalyst mixture was dissolved in chloroform and precipitated in cold methanol where the entire polymer was precipitated. The catalyst containing filtrate was concentrated and recrystrallized from hexane to afford the initial catalyst (verified by ^{1}H NMR, Figures S2.8 and S2.9). The catalyst was reused again (entry 12) confirming its potential to be recovered as

the obtained polymer has similar molecular weights than using freshly prepared catalysts (entry 11, Figure S2.9).

Interestingly, the reaction could be performed in 200 g scale without suffering any color change and similar yield and molecular weights due to the high stability of the organcatalyst as shown in the picture of the polyether obtained in Figure 2.12.
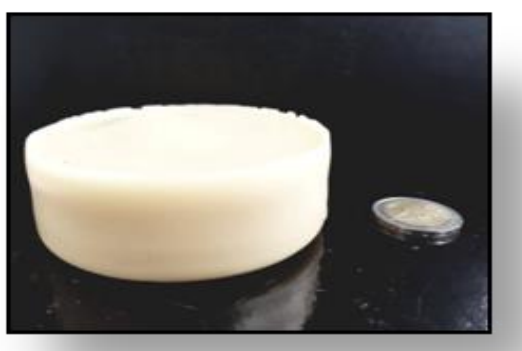

Figure 2.12. 200 g scale poly(oxyhexamethylene).

2.2.3. Synthesis of aliphatic polyethers with different number of methylene units

In order to expand the polymerization scope, NEMOs were investigated for the homopolymerization of a series of aliphatic diols with various number of methylene units. For this purpose, we investigated the homopolymerization of 8 different diols to synthesize the corresponding polyethers. Thus, 1,4-butanediol, 1,5-pentanediol, 1,7-heptanediol, 1,8-octanediol, 1,9-nonanediol, 1,10-decanediol, 1,11-undecanediol and 1-12-dodecanediol, were polymerized under the optimized conditions previously described for 1,6-hexanediol (Figure 2.13).
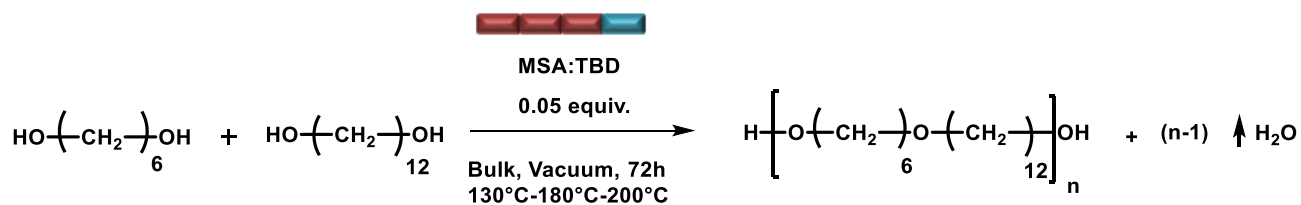
Figure 2.13. Synthesis route of the aliphatic polyethers from different aliphatic diols.

The polymerizations of diols having methylene units from 6 to 12 were confirmed using ^{1}H NMR, ^{13}C NMR and SEC (Figure S2.10-S2.18 and Table 2.2). The ^{1}H NMR results were similar for all the polyethers, obtaining high conversion in all cases. Regarding SEC results, the polyethers had molecular weights between 5000 to 22000 g mol^{-1} and the dispersity values obtained were between 1.9 and 2.5, values that are slightly high for polycondensation reactions.

Although all polymerizations were similar, there is a discret trend between the number of the methylene units and the molecular weight. The polymerization was not successful in the cases of 1,4-butanediol and 1,5-pentanediol. The ^{1}H NMR spectra obtained from the self-condensation of 1,5-pentanediol revealed that no signal attributed to the ending group expected at δ = 3.65 ppm was observed, and only the signal of the protons attributed to the signal adjacent to the ether bound was observed (Figure S2.19).

Table 2.2. Characterization data of the homopolymers synthesized from different aliphatic diols in the presence of 0.05 equiv of MSA:TBD (3:1) catalyst at 130–200 °C.

Monomer	M_n (g mol^{-1})^a	Đ ^{a}	Yield (%)^b	T_m (°C) ^{c}	ΔH_m (J/g) ^{c}	2θ ^{d}	d(nm) ^{d}
1,6-hexanediol	22 000	1.9	70	54.9	83	13.11	0.451
						16.04	0.369
1,7-heptanediol	8 000	2.3	57	65.5	134	14.49	0.408
						15.9	0.372
1,8-octanediol	18 000	2.4	76	67.9	125	13.06	0.453
						15.96	0.370
1,9-nonanediol	9 500	2.5	68	75.6	147	14.38	0.411
						16.04	0.369
1,10-decanediol	8 500	2.5	72	80.4	142	14.38	0.411
						16.03	0.369
1,11-undecanediol	8 000	2.3	79	81.9	138	14.39	0.411
						16.04	0.369
1,12-dodecanediol	5000	2.5	84	84.7	166	14.38	0.411
						16.01	0.369

^{a} Determined by SEC in CHCl$_3$, ^{b} Isolated yield , ^{c} Measured by DSC, ^{d} Obtained by WAXS.

This event suggests that cyclic ethers were obtained instead of linear polymers as it was also reported by Fadret et al. This fact could be associated with the ability of small diols to promote intramolecular etherification giving rise to highly stable 5 and 6 membered cyclic ethers which were removed by the high-vacuum conditions instead of the polyetherification reaction.[14] As previously indicated, the molecular weight decreased with the number of methylene units in the repeating unit. We believe that this fact could be attributed to the higher viscosity of the systems as the number of methylene units increases limiting the diffusion of the water and decreasing the molecular weight.

This has been recently reported in the polycondensation of aliphatic carbonates.[3] To exclude the possible cycle formation, MALDI-TOF analysis were performed and only a

telechelic polymer end-capped with alcohol linear species were detected separated by 100 g mol^{-1} (molecular weight of the poly(oxyhexamethylene) repeating unit), attesting the presence of linear species (Figure 2.14).
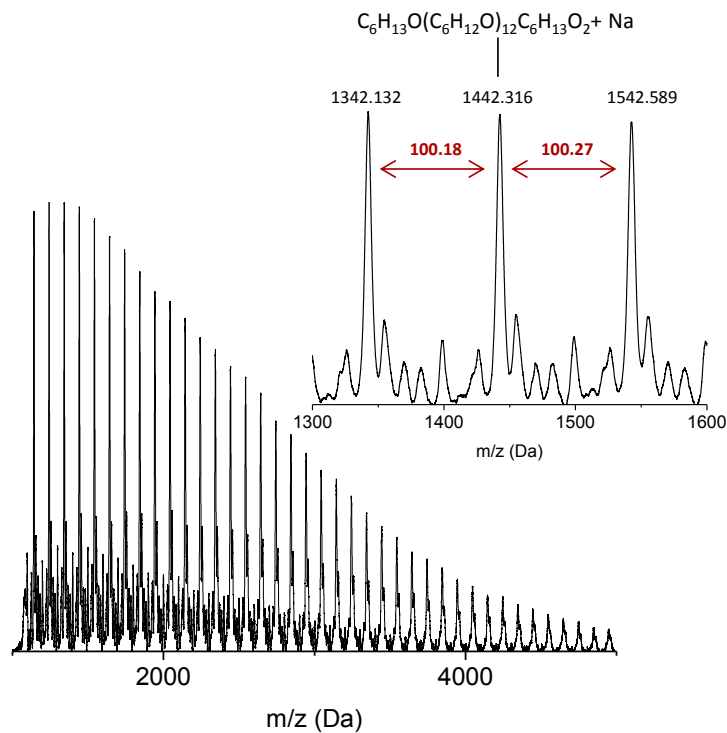

Figure 2.14. MALDI-TOF result of poly(oxyhexamethylene).

The thermal characteristics of the different aliphatic polyethers were measured by DSC (Figure 2.15a). From DSC curves, the melting (T_m) and crystallization temperatures (T_c, Figure S2.20) were determined for all samples. At a first glance, the results revealed that all polyethers were semicrystalline showing T_m values between 54 and 85 °C. All thermal transitions are function of the number of methylenic units along the chain. As the aliphatic chain increases in length (i.e., the number of CH_2 units increases in the chains), the first order thermal transitions of crystallization and melting increase in temperature. At the same time, the latent heats of enthalpy and fusion also increase slightly with the number of methylenic units along the repeating unit of the polyether

chains. On the other hand, due to the high degree of crystallinity in these aliphatic polyethers T_g determinations by DSC were not possible.
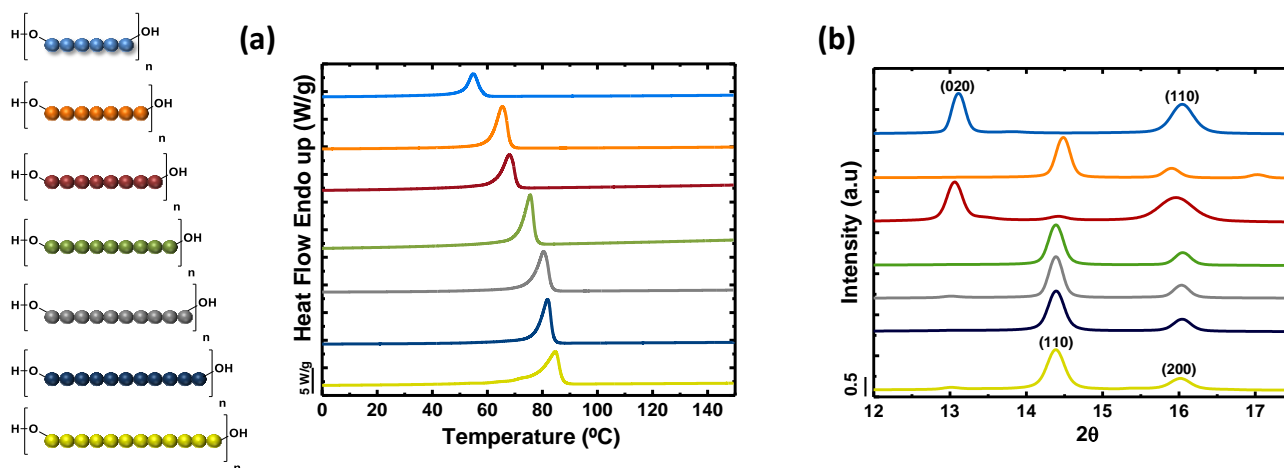
Figure 2.15. a) DSC heating scans of the linear polyethers and b) WAXS diffraction patterns at 25 °C.

The crystal structure of the prepared polyethers was examined by WAXS performed at the synchrotron with a wavelength of 1.0 Å. X-ray diffraction measurements showed that polyethers with 6 and 8 methylene units have a different crystal structure in comparison to polyethers with 7, 9, 10, 11 and 12 methylene units (Figure 2.15b). On the polyether series with 6 and 8 methylene units, very strong (020) and strong (110) reflections are observed at 2θ values of 13.1 ° and 16 °, respectively, which correspond to monoclinic unit cells, similar to the ones reported for polytetrahydrofuran.[13] For polyethers with 9 to 12 methylene units, the crystalline structure is completely different and the reflections associated with (110) and (200) plans appeared at 2θ values of 14.3 ° and 16 ° respectively which are closely similar to the ones reported for the orthorhombic polyethylene unit cell. In the case of poly(oxyheptamethylene) the crystalline form is not related to either of these previous two structures, however its lateral molecular arrangement is quite similar to orthorhombic polyethylene. Table 2.2 shows the diffraction spacings (d) calculated according to Bragg´s Law. These results

are consistent with the crystalline structures reported for polyethers with identical chemical structures but synthesized by different methods.[13]

2.2.4. Synthesis of aliphatic copolyethers and polyether thermosets

In order to broaden the described strategy, copolymerization between different diols was also considered. The synthesis of random copolymers is a good way to modulate the properties and the architecture of homopolymers through selecting functional monomers or varying the copolymer composition.[14,22]

Thus, diols with different length (1,6-hexanediol and 1,12-dodecanediol) were copolymerized in a 50/50 molar ratio and 1,6 hexanediol was also copolymerized with an alcohol with multiple functionalities such as glycerol. The copolyethers were synthetized under the previously reported conditions (Figure 2.16a and b). The copolymer 1,6/1,12 was purified and characterized by ^{1}H NMR spectroscopy (Figure 2.17c). The polyether formation was confirmed by the appearance of the signal 1 at δ = 3.40 ppm attributed to the ether linkage (-CH$_2$-O-CH$_2$-). The molar composition of the copolyether was determined by ^{1}H NMR according to the equation presented in the Experimental Section.
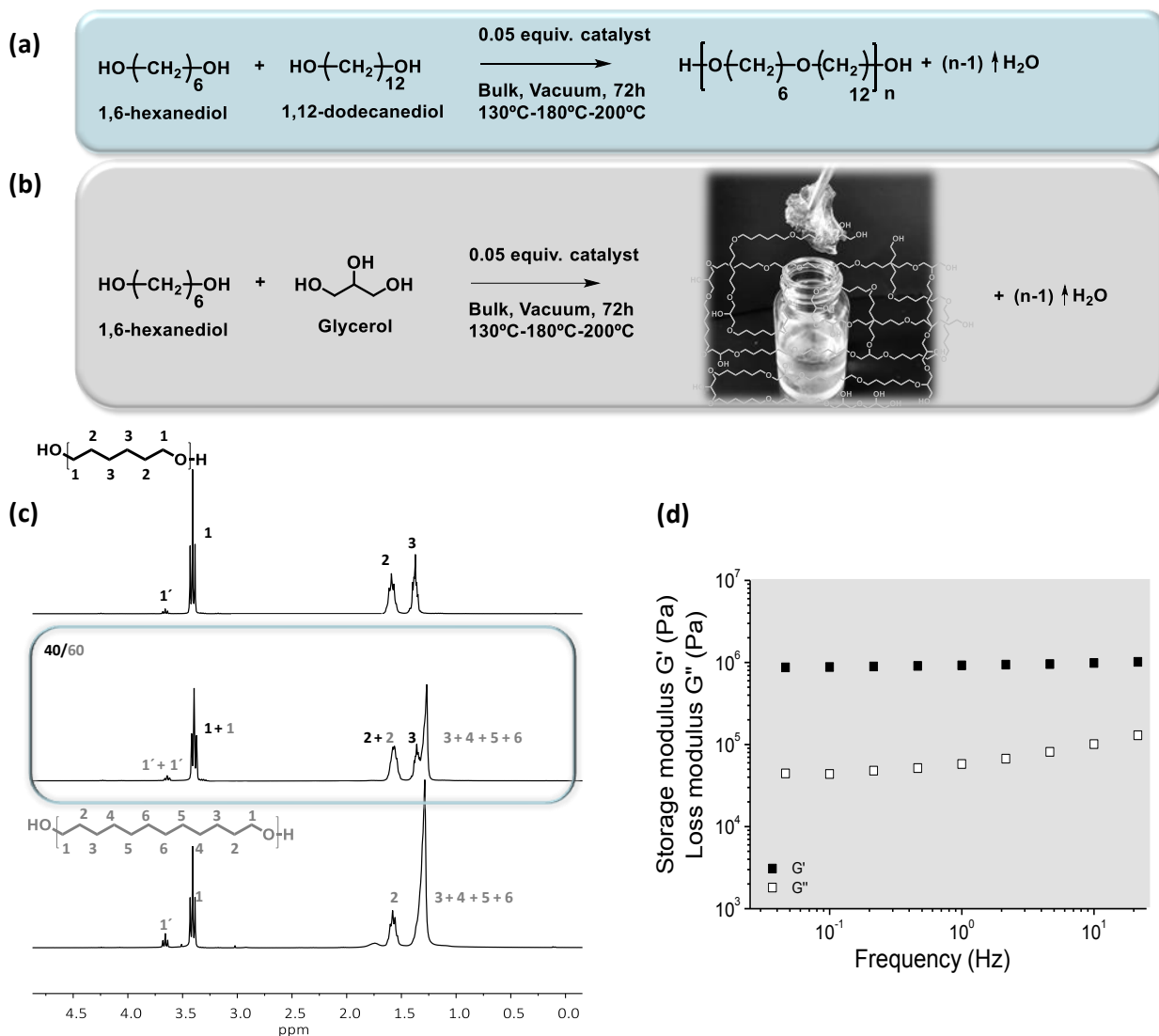
Figure 2.16. Synthesis route of random copolyethers from a) 1,6-hexanediol and 1,12-dodecanediol, b) 1,6-hexanediol and glycerol, c) ^{1}H NMR spectra of poly(oxyhexamethylene), copolyether 1,6/1,12 40/60, and poly(oxydodecamethylene) and d) dynamic mechanical analysis of the polyether thermosets.

We found that the copolymer composition of 1,6-hexanediol/1,12-dodecanediol resulted in 40/60 mol %. This composition differed slightly from the initial feed probably due to partial evaporation of the 1,6-hexanediol during the copolymerization. The copolymer was also characterized by ^{13}C NMR spectroscopy and the presence of dyads in the copolymer chain was observed (Figure S2.21). The

molecular weight and dispersities of the copolymer determined by SEC analysis was similar to the ones of the homopolymers, *i.e.* a M_n of 9800 g mol^{-1} with a Đ of 2.3.

When 1-6-hexanediol was copolymerized with glycerol a cross-linked unsoluble polymer was obtained. Due to the three hydroxy groups of glycerol and the high % of glycerol used in the feed, polyether thermosets were obtained in this case. In order to confirm the polyether formation, FT-IR spectra of the resulting unsoluble polymer was acquired (Figure S2.22). The broad peak around 3000 cm^{-1}, attributed to the –OH stretching from the hydroxyl group significantly reduced its intensity which demonstrates that the self-condensation is ocurring. Whereas a new band characteristic to the C-O-C stretching vibration at 1050 cm^{-1} appreared confirming the formation of ether bonds. The gel formation was confirmed by frequency sweep experiments in compression mode. As observed in Figure 2.16c, the material shows a predominant elastic behaviour (G' > G'') with an elastic modulus value G'~106 Pa. In addition, both G' and G'' values were independent of frequency, as it corresponds to a chemically cross-linked networks. This cross-linked polyether is represented in the image of the Figure 2.16b.

2.3. Conclusion

Polyethers constitute a well-established class of polymers covering a wide range of applications from industrial manufacturing to nanomedicine. Nevertheless, their industrial implementation is limited to short chain aliphatic polyethers such as polyethyleneglycol (PEO or PEG), polypropyleneglycol (PPG) or polytetramethyleneglycol (PTMG) produced by the ring-opening polymerization of the corresponding cyclic ethers. In this chapter we reported a bulk polycondensation method at relatively high temperature and using simple and recyclable organocatalysts

for the production of aliphatic polyethers of medium and large number of methylene units. The molecular structure of the NEMO formed between the non-equimolar mixtures of MSA:TBD were characterized using ^{1}H NMR confirming the presence of a unique compound. This fact was confirmed using DFT calculations. Furthermore, under optimized conditions a series of polyethers with different molecular weights from diols with 6 to 12 methylene units were polymerized using the NEMO MSA:TBD 3:1. Semicrystalline polyethers with molecular weights between 5000 and 22000 g mol^{-1} were obtained. The polyethers showed melting temperatures between 55 and 85 °C which increased with the number of methylene units. Two types of crystal structures were found, the monoclinic polytetrahydrofuran type (for 6 and 8 methylene units) and the orthorhombic polyethylene type (for 7, 9, 10, 11 and 12 methylene units). Moreover, we expanded the self-condensation for the preparation of added value copolymers from different chain length diols and different functionalities, giving rise to different copolymer architectures from linear copolyethers to polyether thermosets. This economic and sustainable synthesis strategy reveals a green potential approach to produce polyethers, copolyethers and thermosets, which could be applied from low temperature thermosets to new soft segments for polyurethane chemistry.

2.4. Experimental Section

2.4.1 Materials

1,12-Dodecanediol (99%, Sigma-Aldrich), 1,11-undecanediol (98%, ABCR), 1,10-decanediol (98%, Sigma Aldrich), 1,9-nonanediol (98%, Sigma-Aldrich), 1,8-octanediol (98%, Sigma-Aldrich), 1,7-heptanediol (95%, Sigma-Aldrich), 1,6-hexanediol (99% Sigma-Aldrich), 1,5-pentanediol (96% Sigma-Aldrich) and 1,4-butanediol (99% Sigma-Aldrich) were used as received after being dried in toluene. Methanesulfonic acid

(MSA, 99%) and 1,5,7-triazabicyclo[4.4.0]dec-5-ene (TBD, 98%), glycerol (99%) phenyl isocyanate (98%), chloroform (CHCl$_3$), methanol (CH$_3$OH) and the rest of the solvents used on this work were supplied by Sigma-Aldrich and used as received.

2.4.2 Preparation of the catalyst mixtures

Different dual catalysts were prepared by mixing methanesulfonic acid (MSA) and 1,5,7-triazabicyclo[4.4.0]dec-5-ene (TBD) at different molar ratios; 3:1 (0.100 g, 1.04 10^{-3} mol of MSA and 0.048 g, 3.46 10^{-4} mol of TBD), 2:1 (0.090 g, 9.36 10^{-4} mol of MSA and 0.065 g, 4.67 10^{-4} mol of TBD), 1:1 (0.070 g, 7.27 10^{-4} mol of MSA and 0.101 g, 7.27 10^{-4} mol of TBD), 1:2 (0.040 g, 4.16 10^{-4} mol of MSA and 0.116 g, 8.33 10^{-4} mol of TBD), 1:3 (0.030 g, 3.12 10^{-4} mol of MSA and 0.130 g, 9.35 10^{-4} mol of TBD).. Afterwards, the mixtures were thermally treated at 90 °C over 30 minutes under stirring until complete formation of homogeneous and transparent liquid solution or salt.

2.4.3 Bulk Self-condensation of 1,6-hexanediol using the catalyst mixtures

The different MSA:TBD complexes were tested in the self-condensation of 1,6-hexanediol. For that 0.05 equiv. (5 mol %, 7.45 10^{-4} mol) of previously prepared protic ionic salt and Non-Eutectic Mixture Organocatalys (NEMO) were mixed with 1.760 g (0.015 mol) of 1,6-hexanediol in a 25 ml Schlenk tube with a magnetic stirrer. The sealed reaction vessel was submerged into a pre-heated oil bath at 180 °C (72 h) under vacuum. The reaction was stopped by rapid cooling in liquid nitrogen. For the purification, the samples were dissolved in chloroform and precipitate in cold methanol. The resulted polyethers were filtrated and dried under vacuum at RT for 24 h before their characterization.

The synthesis of the ≈200 g of polyether was carried out in a 500 ml reactor using an electrical stirrer. For that 200 g of 1,6-hexanediol (1.692 mol) was mixed with a 0.05 equiv. (5 mol %) of previously prepared NEMO 3:1 (0.084 mol, 9.044 g). The reactor was submerged into a pre-heated oil bath at 130 °C (24 h), 180 °C (24 h) and 200 °C (24 h) under vacuum. The reaction was stopped by rapid cooling in liquid nitrogen.

2.4.4 Catalyst recycling

The reaction was carried out mixing 0.05 equiv. (5 mol %, 7.45 10^{-4} mol, 0.080 g) of the NEMO MSA:TBD 3:1 with 1.760 g (0.015 mol) of 1,6-hexanediol in bulk. After performing the polymerization the polymer-catalyst mixture was dissolved in chloroform and precipitated in cold methanol where the entire polymer was precipitated. The catalyst containing filtrate was concentrated and recrystallized from cold hexane to afford the initial catalyst (which was verified by ^{1}H NMR) (93 % yield). The catalyst was reused again to confirm its potential to be recycled.

2.4.5 Bulk Self-condensation of different aliphatic diols

The self-condensation of the diols were accomplished using as catalyst the NEMO formed by the molar mixture of MSA:TBD 3:1. For that, 0.05 equiv. (5 mol %) of MSA:TBD 3:1 (7.45 10^{-4} mol, 0.080g) was mixed with 0.015 mol of the corresponding diol (3.013 g of 1,12-dodecanediol, 2.805 g of 1,11-undecanediol, 2.596 g of 1,10-decanediol, 2.387 g of 1,9-nonanediol, 2.178 g of 1,8-octanediol, 1.969 g of 1,7-heptanediol and 1.760 g of 1,6-hexanediol) in a the Schlenk flask with a magnetic stirrer. The sealed reaction vessel was submerged into a pre-heated oil bath at 130 °C (24 h), 180 °C (24 h) and 200 °C (24 h) under vacuum. The reaction was stopped by rapid cooling in liquid nitrogen.

For the purification, the samples were dissolved in chloroform and precipitated in cold methanol. The resulted polyethers were filtrated and dried under vacuum at RT for 24 h before their characterization.

2.4.6 Calculations of the copolymer molar composition

The molar composition of the copolyether was determined by ^{1}H NMR spectroscopy. It was determined as the integral area ratio of the signals designated in the Figure 2.17c according to the following equation:

$$\frac{X1,6}{X1,12} = \frac{I_3}{I_3 + I_{3+4+5+6}} \qquad (1)$$

Where X1,6 AND X1,12 are the molar fraction of 1,6-hexanediol and 1,12-dodecanediol units, respectively (50/50). I_3 and $I_{3+4+5+6}$ are the integral intensities of the corresponding peaks in the spectra.

2.5. References

(1) Klein, R.; Wurm, F. R. Aliphatic Polyethers: Classical Polymers for the 21st Century. *Macromol. Rapid Commun.* **2015**, *36* (12), 1147–1165. https://doi.org/10.1002/marc.201500013.

(2) Alkattan, M.; Prunet, J.; Shaver, M. P. Functionalizable Stereocontrolled Cyclopolyethers by Ring-Closing Metathesis as Natural Polymer Mimics. *Angew. Chem. Int. Ed.* **2018**, *57* (39), 12835–12839. https://doi.org/10.1002/anie.201805113.

(3) Meabe, L.; Lago, N.; Rubatat, L.; Li, C.; Müller, A. J.; Sardon, H.; Armand, M.; Mecerreyes, D. Polycondensation as a Versatile Synthetic Route to Aliphatic

Polycarbonates for Solid Polymer Electrolytes. *Electrochimica Acta* **2017**, *237*, 259–266. https://doi.org/10.1016/j.electacta.2017.03.217.

(4) Engels, H.-W.; Pirkl, H.-G.; Albers, R.; Albach, R. W.; Krause, J.; Hoffmann, A.; Casselmann, H.; Dormish, J. Polyurethanes: Versatile Materials and Sustainable Problem Solvers for Today's Challenges. *Angew. Chem. Int. Ed.* **2013**, *52* (36), 9422–9441. https://doi.org/10.1002/anie.201302766.

(5) Knop, K.; Hoogenboom, R.; Fischer, D.; Schubert, U. S. Poly(ethylene Glycol) in Drug Delivery: Pros and Cons as Well as Potential Alternatives. *Angew. Chem. Int. Ed.* **2010**, *49* (36), 6288–6308. https://doi.org/10.1002/anie.200902672.

(6) Perry, S.; Hibbert, H. Studies on Reactions Relating to Carbohydrates and Polysaccharides. LXI. The Mechanism of Polymerization of Ethylene Oxide [1]. *J. Am. Chem. Soc.* **1940**, *62* (10), 2599–2604. https://doi.org/10.1021/ja01867a005.

(7) Vandenberg, E. J. Organometallic Catalysts for Polymerizing Monosubstituted Epoxides. *J. Polym. Sci.* **1960**, *47* (149), 486–489. https://doi.org/10.1002/pol.1960.1204714947.

(8) Dreyfuss, M. P.; Dreyfuss, P. A "living" Polymer after Cationic Initiation. *Polymer* **1965**, *6* (2), 93–95. https://doi.org/10.1016/0032-3861(65)90018-2.

(9) Uhrich, K. E.; Hawker, C. J.; Frechet, J. M. J.; Turner, S. R. One-Pot Synthesis of Hyperbranched Polyethers. *Macromolecules* **1992**, *25* (18), 4583–4587. https://doi.org/10.1021/ma00044a019.

(10) Dannecker, P.-K.; Biermann, U.; von Czapiewski, M.; Metzger, J. O.; Meier, M. A. R. Renewable Polyethers via GaBr3-Catalyzed Reduction of Polyesters. *Angew. Chem. Int. Ed.* **2018**, *57* (28), 8775–8779. https://doi.org/10.1002/anie.201804368.

(11) Bossion, A.; Heifferon, K. V.; Meabe, L.; Zivic, N.; Taton, D.; Hedrick, J. L.; Long, T. E.; Sardon, H. Opportunities for Organocatalysis in Polymer Synthesis via Step-

Growth Methods. *Prog. Polym. Sci.* **2019**, *90*, 164–210. https://doi.org/10.1016/j.progpolymsci.2018.11.003.

(12) Rhoad, M. J.; Flory, P. J. The Synthesis of Polymeric Ethers. *J. Am. Chem. Soc.* **1950**, *72* (5), 2216–2219. https://doi.org/10.1021/ja01161a096.

(13) Kobayashi, S.; Tadokoro, H.; Chatani, Y. Structural Studies on Polyethers, [-(CH2)m-O-]n. VI. The Higher Members with M = 6–10, 12. *Makromol. Chem.* **1968**, *112* (1), 225–241. https://doi.org/10.1002/macp.1968.021120120.

(14) Zhang, S.; Féret, A.; Lefebvre, H.; Tessier, M.; Fradet, A. Poly(oxyalkylene) Synthesis in Brønsted Acid Ionic Liquids. *Chem. Commun.* **2011**, *47* (39), 11092–11094. https://doi.org/10.1039/C1CC14162G.

(15) Jehanno, C.; Flores, I.; Dove, A. P.; Müller, A. J.; Ruipérez, F.; Sardon, H. Organocatalysed Depolymerisation of PET in a Fully Sustainable Cycle Using Thermally Stable Protic Ionic Salt. *Green Chem.* **2018**, *20* (6), 1205–1212. https://doi.org/10.1039/C7GC03396F.

(16) Flores, I.; Demarteau, J.; Müller, A. J.; Etxeberria, A.; Irusta, L.; Bergman, F.; Koning, C.; Sardon, H. Screening of Different Organocatalysts for the Sustainable Synthesis of PET. *Eur. Polym. J.* **2018**, *104*, 170–176. https://doi.org/10.1016/j.eurpolymj.2018.04.040.

(17) Flores, I.; Etxeberria, A.; Irusta, L.; Calafel, I.; Vega, J. F.; Martínez-Salazar, J.; Sardon, H.; Müller, A. J. PET-Ran-PLA Partially Degradable Random Copolymers Prepared by Organocatalysis: Effect of Poly(l-Lactic Acid) Incorporation on Crystallization and Morphology. *ACS Sustain. Chem. Eng.* **2019**, *7* (9), 8647–8659. https://doi.org/10.1021/acssuschemeng.9b00443.

(18) García-Argüelles, S.; García, C.; Serrano, M. C.; Gutiérrez, M. C.; Ferrer, M. L.; Monte, F. del. Near-to-Eutectic Mixtures as Bifunctional Catalysts in the Low-Temperature-Ring-Opening-Polymerization of ε-Caprolactone. *Green Chem.* **2015**, *17* (6), 3632–3643. https://doi.org/10.1039/C5GC00348B.

(19) Kelly, J. T.; Knorke, H.; Asmis, K. R. Isolating the Isomeric Hydrogen Bonding Signatures of the Cyanide–Water Complex by Cryogenic Ion Trap Vibrational Spectroscopy. *J. Phys. Chem. Lett.* **2017**, *8* (21), 5349–5354. https://doi.org/10.1021/acs.jpclett.7b02263.

(20) Yang, H.; Zhang, J.; Li, J.; Jiang, S. P.; Forsyth, M.; Zhu, H. Proton Transport in Hierarchical-Structured Nafion Membranes: A NMR Study. *J. Phys. Chem. Lett.* **2017**, *8* (15), 3624–3629. https://doi.org/10.1021/acs.jpclett.7b01557.

(21) Sardon, H.; Engler, A. C.; Chan, J. M. W.; García, J. M.; Coady, D. J.; Pascual, A.; Mecerreyes, D.; Jones, G. O.; Rice, J. E.; Horn, H. W.; et al. Organic Acid-Catalyzed Polyurethane Formation via a Dual-Activated Mechanism: Unexpected Preference of N-Activation over O-Activation of Isocyanates. *J. Am. Chem. Soc.* **2013**, *135* (43), 16235–16241. https://doi.org/10.1021/ja408641g.

(22) He, J.; Burt, S. P.; Ball, M.; Zhao, D.; Hermans, I.; Dumesic, J. A.; Huber, G. W. Synthesis of 1,6-Hexanediol from Cellulose Derived Tetrahydrofuran-Dimethanol with Pt-WOx/TiO2 Catalysts. *ACS Catal.* **2018**, *8* (2), 1427–1439. https://doi.org/10.1021/acscatal.7b03593.

(23) Frisch, M.; Trucks, G.; Schlegel, H.; Scuseria, G.; Robb, M.; Cheeseman, J.; Scalmani, G.; Barone, V.; Mennucci, B.; Petersson, G.; et al. *Gaussian 09, Revision B.01*; 2009.

Chapter 3

Graphical abstract

NEMO

$H_3C-S(=O)(=O)-OH$

1.Copolymerization

$HO-(CH_2)_6-OH$ **+** $HO-(CH_2)_{12}-OH$ $\longrightarrow$ $H-[O-(CH_2)_6-O-(CH_2)_{12}]_n-OH$

BULK 200°C

2.Thermal properties

Isomorphism

T_m

Temperature (°C)

Comonomer content (wt%.)
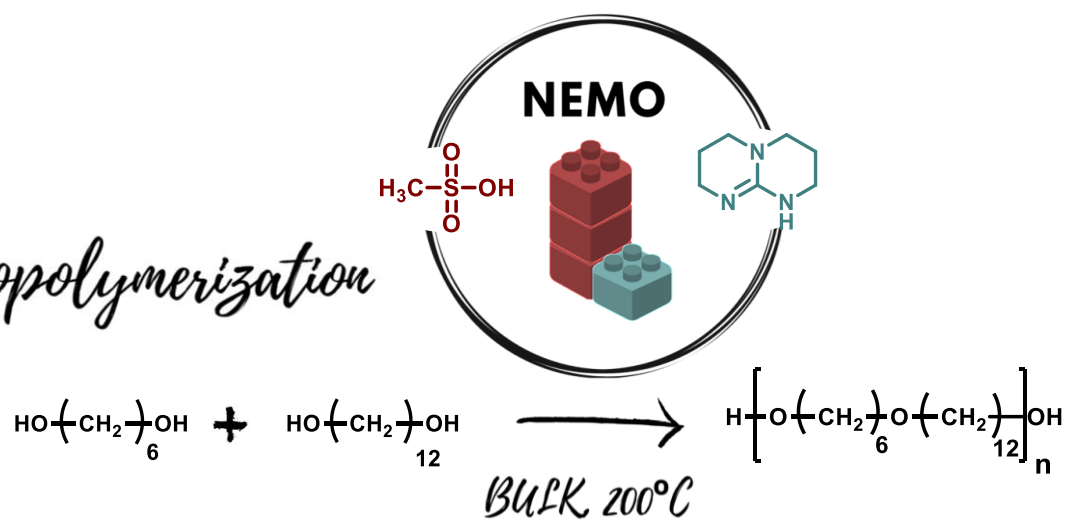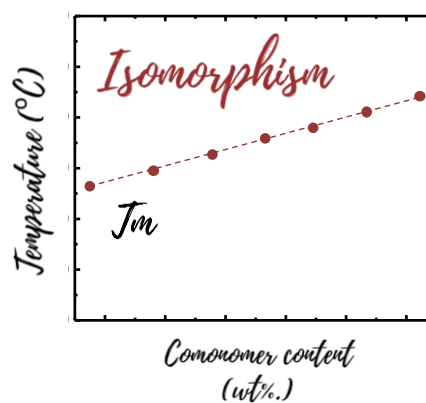
Chapter 3. Isomorphic polyoxyalkylene copolyethers obtained by the self-condensation of 1,6-hexanediol and 1,12-dodecanediol

3.1. Introduction

In the previous chapter, we explored an easy synthesis process of medium-to-long chain aliphatic homopolyethers by the bulk self-condensation of alcohols in the presence of a noneutectic mixture organocatalyst (NEMO) based on methanesulfonic acid (MSA) and 1,5,7-triazabicyclo[4.4.0] dec-5-ene (TBD) (3:1).[1] As a result, highly semicrystalline polyoxyalkylenes with a number of methylene units in the repetitive units ranging from 6 to 12 were obtained. Polyoxyalkylene homopolymers presented semicrystalline behavior showing T_m values between 54 and 85 °C as a function of the number of methylene units along the chain. Furthermore, in a first demonstration, the synthetic approach probed to have potential as a simple way to prepare a series of random copolymers by using different aliphatic diols.

Generally speaking, there are three different manners in which random copolymers could crystallize depending on the exclusion/inclusion balance or, in other words, on the possibility of cocrystallization.[2] These three typical cases are represented in the Figure 3.1: (a) Isomorphims. When comonomeric units can cocrystallize and share a single crystalline unit cell and comonomer exclusion during crystallization never occurs. (b) Total exclusion of second comonomer units in the crystals.
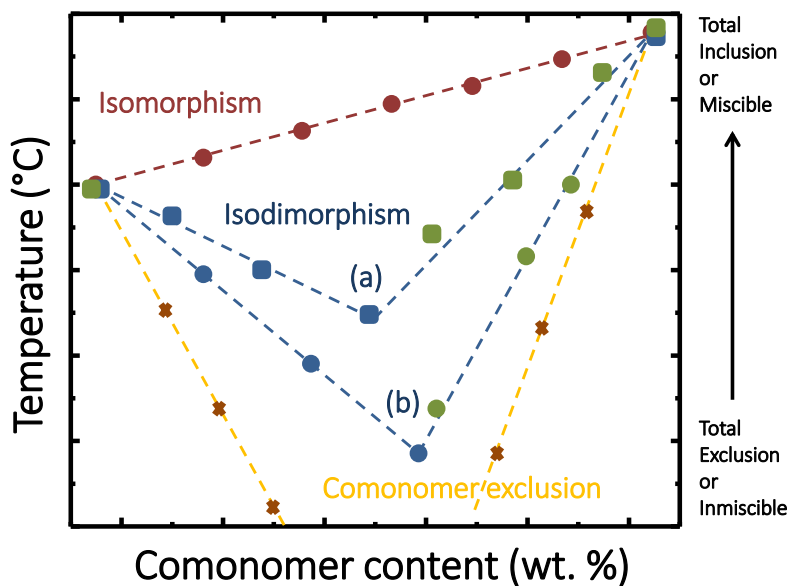
Figure 3.1 Melting (or crystallization) temperature as a function of comonomer content for different possible copolymers. From top to bottom the three typical cases are represented: isomorphic behavior (red), isodimorphic behavior for copolymers with small amount (blue-green, a) and large amount (blue-geen, b) of comonomer exclusion and copolymers with total exclusion of second comonomer (yellow).[2]

This case occurs when only the major component of the copolymer can crystallize and total comonomer exclusion can occur during random copolymers crystallization. (c) Isodimorphism. An intermediate case is that of isodimorphic crystallization. In these copolymers, there is a balance between exclusion and inclusion that depends on the chemical structure of the comonomeric units. Two crystalline phases can be formed depending on composition, and thermal transitions display a pseudo-eutectic point when plotted as a function of composition. Among those crystallization behaviors of random copolymers, the unique crystallization of the major component (case b) can be considered the most frequent, while isomorphic behavior is the less common.[2]

As far as we know, there are no general rules that can unambiguously predict whether a copolymer will display isomorphic, isodimorphic, or no cocrystallization. In fact, even miscible in the amorphous phase, the possibility of forming a mixed crystalline unit cell, or in other words the efficiency of comonomer inclusion, is not easily determined. While cocrystallization has been already demonstrated in some specific type of polyesters or polycarbonates, as far as the authors are aware this crystallization phenomenon has not been seen in other types of polymer families.[3–7]

Herein, we expanded the concept of NEMO-catalyzed bulk self-condensation of diols to prepare a set of copolyethers based on 1,6-hexanediol and 1,12-dodecanediol. The obtained poly(oxyhexamethylene-*ran*-oxydodecamethylene) copolyethers were characterized in terms of molecular weight and composition. The thermal properties and crystallization behavior were studied in detail by DSC and WAXS. The copolyethers showed the ability to crystallize in all the composition range in a single crystal structure while their single melting transition followed a simple rule of mixing. This is the typical behavior of isomorphic crystallization, and the effect of the composition of comonomer units on the crystalline structure was then investigated. To our knowledge, this is the first report on aliphatic copolyethers showing isomorphism. Moreover, a random terpolymer was also synthesized, and it showed similar thermal behavior, suggesting that this chemistry could be further expanded to other copolymers to tune the thermal properties on demand.

3.2. Results and discussion

3.2.1. Synthesis and characterization of poly(oxyhexamethylene-*co*-oxydodecamethylene) copolyethers

In the previous chapter, we reported on the bulk self-condensation of aliphatic diols as a route to aliphatic polyether homopolymers.[1] Following a similar procedure, a series of copolyethers of different compositions were synthesized by self-condensation of 1,6-hexanediol and 1,12-dodecanediol (Figure 3.2). The noneutectic mixture organocatalyst (NEMO) prepared by a simple nonstoichiometric mixture (3:1) of methanesulfonic acid (MSA) and 1,5,7-triazabicyclo[4.4.0]dec-5-ene (TBD) was used as catalyst (Figure S3.1).
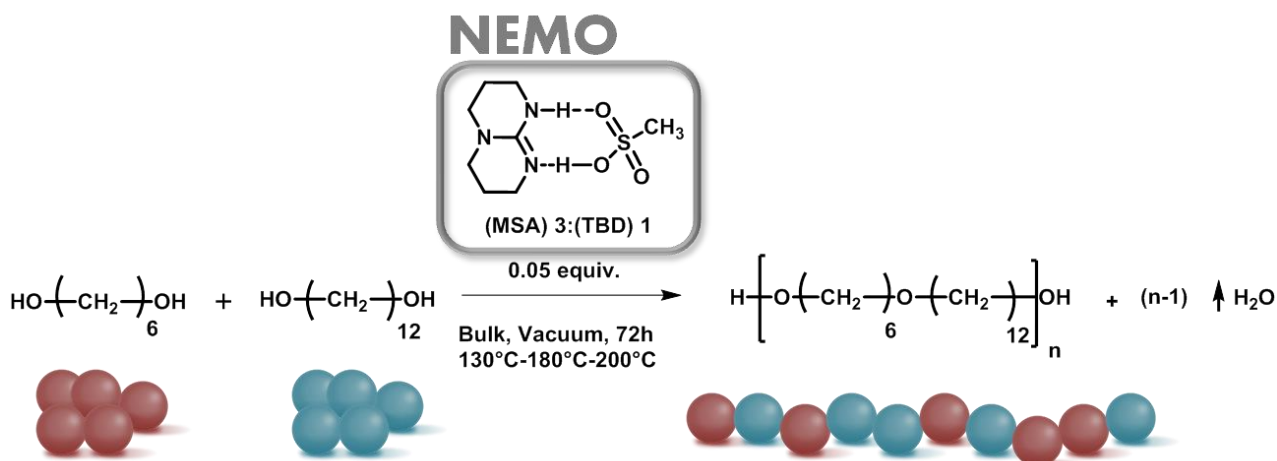
Figure 3.2 Synthesis route of random copolyethers from 1,6-hexanediol and 1,12-dodecanediol in bulk conditions using MSA:TBD (3:1) as NEMO.

In a typical reaction, the corresponding ratios of 1,6-hexanediol and 1,12-dodecanediol were added in the presence of NEMO organocatalyst. The polymerization reaction was performed in various steps: first at 130 °C for 24 h, after which the temperature was raised to 180 °C for 24h, and to 200°C to the last 24h under vacuum, mimicking the conditions used in other polycondensations. The copolymerizations were monitored using ^{1}H NMR by the diagnostic disappearance of

1,6-hexanediol and 1,12-dodecanediol methylene protons (signal δ = 3.65 ppm, adjacent to the alcohol) and their subsequent reappearance at δ = 3.33 ppm due to ether formation.
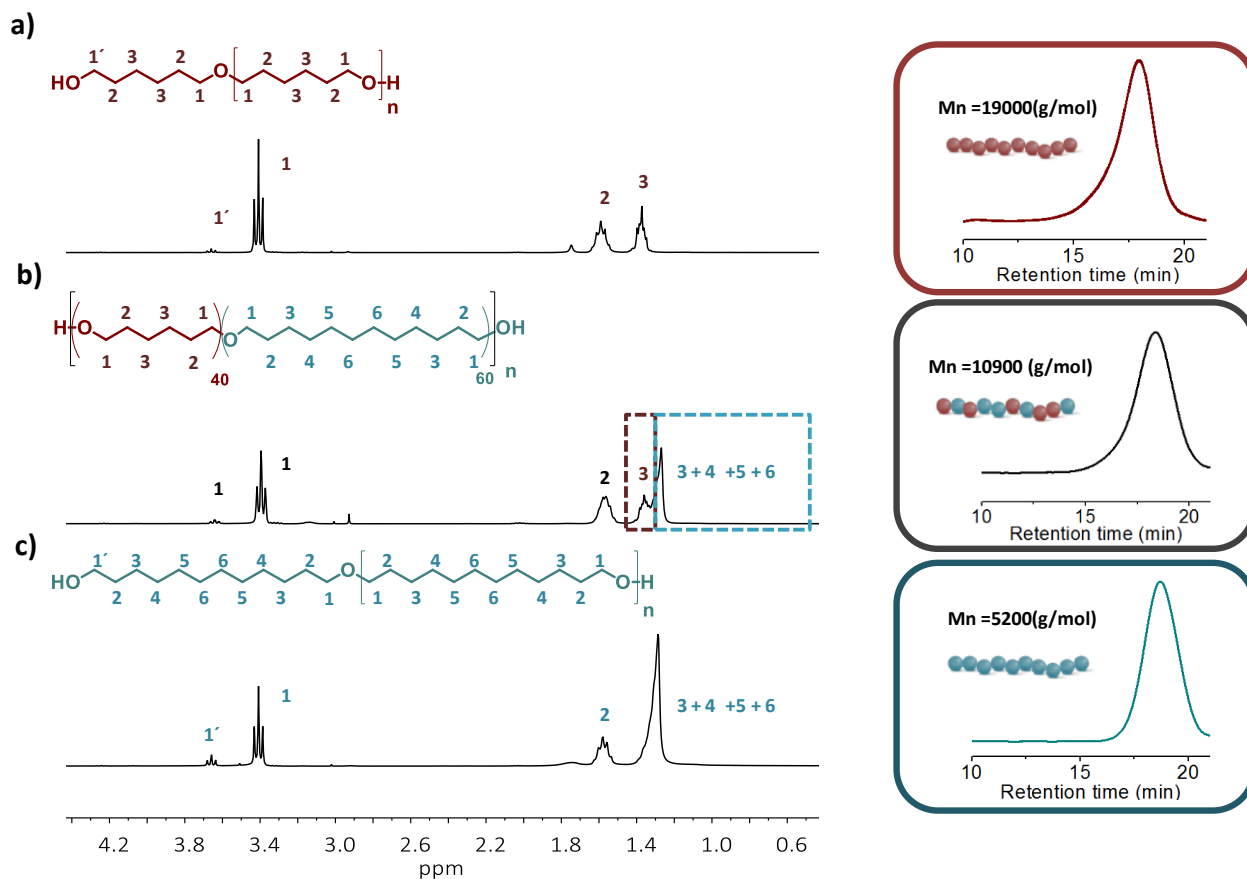
Figure 3.3. ^{1}H NMR spectra and SEC traces of a) poly(oxyhexamethylene) homopolymer, b) poly(oxyhexamethylene-*co*-oxydodecamethylene) copolymer 40/60 and c) poly(oxydodecamethylene) homopolymer.

The molar compositions of the copolyethers were calculated from the ^{1}H NMR spectrum using the relative intensities of the proton signals arising from the 1,6-hexanediol and 1,12-dodecanediol repeating units pointed out as signal 3 (red) and signals 3–6 (blue), respectively (Figure 3.3). It was observed that the content of 1,6-hexanediol was slightly lower in the copolymer composition than in the original feed. This small deviation of ~10% (Table 3.1) could be attributed to the short length of 1,6-hexanediol with respect to 1,12-dodecanediol and the possible cycle formation or

monomer distillation during the reaction. SEC traces showed a single distribution confirming the copolymerization of both comonomers in a single polymer.

Table 3.1. Chemical composition and molecular characteristics of the copolyethers.

Entry	(C6)/(C12) % in the feed	(C6)/(C12) % in the polymer [a]	M_n[a] (g/mol)	M_n[b] (g/mol)	Đ	R[c]
1	100/0	-	10000	19000	2.0	-
3	90/10	88/12	10100	17400	2.1	1.04
4	85/15	80/20	8900	16700	2.2	0.95
6	70/30	74/26	4200	11100	2.4	1.01
7	60/40	51/49	4000	10900	2.3	0.96
8	50/50	40/60	3600	7200	2.4	1.01
10	40/60	32/68	3500	6100	2.0	0.95
11	30/70	17/83	2800	5900	2.1	0.96
14	0/100	-	3200	5200	2.2	-

[a]Determined by ^{1}H NMR spectroscopy in CDCl$_3$, [b]Determined by SEC in CHCl$_3$, [c]Determined by ^{13}C NMR spectroscopy in CDCl$_3$

The microstructure (random, alternating, or blocky) of the copolymer significantly influences the final properties and is a key factor for crystallization. To get a better understanding of the polymer microstructure and to evaluate the randomness character of the copolymers, we analyzed the copolymers using ^{13}C NMR spectroscopy.
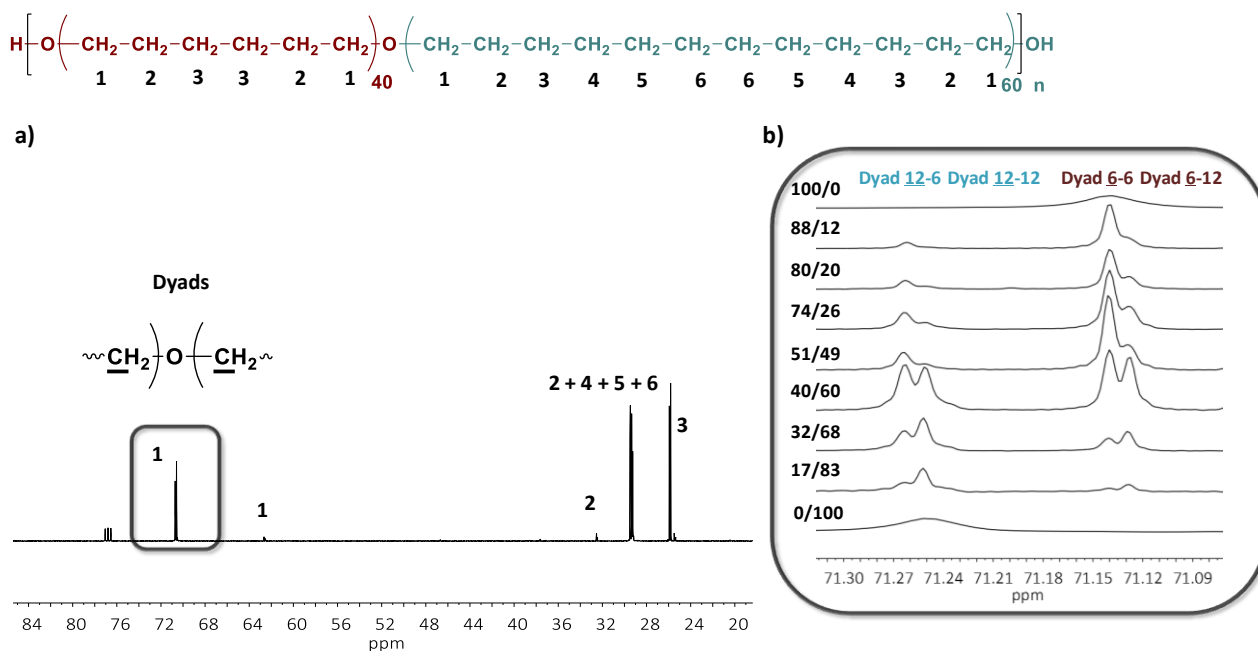
Figure 3.4. a) Chemical structure and ^{13}C NMR spectrum in CDCl$_3$ of the copolyether (40/60) and b) region of the methylene carbons used for the R value determination.

As an example, Figure 3.4 shows the ^{13}C NMR spectrum of the copolymer C6/C12 (40/60) and the scale expanded region of the methylene carbons close to the ether linkage. Detailed ^{13}C NMR spectrum characterization is included in Figure S3.6. In both homopolymers, only one signal attributed to these carbons was observed. When the comonomers are copolymerized, new signals were observed, along with those previously mentioned. These new signals are attributed to the presence of different dyads. Thus, the chemical shift of the methylene group linked to the ether bond would be influenced by the adjacent group (region 71.10–71.30 ppm). These dyads were named as dyad12–6, dyad12–12, dyad6–6, and dyad6–12, which appear at δ = 71.26, 71.25, 71.14 and 71.13 ppm, respectively.

Based on the ^{13}C NMR spectra, the relative molar fraction of the interchange dyad (C6–C12) can be easily determined, and the randomness character value (R) of the copolyethers was calculated using eq 1:

$$R = \frac{(C6\text{-}12)}{2(C6)(C12)} \quad (1)$$

Depending on the value of R, the copolymer can be considered as blocky, random, or alternated. In each case, values of R tend to 0, 1 or 2. Thus, as summarized in Table 3.1, the degree of randomness was 1 or very close to it, indicating the random nature of the prepared copolymers. ^{1}H NMR spectroscopy and SEC analysis were used to determine the molecular weight of all the copolymers. By ^{1}H NMR the values were calculated taking into account the final copolymer composition and by the integration of the methylene end group close to the alcohol that shows a peak at $\delta = 3.65$ ppm and the signal adjacent to the ether linkage at $\delta = 3.33$ ppm. The molecular weight of the copolyethers increased from 5900 to 17400 g/mol as the 1,6-hexanediol content increases. This trend is in agreement with the molecular weight values of the homopolymers, which are lower for poly(oxydodecamethylene). The reason for these differences in molecular weight could be attributed to the increase in melt viscosity of the copolyethers as the number of methylene units in the chain increases. When the viscosity increases, water diffusion and subsequent chain growth are lower and the extent of the step-growth polymerization is limited.[1] We also observed that the molecular weights measured by SEC employing polystyrene standards were higher than those calculated by NMR. Interestingly, they followed the same trend; higher molecular weights were obtained when the content of 1,6-hexanediol increased. In all cases, the SEC traces of the copolymers showed a dispersity close to 2, common for step-growth polymerization materials (Figure 3.2).[8]

3.2.2. Thermal characterization of poly(oxyhexamethylene-*co*-oxydodecamethylene) copolyethers

The crystallization behavior of the random copolymers was investigated by differential scanning calorimetry (DSC) and compared to that of homopolyethers. Figure 3.5a shows the behavior of the materials when they were cooled from the melt; a single crystallization peak is observed for all compositions. When analyzing the subsequent DSC heating scans (Figure 3.5b), a single melting peak is also observed for the whole series of copolyethers. For both crystallization and melting transitions, the peak values corresponding to T_m and T_c strongly depend on the composition (C6/C12) of all copolyethers.

Table 3.2 shows that T_m and T_c values for the copolyethers increase from the characteristic values of poly(oxyhexamethylene) to those of poly(oxydodecamethylene) in a monotonic trend as a function of the composition. Figure 3.5 shows an almost linear trend in the increase of T_m and T_c when the amount of 1,12-dodecanediol increases. It is remarkable that a single first-order crystallization or melting transition is observed in the copolyethers at temperatures in between those of the corresponding homopolymers. Furthermore, despite the fact that the copolymers are random, the prepared copolyethers can crystallize in the entire composition range. These observations can only be possible if comonomer inclusion inside the formed crystals dominates over comonomer exclusion. In other words, the prepared copolymers are probably isomorphic.[2]
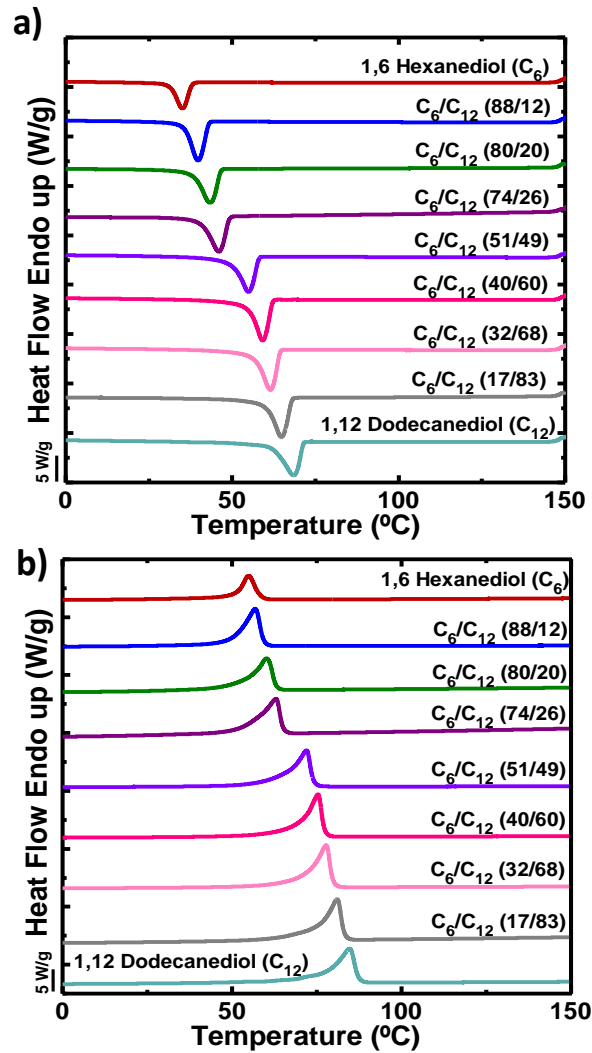
Figure 3.5. a) Cooling DSC scans from the melt and b) subsequent heating scans for the indicated polyethers and copolyethers.

According to the behavior described below (Figure 3.6), the copolyethers prepared here display thermal properties typical of isomorphic random copolymers. Two classes of isomorphism have been reported: (a) chain isomorphism and (b) isomorphism of monomeric units. As we are dealing with random copolyethers, we will focus on the isomorphism of comonomer units.

Isomorphism among monomeric units occurs in copolymerizing monomers that have a chemical nature and shape slightly different from one another (e.g., styrene and o-fluorostyrene). This allows the formation of crystallizable copolymers in the entire composition range. They show physical properties (lattice constants, melting temperatures, etc.) continuously varying between those of the pure homopolymers.[3,5]

Table 3.2. Thermal Properties of the Copolyethers.

Polymer	T_c (˚C)	ΔH_c (J/g)	T_m (˚C)	ΔH_m (J/g)	Xc^*
Poly(oxyhexamethylene)	35.0	-75	54.9	83	0.33
C6/C12 (88/12)	39.7	-123	56.8	133	0.53
C6/C12 (80/20)	43.3	-129	60.2	139	0.55
C6/C12 (74/26)	46.0	-137	62.9	145	0.57
C6/C12 (51/49)	54.8	-141	71.9	152	0.58
C6/C12 (40/60)	59.0	-150	75.3	161	0.62
C6/C12 (32/68)	61.4	-157	77.7	164	0.62
C6/C12 (17/83)	64.7	-150	80.9	164	0.62
Poly(oxydodecamethylene)	68.4	-157	84.7	166	0.62

*Calculated by $X_c = \Delta H_m / \Delta H_m °_{(C6/C12)}$, see Supporting Information.
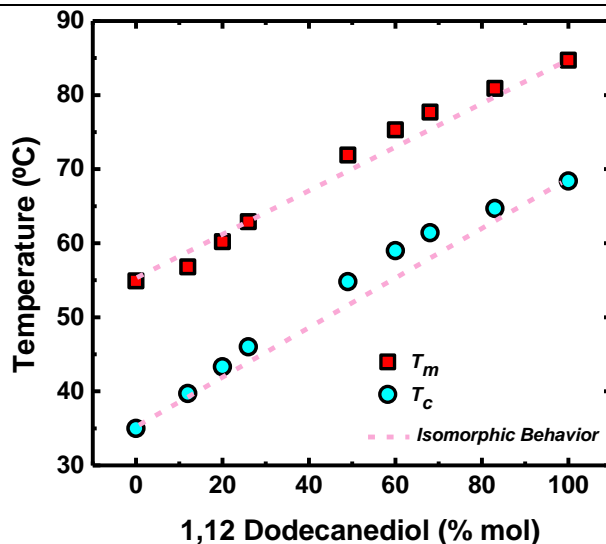
Figure 3.6. Values of T_m and T_c as a function of 1,12-dodecanediol content in the copolyether.

To further confirm the isomorphic behavior of the studied copolymers, they must fulfill requirements that are observed in isomorphic random copolymers.[3,6,7,9,10] One essential requirement is that the copolymers must have approximately the same shape, volume, and compatible conformations of the different comonomer units. In the case of the copolyethers analyzed in this paper, these polymers are made from two homopolyethers, whose chemical structures only differ in the number of methylene units present in the main chain, so it is probable that they fulfill this requirement (as will be confirmed by WAXS studies below). In Figure 3.6, the series of copolymers show single crystallization and melting peaks at intermediate temperatures between those of the homopolymers of reference. This behavior is reported for copolymers of isomorphic comonomeric units and is attributed to the fact that both homopolymers are crystalline and show the same symmetry.[5–7,9] Moreover, both transitions increase when the content of 1,12-dodecanediol in the copolymer is increased. The isomorphic copolymers show a peculiar behavior in their thermal properties when these are plotted as a function of composition.[2,3,5–7,9,10]

Figure 3.6 shows the values of T_m as a function of composition (i.e., 1,12-dodecanediol content), where the experimental results approximately fit a straight line connecting the T_m of the two homopolymers (dotted pink line), i.e., a simple mixing law. Similar behaviors have been reported in the literature for random copolymers where two different comonomers form an isomorphic substitution. [3,5–7,9,10] On the other hand, Table 3.2 shows enthalpy values (and therefore crystallinity values calculated therefrom) in between those of the homopolyethers for all compositions, indicating that the 1,6-hexanediol and 1,12-dodecanediol units cocrystallize, as there is no decrease in the crystallinity degree (expected when exclusion from the crystal lattice takes place). An additional requirement for isomorphism is that the crystalline phases of the two homopolymers must be analogous from the point of view of conformation of the chains and the symmetry of the lattice dimensions. Only in this case would a single crystalline phase be possible with small continuous dimensional changes depending on the composition.[3,9] Kobayashi et al. reported that both homopolyether chains employed here, poly(oxyhexamethylene) and poly(oxydodecamethylene), have essentially a planar zigzag chain conformation in the crystal.[11] On the other hand, poly(oxyhexamethylene) can present two forms of crystal packing (monoclinic and orthorhombic) or a mixture of both depending on the crystallization conditions. Poly(oxydodecamethylene), on the other hand, crystallizes with an orthorhombic unit cell. With regard to the symmetry of the polyethers, it is observed that depending on the number of methylene groups in the chain (even or odd), they present different types of symmetry. Poly(oxyhexamethylene) and poly(oxydodecamethylene) have both even numbers of methylene groups; therefore, they both have the same symmetry. Kobayashi et al. also report the unit cell dimensions for orthorhombic poly(oxydodecamethylene), a = 7.40 Å, b = 4.94 Å, and c = 32.53 Å, and for monoclinic poly(oxyhexamethylene), a = 5.65 Å, b = 9.01 Å, and c = 17.28 Å.[11]

No reports can be found in the literature for the unit cell dimensions of the orthorhombic polymorph of poly(oxyhexamethylene).

Although the dimensions of both homopolyethers unit cells are not similar, it is necessary to remember that the poly(oxyhexamethylene) can also crystallize in an orthorhombic unit cell. It could be possible that in the copolyether both comonomeric units form a single orthorhombic unit cell. This crystalline unit cell could resemble the unit cell of polyethylene, as it is known that polyether chains with long methylene sequences tend to form orthorhombic unit cells that are similar to that of polyethylene.[11,12]
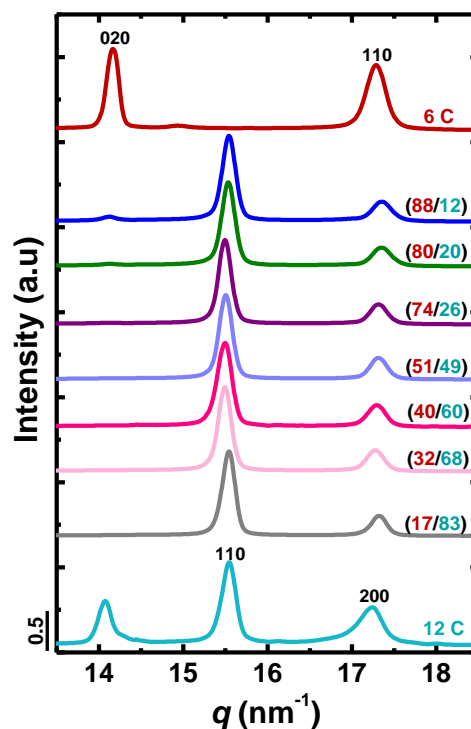
Figure 3.7. WAXS diffraction patterns for copolyethers at 25 ˚C.

Figure 3.7 shows the WAXS patterns obtained for all the prepared copolyethers and homopolyethers at 25 °C, after they were crystallized nonisothermally at 20 °C/min.

It can be seen that the homopolymers poly(oxyhexamethylene) and poly(oxydodecamethylene) show characteristic and distinct reflections that correspond to their reported monoclinic and orthorhombic unit cells.[11]

The reflections obtained for poly(oxyhexamethylene) at q values of 14.16 and 17.29 nm^{-1} correspond to the (020) and (110) crystal planes. In the case of poly(oxydodecamethylene), the reflections at q values of 15.55 and 17.24 nm^{-1} correspond to the (110) and (200) crystal planes. The calculated interplanar distances are reported in Table 3.3, and they are similar to literature values.[11] There is an additional reflection in the case of poly(oxydodecamethylene) at a q value of 14.08 nm^{-1} corresponding to an interplanar distance (dhkl) of 4.46 Å. Further crystallographic work would be needed to reveal the origin of this reflection, which is outside the scope of the present chapter. For the copolyethers, Figure 3.8 shows that all compositions prepared exhibit crystalline reflections at q values of approximately 15.5 and 17.3 that should correspond to diffraction from (110) and (200) crystal planes, respectively. These two reflections resemble those observed for poly(oxydodecamethylene) at similar q values (see Figure 3.8 and Table 3.3). The results suggest that all copolyethers crystallize with a single unit cell, and this unit cell resembles that formed by poly(oxydodecamethylene).

Table 3.3 shows the values obtained in this work for the interplanar distances (dhkl) of the copolyethers. As these are new materials, there are no values reported in the literature for comparison purposes. However, the interplanar distances obtained are comparable to those reported for orthorhombic polyethylene and to our poly(oxydodecamethylene).

Table 3.3. Calculated interplanar distance (d_{hkl}) from Figure 3.7 and comparison with reported values[11]

Polymer	2ϑ	q(nm^{-1})	d_{hkl}(Å)	q(nm^{-1})[a]	d_{hkl}(Å)[a]	Reflection
Poly(oxyhexamethylene)	13.33	14.16	4.436	13.94	4.507	020
	16.29	17.29	3.635	17.08	3.678	110
C6/C12 (88/12)	14.64	15.54	4.042	-	-	110
	16.36	17.36	3.620	-	-	200
C6/C12 (80/20)	14.63	15.53	4.045	-	-	110
	16.35	17.35	3.621	-	-	200
C6/C12 (74/26)	14.59	15.49	4.056	-	-	110
	16.32	17.32	3.628	-	-	200
C6/C12 (51/49)	14.60	15.50	4.053	-	-	110
	16.32	17.31	3.629	-	-	200
C6/C12 (40/60)	14.59	15.50	4.055	-	-	110
	16.30	17.30	3.632	-	-	200
C6/C12 (32/68)	14.59	15.49	4.055	-	-	110
	16.28	17.28	3.636	-	-	200
C6/C12 (17/83)	14.64	15.54	4.043	-	-	110
	16.33	17.33	3.627	-	-	200
Poly(oxydodecamethylene)	13.25	14.08	4.464	13.87	4.530	-
	14.64	15.55	4.041	15.34	4.096	110
	16.25	17.24	3.645	17.05	3.686	200
Polyethylene[b]	-	-	-	15.26	4.115	110
	-	-	-	16.96	3.703	200

[a,b] Reference values[11,13]

From the above-mentioned results it is obvious that a single orthorhombic unit cell is formed in the copolyethers, corroborating that the copolymers prepared here have an isomorphic behavior. Furthermore, when analyzing the values of the interplanar distance (dhkl), calculated using Bragg's law, versus the composition (Figure 3.8), these dhkl values also change linearly with composition, but the observed change is very small. A similar behavior has been reported for systems with isomorphic substitution, which is also an indication that the random copolyethers synthesized here are isomorphic.[7]

Provided that the two crystallizable repeating units meet strict molecular requirements, the copolymers can crystallize in the same crystal lattice, in the entire composition range.
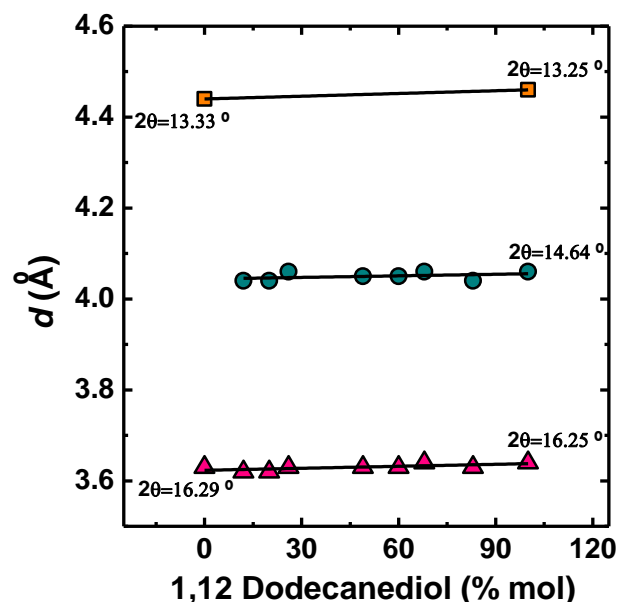
Figure 3.8. Interplanar distance (dhkl) for all reflections at 25 ˚C.

In other words, the two comonomeric units along the chain can cocrystallize regardless of the composition. Therefore, the two comonomers can be considered

miscible in the crystalline state. This case is termed total inclusion of comonomers in a single crystal lattice or isomorphic behavior, and as far as we are aware, it has never been obtained for aliphatic polyethers.

3.2.3. Expanding the scope of the polymerization to terpolymers

To expand the scope of the polymerization, a random terpolymer was also synthesized by the polymerization of 1,6-hexanediol, 1,10-decanediol, and 1,12-dodecanediol using the same synthetic methodology (Figure 3.9, entry 16).

$$HO{\small(}CH_2{\small)}_6 OH \ + \ HO{\small(}CH_2{\small)}_{10} OH \ + \ HO{\small(}CH_2{\small)}_{12} OH \ \xrightarrow[\substack{\text{Bulk, Vacuum, 72h} \\ 130°C-180°C-200°C}]{\text{0.05 equiv of catalyst}} \ H{\small[}O{\small(}CH_2{\small)}_6 O{\small(}CH_2{\small)}_{10} O{\small(}CH_2{\small)}_{12}{\small]}_n OH \ + \ (n-1) \ H_2O$$
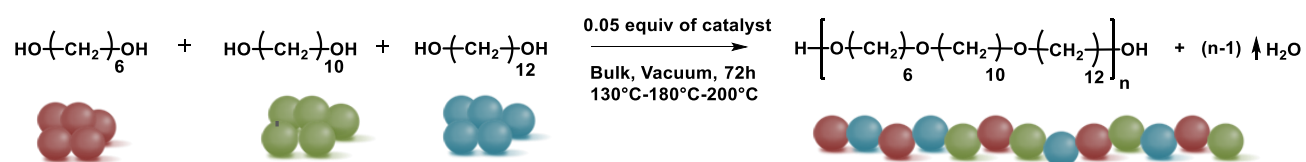
Figure 3.9. Synthesis route of random terpolymer using MSA:TBD (3:1) as catalyst.

Herein, because of the complete overlapping of the H signals corresponding to 1,6-hexanediol, 1,10-decanediol, and 1,12-dodecanediol repetitive units (Figure 3.10), the molar composition of the terpolymer was calculated from the ^{13}C NMR spectrum, and the result was C6/C10/C12 (27/46/27) (Figure 3.11).
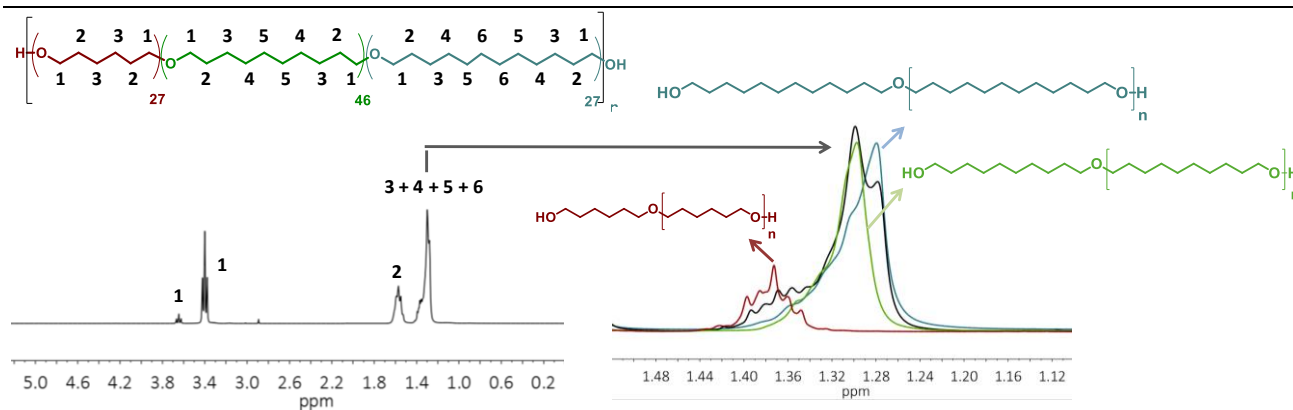
Figure 3.10. Region of the ^{1}H NMR spectra of the terpolymer in comparison to the homopolymers.

The molecular weight was determined by SEC. The SEC trace showed a single distribution, suggesting the presence of the three comonomers in the polymer chain (Figure S3.7).
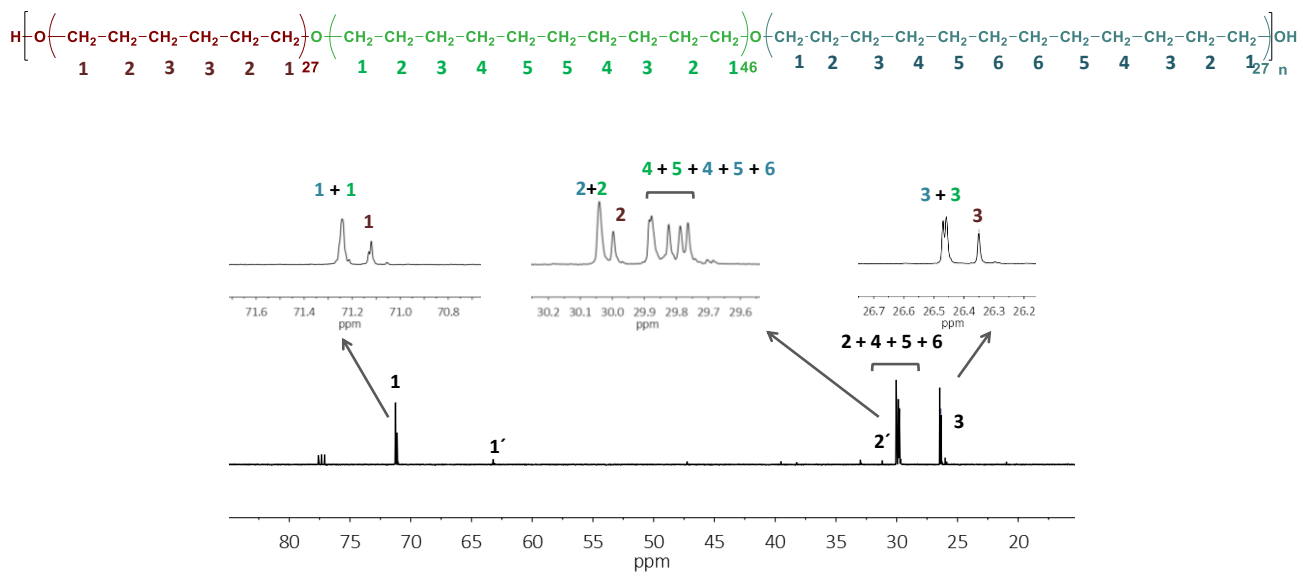
Figure 3.11. ^{13}C NMR spectroscopy in CDCl$_3$ of the terpolymer. Signals 1´and 2´make reference to the corresponding carbons of the ending group.

Table 4. Molecular characteristics of the terpolymer together with the thermal properties.

Entry	(C6/C10/C12) % in the feed	(C6/C10/C12) % in the polymer [a]	M_n[a] (g/mol)	M_n[b] (g/mol)	Đ	T_c (°C)	ΔH_c (J/g)	T_m (°C)	ΔH_m (J/g)
14	0/0/100	-	3200	5200	2.2	68.4	-157	84.7	166
15	0/100/0	-	6800	8200	2.1	63.0	-135	80.4	142
16	33/33/33	27/46/27	4100	6900	2.0	56.0	-173	75.1	179

[a] Determined by ^{13}C NMR spectroscopy in CDCl$_3$, [b] Determined by SEC in CHCl$_3$

In addition to the comprehensive thermal characterization performed to the copolyethers, the nonisothermal crystallization behavior of the random terpolymer was investigated by DSC and compared to the three poly(oxyhexamethylene), poly(oxydecamethylene), and poly(oxydodecamethylene) homopolyethers. The heating and cooling scans of the materials are represented in Figure 3.12. As observed in the copolymers, the terpolymer also shows a single melting and crystallization peak with T_m and T_c values for the terpolymer in between the values given by the homopolymers. Further analysis would be needed to ascertain if this terpolymer is also crystallizing in a single unit cell as well as exploring the effects of composition. However, that is outside the scope of the present work, and we just wanted to show the potentiality of the synthetic path to prepare novel terpolyethers.
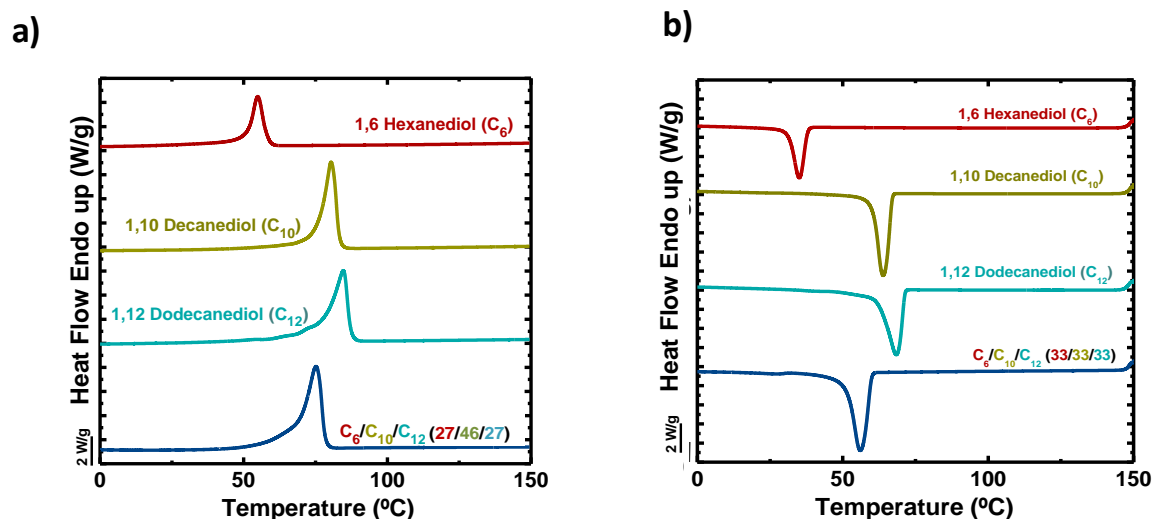
Figure 3.12. a) DSC heating scans and b) DSC cooling scans for the indicated polyethers and terpolyether.

3.3. Conclusion

In this chapter, the potential of the NEMO MSA:TBD 3:1 was expanded to the synthesis of a series of aliphatic poly(oxyhexamethylene-*ran*-oxydodecamethylene)s random copolyethers by self-condensation of two different diols differing in chain length: 1,6-hexanediol and 1,12-dodecanediol. The seven copolymers prepared with different compositions were completely random according to NMR spectroscopy, and their number-average molecular weights varied between 5900 and 17400 g mol^{-1}. According to DSC and WAXS, these random copolyethers exhibit the following general behavior: (a) they crystallize in the entire composition range despite being random, (b) their melting points varied with composition according to a simple rule of mixtures, and (c) WAXS results show that they crystallize in a single unit cell whose dimensions exhibit a weak but linear variation with copolymer composition. Thus, we can conclude that the copolyethers prepared here are isomorphic. Finally, a random terpolyether was also synthesized with the same route previously employed to obtain the copolyethers, and a material with a single melting point was also obtained.

Therefore, this synthetic route can be tailored to prepare long chain aliphatic copolyethers and terpolyethers with a given melting temperature.

3.4. Experimental Section

3.4.1 Materials

1,12-Dodecanediol (99%, Sigma-Aldrich), 1,10-decanediol (99%, Sigma-Aldrich) and 1,6-hexanediol (99% Sigma-Aldrich) were used as received after being dried in toluene. Methanesulfonic acid (MSA, 99%) and 1,5,7-triazabicyclo[4.4.0]dec-5-ene (TBD, 98%), chloroform ($CHCl_3$), methanol (CH_3OH) and the rest of the solvents used on this work were supplied by Sigma-Aldrich and used as received.

3.4.2 Synthesis of the copolyethers

The synthesis of copolyethers was performed by self-condensation of two different diols: a short chain aliphatic diol (1,6-hexanediol) and a long chain one (1,12-dodecanediol). The copolymers were named as C6/C12 mol% as the molar percentage of 1,6-hexanediol and 1,12-dodecanediol used in the feed.

In the first step the NEMOs were prepared by simple non-stoichiometric mixture (3:1) of methanesulfonic acid (MSA) and 1,5,7-triazabicyclo[4.4.0]dec-5-ene (TBD). The mixtures were thermally treated at 90 °C over 30 minutes under stirring until complete formation of homogeneous and transparent liquid solution. After the catalyst preparation, a mixture of monomers containing different 1,6-hexanediol/1,12-dodecanediol (C6/C12) ratios: 90/10 (4.20 g, 0.036 mol/0.80 g, 3.95 10^{-3} mol), 85/15 (3.84 g, 0.032 mol/1.16 g, 5.73 10^{-3} mol), 70/30 (2.88 g, 0.024 mol/2.12 g, 0.010 mol), 60/40 (2.33 g, 0.020 mol/2.67 g, 0.013 mol), 50/50 (1.84 g, 0.016 mol/3.16g, 0.016

mol), 40/60 (1.40 g, 0.012 mol/3.60 g, 0.018 mol), 30/70 (1.00 g, 8.47 10^{-3} mol/4.00 g, 0.020 mol) and were added respectively to 0.05 equiv. organocatalyst. Likewise, for the synthesis of the terpolymer, a mixture of monomers contained (C6/C10/C12) 33/33/33: 0.010 mol (1.194 g/1.761 g/ 2.045 g) was also added also with 0.05 equiv. organocatalyst.

The sealed reaction vessels were then submerged into a pre-heated oil bath at 130 °C under vacuum. The self-condensation process was performed in three steps. After the first 24 h at 130 °C, the temperature was increased to 180 °C for 24 h and to 200 °C for the last 24 h. After completion, the copolyethers were cooled to room temperature naturally. For the purification, the samples were dissolved in chloroform and precipitated in cold methanol. The resulted copolyethers were filtrated and dried under vacuum at RT for 24 h before their characterization. Homopolymers from 1,6-hexanediol 1,10-decanediol and 1,12-dodecanediol were synthesized and purified by the same procedure.

3.5. References

(1)   Basterretxea, A.; Gabirondo, E.; Jehanno, C.; Zhu, H.; Flores, I.; Müller, A. J.; Etxeberria, A.; Mecerreyes, D.; Coulembier, O.; Sardon, H. Polyether Synthesis by Bulk Self-Condensation of Diols Catalyzed by Non-Eutectic Acid–Base Organocatalysts. *ACS Sustain. Chem. Eng.* **2019**, *7* (4), 4103–4111. https://doi.org/10.1021/acssuschemeng.8b05609.

(2)   Pérez-Camargo, R. A.; Arandia, I.; Safari, M.; Cavallo, D.; Lotti, N.; Soccio, M.; Müller, A. J. Crystallization of Isodimorphic Aliphatic Random Copolyesters: Pseudo-Eutectic Behavior and Double-Crystalline Materials. *Eur. Polym. J.* **2018**, *101*, 233–247. https://doi.org/10.1016/j.eurpolymj.2018.02.037.

(3) Allegra, G.; Bassi, I. W. Isomorphism in Synthetic Macromolecular Systems. In *Fortschritte der Hochpolymeren-Forschung*; Advances in Polymer Science; Springer Berlin Heidelberg, 1969; pp 549–574.

(4) Liang, Z.; Pan, P.; Zhu, B.; Inoue, Y. Isomorphic Crystallization of Aliphatic Copolyesters Derived from 1,6-Hexanediol: Effect of the Chemical Structure of Comonomer Units on the Extent of Cocrystallization. *Polymer* **2011**, *52* (12), 2667–2676. https://doi.org/10.1016/j.polymer.2011.04.032.

(5) Natta, G.; Corradini, P.; Sianesi, D.; Morero, D. Isomorphism Phenomena in Macromolecules. *J. Polym. Sci.* **1961**, *51* (156), 527–539. https://doi.org/10.1002/pol.1961.1205115610.

(6) Ye, H.-M.; Wang, R.-D.; Liu, J.; Xu, J.; Guo, B.-H. Isomorphism in Poly(butylene Succinate-Co-Butylene Fumarate) and Its Application as Polymeric Nucleating Agent for Poly(butylene Succinate). *Macromolecules* **2012**, *45* (14), 5667–5675. https://doi.org/10.1021/ma300685f.

(7) Yu, Y.; Sang, L.; Wei, Z.; Leng, X.; Li, Y. Unique Isodimorphism and Isomorphism Behaviors of Even-Odd Poly(hexamethylene Dicarboxylate) Aliphatic Copolyesters. *Polymer* **2017**, *115*, 106–117. https://doi.org/10.1016/j.polymer.2017.03.034.

(8) Bossion, A.; Heifferon, K. V.; Meabe, L.; Zivic, N.; Taton, D.; Hedrick, J. L.; Long, T. E.; Sardon, H. Opportunities for Organocatalysis in Polymer Synthesis via Step-Growth Methods. *Prog. Polym. Sci.* **2019**, *90*, 164–210. https://doi.org/10.1016/j.progpolymsci.2018.11.003.

(9) Ceccorulli, G.; Scandola, M.; Kumar, A.; Kalra, B.; Gross, R. A. Cocrystallization of Random Copolymers of ω-Pentadecalactone and ε-Caprolactone Synthesized by Lipase Catalysis. *Biomacromolecules* **2005**, *6* (2), 902–907. https://doi.org/10.1021/bm0493279.

(10) Latere Dwan'Isa, J.-P.; Lecomte, P.; Dubois, P.; Jérôme, R. Synthesis and Characterization of Random Copolyesters of ε-Caprolactone and 2-Oxepane-1,5-Dione. *Macromolecules* **2003**, *36* (8), 2609–2615. https://doi.org/10.1021/ma025973t.

(11) Kobayashi, S.; Tadokoro, H.; Chatani, Y. Structural Studies on Polyethers, [-(CH2)m-O-]n. VI. The Higher Members with M = 6–10, 12. *Makromol. Chem.* **1968**, *112* (1), 225–241. https://doi.org/10.1002/macp.1968.021120120.

(12) Wunderlich, B. CHAPTER III - The Crystal Morphology. In *Macromolecular Physics*; Wunderlich, B., Ed.; Academic Press, 1973; pp 178–379. https://doi.org/10.1016/B978-0-12-765601-4.50008-1.

(13) *Physical Properties of Polymers Handbook*, 2nd ed.; Mark, J. E., Ed.; Springer-Verlag: New York, 2007

Chapter 4

Graphical abstract

1. Copolymerization

2. Thermal properties

BULK 200°C

NEMO
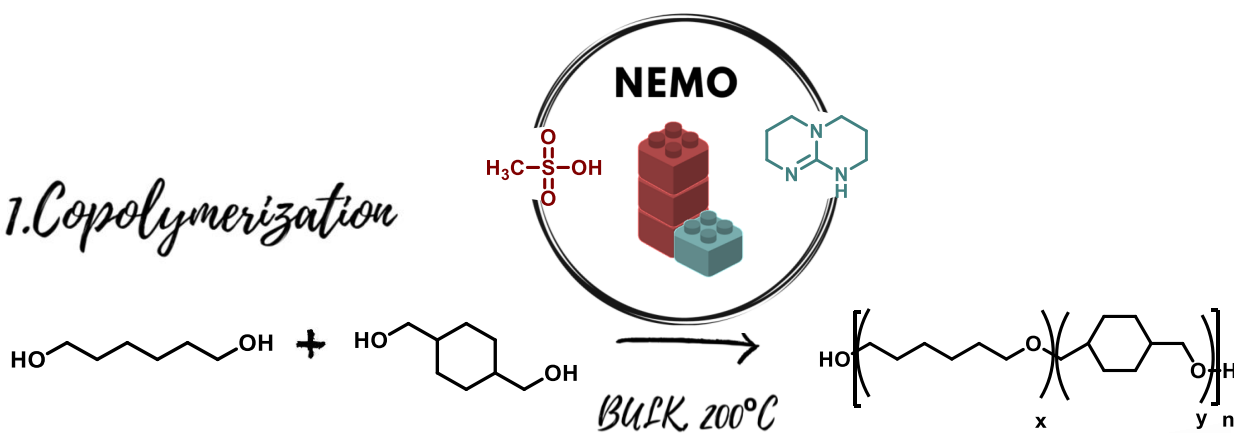
Fully Bio-based Polyethers

Chapter 4. Synthesis and characterization of fully bio-based poly(oxyhexamethylene-co-1,4-cyclohexanedimethanol) copolyethers.

5.1. Introduction

In the past few years, a remarkable progress has been made in the development of renewable polymeric materials derived from biomasses.[1–3] As a consecuence of the increasing demand of unconventional polymer architectures together with the rapid depletion of petroleum raw materials, synthesis routes to obtain renewable sources are becoming more consistent.[4–6] In addition, the prices of these bio-based monomers are decreasing making them in some cases more competitive monomers with respect to the corresponding fossil-based counterparts.[7,8]

Among several biobased monomeric units that have been presented in the past few years, well estabilished diols and polyols such as 1,4-propanediol, 1,6-hexanediol, glycerol or isomanide are becoming increasingly studied and derived from renewable resources.[3,9] Their interest in the field of polymer chemistry comes enhanced from their bioavailability, good thermal stability and the hydroxyl groups at the molecule terminals structure that make them ideal monomers for the synthesis of polycondensates such as polyesters, polyurethanes or polycarbonates.[10–14] Even though the incorporation of these bio-based diols in the polymer backbone is relatively easy to achieve, it comes strongly dictated by the mechanical, thermal, rheological, and other physical properties required for the final material. For this reason, for the most of the part, bio-based polymers comprise only of biobased

building blocks, being the percentage of renewable monomers included in the polymer network only within the 40-60%.[15]

One of the industries that are demanding more and more biobased monomers is the industry of polyurethanes. From a green and sustainable chemistry standpoint, the current challenge in the polyurethane's industry is to switch from petrobased polyurethanes (PUs) to biobased polyurethanes in a cost-effective manner. With a global production forecast of 26.5 million tons for 2021, PUs are today the sixth most widespread group of polymers due to their versatility. Current trends are focused on the use of chemical platforms based on vegetable oils/sources and involving the valorization of natural polyols.[12,14,16–19] Most (75%) of the polyols used for PU synthesis are polyether polyols, obtained from the reaction between a "starter" polyol and an alkylene oxide, both petrobased. These low molecular wright polyether polyols such as polyethylene glycol (PEG), polypropylene glycol (PPG) or polytetramethylene glycol (PTMG), impart to the material low T_g (in the range of -60 °C) and have enabled the preparation of phase separated polyurethane elastomers, coating and foams. In spite of the greater use of polyether polyols rather than polyester polyols for polyurethane industry, the development of bio-based polyether polyols is far behind the development of polyester polyols. Only few examples are found in the literature and all of them are based on isosorbide, which gives rise to relatively rigid polyethers.[20–22] As an example, Saxon and his co-workers syntesized very recently fully bio-based polyethers based on isosorbide via Ring-Opening Polymerization (ROP) giving as a result both cyclic and linear polyethers.[21]

In light of this, the present chapter reports the preparation of a variety of polyether polyols with low T_g. For that purpose we prepared polyols by the self condensation of different bio-source diols as a simple and scalable method of synthesis of new fully

renewable source polyethers. We hypothesize that by combining long-chain aliphatic diol 1,6-hexanediol (HDO) with cyclic diol 1,4-cyclohexanedimethanol (CHDM) we will be able to prepare both amorphous and semycristalline polyethers.
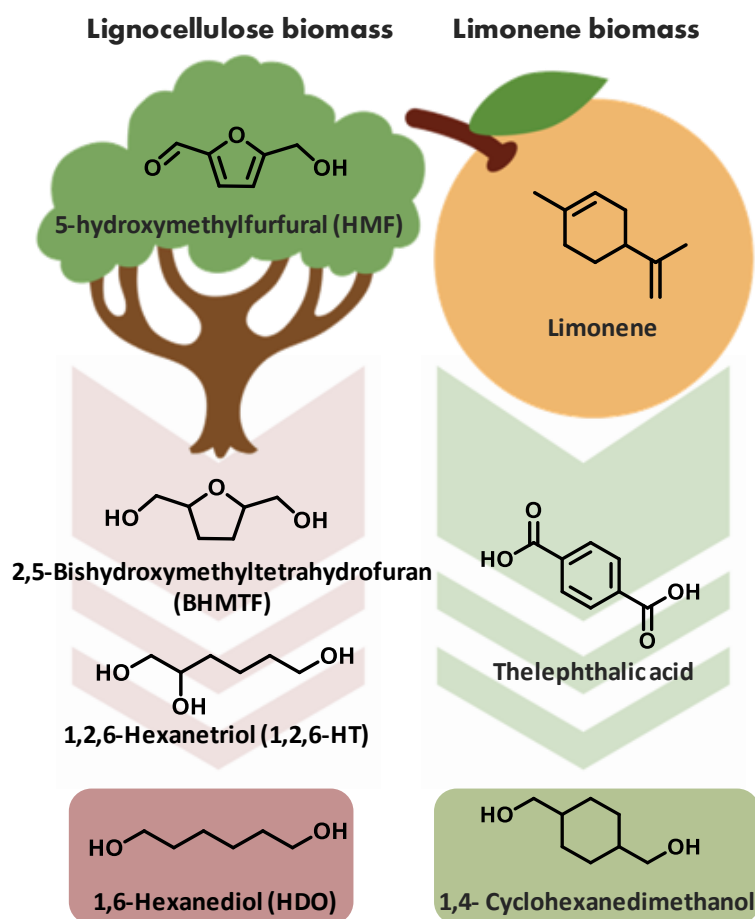
Figure 4.1. Scheme of the plausible synthesis pathway of 1,6-hexanediol and 1,4-cyclohexanedimethanol from biomass.[23,24]

1,6-Hexanediol (HDO) can be easily obtained from lignocelulosic biomass through the hydrogenation of 5-hydroxymethylfurfural (HMF) and is widely used in polyurethane and polyester synthesis acting as chain extender (Figure 4.1).[23,25,26] Considering the literature, the incorporation of 1,6-hexandiol in the polymer backbone gives superior properties in flexibility and hydrolytic stability than other well known diols such as ethylene glycol. As it contains a fairly long hydrocarbon chain it provides better

mechanical strength and low glass transition temperature (T_g).[26–28] On the other hand, 1,4-cyclohexanedimethanol (CHDM) is considered as a flexible monomer and has been extensively used to enhance the flexibility of polyesters and polycarbonates.[11,13,29–32]. Its preparation from limonene terpenes biomass through the terephthalic acid synthesis was recently reported (Figure 4.1).[24] In addition, it has been observed that not only the content of cyclohexylene moieties strongly influences the comprehensive properties of polymers, but also their steric conformation (*trans* or *cis* isomers). In general the *trans* isomer favors the formation of stable crystals, while the *cis* isomer trends to disturb or hinder the crystallization.[29,33–35]

In view of these considerations, fully bio-based series of poly(oxyhexamethylene-co-1,4-cyclohexanedimethanol) copolyethers have been prepared by a simple self-condensation method. For that, using the NEMO catalyst employed in previous works aliphatic copolyethes were synthetized varying the HDO-CHDM comonomer content. Their chemical structures, composition and molecular weight were determined by Nuclear Magnetic Resonance (NMR) and Size Exclusion Chromatography (SEC). We envision that due to the bulky character of the 1,4-cyclohexanedimethanol, the crystallization of the copolyethers will be hindered. Hence, we believe that the bio-based copolyethers could be tuned from higly semi-crystalline to amorphous low T_g containing polyols just by increasing the CHDM content in the backbone.

4.2. Results and discussion

4.2.1. Synthesis and characterization of poly(oxyhexamethylene-co-1,4-cyclohexanedimethanol) copolyethers

In the previous chapter we reported on the bulk self-condensation of two different aliphatic diols as a route to prepare higly semicrystalline aliphatic copolyethers[36]

Herein, a similar procedure was followed to obtain fully bio-based copolyethers derived from the self-condensation of 1,6-hexanediol (HDO) and 1,4-cyclohexanedimethanol (CHDM) (Figure 4.2). As catalyst, the non-eutectic mixture organocatalyst (NEMO) prepared by the nonstoichiometric mixture (3:1) of methanesulfonic acid (MSA) and 1,5,7-triazabicyclo[4.4.0]dec-5-ene (TBD) was used as it was the best in terms of conversion and molecular weights.
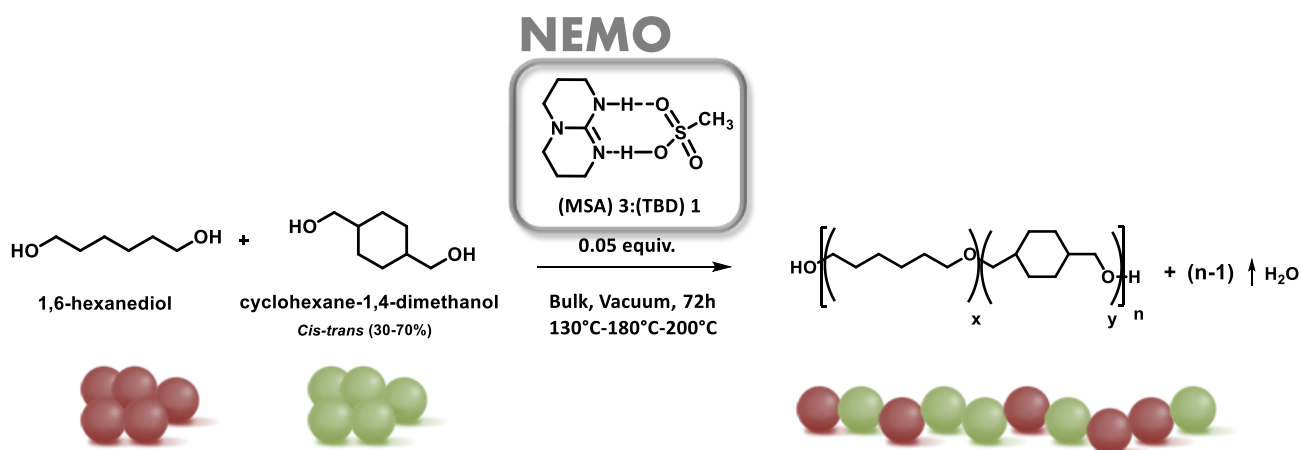
Figure 4.2. Synthesis route of random copolyethers from 1,6-hexanediol and 1,4-cyclohexanedimethanol in bulk conditions using MSA:TBD (3:1) as NEMO.

Different ratios of 1,6-hexanediol (HDO) and 1,4-cyclohenamedimethanol (CHDM) were loaded into the reactor together with the NEMO organocatalyst. The polymerization reaction was performed in various steps: first at 130 °C for 24 h, after the temperature was raised to 180 °C for 24h and the reaction was completed at 200 °C for 24h, all three steps under vacuum.

The corresponding homopolymers of both monomers were also prepared under the same reaction conditions. It is worth to specify that the CHDM employed owned a mixture of *cis/trans* isomer ratio equal to 70/30 which can greatly influence the crystallization of the materials.
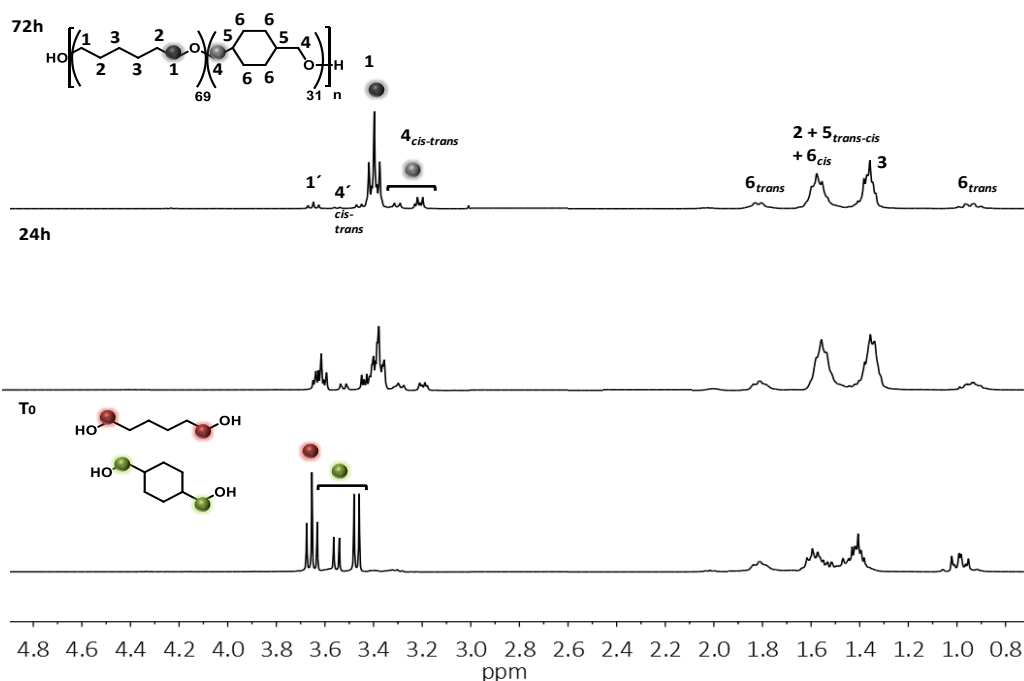
Figure 4.3. ^{1}H NMR spectra of the reaction media during the course of the reaction. The proton signals distinguished with color dots were used for the calculation of the monomer conversion.

The polymerizations were monitored using ^{1}H NMR by the diagnostic disappearance of 1,6-hexanediol (red signal δ= 3.65 ppm, adjacent to the alcohol) and 1,4-cyclohexanedimethanol (green signals δ= 3.54-3.45 ppm, adjacent to the alcohol) and their both subsequent reappearance at δ= 3.39 ppm and δ= 3.30-3.19 ppm, respectively, due to ether formation (Figure 4.3, black and grey signals respectively). Monomer conversion above 90 mol % was obtained for all the samples.

When the reaction finished, the copolymers were purified and the molar compositions of the copolyethers were calculated from the ^{1}H NMR spectrum using the relative intensities of the proton signals arising from the 1,6-hexanediol and 1,4-cyclohexanedimethanol repeating units pointed out as signal 1 and signal 4, in the Figure 4.4. The values obtained for the final copolymer composition was very similar to the feeding composition for all the samples (Table 4.1).In addition, the *cis/trans* isomer

content of the CHDM in the copolymer were also determined by ^{1}H NMR using the signals attributed to *cis* isomer (δ= 3.29 ppm) and *trans* isomer (δ= 3.29 pmm). We did not observe any change in the isomer content in the final polymers confirming the absence of any isomerization reaction during the polymerization which agrees with literature data .[29,37]
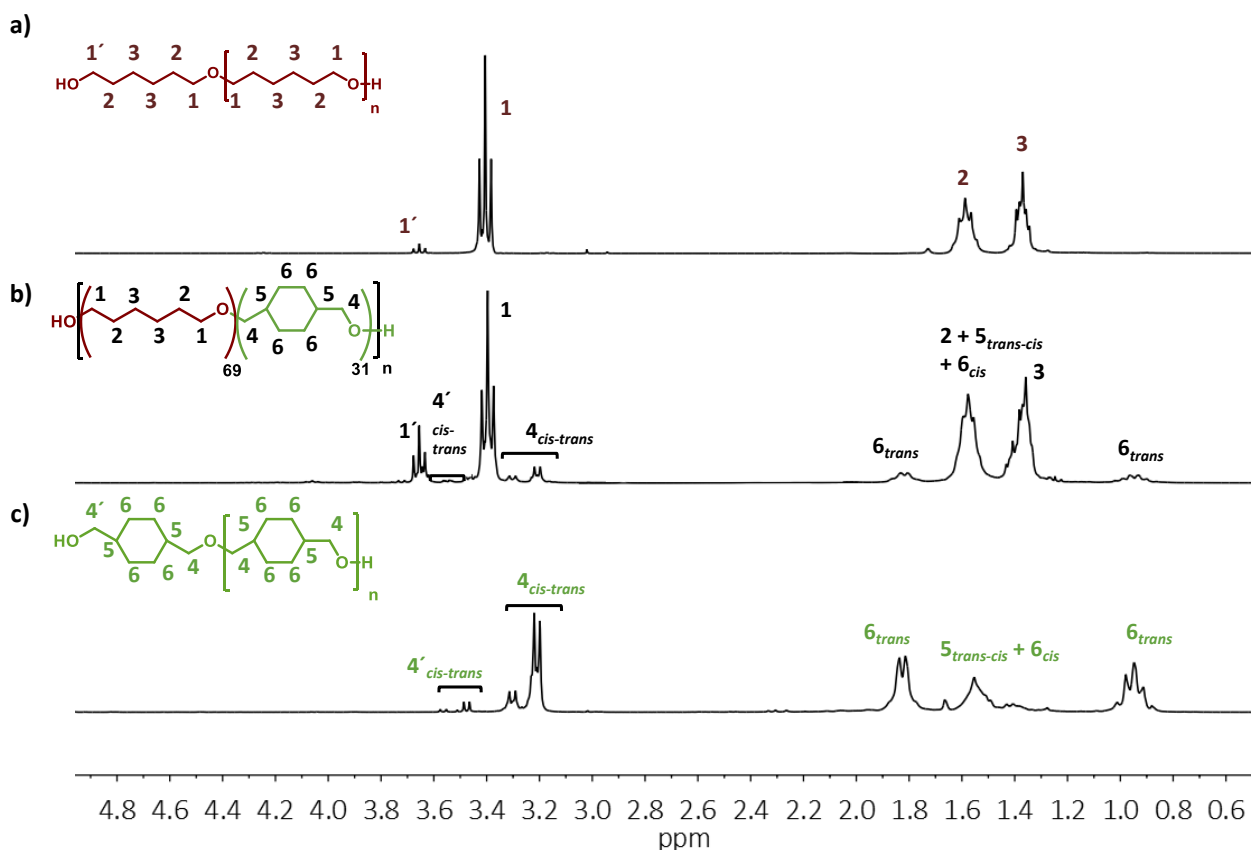
Figure 4.4. ^{1}H NMR spectra of a) poly(oxyhexamethylene) homopolymer, b) poly(oxyhexamethylene-co-1,4-cyclohexanedimethanol) copolymer 69/31 and c) poly(1,4-cyclohexanedimethanol) homopolymer.

The molecular weights were analyzed by SEC and a monomodal distribution was obtained for all the samples confirming the copolymerization of both comonomers in a single polymer. The molecular weights obtained ranged from 7900 to 12300 g mol $^{-1}$ (Figure S4.2-4.9).

Table 4.1. Chemical composition and molecular characteristics of the copolyethers.

Entry	(HDO)/(CHDM) % in the feed	(HDO)/(CHDM) % in the polymer [a]	(CHDM) % cis/trans in the polymer[a]	M_n[b] (g/mol)	Đ	R[c]
1	100/0	-	-	10000	1.8	-
2	90/10	91/9	34/66	8000	1.7	1.4
3	80/20	83/17	28/72	8600	2.0	1.1
4	70/30	69/31	29/71	8700	1.5	0.98
5	50/50	52/48	30/70	7900	1.8	1.0
6	30/70	31/69	31/69	9100	1.7	1.0
7	20/80	22/78	27/73	10300	1.6	1.2
8	0/100	-	-	12300	2.0	

[a]Determined by ^{1}H NMR spectroscopy in CDCl$_3$, [b]Determined by SEC in CHCl$_3$, [c]Determined by ^{13}C NMR spectroscopy in CDCl$_3$

As it was also reported on Chaper 3 the copolymer microstructure (random, alternating, or blocky) has an enormous impact on the copolymer properties. Thus, the randomness character of the copolymers was evaluated using ^{13}C NMR spectroscopy.
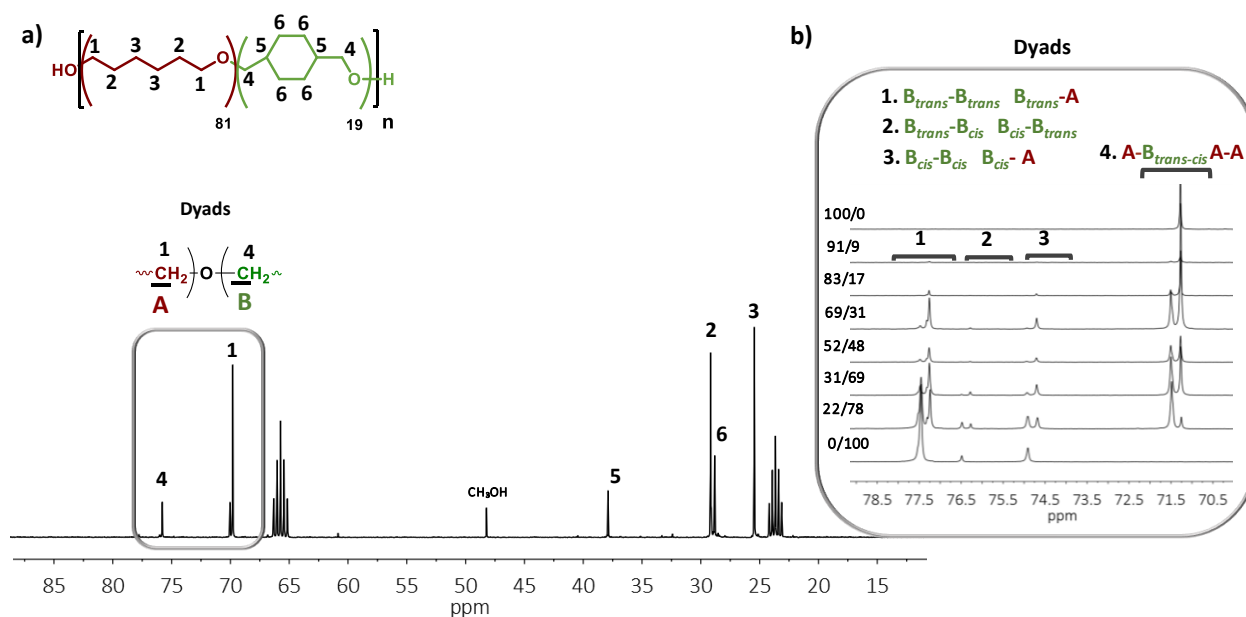
Figure 4.5. a) Chemical structure and ^{13}C NMR spectrum in deurerated THF of the copolyether (81/19) and b) region of the methylene carbons used for the R value determination.

Figure 4.5 shows the ^{13}C NMR spectrum of the copolymer HDO/CHDM (81/19) and the expanded region of the methylene carbons next to the ether linkage. In both homopolymers only one signal attributed to these carbons is observed. However, in the spectra of the copolymers new signals are observed along with those previously mentioned. These new signals are attributed to the presence of different dyads and were numbered from 1 to 4. The chemical shift of the methylene group linked to the ether bond corresponding to HDO and CHDM comonomers would be influenced by the adjacent group (region δ= 70.50-78.50 ppm). Together with the dyads 1 (CHDM-CHDM and CHDM-HDO) and 4 (HDO-HDO and HDO-CHDM) the influence of the isomer *cis* and *trans* in the shift of the carbon of the methylene group could also be noticed in dyads 2 and 3.

Based on the ^{13}C NMR spectra, the relative molar fraction of the interchange dyad numbered as 1 and 4 in the Figure 4.5 were determined, and the randomness character value (R) of the copoyethers was calculated using eq 1:

$$R = \frac{(\text{HDO-CHDM})}{2(\text{HDO})(\text{CHDM})} \quad (1)$$

Depending on the value of R, the copolymer can be considered blocky, random, or alternated. The values of R tend to 1 in all cases as summarized in Table 4.1, indicating the random nature of the prepared copolymers (Figure 4.5).

4.2.2. Thermal characterization of poly(oxyhexamethylene-co-1,4-cyclohexanediomethanol) copolyethers

The thermal properties of the random copolymers were investigated by Differential Scanning Calorimetry (DSC). The DSC curves for the copolymers were compared to that of homopolymers and are shown in the Figure 4.6. The related data obtained is summarized in Table 4.2.
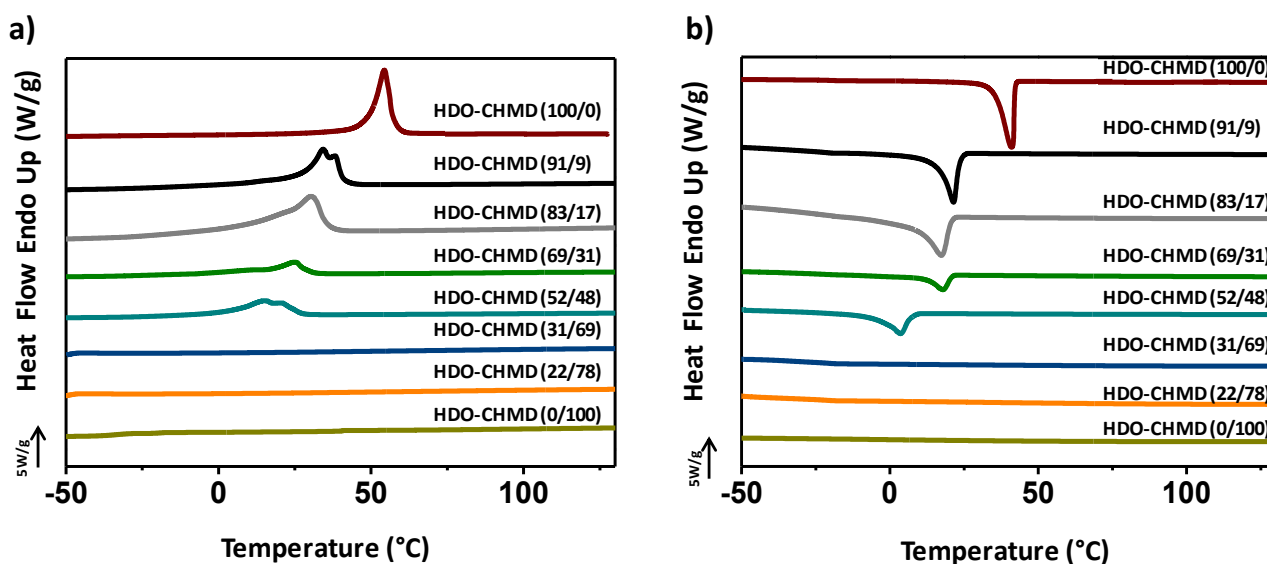
Figure 4.6. (a) Heating DSC scans and (b) subsequent cooling from the melt for the indicated polyethers and copolyethers.
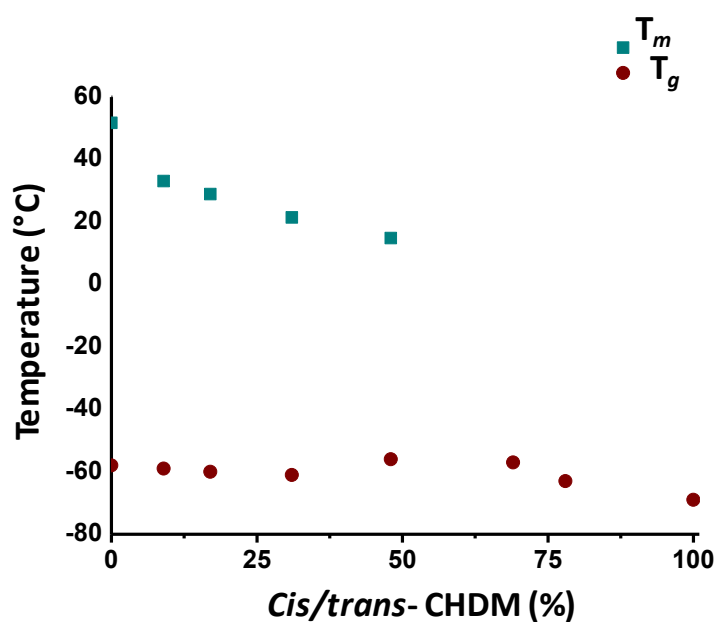
Figure 4.7. T_m and T_g variation in functions of *trans*-CHDM content in the copolymers.

Observing Figure 4.6, when the materials were cooled from the melt, it was noticed that crystallinity of the copolymers decreased with the increase of the CHDM content. The same behavior was observed for the melting temperature when analyzing the subsequent DSC heating scans. The decrease of the crystallizability is reasonable and it can be the result of the decrease of the symmetry and rigidity of CHDM which is a mixture of *cis- and trans*-isomers. Furthermore, the homopolyether synthetized from CHDM also shows an amorphous behavior. It is well known that when a mixture of isomers is used it can potentially decrease the chain regularity disturbing or hindering the crystallization of the material. Based on above DSC results, the determination of the T_g values of the copolyethers was not possible specially in the highly crystalline materials. Therefore, fast scanning calorimetry (FSC) measurements were carried in order to cool down the samples as fast as possible and be able to determine the $T_{g\ onset}$. In all cases low $T_{g\ onset}$ were reported and a small decrease of $T_{g\ onset}$ was observed when the CHDM content increases. Neverhteless, in all cases low $T_{g\ onset}$ materials were obtained with tunable crystallizations (Figure 4.7).

Table 4.2. Thermal Properties of the Copolyethers.

Sample (HDO/CHDM)	T_c (°C)	ΔH_c (J/g)	T_m (°C)	$T_{g\ onset}$ (°C)
100/0	33.0	-70	51.7	-58
91/9	22.4	-47	33.1	-59
83/17	17.5	-36	28.9	-60
69/31	13.1	-26	21.4	-61
52/48	4.7	-10	14.8	-56
31/69	-	-	-	- 57
22/78	-		-	-63
0/100	-		-	-69

4.2.3. Influence of CHDM cis-trans isomeric configuration on the thermal properties

In order to investigate the influence of the isomer content on the copolymer properties CHDM moieties with different content of *cis* and *trans* isomers were used. The 99 % *trans*-CHDM was used as received while the CHDM with higher *cis* isomer content was prepared and isolated following the method developed by Wang et al. Briefly the commercially available *cis/trans*-CHDM 30/70 was treated with acetic anhydride in order to obtain the diacetate derivates.[29] Then, *trans*-1,4-cyclohexanedimethanol diacetate and *cis*-1,4 cyclohexanedimethanol diacetate were isolated by crystallization in n-hexane. In order ot obtain the diol, *cis*-1,4-cyclohexanedimethanol diacetate was treated with aqueous sodium hydroxyde. We were able to reach a maximum of 90 % *cis*-CHDM confirmed by ^{1}H-NMR (Figure 4.8) Detailed process is included in the Experimental Section.
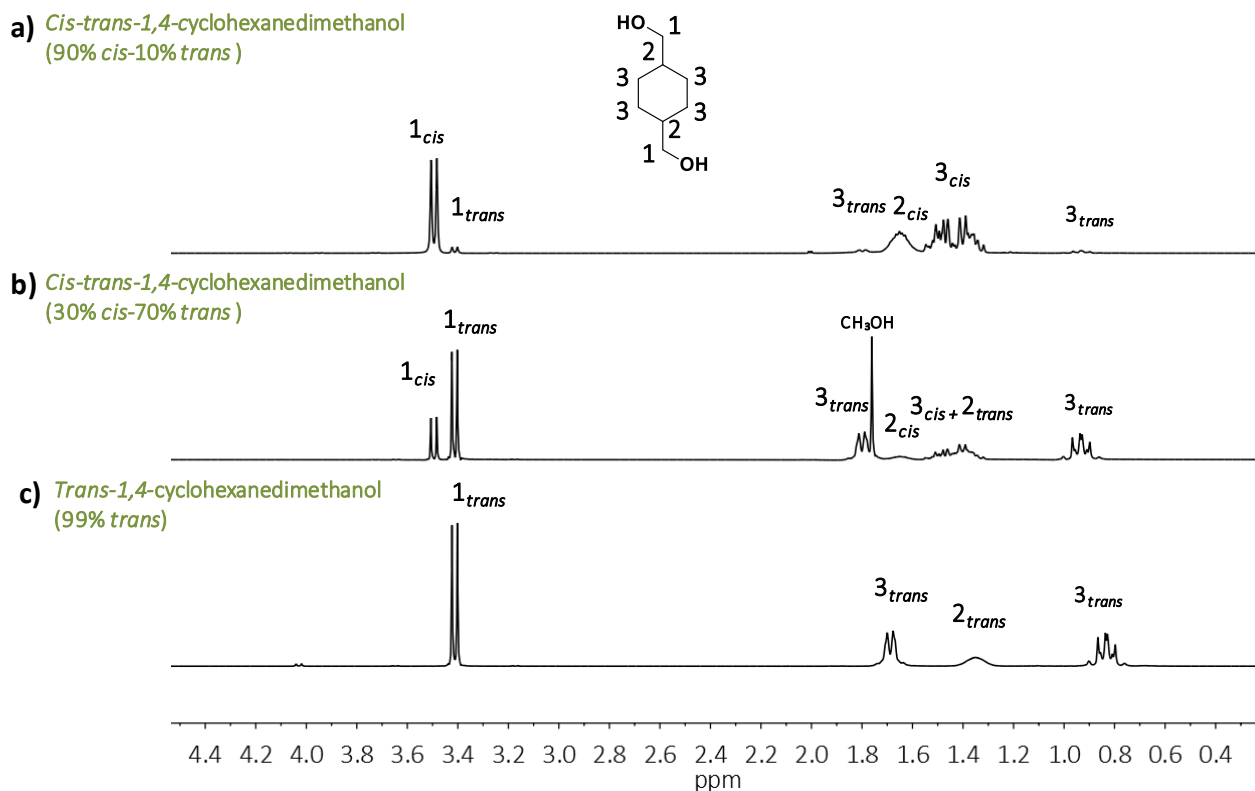
Figure 4.8. ^{1}H NMR spectra of a) 90/10% cis/trans-1,4-cyclohexanedimethanol, b) 30/70% cis/trans-1,4-cyclohexanedimethanol and c) 1/99% *cis/trans*-1,4-cyclohexanedimethanol.

With the comonomers 99% *trans*-CHDM and 90% *cis*-CHDM, copolymers were prepared at 3 different compositions 80/20, 50/50 and 20/80 to evaluate the effect of the isomer content in the thermal properties of the copolymers. Following the same procedure that in the previous section, the composition of the copolymers and the isomer *cis/trans* ratio were determined, and as it was expected, no changes in the isomer composition were observed and the (HDO)/(CHDM) % in the polymer was very similar to the % in feed (Table S4.1). In addition, a homopolymer containing 99% *trans*-CHDM was also synthetized and the DSC curve included in the Figure S4.14 proved its semicrystalline behavior. The related data obtained for these latest samples is summarized in the Table 4.3.

Table 4.3. Thermal Properties of the Copolyethers.

(CHDM) %*trans* in the feed	Sample (HDO/CHDM)	T_c (˚C)	ΔH_c (J/g)	T_m (˚C)
99	0/100	25	-39	45.2
99	80/20	21	-38	35.4
10	80/20	5.5	-11	12.1
99	50/50	7.3	-23	18.2
10	50/50	2.2	-5	7.7
99	20/80	17	-25	29.9
10	20/80	-	-	-

For a better reading, the Figure 4.9 represents the dependence of T_m in function of the (CHDM) % content in the copolymer and also in function of the *trans* isomer content of the CHDM comonomer.
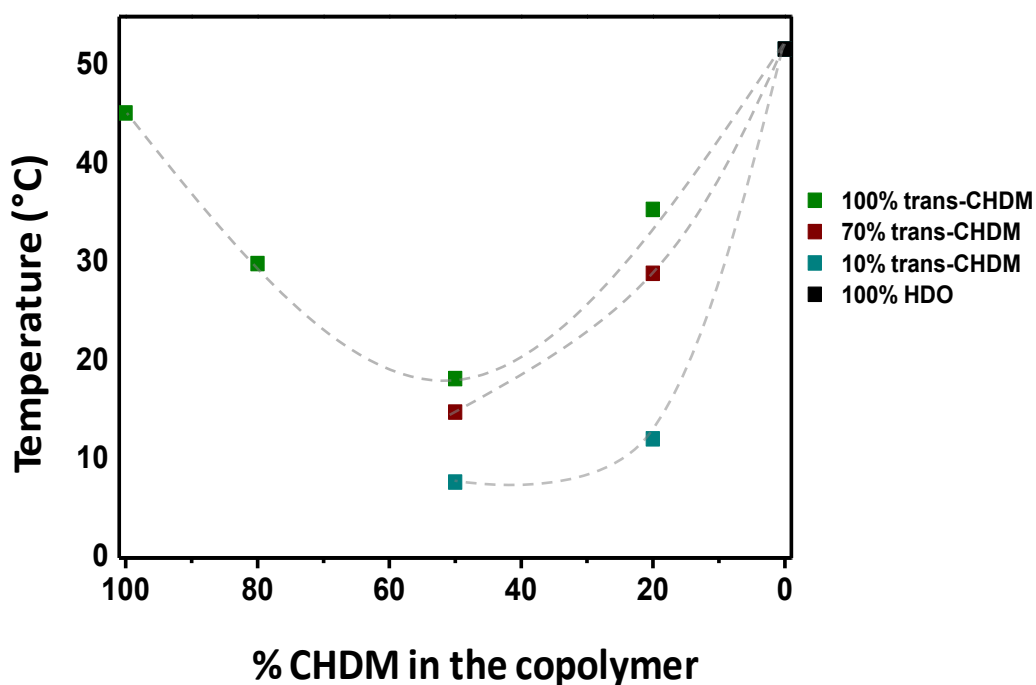
Figure 4.9. T_m variation in functions of *trans*-CHDM content in the CHDM comonomer and CHDM content in the copolymer

The copolymer HDO/CHDM 20/80 proved to be amorphous when containing 90% *cis*-CHDM but semicrystalline when containing 99% *trans*-CHDM. For the copolymers HDO/CHDM 80/20 and 50/50 the *trans/cis* ratio of the aliphatic ring led to significant variations in the T_m. In particular, by increasing the *trans* content, T_m showed a considerable increment. This trend was due to the stretched *trans* configuration of CHDM which improved the symmetry of the chain and the packing towards stable crystals.

The reason for the different effect of *cis/trans* configuration has been attributed to that the *trans* isomer is more symmetrical and favors the formation of stable crystals, while the *cis* isomer will disturb or hinder the crystallization.[29]

4.3. Conclusion

A series of fully biobased aliphatic poly(oxyhexamethylene-ran-1,4-cyclohexanedimethanol) copolyethers were synthesized by self-condensation of 1,6-hexanediol and 1,4-cyclohexanedimethanol using the NEMO MSA:TBD. The molecular structures of the copolymers were confirmed by NMR and the microstructure resulted to be random for all the samples. Their number-average molecular weights was determined by SEC and varied between 7900 and 10300 g mol^{-1}. Regarding to DSC, the crystallinity of the copolymers decreased with the increase of the CHDM content. The asymmetric nature of the CHDM employed which owned a mixture of isomers *cis*/*trans* could contribute to hinder the crystallization of the material. Due to the the cycloaliphatic nature of the diol an increase we did not observe significant changes in the $T_{g\ onset}$ of the materials. In a second part, it was observed that not only the content of CHDM comonomer led to variations in the thermal properties of the copolymers, but also their spatial conformation (*trans* or *cis* isomers).

When near pure *trans*-CHDM was used the melting temperature as well as the enthalpy of fushion increased substantially. On the other hand, the opposite effect was observed for the CHDM rich on *cis* isomer.

This behavior confirms the fact that by the increasing the *trans* isomer content the T_m increases, while the *cis* isomer trends to disturb or hinder the crystallization. This polycondensation route shows a simple and sustainable way to synthesize fully bio-based polyethers with comprehensive properties and turnable crystallinity while maintaining the $T_{g\ onset}$ low which make them ideal candidates for the preparation of a great variety of elastomers.

4.4. Experimental Section

4.4.1 Materials

1,6-Hexanediol (99% Sigma-Aldrich), 1,4-cyclohexanedimethanol (99% and *cis/trans* 30/70% Sigma-Aldrich) were used as received after being dried in toluene. Methanesulfonic acid (MSA, 99%) and 1,5,7-triazabicyclo[4.4.0]dec-5-ene (TBD, 98%), sodium hydroxide (NaOH), acetic anhydride (($CH_3CO)_2O$), n-hexane (C_6H_{14}), chloroform ($CHCl_3$), methanol (CH_3OH) and the rest of the solvents used on this work were supplied by Sigma-Aldrich and used as received.

4.4.2 Synthesis of the copolyethers

The synthesis of copolyethers was performed by self-condensation of two different diols: 1,6-hexanediol and 1,4-cyclohexanedimethanol. The copolymers were named as HDO/CHDM mol% as the molar percentage of 1,6-hexanediol and 1,4-cyclohexanedimethanol used in the feed.

In the first step the NEMOs were prepared by simple non-stoichiometric mixture (3:1) of methanesulfonic acid (MSA) and 1,5,7-triazabicyclo[4.4.0]dec-5-ene (TBD). The mixtures were thermally treated at 90 °C over 30 minutes under stirring until complete formation of homogeneous and transparent liquid solution.

After the catalyst preparation, a mixture of monomers containing different 1,6-hexanediol/1,4-cyclohexanedimethanol (HDO/CHDM) ratios: 100/0 (5.00 g, 0.042 mol), 90/10 (4.40 g, 0.037 mol/0.60 g, 4.14 10^{-3} mol), 80/20 (3.83 g, 0.032 mol/1.17 g, 8.10 10^{-3} mol), 70/30 (3.28 g, 0.028 mol/1.72 g, 0.012 mol), 50/50 (2.25 g, 0.019 mol/2.75 g, 0.019 mol), 30/70 (1.30 g, 0.011 mol/3.70 g, 0.026 mol), 20/80 (0.85 g, 7.19 10^{-3}/4.15 g, 0.029 mol), 0/100 (5.00 g, 0.035 mol) and were added respectively to 0.05 equiv. organocatalyst.

The sealed reaction vessels were then submerged into a pre-heated oil bath at 130 °C under vacuum. The self-condensation process was performed in three steps. After the first 24 h at 130 °C, the temperature was increased to 180 °C for 24 h and to 200 °C for the last 24 h. After completion, the copolyethers were slowly cooled down to room temperature. For the purification, the samples were dissolved in chloroform and precipitated in cold methanol. The resulted copolyethers were filtrated and dried under vacuum at RT for 24 h before their characterization. Homopolymers from 1,6-hexanediol and 1,4-cyclohexanedimethanol were synthesized and purified by the same procedure.

4.4.3 Preparation of *cis/trans*-CHDM 90/10%

75 g (0.52 mol, 1 eq.) of commercially available CHDM mixture with a content of 32 % of *cis* isomer and acetic anhydride, 127 g (1.25 mol, 2.4 eq.) was added to a round-bottom flask and refluxed at 140 °C for 3 h. After removal the acetic acid formed at the acylation step under reduced pressure, the obtained solid was dissolved in a minimum

amount of n-hexane at 50 °C for crystallization. The solution was gradually cooled down and kept at the freezer overnight. Then the crystals were formed they were collected via filtration. The solvent was removed from the *cis*-isomer rich filtrate under reduced pressure and the obtained solid was dissolved in 20 mL of ethanol.

To this solution, 200 mL of 4 M aqueous NaOH solution was slowly added and stirred at 40 °C for 2 h. Afterwards, 400 mL of ethyl acetate was added into the previous solution for product extraction. The ethyl acetate solution was dried using anhydrous magnesium sulfate and the solvent was removed using reduced pressure. 10 g of product was obtained with a *cis*-CHDM content of 90 % confirmed by ^{1}H-NMR.

4.5. References

(1) Brodin, M.; Vallejos, M.; Opedal, M. T.; Area, M. C.; Chinga-Carrasco, G. Lignocellulosics as Sustainable Resources for Production of Bioplastics – A Review. *J. Clean. Prod.* **2017**, *162*, 646–664. https://doi.org/10.1016/j.jclepro.2017.05.209.

(2) Christensen, C. H.; Rass-Hansen, J.; Marsden, C. C.; Taarning, E.; Egeblad, K. The Renewable Chemicals Industry. *ChemSusChem* **2008**, *1* (4), 283–289. https://doi.org/10.1002/cssc.200700168.

(3) Galbis, J. A.; García-Martín, M. de G.; de Paz, M. V.; Galbis, E. Synthetic Polymers from Sugar-Based Monomers. *Chem. Rev.* **2016**, *116* (3), 1600–1636. https://doi.org/10.1021/acs.chemrev.5b00242.

(4) Liang, Y.; Li, L.; Scott, R. A.; Kiick, K. L. 50th Anniversary Perspective: Polymeric Biomaterials: Diverse Functions Enabled by Advances in Macromolecular Chemistry. *Macromolecules* **2017**, *50* (2), 483–502. https://doi.org/10.1021/acs.macromol.6b02389.

(5)   Sheldon, R. A. Metrics of Green Chemistry and Sustainability: Past, Present, and Future. *ACS Sustain. Chem. Eng.* **2018**, *6* (1), 32–48. https://doi.org/10.1021/acssuschemeng.7b03505.

(6)   Iwata, T. Biodegradable and Bio-Based Polymers: Future Prospects of Eco-Friendly Plastics. *Angew. Chem. Int. Ed.* **2015**, *54* (11), 3210–3215. https://doi.org/10.1002/anie.201410770.

(7)   Sheldon, R. A. The Road to Biorenewables: Carbohydrates to Commodity Chemicals. *ACS Sustain. Chem. Eng.* **2018**. https://doi.org/10.1021/acssuschemeng.8b00376.

(8)   Papageorgiou, G. Z. Thinking Green: Sustainable Polymers from Renewable Resources. *Polymers* **2018**, *10* (9), 952. https://doi.org/10.3390/polym10090952.

(9)   Vilela, C.; Sousa, A. F.; Fonseca, A. C.; Serra, A. C.; Coelho, J. F. J.; Freire, C. S. R.; Silvestre, A. J. D. The Quest for Sustainable Polyesters – Insights into the Future. *Polym. Chem.* **2014**, *5* (9), 3119–3141. https://doi.org/10.1039/C3PY01213A.

(10)   Caretto, A.; Passoni, V.; Brenna, N.; Sitta, M.; Ogliosi, L.; Catel, G.; Turri, S.; Griffini, G. Fully Biobased Polyesters Based on an Isosorbide Monomer for Coil Coating Applications. *ACS Sustain. Chem. Eng.* **2018**. https://doi.org/10.1021/acssuschemeng.8b02659.

(11)   Park, S.-A.; Choi, J.; Ju, S.; Jegal, J.; Lee, K. M.; Hwang, S. Y.; Oh, D. X.; Park, J. Copolycarbonates of Bio-Based Rigid Isosorbide and Flexible 1,4-Cyclohexanedimethanol: Merits over Bisphenol-A Based Polycarbonates. *Polymer* **2017**, *116*, 153–159. https://doi.org/10.1016/j.polymer.2017.03.077.

(12)   Furtwengler, P.; Perrin, R.; Redl, A.; Avérous, L. Synthesis and Characterization of Polyurethane Foams Derived of Fully Renewable Polyester Polyols from Sorbitol. *Eur. Polym. J.* **2017**, *97*, 319–327. https://doi.org/10.1016/j.eurpolymj.2017.10.020.

(13) Kasmi, N.; Majdoub, M.; Papageorgiou, G. Z.; Bikiaris, D. N. Synthesis and Crystallization of New Fully Renewable Resources-Based Copolyesters: Poly(1,4-Cyclohexanedimethanol-Co-Isosorbide 2,5-Furandicarboxylate). *Polym. Degrad. Stab.* **2018**, *152*, 177–190. https://doi.org/10.1016/j.polymdegradstab.2018.04.009.

(14) Chen, T.; Jiang, G.; Li, G.; Wu, Z.; Zhang, J. Poly(ethylene Glycol-Co-1,4-Cyclohexanedimethanol Terephthalate) Random Copolymers: Effect of Copolymer Composition and Microstructure on the Thermal Properties and Crystallization Behavior. *RSC Adv.* **2015**, *5* (74), 60570–60580. https://doi.org/10.1039/C5RA09252C.

(15) Caretto, A.; Passoni, V.; Brenna, N.; Sitta, M.; Ogliosi, L.; Catel, G.; Turri, S.; Griffini, G. Fully Biobased Polyesters Based on an Isosorbide Monomer for Coil Coating Applications. *ACS Sustain. Chem. Eng.* **2018**. https://doi.org/10.1021/acssuschemeng.8b02659.

(16) Winnacker, M.; Rieger, B. Biobased Polyamides: Recent Advances in Basic and Applied Research. *Macromol. Rapid Commun.* **2016**, *37* (17), 1391–1413. https://doi.org/10.1002/marc.201600181.

(17) Moran, C. S.; Barthelon, A.; Pearsall, A.; Mittal, V.; Dorgan, J. R. Biorenewable Blends of Polyamide-4,10 and Polyamide-6,10. *J. Appl. Polym. Sci.* **2016**, *133* (45). https://doi.org/10.1002/app.43626.

(18) Zhang, C.; Kessler, M. R. Bio-Based Polyurethane Foam Made from Compatible Blends of Vegetable-Oil-Based Polyol and Petroleum-Based Polyol. *ACS Sustain. Chem. Eng.* **2015**, *3* (4), 743–749. https://doi.org/10.1021/acssuschemeng.5b00049.

(19) Smith, P. B. Bio-Based Sources for Terephthalic Acid. In *Green Polymer Chemistry: Biobased Materials and Biocatalysis*; ACS Symposium Series; American Chemical

Society, 2015; Vol. 1192, pp 453–469. https://doi.org/10.1021/bk-2015-1192.ch027.

(20) Chatti, S.; Bortolussi, M.; Loupy, A.; Blais, J. C.; Bogdal, D.; Majdoub, M. Efficient Synthesis of Polyethers from Isosorbide by Microwave-Assisted Phase Transfer Catalysis. *Eur. Polym. J.* **2002**, *38* (9), 1851–1861. https://doi.org/10.1016/S0014-3057(02)00071-X.

(21) Saxon, D. J.; Nasiri, M.; Mandal, M.; Maduskar, S.; Dauenhauer, P. J.; Cramer, C. J.; LaPointe, A. M.; Reineke, T. M. Architectural Control of Isosorbide-Based Polyethers via Ring-Opening Polymerization. *J. Am. Chem. Soc.* **2019**, *141* (13), 5107–5111. https://doi.org/10.1021/jacs.9b00083.

(22) Hammami, N.; Majdoub, M.; Habas, J.-P. Structure-Properties Relationships in Isosorbide-Based Polyacetals: Influence of Linear or Cyclic Architecture on Polymer Physicochemical Properties. *Eur. Polym. J.* **2017**, *93*, 795–804. https://doi.org/10.1016/j.eurpolymj.2017.03.050.

(23) Tang, X.; Wei, J.; Ding, N.; Sun, Y.; Zeng, X.; Hu, L.; Liu, S.; Lei, T.; Lin, L. Chemoselective Hydrogenation of Biomass Derived 5-Hydroxymethylfurfural to Diols: Key Intermediates for Sustainable Chemicals, Materials and Fuels. *Renew. Sustain. Energy Rev.* **2017**, *77*, 287–296. https://doi.org/10.1016/j.rser.2017.04.013.

(24) Berti, C.; Binassi, E.; Colonna, M.; Fiorini, M.; Kannan, G.; Karanam, S.; Mazzacurati, M.; Odeh, I. Bio-Based Terephthalate Polyesters. US20100168372A1, July 1, 2010.

(25) He, J.; Burt, S. P.; Ball, M.; Zhao, D.; Hermans, I.; Dumesic, J. A.; Huber, G. W. Synthesis of 1,6-Hexanediol from Cellulose Derived Tetrahydrofuran-Dimethanol with Pt-WOx/TiO2 Catalysts. *ACS Catal.* **2018**, *8* (2), 1427–1439. https://doi.org/10.1021/acscatal.7b03593.

(26) Xiao, B.; Zheng, M.; Li, X.; Pang, J.; Sun, R.; Wang, H.; Pang, X.; Wang, A.; Wang, X.; Zhang, T. Synthesis of 1,6-Hexanediol from HMF over Double-Layered Catalysts of Pd/SiO2 + Ir–ReOx/SiO2 in a Fixed-Bed Reactor. *Green Chem.* **2016**, *18* (7), 2175–2184. https://doi.org/10.1039/C5GC02228B.

(27) Lligadas, G.; Ronda, J. C.; Galià, M.; Cádiz, V. Polyurethane Networks from Fatty-Acid-Based Aromatic Triols: Synthesis and Characterization. *Biomacromolecules* **2007**, *8* (6), 1858–1864. https://doi.org/10.1021/bm070157k.

(28) Tatara, A. M.; Watson, E.; Satish, T.; Scott, D. W.; Kontoyiannis, D. P.; Engel, P. S.; Mikos, A. G. Synthesis and Characterization of Diol-Based Unsaturated Polyesters: Poly(diol Fumarate) and Poly(diol Fumarate-Co-Succinate). *Biomacromolecules* **2017**, *18* (6), 1724–1735. https://doi.org/10.1021/acs.biomac.7b00044.

(29) Wang, J.; Liu, X.; Jia, Z.; Sun, L.; Zhang, Y.; Zhu, J. Modification of Poly(ethylene 2,5-Furandicarboxylate) (PEF) with 1, 4-Cyclohexanedimethanol: Influence of Stereochemistry of 1,4-Cyclohexylene Units. *Polymer* **2018**, *137*, 173–185. https://doi.org/10.1016/j.polymer.2018.01.021.

(30) Tsai, Y.; Fan, C.-H.; Hung, C.-Y.; Tsai, F.-J. Amorphous Copolyesters Based on 1,3/1,4-Cyclohexanedimethanol: Synthesis, Characterization and Properties. *J. Appl. Polym. Sci.* **2008**, *109* (4), 2598–2604. https://doi.org/10.1002/app.28385.

(31) Chen, T.; Zhang, W.; Zhang, J. Alkali Resistance of Poly(ethylene Terephthalate) (PET) and Poly(ethylene Glycol-Co-1,4-Cyclohexanedimethanol Terephthalate) (PETG) Copolyesters: The Role of Composition. *Polym. Degrad. Stab.* **2015**, *120*, 232–243. https://doi.org/10.1016/j.polymdegradstab.2015.07.008.

(32) Mondschein, R. J.; Dennis, J. M.; Liu, H.; Ramakrishnan, R. K.; Sirrine, J. M.; Weiseman, T.; Colby, R. H.; Nazarenko, S.; Turner, S. R.; Long, T. E. Influence of Bibenzoate Regioisomers on Cyclohexanedimethanol-Based (Co)polyester Structure–Property Relationships. *Macromolecules* **2019**. https://doi.org/10.1021/acs.macromol.8b02411.

(33) Vanhaecht, B.; Teerenstra, M. N.; Suwier, D. R.; Willem, R.; Biesemans, M.; Koning, C. E. Controlled Stereochemistry of Polyamides Derived from Cis/Trans-1,4-Cyclohexanedicarboxylic Acid. *J. Polym. Sci. Part Polym. Chem.* **2001**, *39* (6), 833–840. https://doi.org/10.1002/1099-0518(20010315)39:6<833::AID-POLA1056>3.0.CO;2-5.

(34) Celli, A.; Marchese, P.; Sisti, L.; Dumand, D.; Sullalti, S.; Totaro, G. Effect of 1,4-Cyclohexylene Units on Thermal Properties of poly(1,4-Cyclohexylenedimethylene Adipate) and Similar Aliphatic Polyesters. *Polym. Int.* **2013**, *62* (8), 1210–1217. https://doi.org/10.1002/pi.4409.

(35) Berti, C.; Celli, A.; Marchese, P.; Marianucci, E.; Barbiroli, G.; Credico, F. D. Influence of Molecular Structure and Stereochemistry of the 1,4-Cyclohexylene Ring on Thermal and Mechanical Behavior of Poly(butylene 1,4-Cyclohexanedicarboxylate). *Macromol. Chem. Phys.* **2008**, *209* (13), 1333–1344. https://doi.org/10.1002/macp.200800125.

(36) Wang, J.; Mahmud, S.; Zhang, X.; Zhu, J.; Shen, Z.; Liu, X. Biobased Amorphous Polyesters with High Tg: Trade-Off between Rigid and Flexible Cyclic Diols. *ACS Sustain. Chem. Eng.* **2019**. https://doi.org/10.1021/acssuschemeng.9b00285.

(37) Basterretxea, A.; Gabirondo, E.; Flores, I.; Etxeberria, A.; Gonzalez, A.; Müller, A. J.; Mecerreyes, D.; Coulembier, O.; Sardon, H. Isomorphic Polyoxyalkylene Copolyethers Obtained by Copolymerization of Aliphatic Diols. *Macromolecules* **2019**. https://doi.org/10.1021/acs.macromol.9b00469.

(38) Brunelle, D. J.; Jang, T. Method for Preparing poly(1,4-Cyclohexanedicarboxylates). US6084055A, July 4, 2000.

Chapter 5

Graphical abstract
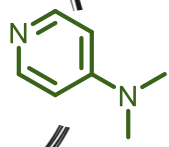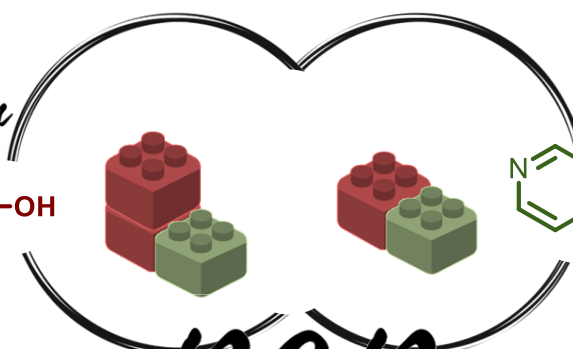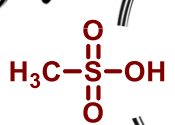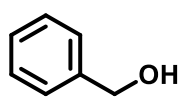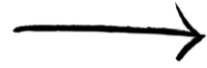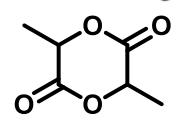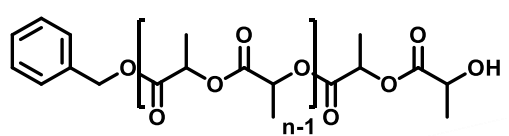
Chapter 5. Bulk Ring-Opening Polymerization (ROP) of L-lactide catalyzed by a Non-Eutectic Mixture Organocatalyst (NEMO)

5.1. Introduction

The development of sustainable polymers is one of the most significant challenges of the 21st century.[1] Our current plastic production model is far from being sustainable. One option to reduce the demand for petroleum derived materials and to minimize the negative impact on the environment is the development of a circular economy approach where polymers can be obtained from the biomass for which biodegradability is included in their performance. Among the polymers that can be both biosourced and biodegradable, polylactide (PLA) attracts special attention since it has demonstrated to be a successful substitute for plastics of petroleum origin, specially in short term food packaging applications.[2–4] Typically, they are strong but brittle materials with comparable mechanical properties to polystyrene. Owing to their intrinsic biodegradability, biocompatibility and mechanical properties PLA has become one of the most consumed biomaterial in the world in many different areas of life including biomedicine, pharmacy, or packaging.[5] PLA can be produced by the polycondensation of lactic acid or by the ring-opening polymerization (ROP) of the L/D-lactide cyclic esters.[2,6]

The actual industrial production of PLA requires the use of metal catalysts such as SnOct$_2$ which show high thermal stability and activity at low catalyst loadings. However, the elimination of the catalyst is complicated, which compromises in some cases its applicability and could generate some problems when the PLA is degraded in

the environment.[7–10] Considering that the PLA is mainly aimed at biomedical and packaging applications, the new European Union regulations are increasingly restricting the use of tin-based catalysts since it has been shown that the residual catalyst in the polymer can penetrate the tissues and the circulation system of the blood causing toxicity effects.[11] In addition, the residual catalyst can also provoke detrimental effects on the ageing of the final material. In light of this, both industry and acamedia are looking for alternatives in order to implement more sustainable chemistries for the production of PLA.[12,13]

Some of such organocatalysts present lower toxicity than their organometallic counterparts and, for the most, can be safely used in biomedical and electronic applications while they can be easily removed from the final PLA material. However, while numeours publications could be found in the literature related with the ROP of L-lactide in solution, there remains a significant challenge before such approaches can be applied to bulk polymerizations which require temperatures above 130 °C. Besides the difficulty of avoiding side reactions such as racemizations, transesterifications or macrocyclizations, organocatalysts suffer from a low thermal stability and the harsh used-conditions lead to their deactivation, gender a poor control over the reaction and indirectly induce the brownish of the final product.[14,15] Thus, overcoming these issues and substitute metal complexes by organic compounds presents significant challenges (Figure 5.1). [16,17]
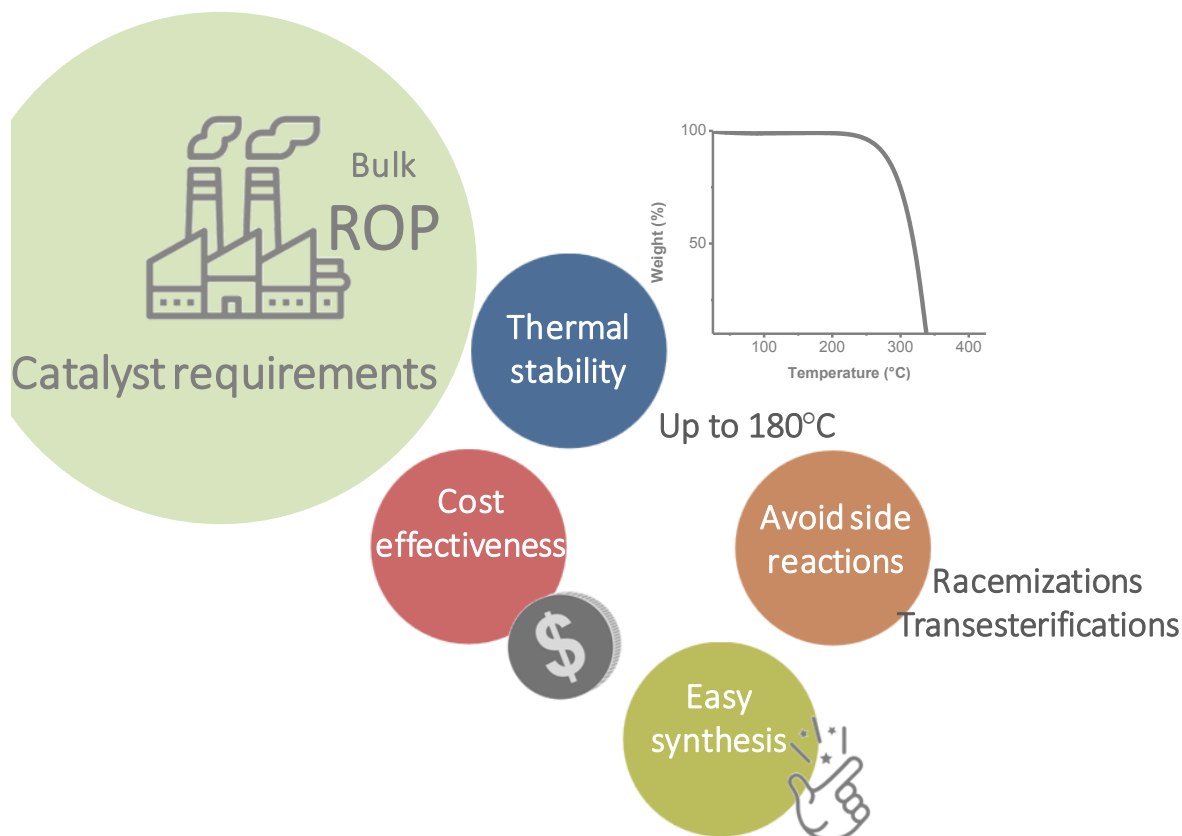
Figure 5.1. Scheme of the requirements that an organocatalyst has to meet in order to be efficient in industrial PLA synthesis.

The organic candidate should resist to temperatures of at least 130 °C (temperature required in bulk conditions) without suffering any catalyst deactivation. The catalyst must also be cost-effective and accessible. Regarding the final product, polymers with high yield, controlled molecular weights and narrow dispersities should be obtained. Besides that, racemization, transesterification reactions and macrocyclizations should be minimized in order to obtain high molecular weight PLLA with high cristallinity degrees. [18,19].

To the best of our knowledge an organic substitute to metallic catalysts with similar performance has not been reported for the ROP of L-lactide in bulk.

However, significant advances have been made over the last decades. A variety of

organic molecules, enzymes, bicomponent and nature inspired systems have been considered as potential catalysts of a well controlled bulk ROP of lactide[17,20–23]. One possibility which is gaining more and more attention is related with the use of acid-base adducts as strategy to address the challenge of the catalyst's thermal stability.[24–26] These acid-base mixture organocatatlys have demonstrated to allow the implementation of industrial bulk conditions in diverse organocatalyzed polymerizations and moreover, they comply with some of the aforementioned requirements since they are inexpensive, widely available and easy to prepare by the combination of different acidic and basic organic molecules. In particular, acid-base complexes based on 4-dimethylaminopyridine (DMAP) have shown great advances in the ROP of LA during the last years. More than a decade after DMAP was first employed as organocatalyst of the ROP of LA, it still is among the the most efficient catalyst in terms of reaction productivity. It shows excellent ROP activity, high reaction rates and has even been tested at 185 °C in spite of its relative poor thermal stability which generates important coloration of the PLA.[27] In addition DMAP is a highly active catalyst which promotes the polymerization in an uncontrolled manner. In this regard, a way to enhance its thermal stability and to reduce its strong activity is the formation of H-bond adducts by combining the DMAP with an organic acid resulting in a more thermally stable catalyst.[17,28–30]

Hence, the group of Peruch explored different Non-Eutectic Mixtures Organocatalyst (NEMO) DMAP:HX (2:1) in the ROP of LLA in the presence of protic initiators at 100 °C.[28] Between different acids tested the combination of DMAP and triflic acid 2:1 (DMAP:HOTf) displayed an outstanding catalytic activity and ables to mediate the synthesis of PLLA with M_n up to 14 kg mol^{-1} in 1 h. Monomer conversions up to 80%, no observed transesterification and narrow dispersities were also obtained.

However, when increasing the temperature to 130 °C, significant racemization reactions were observed. Following the same concept, a very recent study using DMAP and saccharin system 1:1 (DMAP:Sac) as L-lactide (LLA) and δ-valerolactone (VL) ROP catalyst in bulk at 140 °C was published.[31] For that purpose authors combined three commercial pyridines including DMAP, PPY, and pyridine with a stoichiometric ratio of saccharine. They observed that DMAP:Sac (1:1) was the most efficient salt for the ROP of LA. Thus, using a benzyl alcohol (BnOH) as an initiator resulted in high molecular weights (M_n= 14.32 $kg\,mol^{-1}$) and narrow dispersity indices within 11 h. However, they did not show any result to increase the molecular weights.

In this chapter we disclose two protic organic ionic complexes that allow us to obtain PLLA of molecular weights higher than 15 kg mol^{-1} in bulk without coloration of the sample. A stoichimetric (1:1) and non-stoichiometric (2:1) mixtures of MSA and DMAP were performanced as catalysts in the ROP of L-lactide in bulk at 130 °C. First, the two mixtures of MSA and DMAP were prepared forming two different acid-base complexes which were extensively characterized. Their catalytic activity was assessed in the ROP of L-lactide in bulk obtaining good yields and narrow dispersities. The resulted PLA were deeply characterized and the differences in terms of kinetics and stereoregularity of the samples were attested. To expand the scope of the Non-Eutectic Mixture Organoctalyst (NEMO) MSA:DMAP (2:1) the catalyst was employed at industrially relevant temperature (180 °C) with great success and was also implemented for the synthesis of both poly(ε-caprolactone) and poly(L-lactide)-*b*-poly(ε-caprolactone) diblock copolymers.

5.2. Results and discussion

5.2.1. Characterization of the acid base organocatalysts based on MSA and DMAP

Firstly, we synthesized and characterized the acid-base mixture organocatalysts. For that, a stoichiometric mixture (1:1) and a non-stoichiometric mixture (2:1) of methanesulfonic acid (MSA) and 4-dimethylaminopyridine (DMAP) were prepared at 90 °C for 30 minutes (Figure 5.2). A white homogeneous solid was obtained for the 1:1 mixture and the 2:1 mixture resulted in a transparent liquid. In order to confirm the proton exchange and the formation of complexes the resulting mixtures were characterized by ^{1}H NMR and ^{15}N NMR spectroscopies in DMSO.
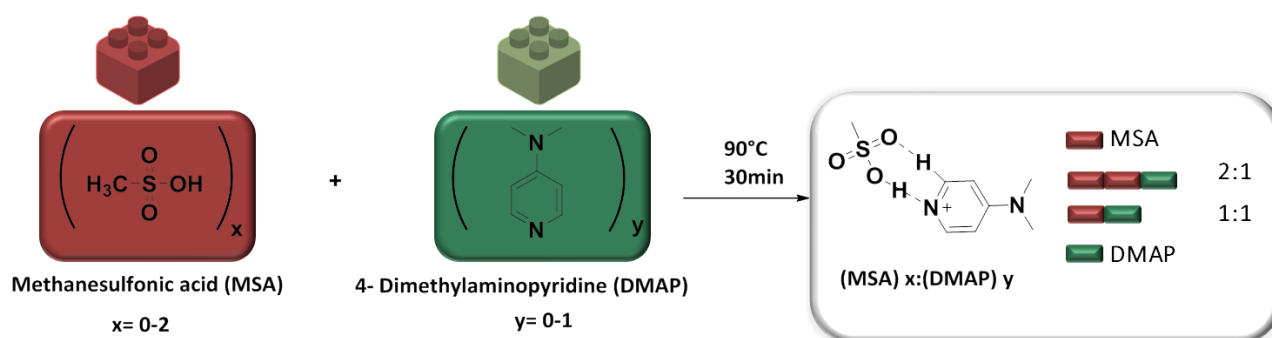
Figure 5.2. Scheme of the synthesis of the protic ionic compound (1:1) and the Non-Eutectic acid base Organocatalysts (NEMOs: 2:1).

^{1}H NMR spectra of pure MSA and DMAP show the characteristic O-H proton of the acid of MSA at δ = 14.16 ppm and the proton signals of the aromatic ring of DMAP at δ = 8.09 and 6.59 ppm.
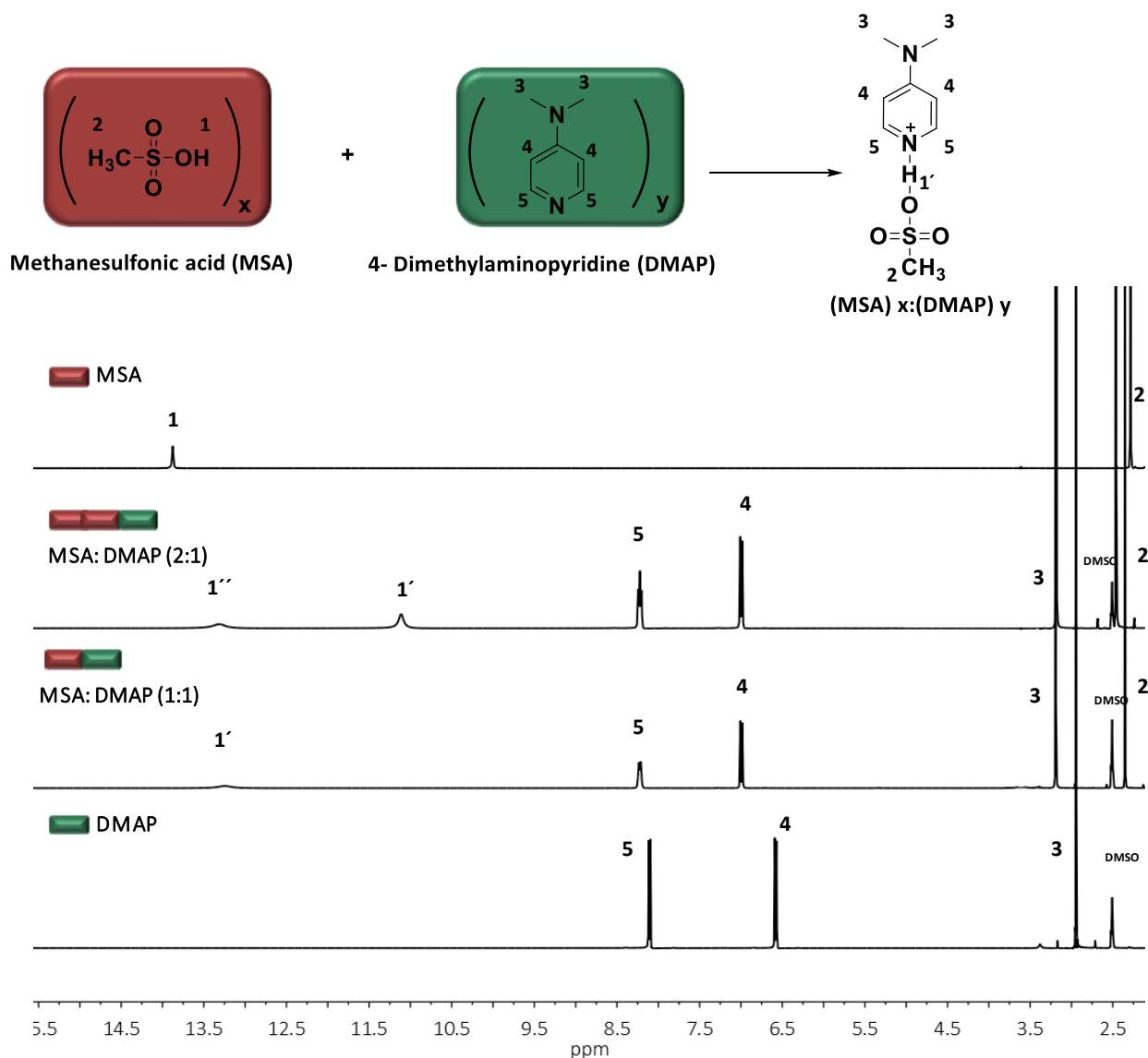
Figure 5.3. ^{1}H NMR spectroscopy in DMSO of the methanesulfonic acid (MSA), 14-Dimethylaminopyridine (DMAP) and the acid base mixtures (2:1 and 1:1).

In contrast, for the (1:1) mixture, due to the protonation of the N of the aromatic ring of the DMAP their proton signals sifted from δ = 8.09 and 6.59 ppm to 8.22 and 6.98 ppm as well as the signal of the acid proton of the MSA which shifted to lower ppm values, from δ = 14.16 ppm to δ = 13.26 ppm. Also, the signal corresponding o the methyl protons also shifted from δ = 2.95 ppm to δ = 3.61 ppm. This demonstrates the formation of the protic ionic salt by a proton transfer from MSA to DMAP (Figure 5.3).

For the NEMO 2:1 the same behavior was observed for the protons corresponding to the aromatic ring of the DMAP. However, in this case, we believe that the proton signal corresponding to the protonated aromatic ring shifted to even lower ppm (δ = 11.11 ppm) in comparison to the same proton signal but of the 1:1 sample. Together with that, the proton of the additional MSA of the mixture 2:1 was attributed to the signal at δ = 11.11 ppm. The appearance of chemical shifts in the ^{1}H NMR spectra of both mixtures as compared to these of the pure components confirms the presence of intramolecular H-bonds between all components of the mixture (Figure 5.3). To gain better insights, ^{15}N NMR spectroscopy was also used to ensure the protonation of the DMAP and the formation of the protic ionic complexes. As it is represented in Figure 5.4 for both MSA:DMAP mixtures the N signals attributed to the N in aromatic ring (brown) and the N of the amine group $N(CH_3)_2$ (green) are shifted to lower field upon protonation, being the N in aromatic ring (brown) more shifted when considering the pure DMAP signals. This result hints that the N of the aromatic ring is the one protonated in both acid-base mixtures. In addition, the small N intensity of the amine group can be probably the result of the extremely long relaxation time of the unprotonated nitrogen site.
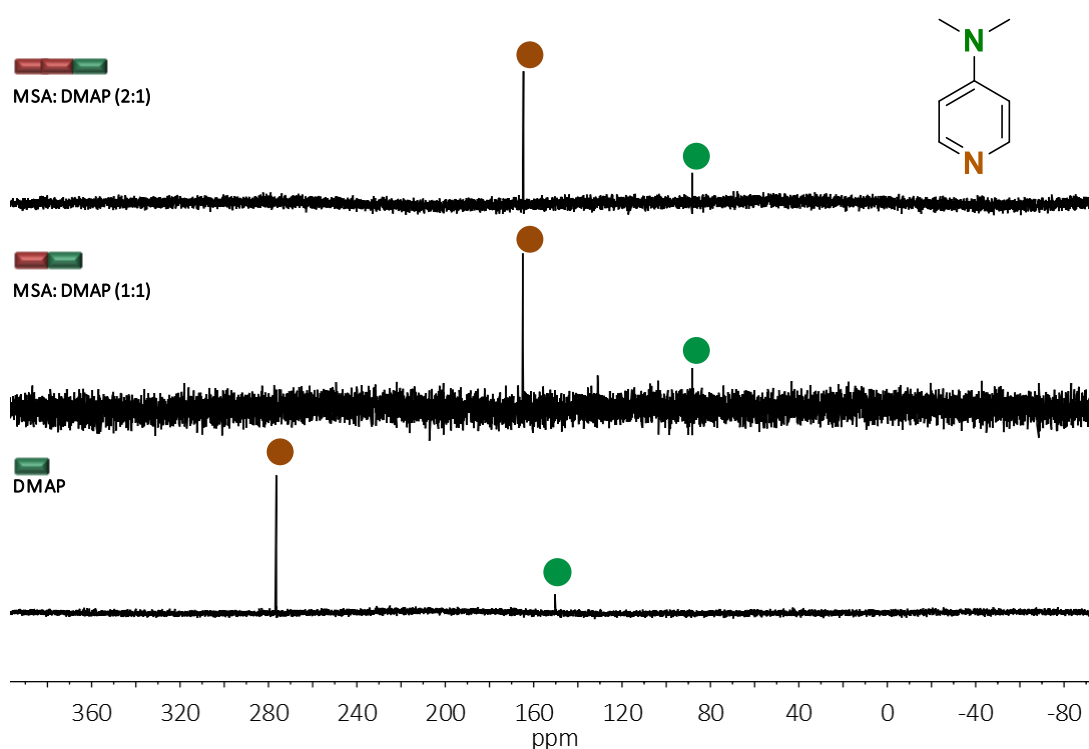
Figure 5.4.^{15}N NMR spectroscopy in DMSO of the different MSA:DMAP stoichiometric and non-stochiometric mixtures and DMAP.

According to these evidences of both NMRs it is suggested that for the NEMO MSA:DMAP 2:1 not only does one of the acidic proton of MSA$_1$ transfer to the basic N of the aromatic ring of the DMAP, but also that the acidic proton of MSA$_2$ forms a hydrogen bond with probably the MSA$_1$ without protonating the aliphatic N. To try to clarify the statements made and to get better insights into the molecular structures of MSA:DMAP (2:1) and (1:1), both complexes have been investigated by means of quantum chemical calculations using ωB97XD/6-311++G(2df,2p) (Figure 5.5).
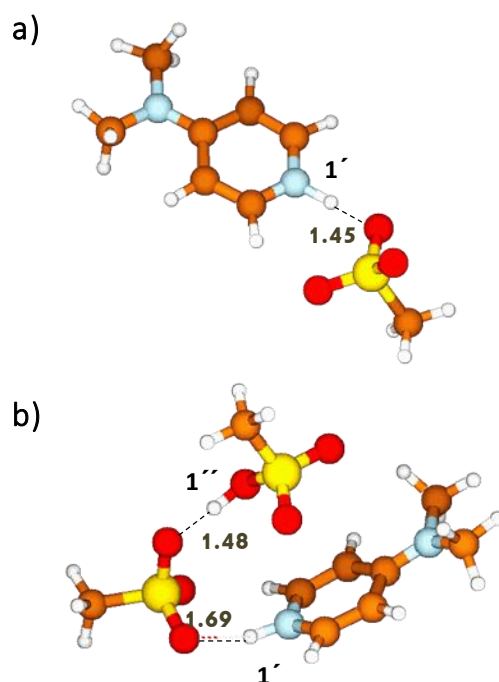
Figure 5.5 Calculated structures of MSA:DMAP (2:1) and (1:1).

The results obtained confirm two of the evidences previously observed. The first one refers the attribution of the MSA protons in the NMR spectra of both mixtures (Figure 5.3). Considering the distance in angstrom (Å) between the O of the MSA and the protonated N of the DMAP for the both optimized structures 1:1 and 2:1 (Figure 5.5 a and b, respectively) the distance observed for the NEMO 2:1 is higher (1.69 Å) than for the 1:1 (1.45 Å). This could explain the differences in ppm values observed in the NMR spectra, since the farther proton to the O of the MSA would be less acidic and thus it will appear at lower ppm values. Likewise, the distance obtained for the H of the MSA_2 and the MSA_1 is 1.48 Å, which is almost the same than the observed for the MSA:DMAP 1:1. This clarifies the similar ppm values observed for these two different prontons in the ^1H NMR spectra. Secontdly, these calculations also support the ^{15}N NMR analysis where only the protonation of the N of the aromatic ring was suggested.

In addition, the dissociation energy encountered using DFT calculations of the NEMO 2:1 was particularly high (41.3 kcal.mol^{-1}), being even higher than the dissociation energy obtained for the system 1:1 (19.4 kcal.mol^{-1}).

Thermogravimetric analyses (TGA) were also carried out to determine the resistance of both complexes to high temperature values in comparison to the individual components and the results supported previous DFT results (Figure 5.6). Among all, both catalytic systems resulted to be prominently stable up to 250 °C. These results revealed that the mixtures 1:1 and 2:1 were better resisting to temperature than MSA or DMAP as individual components, which is in good agreement with the high dissociation energies of both catalysts. Moreover, we found that the mixture 2:1 is forming a more thermally stable complex corroborating the calculations obtained by DFT.
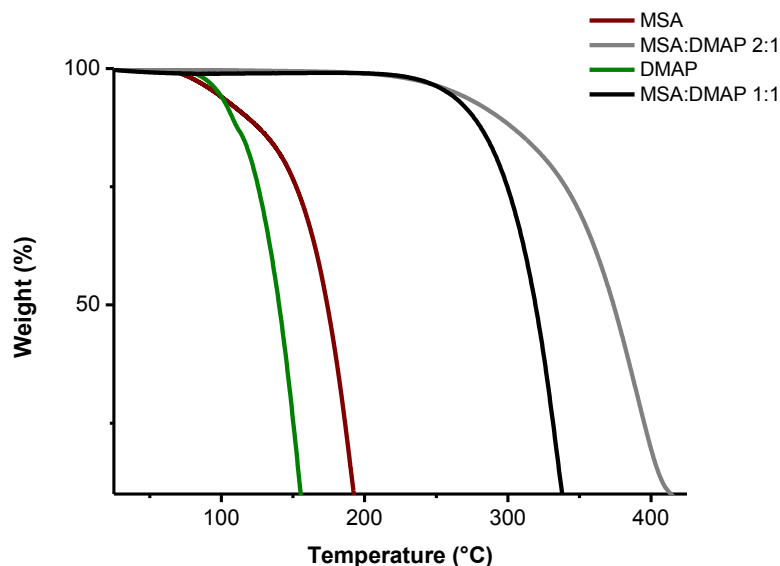
Figure 5.6 Thermogravimetric analysis of methanesulfonic acid (MSA), 14-Dimethylaminopyridine (DMAP) and the acid base mixtures (2:1 and 1:1).

5.2.2. Catalyst evaluation in the Ring Opening Polymerization of L-lactide in bulk
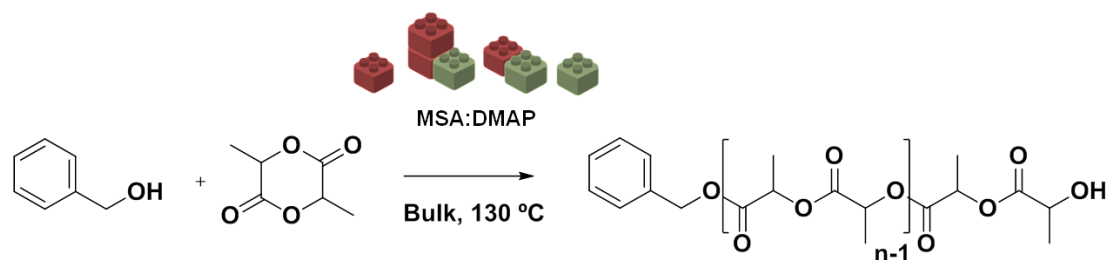
Figure 5.7. General scheme of the ROP of L-lactide catalyzed using different catalysts.

The catalytic activities of the MSA:DMAP organic systems (1:1 and 2:1) were first assessed for the ROP of L-lactide in bulk at 130 °C (Figure 5.7). Polymerizations were evaluated with BnOH as initiator targeting a total degree of polymerization of 100 ($DP_{tot}=[LLA]_0/[BnOH]_0 =100$) (Table 5.1., entries 3 and 4). Pure MSA and DMAP were also utilized as catalysts under the same experimental conditions (entries 1 and 2) as control experiments. In order to determine the performance of each catalyst, kinetic data were recordered for polymerizations performed at different reaction times. Aliquots of each kinetics were analyzed by ^{1}H NMR spectroscopy and quantitative monomer conversion values were calculated. For that, we monitored the diagnostic disappearance of the methine protons of the L-lactide monomer (signal at δ = 5.04 ppm) and their subsequent reappearance at δ = 5.17 ppm due to ring-opening (Figure 5.8).
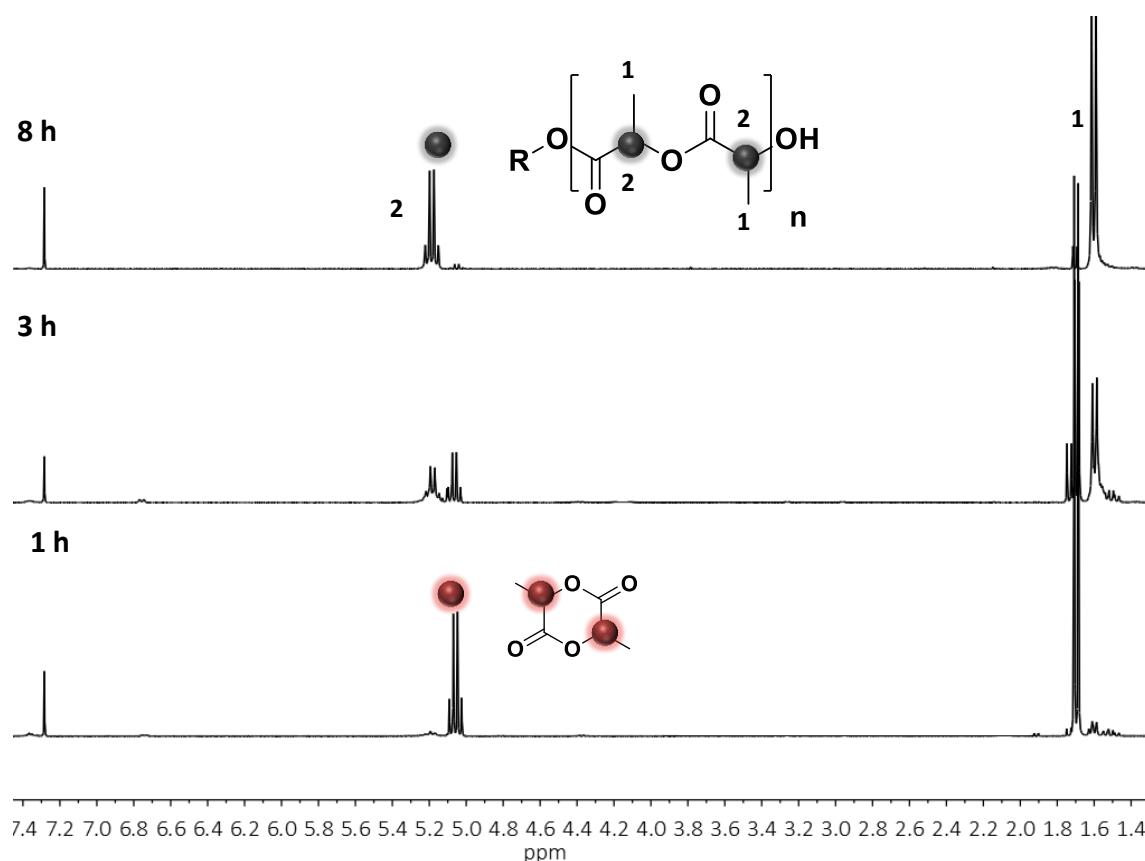
Figure 5.8 ^{1}H NMR spectra of the reaction media during the course of the reaction. The proton signals distinguished with red and grey dots were used for the calculation of the monomer conversion.

By using pristine MSA catalyst, only 20% conversion was achieved after 2 hours (entry 1). The plateau observed in the conversion evolution associated to the brownish color of the medium suggested the degradation of the catalyst at high temperature. In contrast, DMAP as individual catalyst resulted in 96% of monomer conversion after 3 h. Unfortunately, and as reported in the state-of-the-art, the polymer was yellowish due to its poor thermal stability (entry 2). The 1:1 catalytic system showed the best catalytic efficiency. After 2 h, 99% of monomer conversion was observed and the PLLA was transparent (entry 3).

Table 5.1. Results and conditions of the ROP OF LLA in bulk initiated by BnOH.

Entry	[MSA]-[DMAP]	[BnOH]-[catalyst]-[M]	Time (h)	Conv. [a] (%)	$M_{n\,Theo}$ (g mol-1)[b]	M_n (^{1}H NMR)[a]	M_n-SEC(g mol-1)[c]	Đ[c]
1	1/0	1/1/100	2	20	-	-	-	-
2	0/1	1/1/100	3	96	13900	12000	13000	1.4
3	1/1	1/1/100	2	99	14400	14580	15000	1.2
4	2/1	1/1/100	15	97	14100	13720	15700	1.2
5	1/1	1/1/50	1	98	7200	6500	9000	1.2
6	2/1	1/1/50	4	96	7000	6600	8200	1.2
7	2/1	1/2/100	8	98	14200	14500	14300	1.2
8	2/1	1/2/100[e]	6	96	13900	14400	15200	1.2
9	2/1	1/2/100[f]	6	98	14200	14700	15800	1.2
10	2/1	1/2/200[e]	14	99	28600	32100	24500	1.2
11	2/1	1/2/400[e]	26	98	56600	56500	40100	1.3
12[g]	2/1	1/2/100	4	94	98	11100	9000	1.2

[a] Calculated by ^{1}H NMR [b] Calculated from the molar mass of l-lactide (144.12 g·mol^{-1}) × conversion × [the initial monomer]/[initiator ratio] plus the molar mass of the initiator [c]Determined by SEC in THF using polystyrene standards and correction factors, [d]DSC, [e]150 °C [f]180 °C [g]CLO

Similarly, in the system 2:1 the polymer was colorless but the reaction took much longer time to reach 97 % conversion (15 h) (entry 4). The kinetic plot (Figure 5.9a) displayed relationship of $\ln([M]_0/[M]_t)$ vs. time for a polymerization performed from a initial $[LA]_0/[BnOH]_0/[catalyst]_0$ of 100/1/1. Owing to the long reaction time required for the polymerization catalyzed by MSA:DMAP 2:1 the kinetic plot does not represent the whole course of the reaction but we found that in these 3 last cases (entry 2,3 and 4) the polymerization was showing a linear monomer conversion versus time since the beginning of the reaction the plot. Interestingly, we found that the slope in the case of 1:1 was similar to the slope of DMAP as invididual catalyst. Neverthteless in the case of 2:1 the polymerization process was much slower than in the other 2 cases.
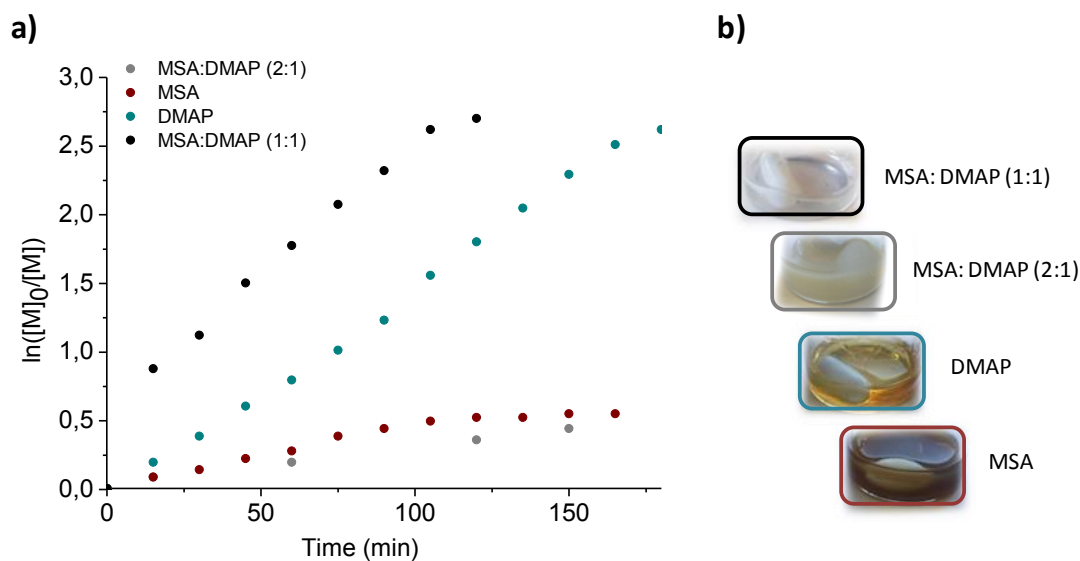
Figure 5.9. a) Semi-logarithmic kinetic plot of the polymerization of LLA at different reaction times catalyzed by different the different MSA:DMAP mixtures and b) pictures of the final polymers obtained with the different catalysts.

To gain more insight about the differences in polymerization kinetics between the system 1:1 and 2:1, the interaction between LLA and the catalyst was investigated by ^{13}C NMR. For that, model reactions were prepared consisting in the mixture of equimolar amounts of LLA and both MSA:DMAP 1:1 and 2:1 catalysts . These mixtures were analyzed by ^{13}C NMR in CDCl$_3$. Figure 5.10c represents the carbonyl region of the LLA for which the carbonyl carbon resonates at δ = 168.19 ppm. In presence of catalysts, the coordination of the LLA carbonyl is signficiantly affected. Interestingly, the effect is more pronounced when the LLA is in presence of one molar equivalent of a MSA:DMAP 1:1 catalyst. As clearly observed during or kinetics investigation, this higher shielding effect suggests that the carbonyl will be more active towards a nucleophilic attack explaining then the faster process of reaction observed when catalyzed by a MSA:DMAP 1:1 catalyst as compared to the 2:1.
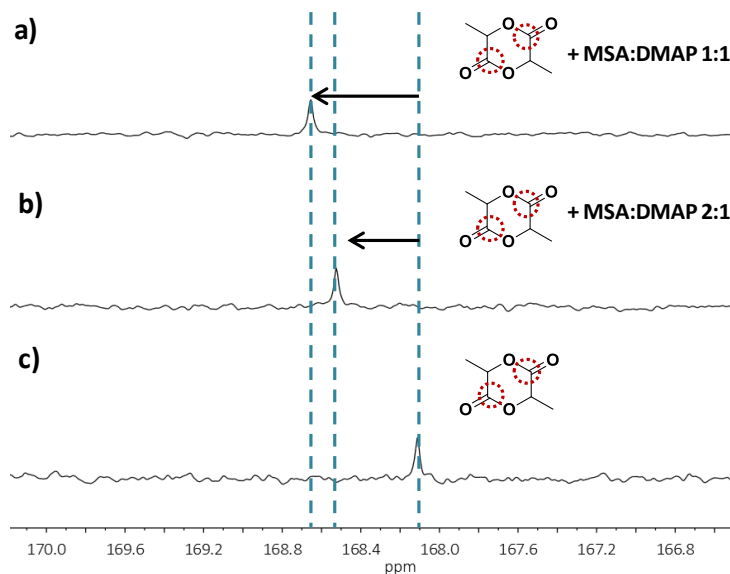
Figure 5.10. ^{13}C NMR spectra of the carbonyl carbon of a) an equimolar mixture of LLA and MSA:DMAP 1:1 and b) an equimolar mixture of LLA and MSA:DMAP 2:1 and c) LLA.

To determine if MSA:DMAP catalysts could efficiently triggering the ROP of LLA at 130 °C, the obtained polymers were characterized in detail. ^{1}H NMR spectroscopy provides the first insights of the PLLA synthesis (Figure 5.11a).

First, the characteristic peaks attributed to PLLA formation were observed at δ = 5.17 ppm and δ = 1.56 ppm. After, the molecular weights were determined by the integration of the signal assigned to the the repeating methine protons of the lactidyl sequence (signal at δ = 5.17 ppm) and the integration of the signals of the aromatic proton of the BnOH (signal at δ = 7.34 used for the initiation. The molecular weights obtained are in agreement with the theoretical ones indicating that the ROP of LLA was strictly initiated by the exogeneous BnOH in all cases (Table 5.1, entries 2-4) and attesting the efficiency of the system.

a)

b)
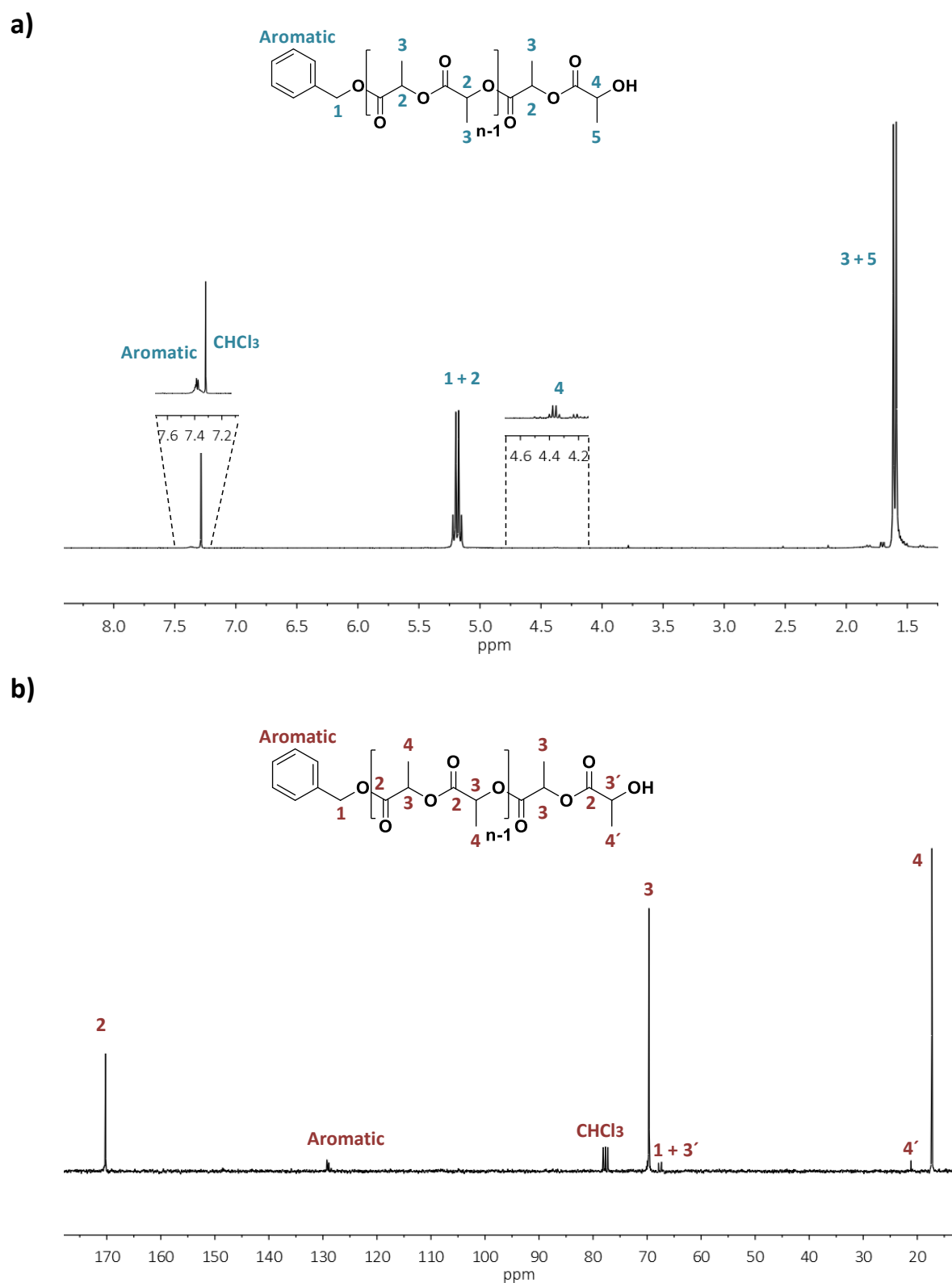
Figure 5.11. a) ^{1}H NMR spectrum of PLLA initiated by BnOH and b) ^{13}C NMR spectrum of PLLA initiated by BnOH.

SEC analyses revealed dispersity values of 1.2 for both catalytic systems, a bit narrower than the Đ = 1.4 obtained with DMAP only. To demonstrate the versatility of this organocatalyzed ROP in terms of end-group fidelity, 1-pyrenebutanol was used as initiator. In this case SEC analysis was performed by using both RI and UV detectors. As shown in the Figure 5.12, the UV-vis and RI SEC traces for PLLA are perfectly overlaid, indicating that pyrene moieties are end-capping of PLLA chains attesting the absence of side reactions.
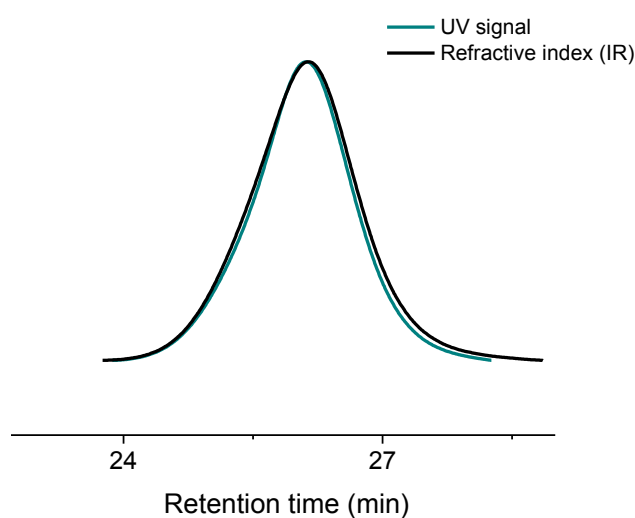
Figure 5.12. SEC trace with UV and refractive-index signals for [1-Pyrenebutanol]-[MSA]-[DMAP]-[LLA]=1-2-1-100.

To evaluate the living nature of the polymerization, a study of the evolution of the molecular weight of a PLA was realized for an initial degree of polymerization of 50 catalyzed by both MSA:DMAP catalytic systems (entries 5 and 6). As shown by Figures 5.13 and 5.14, both evolutions of $M_{n,SEC}$ are linear whatever the catalytic system showing a first-order kinetics.
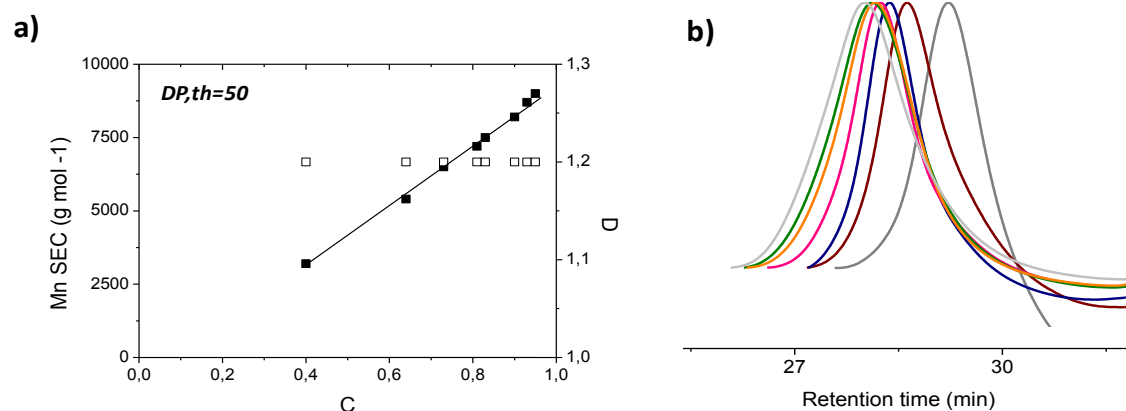
Figure 5.13. a) Dependence of molecular weight (Mn SEC) and dispersity (Đ) versus the monomer conversion for entry 5 and b) SEC traces of the monitored kinetics (eluent THF).
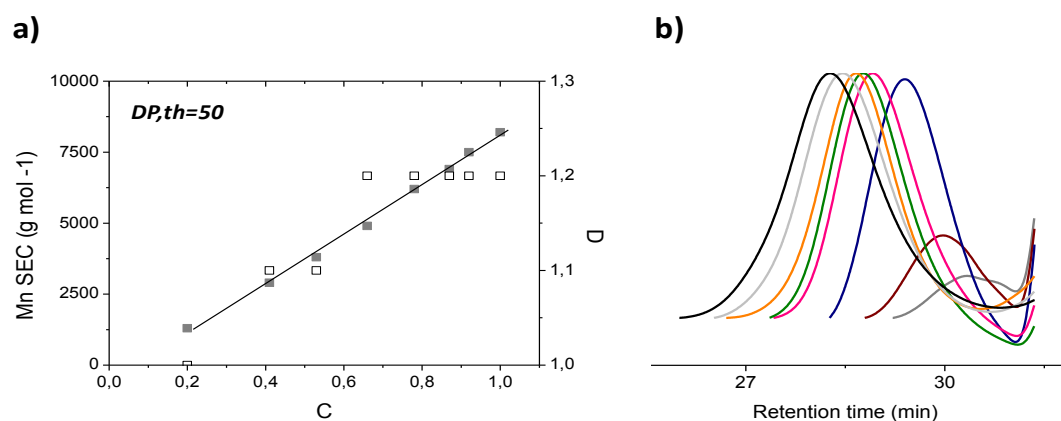
Figure 5.14. a) Dependence of molecular weight (Mn SEC) and dispersity (Đ) versus the monomer conversion for entry 6 and b) SEC traces of the monitored kinetics (eluent THF).

Apart from achieving good reactivity and good end-group fidelity one of the main challenges in the ROP of lactide is to avoid side reactions such as transesterification and epimerization during the polymerization. The main reason behind that is that only 2 % of epimerization can detrimentally affect the PLLA crystallization kinetics. Therefore, we closely analyzed the obtained PLLA using NMR spectroscopy techniques (Figure 5.15) starting with the multiplicity of the the methine proton signals (δ = 5.3-

5.1 ppm). Multiplicities of the signals were different when comparing the polymer catalyzed by the system 1:1 (a) and the one catalyzed with the system 2:1 (a´) (Table 5.1, entries 3 and 4, respectively). For PLLA catalyzed by 1:1 (a) the signal is not as well defined as in the case of 2:1 which in most cases is associated to a poorer control of polymerization. It seems that the 2:1 catalyst is providing more steroregular PLLA than the 1:1 or as compared to the prisitine DMAP catalyst. To support this result, both methine carbon signal (δ = 69-70 ppm) and methyl carbon signal (δ = 169-161 ppm) of the PLLA repeating unit were analyzed by using the ^{13}C NMR spectroscopy (Figures 5.15b and b´). As expected, when using the system 2:1 a single peak attributed to *mmm* tetrad is observed confirming that the regularity is maintained during the polymerization. However, in the polymer obtained with the system 1:1, in addition to the *mmm* tetrad, new peaks corresponding to different tetrads are also observed suggesting the presence of side reactions such as racemization, epimerization or transesterification during the polymerization.
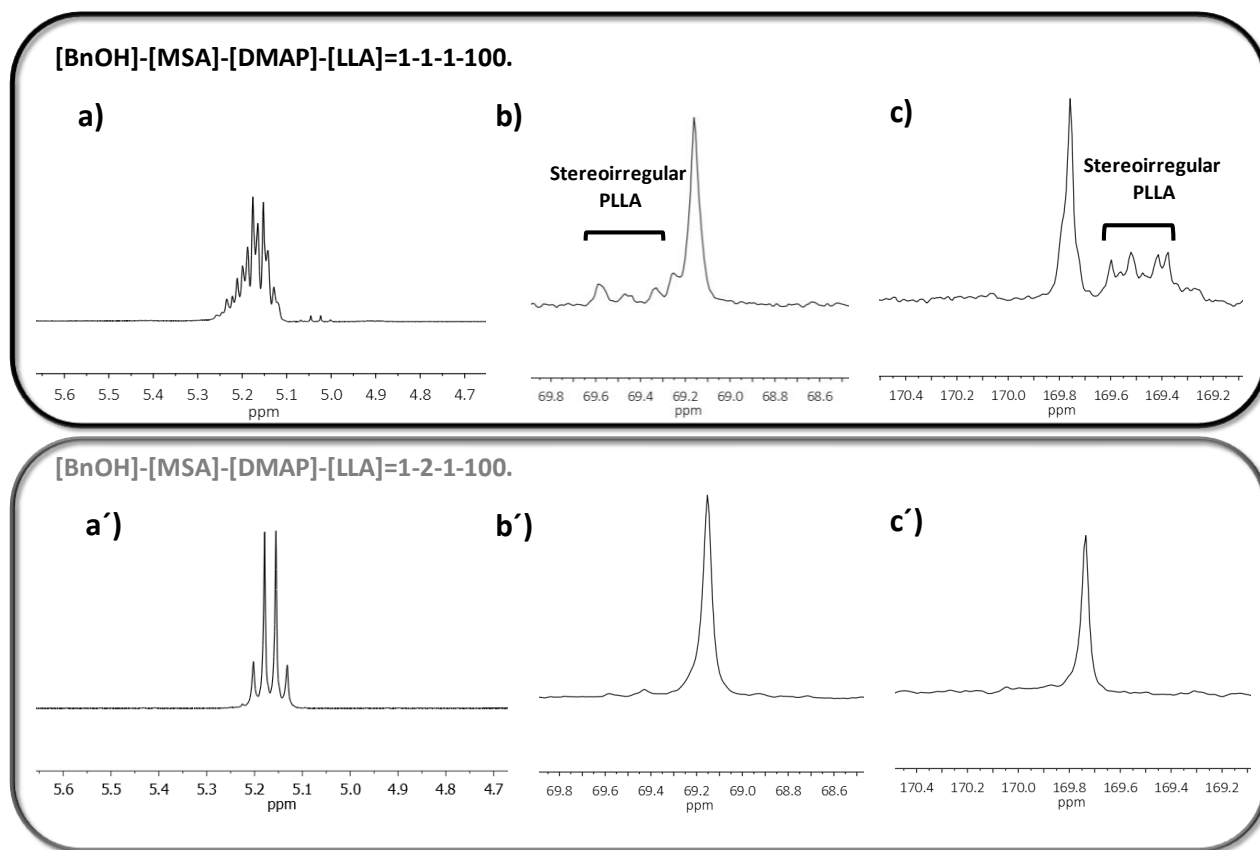
Figure 5.15. a) and a′) 1H NMR region of the methine protons of PLLA [entries 3 and 4, respectively], b) and b′) 13C NMR region of the methine carbons of PLLA [entries 3 and 4, respectively] and c) and c′) 13C NMR region of the carbonyl carbons of PLLA [entries 3 and 4, respectively].

To further confirm (or not) the absence of racemization or epimerization during the polymerization courses, polymers obtained from two MSA:DMAP 1:1 and 2:1 catalysts (entry 3 and 4) were analyzed by Gas Chromatography (GC)analyses. Columns employed for those analyses present a chiral stationary phase suitable for a L- and D-enantiomers separation. Analyses were performed by Corbion and the results are unambiquitous. with the PLA prepared from a MSA:DMAP 1:1 presents, after hydrolysis, a L-to-D isomer ratio of 82-18 while the sample obtained from the NEMO is characterized by a 98-2 ratio confirming then the well beter control obtained when using a non-eutectic catalytic mixture.

Finally, the control of the polymer microstructure has been demonstrated of significant importance since it affects the physical properties of the PLLA obtained polymer. Thermal properties of the PLLA can predict differences in the polymer stereoregulatity. Depending on their molecular weight and their enantiomeric repeating units, PLLA/PLA polymers range from amorphous to semicrystalline with glass transition temperatures around 40 to 60 °C and melting temperatures ranging from 130 °C to 180 °C. The melting temperature (T_m), and the glass transition temperature (T_g) of PLA decrease with decreasing amounts of PLLA [33,34]. Therefore, samples (entry 3 and 4) obtained from both 1:1 and 2:1 catalysts were analyzed by DSC (Figure 5.16). We found that, amorphous PLA was obtained with MSA:DMAP 1:1 and semicrystalline PLLA was obtained with MSA:DMAP 2:1 with a T_m of 149.6 °C. The glass transition temperatures (T_g) of both samples were similar being the one of the amorphous PLA slightly lower.
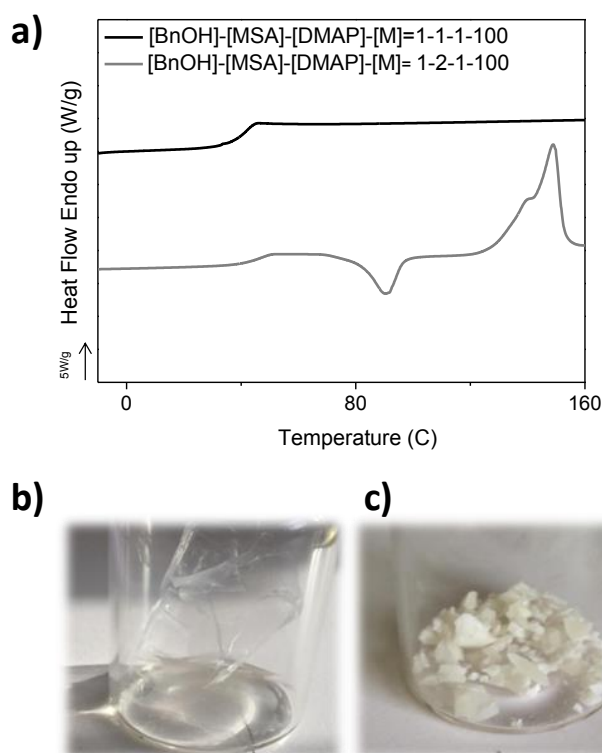
Figure 5.16. a) DSC cooling scans of the two PLA obtained from a 1:1 catalytic mixture (entry 3, Table 5.1) and a 2:1 catalytic mixture (entry 4, Table 5.1); b) and c) refer to the visual aspects of both polymers : figure b presenting the amorphous PLA (entry 3) while figure c showing the semicrystalline PLLA (entry 4).

5.2.3. Step towards high temperarute polymerization of PLA

To attain the objective of the metal-free industrial polymerization, the catalysts must be tested in industrially relevant condtions. As previously shown, the catalyst based on MSA:DMAP 2:1 seems the most promising to avoid side reactions during the polymerization, but the polymerization kinetics were relatively slow for an industrial process (Table 5.1, entry 4). In order to speed up the polymerization process, the catalyst loading was doubled (entry 7) and the polymerization temperature was raised from to 130 °C (enrty 4) to 150 °C (entry 8) and 180 °C (entry 9). As compared to the 15 hours required when using one equimolar equivalent of NEMO, doubling the

133

catalyst loading allowed the kinetics to be reduced to 8 h without affecting the polymer architecture (entry 7). The polymerization time was further reduced to 6 h by increasing the temperature to 150 °C, still maintaining a good end-group fidelity and a good control over the polymerization. Increasing the temperature to 180°C did not significantly improve the polymerization rate, but affected the dispersity values by increasing them slightly.

In spite of the great advances of the MSA:DMAP 2:1 catalyst to promote the LLA ROP of LLA at elevated temperatures without suffering from side reactions, one of the remaining challenges is to be able to obtain molecular weights that could be more practical for an industrial implementation. Therefore polymerizations targeting monomer to initiator ratios of 200 and 400 were realized (Table 5.1, entries 10 and 11). Herein, PLLA with molecular weight of $M_{n\,NMR}$= 32100 g mol^{-1} and $M_{n\,NMR}$= 56500 g mol^{-1} were obtained (up to 40 kDa by SEC). The Figure 5.17a exhibited SEC traces of the PLLAs prepared for different DPs. For each sample, a narrow and symmetrical profile is observed. When targeting higher molecular weights, the stereoregularity was maintained as it is shown in the DSC scans which demonstrated the semicrystalline nature of the samples (Figure 5.17b).
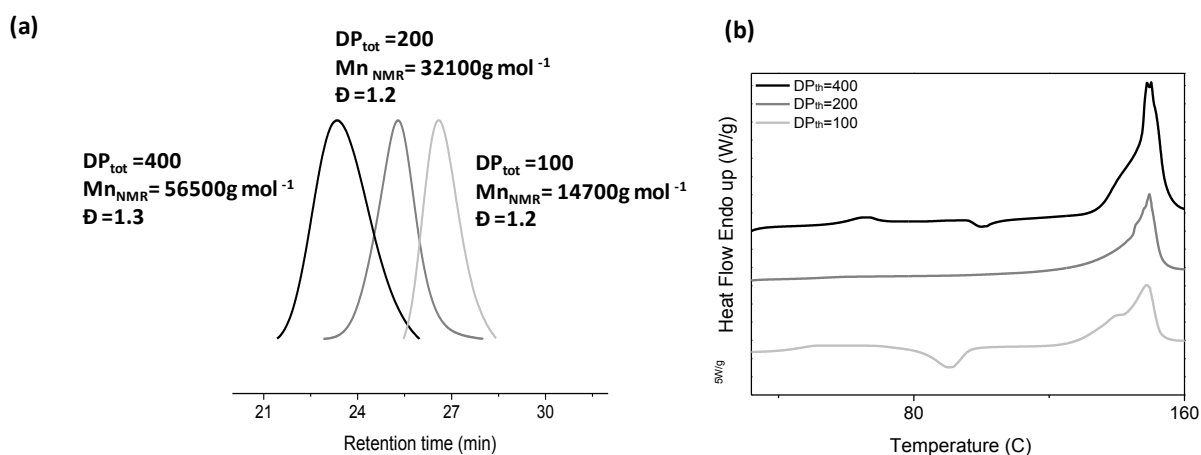
Figure 5.17. a) SEC traces of the obtained PLLA samples with series ratios of $[LLA]_0/[BnOH]_0=100,200$ and 400 (eluent THF) and b) DSC cooling scan for entry 4,12 and 13).

5.2.4. Expanding the scope of the polymerization process

In order to expand the scope of such catalytic process, we decided to investigate the feasibility of a MSA:DMAP 2:1 catalyst to polymerize other cyclic monomers. The ROP of CLO was performed at 130°C and using as catalyst the MSA:DMAP 2:1. After 4 h the reaction was finished (entry 12, Figure S5.10) and the thermal behavior was analyzed by DSC (Figure 5.19)
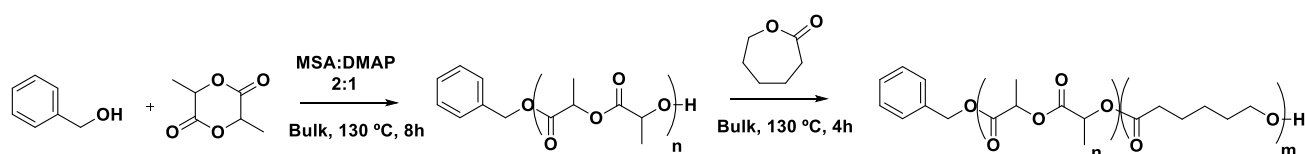
Figure 5.18. One-pot synthesis of diblock copolymers by ROP of LLA and ε-caprolactone (CLO) using MSA:DMAP 2:1 as catalyst.

To finish, in order to evaluate the "living" nature of the copolymerization, the ROP of L-lactide was first carried out at 130°C using a $[BnOH]_0$-$[MSA]_0$-$[DMAP]_0$-$[LLA]_0$ initial molar ratio of 1-4-2-100. Subsequently, after achieving a full conversion in L-lactide (~ 8 hours), 100 molar equivalents of ε-caprolactone (CLO) (as compared to BnOH) were

added to the reaction medium and the ROP was kept at 130°C for 4 extra hours (Figure 5.18). SEC analyses were performed before and after the addition of the CLO (Figure 5.19 b). As expected after the CLO addition, the SEC trace is shifted to higher molecular weights, maintaining a narrow dispersity and confirming the copolymer formation. Finally, after purification, the copolymer composition was determined by ^{1}H NMR and concluded on the obtention of a PLLA-*b*-PCLO composed by a LA-to-CL ratio of 60/40.

a) b)
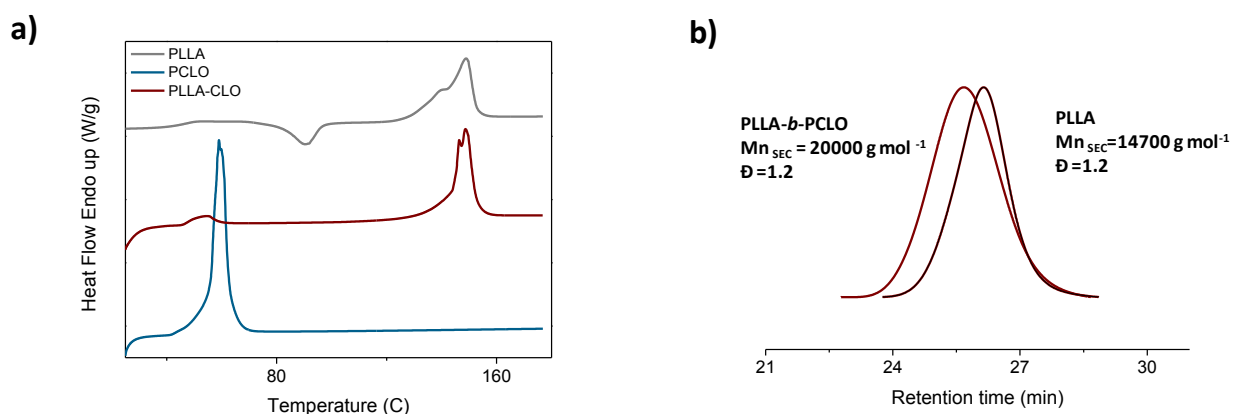
Figure 5.19.a) DSC cooling scans of PLLA, PCLO and PLLA-*b*-PLCO and c) SEC traces of the PLLA before the addition of CLO and before the addition and polymerization of CLO (eluent THF).

In order to confirm the formation of block copolymers the thermal properties of the material were analyzed by DSC. Two melting temperatures were observed (Figure 5.19a). This result confirmed the stereoregular character of the PLLA along the copolymer chain and the blocky character of the copolymer.

5.3. Conclusion

The solvent-free ROP of L-lactide at elevated temperatures was succesfully performed using and acid-base mixtures. Two different acid-base mixtures were used based on MSA and DMAP, the stoichiometric mixture (1:1) and the non-stoichiometric mixture

(2:1). On one hand, the 1:1 MSA:DMAP mixture is shown to promote the organocatalyzed ROP of LLA (DP$_{theo}$ 100) in remarkable low reaction times (2 h) with an appreciable and precise degree of control over the molar masses and dispersities. In addition, the absence of colour of the sample demonstrated the thermal stability of the system in comparison to individual DMAP and MSA. However, due to the particularly high reactivity rates, side reactions were occurring during the polymerization such as transesterification and racemization leading to amorphous PLAs. On the other hand, in spite of the reduced catalytic activity of MSA:DMAP (2:1) catalyst, the polymerization control was greatly improved. As demonstrated by gas chromatography and DSC analyses, semicrystalline PLLAs with chiral purity up to 98% were obtained, which is unprecedented for an organocatalyst in bulk conditions. This good catalytic performance was exploited to synthesize high molecular weight PLLA of M_n= 56500 g mol^{-1} at higher temperature (150°C) and in a relatively short period of times mimicking industrially relevant condtions maintaining the good control over the polymerization. Finally, due to the living character of the polymerization, we further exploited the catalyst to produce PCLO and a block copolymer based on LA and CLO with double crystalline behavior. Up to our knowledge, this study approaches for the first time to a thermally stable organocatalyst able to promote the polymerization of L-LA in conditions close to the industrial without deterioring the stereoregulality of the PLLA during the polymerization. However, further characterization of the materials must be carried out and the mechanisms of reaction must be studied in order to get a better understanding of the synthetic processes.

5.4. Experimental Section

5.4.1 Materials

L-Lactide (L-LA, 98%, TCI) was recrystallized three times from toluene and dried under

vacuum for two days. ε-Caprolactone (CLO, 99%, Sigma Aldrich), benzyl alcohol (BnOH, 99%, Sigma Aldrich) were dried over CaH_2 for 48 hours prior to their distillation under reduced pressure and were stored on molecular sieves and 1-pyrenebutanol (99%, Sigma Aldrich) were also dried under vaccum. Compounds were stored in a glove box (O_2 ≤ 1 ppm, H_2O ≤ 0.5 ppm). Methanesulfonic acid (MSA, 99%) and 4-(dimethylamino)pyridine (DMAP, 98%), chloroform ($CDCl_3$), methanol (CH_3OH) and the rest of the solvents used on this work were supplied by Sigma-Aldrich and used as received.

5.4.2 General procedure of the preparation of the catalyst MSA:DMAP

In a glove box, different dual catalysts were prepared by mixing methanesulfonic acid (MSA) (1.38×10^{-4} mol, 0.013 g, 9 μl) and 4-dimethylaminopyridine (DMAP) (1.38×10^{-4} mol, 0.017 g) for the mixture 1:1 while methanesulfonic acid (MSA) and (2.76×10^{-4} mol, 0.026 g, 18 μl) and 4-dimethylaminopyridine (DMAP) (1.38×10^{-4} mol, 0.017 g) were used for the preparation of the mixture 2:1. Afterwards, the mixtures were thermally treated at 90 °C over 30 minutes under stirring until complete formation of homogeneous and transparent liquid solution or salt. The good formation of those complexes was attested by ^1H NMR spectroscopy prior their use.

5.4.3. General procedure of the Ring-Opening Polymerization of L-lactide and ε-caprolactone catalyzed by the MSA:DMAP mixtures

In a glove box, previously dried vials were charged with LLA (1 g), the MSA:DMAP catalyst (1:1, 2:1) and a stir bar. Then the initiator (BnOH,) was added via a 5 or 10 μL syringe. The sealed vials were immersed in a pre-heated oil bath at the desired temperature (130 °C–180 °C). The conversion of the monomer was monitored by ^1H NMR spectroscopy with solution of $CDCl_3$ until reached at least 95%. The reaction was

stopped by cooling down the medium at room temperature. For the purification, the crude polymer was dissolved in chloroform and precipitated in cold methanol. The resulted PLLA were filtrated and dried under vacuum at RT for 24 h before their characterization. The same procedure was used in the ROP of ε -caprolactone.

5.4.4. Diblock copolymerization of L-lactide and ε-caprolactone

In a glove box, LLA (0.5 g) the MSA:DMAP 2:1 and a stir bar were added to a dry vial .Then, the BnOH initiator was added via a 5 or 10 µL syringe and the sealed vial was immersed, out of the glovebox, in pre-heated oil bath thermostatized at 130°C. The LLA conversion of LLA was followed by ^{1}H NMR (in CDCl$_3$) When the conversion value was of 90% (~8 hours), the polymerization medium was cooled down at RT and the CLO (0.4 g) was added in the vial by the use of a glove box. Very quickly, the vial was re-immersed at 130°C. After 4 h, the copolymer (PLLA-*b*-PCLO) was isolated by dissolving it in chloroform prior its precipitation in cold methanol. After decantation, the copolymer was filtered out and dried under vacuum.

5.5. References

(1) Sheldon, R. A. Metrics of Green Chemistry and Sustainability: Past, Present, and Future. *ACS Sustain. Chem. Eng.* **2018**, *6* (1), 32–48. https://doi.org/10.1021/acssuschemeng.7b03505.

(2) Gupta, A. P.; Kumar, V. New Emerging Trends in Synthetic Biodegradable Polymers − Polylactide: A Critique. *Eur. Polym. J.* **2007**, *43* (10), 4053–4074. https://doi.org/10.1016/j.eurpolymj.2007.06.045.

(3) Schneiderman, D. K.; Hillmyer, M. A. 50th Anniversary Perspective: There Is a Great Future in Sustainable Polymers. *Macromolecules* **2017**, *50* (10), 3733–3749. https://doi.org/10.1021/acs.macromol.7b00293.

(4) Llevot, A.; Dannecker, P.-K.; von Czapiewski, M.; Over, L. C.; Söyler, Z.; Meier, M. A. R. Renewability Is Not Enough: Recent Advances in the Sustainable Synthesis of Biomass-Derived Monomers and Polymers. *Chem. – Eur. J.* **2016**, *22* (33), 11510–11521. https://doi.org/10.1002/chem.201602068.

(5) Castro-Aguirre, E.; Iñiguez-Franco, F.; Samsudin, H.; Fang, X.; Auras, R. Poly(lactic Acid)-Mass Production, Processing, Industrial Applications, and End of Life. *Adv. Drug Deliv. Rev.* **2016**, *107*, 333–366. https://doi.org/10.1016/j.addr.2016.03.010.

(6) Auras, R.; Harte, B.; Selke, S. An Overview of Polylactides as Packaging Materials. *Macromol. Biosci.* **2004**, *4* (9), 835–864. https://doi.org/10.1002/mabi.200400043.

(7) Drumright, R. E.; Gruber, P. R.; Henton, D. E. Polylactic Acid Technology. *Adv. Mater.* **2000**, *12* (23), 1841–1846. https://doi.org/10.1002/1521-4095(200012)12:23<1841::AID-ADMA1841>3.0.CO;2-E.

(8) Sosnowski, S.; Lewinski, P. L-Lactide Polymerization Catalysed by tin(II) 2-Ethyl-Hexanoate. A Deeper Look at Chain Transfer Reactions. *Polym. Chem.* **2015**, *6* (35), 6292–6296. https://doi.org/10.1039/C5PY00748H.

(9) Badoux, M.; Drechsler, S.; Pal, S.; Kilbinger, A. F. M. Facile Synthesis of a High Molecular Weight Amphiphilic Aramid–ROMP Block Copolymer. *Macromolecules* **2017**, *50* (23), 9307–9314. https://doi.org/10.1021/acs.macromol.7b01989.

(10) Kricheldorf, H. R.; Kreiser-Saunders, I.; Stricker, A. Polylactones 48. SnOct2-Initiated Polymerizations of Lactide: A Mechanistic Study. *Macromolecules* **2000**, *33* (3), 702–709. https://doi.org/10.1021/ma991181w.

(11) Bossion, A.; Heifferon, K. V.; Meabe, L.; Zivic, N.; Taton, D.; Hedrick, J. L.; Long, T. E.; Sardon, H. Opportunities for Organocatalysis in Polymer Synthesis via Step-Growth Methods. *Prog. Polym. Sci.* **2019**, *90*, 164–210. https://doi.org/10.1016/j.progpolymsci.2018.11.003.

(12) Nachtergael, A.; Coulembier, O.; Dubois, P.; Helvenstein, M.; Duez, P.; Blankert, B.; Mespouille, L. Organocatalysis Paradigm Revisited: Are Metal-Free Catalysts Really Harmless? *Biomacromolecules* **2015**, *16* (2), 507–514. https://doi.org/10.1021/bm5015443.

(13) Mezzasalma, L.; Harrisson, S.; Saba, S.; Loyer, P.; Coulembier, O.; Taton, D. Bulk Organocatalytic Synthetic Access to Statistical Copolyesters from L-Lactide and ε-Caprolactone Using Benzoic Acid. *Biomacromolecules* **2019**, *20* (5), 1965–1974. https://doi.org/10.1021/acs.biomac.9b00190.

(14) Dove, A. P. Organic Catalysis for Ring-Opening Polymerization. *ACS Macro Lett.* **2012**, *1* (12), 1409–1412. https://doi.org/10.1021/mz3005956.

(15) Mezzasalma, L.; Dove, A. P.; Coulembier, O. Organocatalytic Ring-Opening Polymerization of L-Lactide in Bulk: A Long Standing Challenge. *Eur. Polym. J.* **2017**, *95*, 628–634. https://doi.org/10.1016/j.eurpolymj.2017.05.013.

(16) Zhong, Z.; Dijkstra, P. J.; Feijen, J. [(salen)Al]-Mediated, Controlled and Stereoselective Ring-Opening Polymerization of Lactide in Solution and without Solvent: Synthesis of Highly Isotactic Polylactide Stereocopolymers from Racemic D,l-Lactide. *Angew. Chem. Int. Ed.* **2002**, *41* (23), 4510–4513. https://doi.org/10.1002/1521-3773(20021202)41:23<4510::AID-ANIE4510>3.0.CO;2-L.

(17) Wei, F.; Zhu, H.; Li, Z.; Wang, H.; Zhu, Y.; Zhang, L.; Yao, Z.; Luo, Z.; Zhang, C.; Guo, K. Food Sweetener Saccharin in Binary Organocatalyst for Bulk Ring-Opening Polymerization of Lactide. *Adv. Synth. Catal.* **2019**, *361* (6), 1335–1347. https://doi.org/10.1002/adsc.201801319.

(18) Yu, Y.; Storti, G.; Morbidelli, M. Ring-Opening Polymerization of L,l-Lactide: Kinetic and Modeling Study. *Macromolecules* **2009**, *42* (21), 8187–8197. https://doi.org/10.1021/ma901359x.

(19) Yu, Y.; Storti, G.; Morbidelli, M. Kinetics of Ring-Opening Polymerization of L,l-Lactide. *Ind. Eng. Chem. Res.* **2011**, *50* (13), 7927–7940. https://doi.org/10.1021/ie200117n.

(20) Zhang, D.; Jardel, D.; Peruch, F.; Calin, N.; Dufaud, V.; Dutasta, J.-P.; Martinez, A.; Bibal, B. Azaphosphatranes as Hydrogen-Bonding Organocatalysts for the Activation of Carbonyl Groups: Investigation of Lactide Ring-Opening Polymerization. *Eur. J. Org. Chem.* **2016**, *2016* (8), 1619–1624. https://doi.org/10.1002/ejoc.201600080.

(21) Chesterman, J. P.; Amsden, B. G. Triethylamine-Based Catalysts for the Melt Polymerization of Carbonate Monomers. *Polym. Chem.* **2016**, *7* (45), 6946–6953. https://doi.org/10.1039/C6PY01248E.

(22) Mezzasalma, L.; Winter, J. D.; Taton, D.; Coulembier, O. Benzoic Acid-Organocatalyzed Ring-Opening (Co)polymerization (ORO(c)P) of L-Lactide and ε-Caprolactone under Solvent-Free Conditions: From Simplicity to Recyclability. *Green Chem.* **2018**, *20* (23), 5385–5396. https://doi.org/10.1039/C8GC03096K.

(23) Mezzasalma, L.; Winter, J. D.; Taton, D.; Coulembier, O. Extending the Scope of Benign and Thermally Stable Organocatalysts: Application of Dibenzoylmethane for the Bulk Copolymerization of L-Lactide and Ɛ-Caprolactone. *J. Polym. Sci. Part Polym. Chem.* **2018**, *56* (5), 475–479. https://doi.org/10.1002/pola.28921.

(24) Basterretxea, A.; Gabirondo, E.; Jehanno, C.; Zhu, H.; Flores, I.; Müller, A. J.; Etxeberria, A.; Mecerreyes, D.; Coulembier, O.; Sardon, H. Polyether Synthesis by Bulk Self-Condensation of Diols Catalyzed by Non-Eutectic Acid–Base Organocatalysts. *ACS Sustain. Chem. Eng.* **2019**, *7* (4), 4103–4111. https://doi.org/10.1021/acssuschemeng.8b05609.

(25) Jehanno, C.; Flores, I.; Dove, A. P.; Müller, A. J.; Ruipérez, F.; Sardon, H. Organocatalysed Depolymerisation of PET in a Fully Sustainable Cycle Using

Thermally Stable Protic Ionic Salt. *Green Chem.* **2018**, *20* (6), 1205–1212. https://doi.org/10.1039/C7GC03396F.

(26) Flores, I.; Demarteau, J.; Müller, A. J.; Etxeberria, A.; Irusta, L.; Bergman, F.; Koning, C.; Sardon, H. Screening of Different Organocatalysts for the Sustainable Synthesis of PET. *Eur. Polym. J.* **2018**, *104*, 170–176. https://doi.org/10.1016/j.eurpolymj.2018.04.040.

(27) Nederberg, F.; Connor, E. F.; Möller, M.; Glauser, T.; Hedrick, J. L. New Paradigms for Organic Catalysts: The First Organocatalytic Living Polymerization. *Angew. Chem. Int. Ed.* **2001**, *40* (14), 2712–2715. https://doi.org/10.1002/1521-3773(20010716)40:14<2712::AID-ANIE2712>3.0.CO;2-Z.

(28) Kadota, J.; Pavlović, D.; Hirano, H.; Okada, A.; Agari, Y.; Bibal, B.; Deffieux, A.; Peruch, F. Controlled Bulk Polymerization of L-Lactide and Lactones by Dual Activation with Organo-Catalytic Systems. *RSC Adv.* **2014**, *4* (28), 14725–14732. https://doi.org/10.1039/C4RA01239A.

(29) Kadota, J.; Pavlović, D.; Desvergne, J.-P.; Bibal, B.; Peruch, F.; Deffieux, A. Ring-Opening Polymerization of L-Lactide Catalyzed by an Organocatalytic System Combining Acidic and Basic Sites. *Macromolecules* **2010**, *43* (21), 8874–8879. https://doi.org/10.1021/ma101688d.

(30) Guillerm, B.; Lemaur, V.; Ernould, B.; Cornil, J.; Lazzaroni, R.; Gohy, J.-F.; Dubois, P.; Coulembier, O. A One-Pot Two-Step Efficient Metal-Free Process for the Generation of PEO-B-PCL-B-PLA Amphiphilic Triblock Copolymers. *RSC Adv.* **2014**, *4* (20), 10028–10038. https://doi.org/10.1039/C3RA47204C.

(31) Wei, F.; Zhu, H.; Li, Z.; Wang, H.; Zhu, Y.; Zhang, L.; Yao, Z.; Luo, Z.; Zhang, C.; Guo, K. Food Sweetener Saccharin in Binary Organocatalyst for Bulk Ring-Opening Polymerization of Lactide. *Adv. Synth. Catal.* **0** (0). https://doi.org/10.1002/adsc.201801319.

(32) Culkin, D. A.; Jeong, W.; Csihony, S.; Gomez, E. D.; Balsara, N. P.; Hedrick, J. L.; Waymouth, R. M. Zwitterionic Polymerization of Lactide to Cyclic Poly(Lactide) by Using N-Heterocyclic Carbene Organocatalysts. *Angew. Chem.* **2007**, *119* (15), 2681–2684. https://doi.org/10.1002/ange.200604740.

(33) Farah, S.; Anderson, D. G.; Langer, R. Physical and Mechanical Properties of PLA, and Their Functions in Widespread Applications — A Comprehensive Review. *Adv. Drug Deliv. Rev.* **2016**, *107*, 367–392. https://doi.org/10.1016/j.addr.2016.06.012.

(34) J. Stanford, M.; P. Dove, A. Stereocontrolled Ring-Opening Polymerisation of Lactide. *Chem. Soc. Rev.* **2010**, *39* (2), 486–494. https://doi.org/10.1039/B815104K.

Conclusions and Perspective

Organocatalysts have undoubtedly made a significant impact in the field of polymerization owing to their ``greener´´ character, good selectivity and their unique versatility. However, it is a known fact that despite they are broadly use on research laboratories under mild conditions, when they are employed at elevated temperatures they lose performance due to degradation or deactivation. This clearly limits its implementation in industrial synthesis processes.

A solution to this can be found in the employment of acid-base mixture organocatalysts as their synthesis is simple and they have shown to be stable at elevated temperatures. Recent advances in the field were summarized in the introduction of the thesis providing the keys to their formation and use. These catalysts can be prepared through stoichiometric and non-stoichiometric acid-base mixtures resulting in protic ionic mixtures or Non-Eutectic Mixtures Organocatalysts (NEMOs). This plethora of possibilities allows the preparation of thermally stable catalysts which may show a stronger acidic or basic nature.

This concept was applied first in the synthesis of poyethers by self-condensation at high temperatures. To do so, considerably cheap, and thermo stable ogancatalysts were prepared by different mixtures of a common acid, MSA and a common base, TBD. The non-stoichiometric mixtures high in MSA demonstrated to be highly efficient as catalysts and were named as Non-Eutectic Mixture Organocatalys (NEMOs). Their use as catalysts in the synthesis of polyethers by self-condensation in bulk conditions led to medium to long chain aliphatic poly(oxyalkylene)s which could have potential applications as new soft segments for polyurethane chemistry. Their potential can reside in the superior properties in hydrolytic stability and tunable flexibility than other commonly used polyols such as PEG. In addition, since one of the most well-known

innerent advantage in the use of organocatalysts is the reclycability; the NEMO was recycled demonstrating major cost-effectiveness.

Taking advantage of the good performance of the NEMO MSA:TBD random copolyethers were also prepared. Copolymerization methods bring tunability to the properties of the materials broadening their strengths. On the light of this, medium chain diol (1,6-hexanediol) and long chain diol (1,12-dodecanediol) were copolymerized and aliphatic copolyethers with isomorphic behavior were obtained. This discovery contributes to the first report of this crystallization behavior in polyether based materials.

Similarly, fully bio-based copolyethers were synthetized by using 1,6-hexanediol and 1,4-cyclohexanedimethanol. Research on bio-based materials brings to the polymerization process a sustainable profit when contrasted with the use of petroleum-based materials. Using the innovative NEMO, bio-based copolyethers with tunable crystallinity, from highly semicrystalline to amorphous, were obtained. Interestingly, changes in the the T_g were not reported. This route shows a simple and sustainable way to synthesize fully bio-based polyethers which can be ideal candidates as polyols of synthesis of PU or for the preparation of a great variety of elastomers.

To finish, the ROP of LA considered one of the long-standing challenges in organocatalysis was also discussed. In this part of the thesis, the optimization labor of a new acid-base mixture oragnocatalyst was also performed being MSA and DMAP the constituents of the mixture. The stoichiometric mixture (1:1) and the NEMO (2:1) showed extraordinary thermal resistance and particular effectivity for the catalysis of ROP. Interestingly, the salt MSA:DMAP 1:1 and the NEMO 2:1 displayed different

catalytic behavior resulting in important differences in the final polymer. While the MSA:DMAP 1:1 showed high reactivity rates, side reactions were occurring during the polymerization such as transesterification or racemization leading to amorphous PLA, but contrarily, the NEMO 2:1 promoted a controlled polymerization resulting in a semicrystalline PLLA with chiral purity up to 98%. Even though further studies must be done to understand the reaction mechanism that promote these differences, with this study we contribute for the first time to a thermally stable organocatalyst able to promote the polymerization of L-LA without deterioring the stereoregulality of the PLLA during the polymerization.

In the light of these results, acid-base organocatalysts and in particular the NEMO presented in this work have undoubtedly demonstrated to be easy to synthetize and to own outstanding thermal stabiliby, recyclability and good catalytic activity bringing simplicity a two valuable polymerizations. Making reference to the objectives that the industrial chemical community has to face and that were mentioned in the intruction, with this work we have contributed to all points. Showing the good efficiency and selectivity of organocatalysts at high temperatures can set the removal of organometallic catalysts from the polymerization processes and thus favoring the recyclability of the final material and encouraging greener procedures. Also, we have introduced new renewable raw materials that can be polymerized by polycondensation. Polycondensation as a polymerization method has played an important role in this work. It can be considered a simplistic and versatile way of synthesis which avoids the use of solvents and decreases the wastes generated since implies water removal as polycondensate.

None-the-less, beyond all the efforts highlighted, significant progress has still need to be made. 1) The reactivity rates and the molecular weights achieved in polymerization reactions are still low when compared to metal-based species. 2) The majority of the most efficient acid base mixtures are based on expensive organocatalysts such as TBD making their implementation in the industry economically unviable. 3) The catalyst loading of these acid-base mixtures are much superior to the organometallic catalyst and even though these organocatalysts is easier to remove from the polymer by precipitation/extraction, industrially this additional steps will increase the production costs and must be evaluated in advance.

On the basis of these considerations, a number of innovations are required to make the implementation of acid base organocatalysts in industry a closer reality. The high cost of the methodologies (i.e. inert atmosphere), as well as the reagents used (i.e. organic bases) together with the high catalyst loadings are key limiting factors for this technology at present. In this regard, the innovation should involve the development of cheap, non-toxic and highly selective acid-base mixtures to be used at industrially relevant temperatures. Beyond this, technical challenges for scaling up these processes have not been addressed and closer interaction between academia and industry will be beneficial for the implementation of these acid-base mixtures at industrial scales.
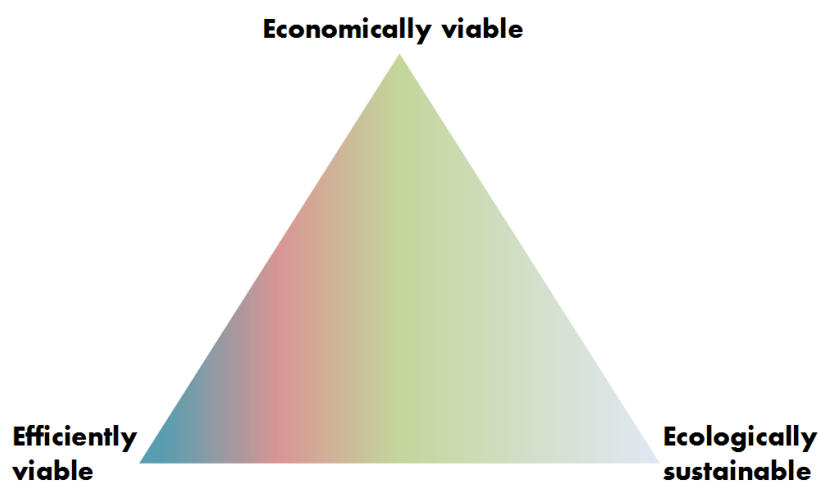
Figure1. The three points of sustainable polymerization process.

Overall, great strides are still to be made to gather the foundation of a sustainable organocatalyzed development which fully combines the three pillars of the sustainable development vector adapted to industrial polymerizations: efficiency, ecomomically viable and ecologically sustainable. During this period, in addition to a good environmental practice the research efforts must continue into reducing toxic compounds of the materials for an easy reusability and favour the circular economy. With the advances underlined in this work we want to encourage scientists on the use of acid-base organocatalysts in (de)polymerization in order to expand their use and to develop new catalytic strategies that could find their way to the market.

The sustainable challenges facing polymer chemistry today can sometimes seem overwhelming. But change is as possible as inevitable and even narrow topics such as organocatalytic polymerization processes can be formidable in scope.

``Change is inevitable; change is constant´´- *Benjamin Disrael*

Methods

Size Exclusion Chromatography (SEC)

Size Exclusion Chromatography (SEC) was performed in chloroform at 30 °C using a Waters chromatograph equipped with four 5 mm Waters columns (300 mm "x" 7.7 mm) connected in series with increasing pore sizes. Toluene was used as a marker. Polystyrenes of different molecular weights were used for the calibration.

Fourier Transform Infrared Spectroscopy (FT-IR)

Fourier Transform Infrared pectrophotometer (Nicolet 6700 FT-IR, Thermo Scientific Inc., USA) was used using attenuated total reflectance (ATR) technique (Golden Gate, spectra Tech). Spectra were recorded between 4000-525 cm^{-1} with a spectrum resolution of 4 cm^{-1}. All spectra were averaged over 10 scans.

Differential Scanning Calorimetry (DSC)

Differential Scanning Calorimeter (DSC-Q2000, TA Instrument Inc., USA) was used to analyze the thermal behavior of the samples. A total of 6-8 mg of samples were first scanned from -80 °C to 150 °C at a heating rate of 20 $°C.min^{-1}$ to eliminate interferences due to moisture. The samples were then cooled to -80 °C to remove the thermal history and reheated to 150 °C at 20 $°C.min^{-1}$. The glass transition and melting temperatures were calculated from the second heating run.

Nuclear Magnetic Resonance (NMR) spectroscopy

^{1}H and ^{13}C Nuclear Magnetic Resonance (NMR) spectroscopy.was recorded in a Bruker Avance DPX 300 at 300.16 MHz and at 75.5 MHz of resonance frequency respectively, using deuterated chloroform ($CDCl_3$), dimethyl sulfoxide (DMSO) or tetrahydrofuran (THF) as solvent at room temperature. Experimental conditions were as follows: a) for

^{1}H NMR spectroscopy: 10 mg of sample; 3 s acquisition time; 1 s delay time; 8.5 μs pulse; spectral width 5000 Hz and 32 scans; b) for ^{13}C NMR spectroscopy: 40 mg; 3 s acquisition time; 4 s delay time; 5.5 μs pulse; spectral width 18800 Hz and more than 10000 scans. ^{15}N NMR measurements were performed on a Bruker Avance III 500M solution-state NMR (standard bore). Recycle delays are 10s, 10k ~ 20 k scans were accumulated to get sufficient signal-to-noise ratio.

Thermogravimetric analyses (TGA)

Thermogravimetric analyses (TGA) were carried out using a Q500 Thermogravimetric Analyzer from TA Instruments. Samples were heated from room temperature to 600 ˚C at a rate of 10 °C/min under a constant N_2 flow.

Density functional theory (DFT)

The electronic structure calculations were carried out using the Gaussian 09 suite of programs[23]. Geometry optimization were performed using ωB97XD functional with the 6-31+G(d,p) basis set. Vibrational frequencies were calculated at the same level of theory to ensure that the optimized structures were minima in the potential energy surface (no imaginery frequencies) and to determine the zero-point vibrational energy (ZPVE) and the thermal vibrational corrections at T = 298 K. Single-point energy calculations were performed at the ωB97XD/6-311++ G(2df,2p) level of theory in order to refine the electronic energy.

Wide Angle X-RAY Scattering (WAXS)

The samples in DSC pans were examined at 25 ˚C by WAXS performed at beamline BL11-NCD at the ALBA Synchrotron radiation facility (Barcelona, Spain). The

wavelength was λ=1.0 Å. WAXS patterns were recorded using a Rayonix LX255-HS detector with an active area of 85 x 255 mm2 (pixel size 40 µm2) the sample to detector distance employed was 154.69 mm with tilt angle 0f 29.23˚. The intensity profile is reported as the plot of the scattering intensity vs scattering angle (2θ). The scattering vector was calibrated using chromium (III) oxide.

Dynamic Mechanical Analysis (DMA)

Small amplitude oscillatory shear experiments were conducted in a Dynamic Mechanical Analyser, Triton 2000 DMA from Triton Technology (Mansfield, UK), in compression mode. Frequency sweep experiments were carried out in linear viscoelastic conditions at 25°C in the range of 0.01 and 21.5 Hz.

Matrix Assisted Laser Desorption Ionization Time of Flight Mass Spectrometry (MALDI-TOF MS)

Matrix Assisted Laser Desorption Ionization Time of Flight Mass Spectrometry (MALDI-TOF MS) measurements were S5 performed on a Bruker Autoflex Speed system (Bruker, Germany) instrument, equipped with a 355 nm NdYAG laser.

Enantioselective Gas chromatography (GC)

The gas chromatograph (GC2014C) and GC Solution were purchased from Shimadzu Corporation, Japan. The capillary column (SPB-5) was obtained from SUPELCO Inc., U.S. The temperatures used for the injector, the detector (FID) and the column oven were set at 250, 250 and 140 ° C, respectively. The flow rate and the carrier gas division ratio (N2) were 2.0 mL / min and 20: 1, respectively. The lactide (1.0%, w / v) was dissolved in dichloromethane and the injection volume was 0.40 µl. The automatic potentiometric titrant equipped with a non-aqueous pH electrode used 0.1 mol / L

KOCH$_3$ in methanol as a standard volumetric solution. Standard references of pure L and D-lactides (Corbion Purac) were used.

Fast scanning calorimetry measurements (FSC)

Fast scanning calorimetry (FSC) measurements were carried in a Flash DSC 1 from Mettler Toledo equipped with an intracooler used to cool sample down to -100 °C, and nitrogen purge. The measurements were performed under a 20 mL·min^{-1} nitrogen flow. Samples were directly placed on the backside of the chip sensor. To improve the contact between the sensor and the sample a thin layer of fluorinated oil was use.

Appendix

Chapter 2.
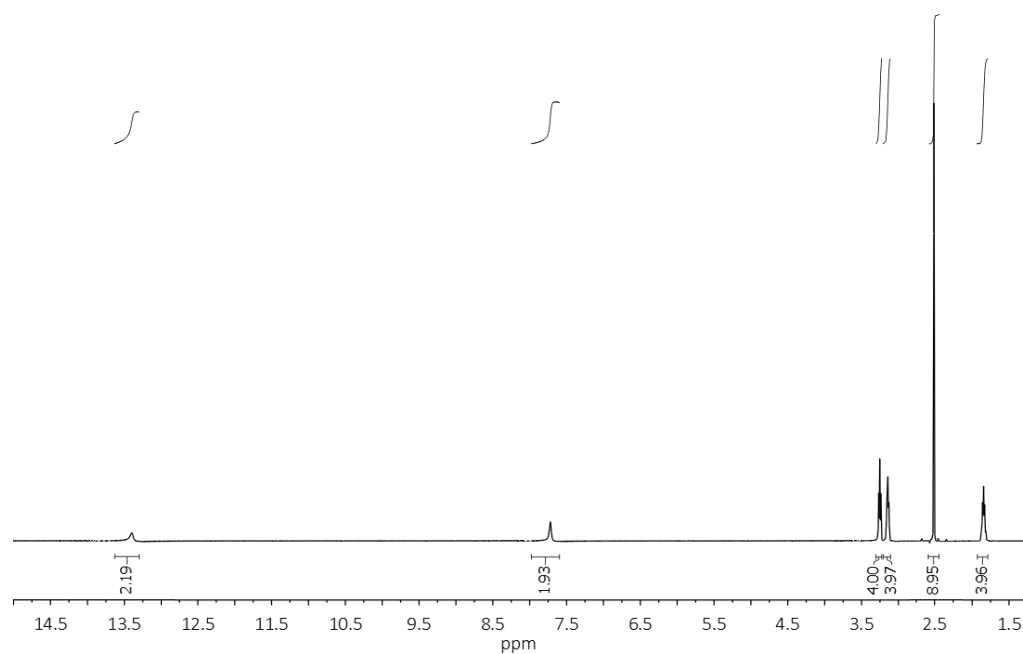
Figure S2.1. ^{1}H NMR spectroscopy in DMSO-d6 of the catalyst MSA:TBD (3:1). δ (ppm) 13.14, (s, 2H, OH, MSA), 7.72, (s, 2H, N-H-O), 3.25 (t, 4H, CH2, TBD), 3.14 (t, 4H, CH2, TBD), 2.52 (s, 9H, CH$_3$, MSA). 1.85 (q, 4H, CH$_2$, TBD).
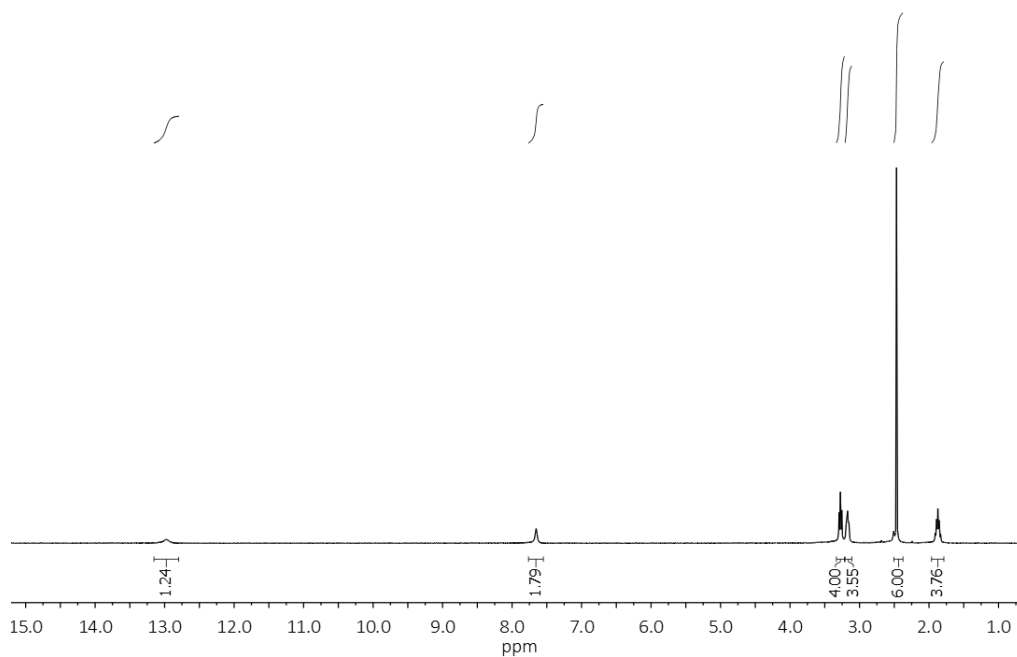
Figure S2.2. ^{1}H NMR spectroscopy in DMSO-d_6 of the catalyst MSA:TBD (2:1). δ (ppm) 13.14, (s, 1H, OH, MSA), 7.72, (s, 2H, N-H-O), 3.25 (t, 4H, CH2, TBD), 3.14 (t, 4H, CH2, TBD), 2.52 (s, 6H, CH$_3$, MSA). 1.85 (q, 4H, CH$_2$, TBD).
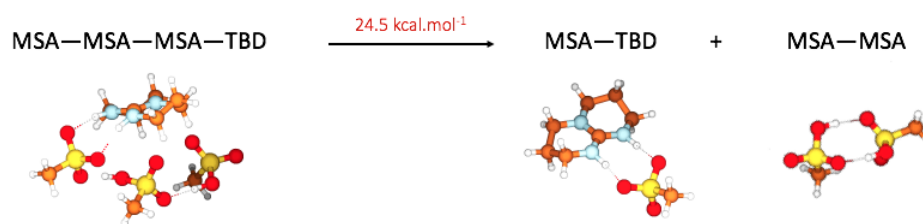
Figure S2.3. Dissociation pathway for MSA:TBD (3:1)
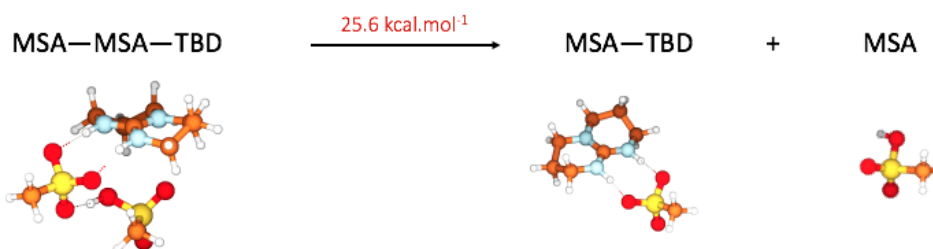
Figure S2.4. Dissociation pathway for MSA:TBD (2:1)
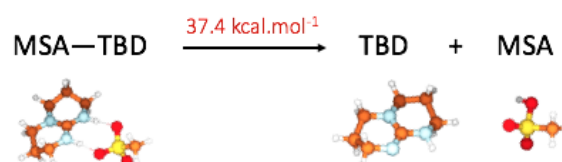
Figure S2.5. Dissociation pathway for MSA:TBD (1:1)
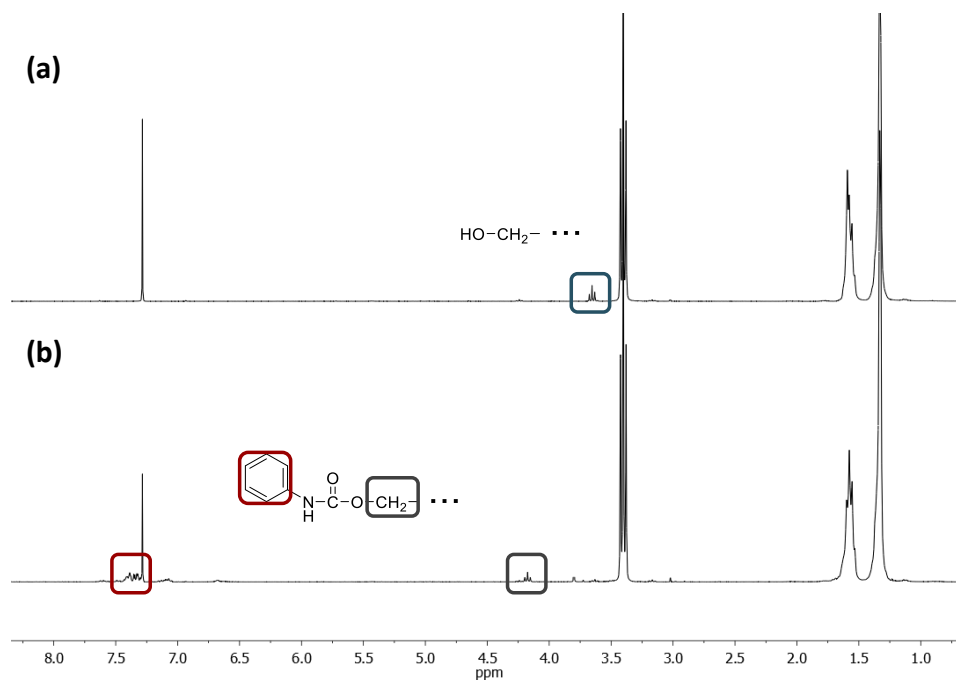
Figure S2.6. ¹H NMR of spectroscopy in d-CDCl₃ the a) poly(oxyhexamethylene) purified and b) poly(oxyhexamethylene) capped with pheny lisocyanate.
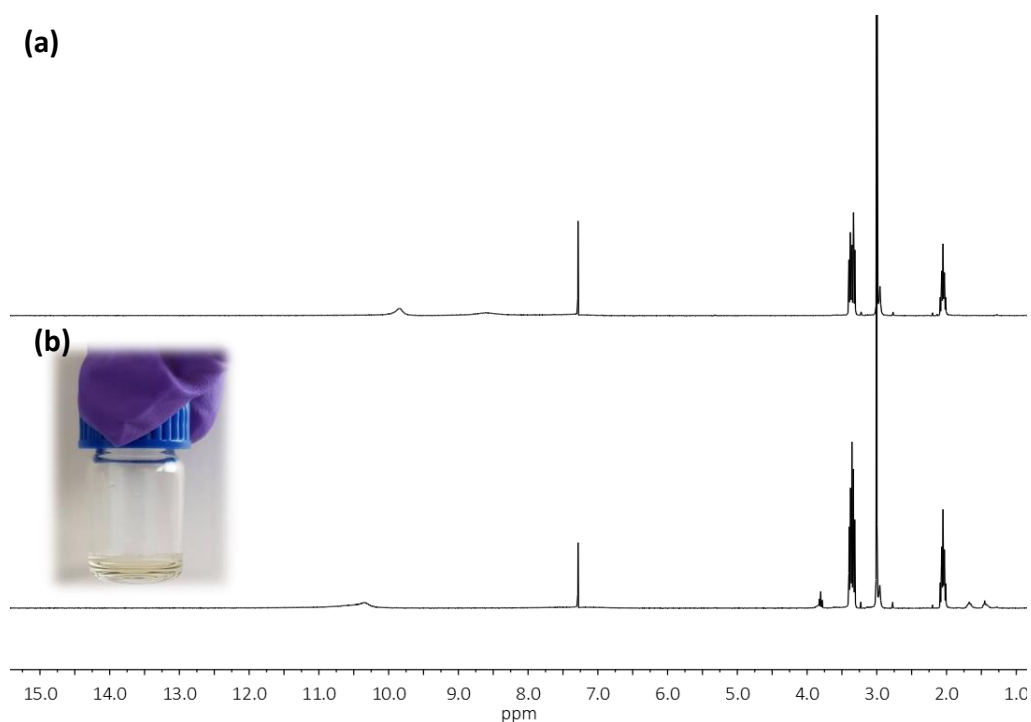
Figure S2.7. ¹H NMR of spectroscopy in d-CDCl₃ of a) the non-eutectic acid base mixture MSA:TBD 3:1 recrystrallized and b) the non-eutectic mixture MSA:TBD 3:1 recovered.
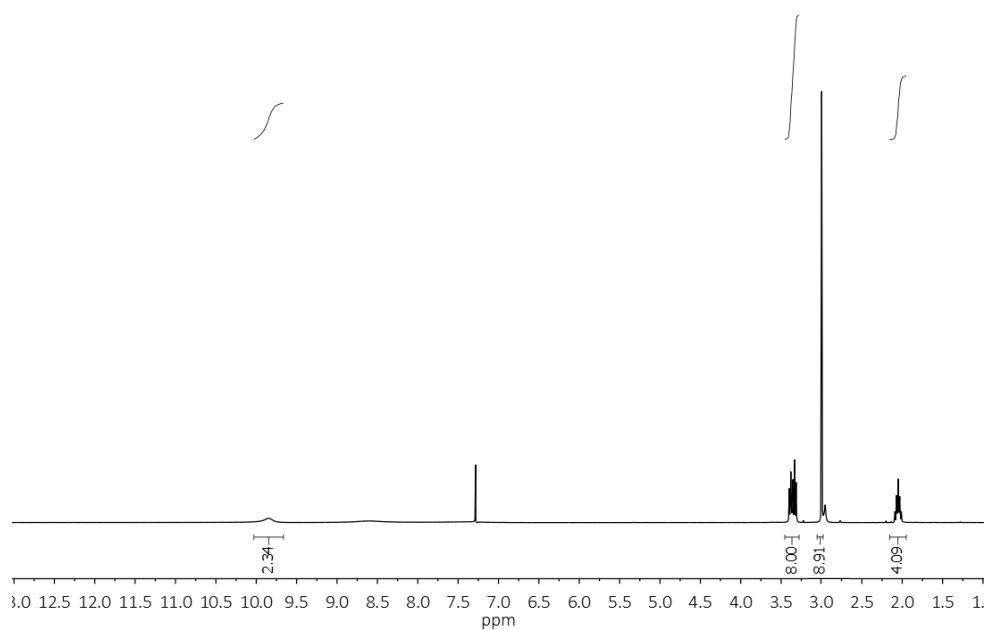
Figure S2.8. ^{1}H NMR of spectroscopy in d-CDCl$_3$ of the non-eutectic acid base mixture MSA:TBD 3:1 recrystrallized.
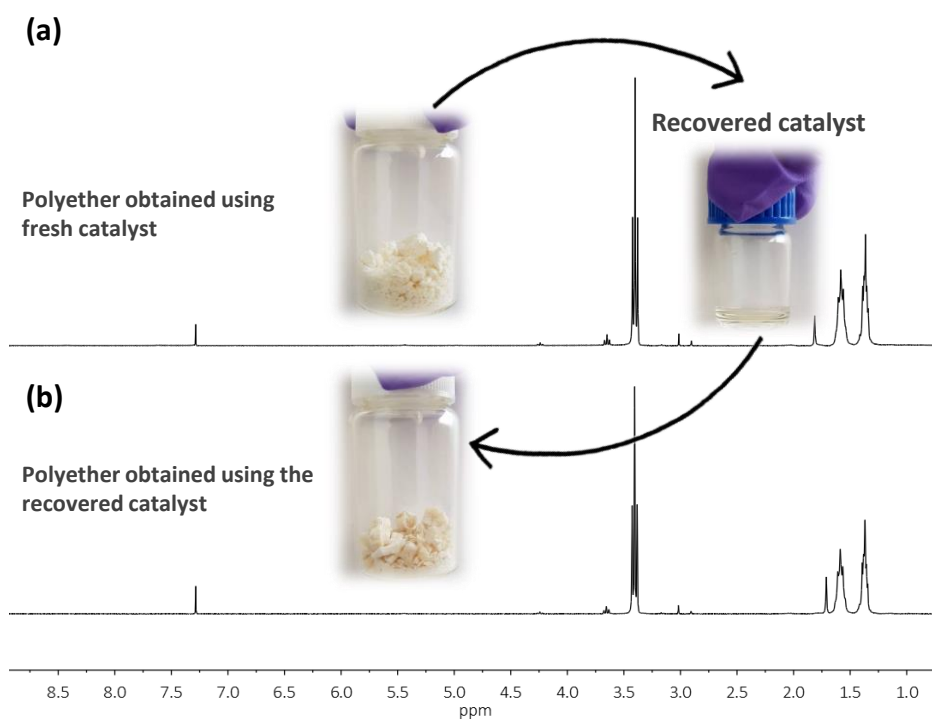
Figure S2.9. a) ^{1}H NMR of spectroscopy in d-CDCl3 the a) poly(oxyhexamethylene) and b) poly(oxyhexamethylene) obtained using the recycled catalyst.
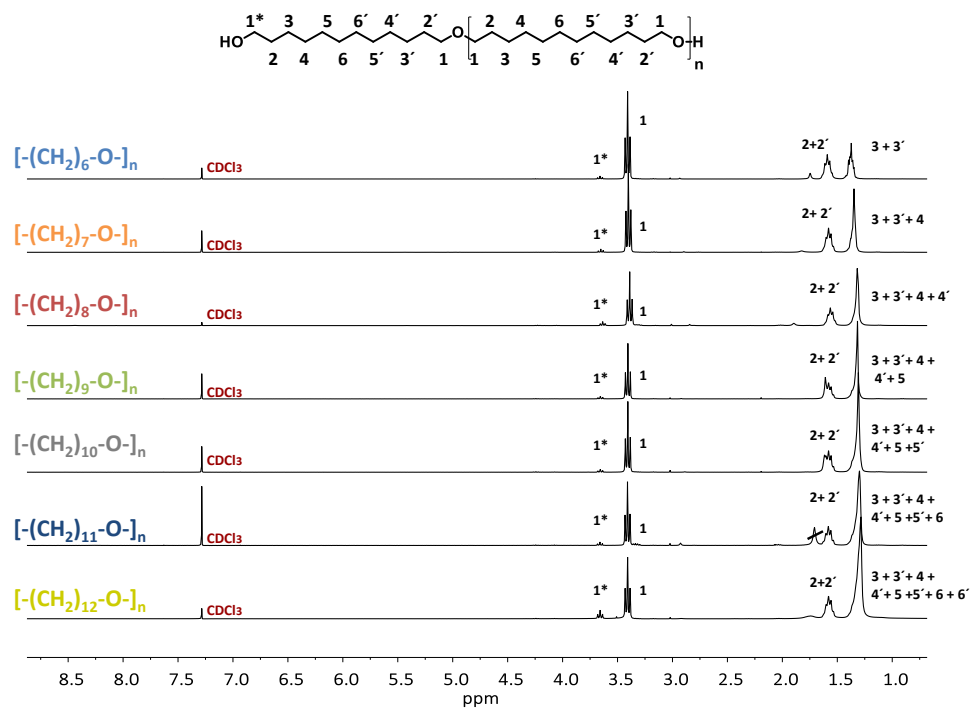
Figure S2.10. ^{1}H NMR spectroscopy in d-CDCl3 of the polyethers.
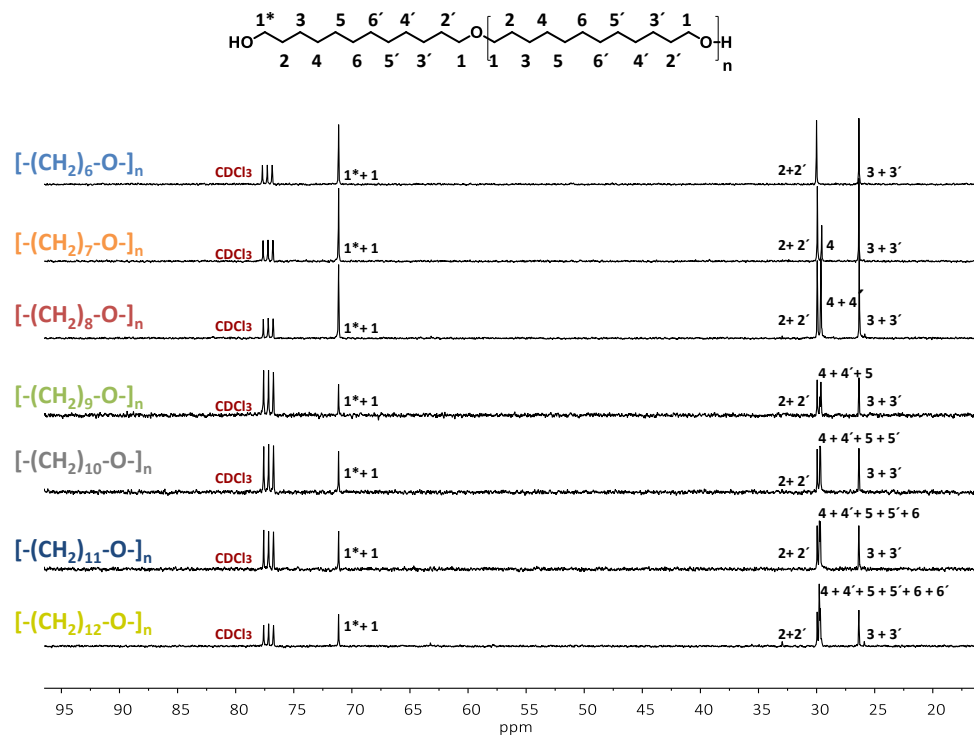
Figure S2.11. ^{13}C NMR spectroscopy in d-CDCl3 of the polyethers.
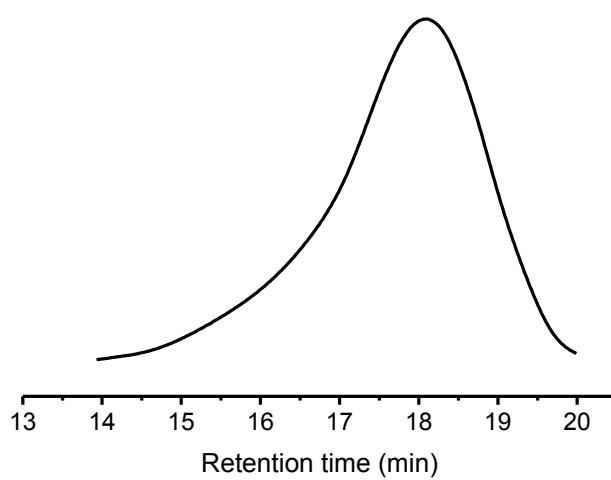
Figure S2.12. SEC chromatograms of $[-(CH_2)_6-O-]_n$.
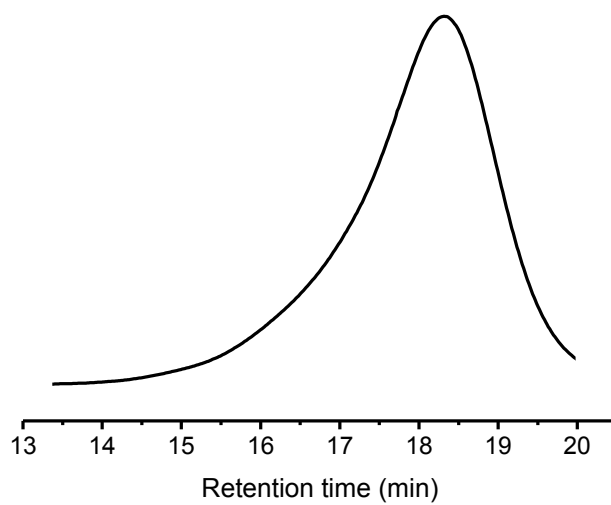
Figure S13. SEC chromatograms of $[-(CH_2)_7-O-]_n$.
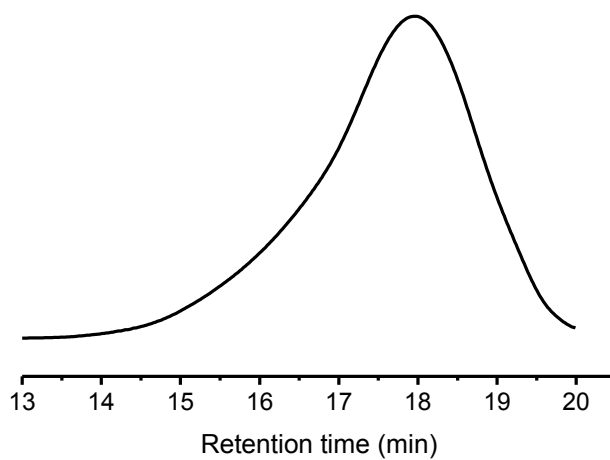
Figure S2.14. SEC chromatograms of $[-(CH_2)_8-O-]_n$.
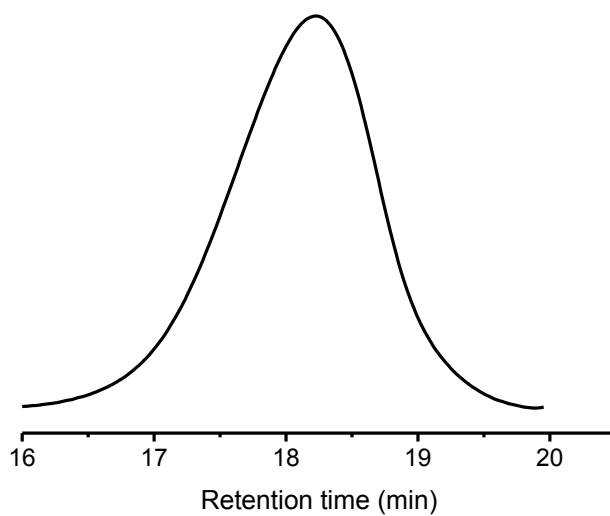
Figure S2.15. SEC chromatograms of $[-(CH_2)_9-O-]_n$.
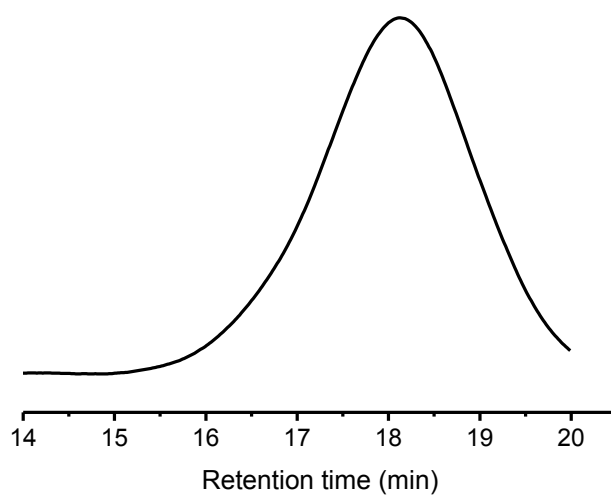
Figure S2.16. SEC chromatograms of $[-(CH_2)_{10}-O-]_n$.
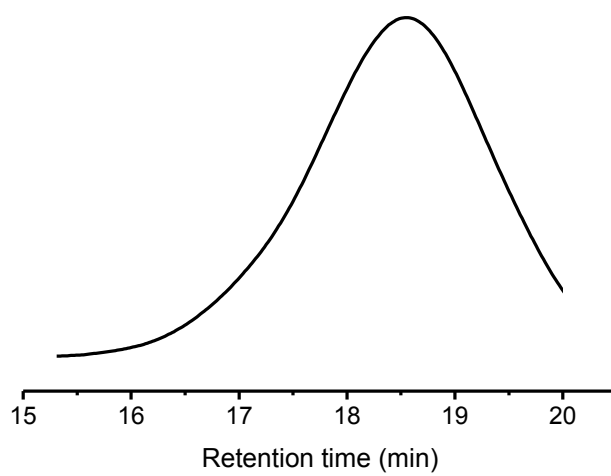
Figure S2.17. SEC chromatograms of $[-(CH_2)_{11}-O-]_n$.
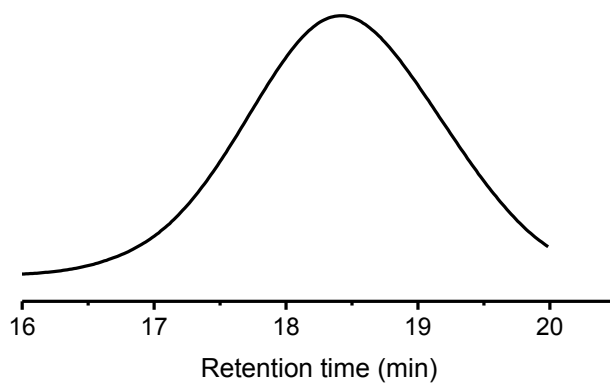
Figure S2.18. SEC chromatograms of $[-(CH1_2)_{12}-O-]_n$.
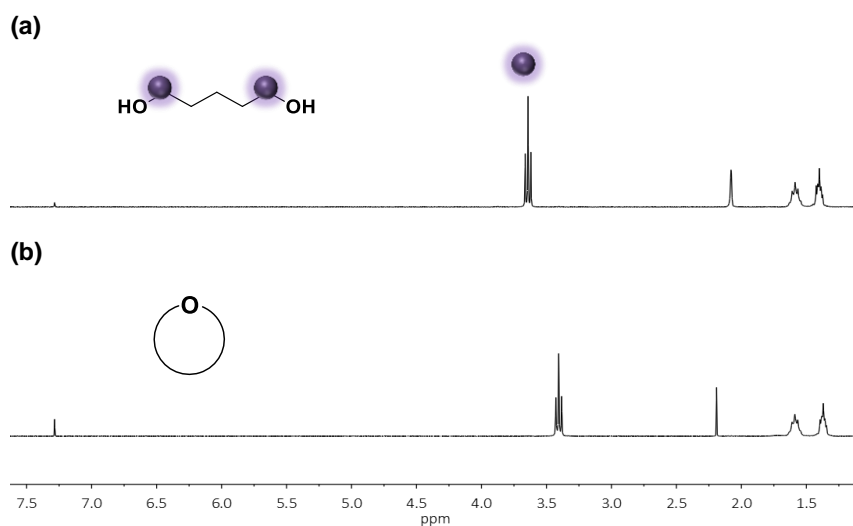
Figure S2.19. ^1H NMR of spectroscopy in d-CDCl$_3$ of a) 1,5-pentanediol monomer and b) cycles obtained after the self-condensation of 1,5- pentanediol. No signal at 3.65ppm corresponding to the ending group was observed.
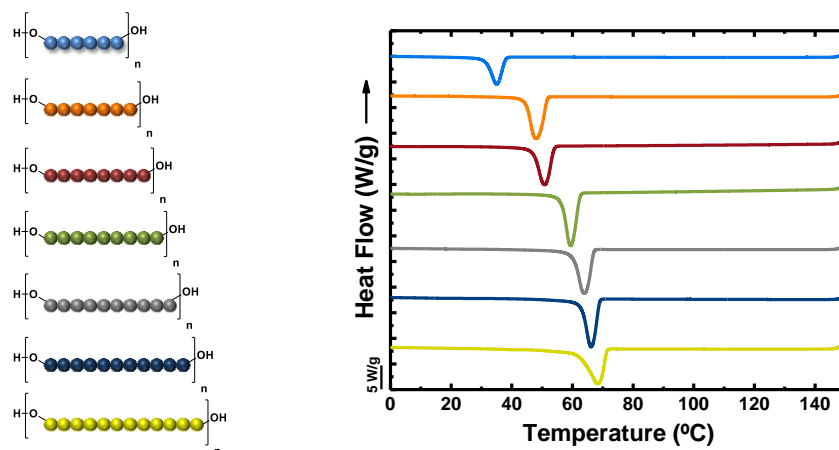
Figure S2.20. DSC cooling scan of the polyethers.

Table S2.1. Calculated Diffraction Spacings (*d*)

Sample	2θ	2θ*	q(nm-1)	q(nm-1)*	d(nm)	d(nm)*	Reflection
Polytetrahydrofuran	-	20	-	14.15	-	0.444	020
	-	24.4	-	17.22	-	0.365	110
$[-(CH_2)_6-O-]_n$	13.11	19.7	13.92	13.94	0.451	0.451	020
	16.04	24.2	17.02	17.08	0.369	0.368	110
$[-(CH_2)_7-O-]_n$	14.49	21.9	15.38	15.48	0.408	0.406	110
	15.9	24.12	16.88	17.03	0.372	0.369	200
$[-(CH_2)_8-O-]_n$	13.06	19.6	13.88	13.87	0.453	0.453	020
	15.96	24.15	16.94	17.05	0.370	0.369	110
$[-(CH_2)_9-O-]_n$	14.38	21.65	15.28	15.31	0.411	0.411	110
	16.04	24.2	17.03	17.08	0.369	0.368	200
$[-(CH_2)_{10}-O-]_n$	14.38	21.6	15.28	15.27	0.411	0.411	110
	16.03	24.15	17.01	17.05	0.369	0.369	200
$[-(CH_2)_{11}-O-]_n$	14.39	-	15.28	-	0.411	-	110
	16.04	-	17.02	-	0.369	-	200
$[-(CH_2)_{12}-O-]_n$	14.38	21.7	15.28	15.34	0.411	0.410	110
	16.01	24.15	17.00	17.05	0.369	0.369	200
Polyethylene	-	21.7	-	15.34	-	0.410	110
	-	24.1	-	17.01	-	0.369	200

2θ* values were taken from the graphs reported by Kobayashi, using these values, q* and d* were calculated employing the wavelength reported in the article (λ = 1.542 Å)[1].
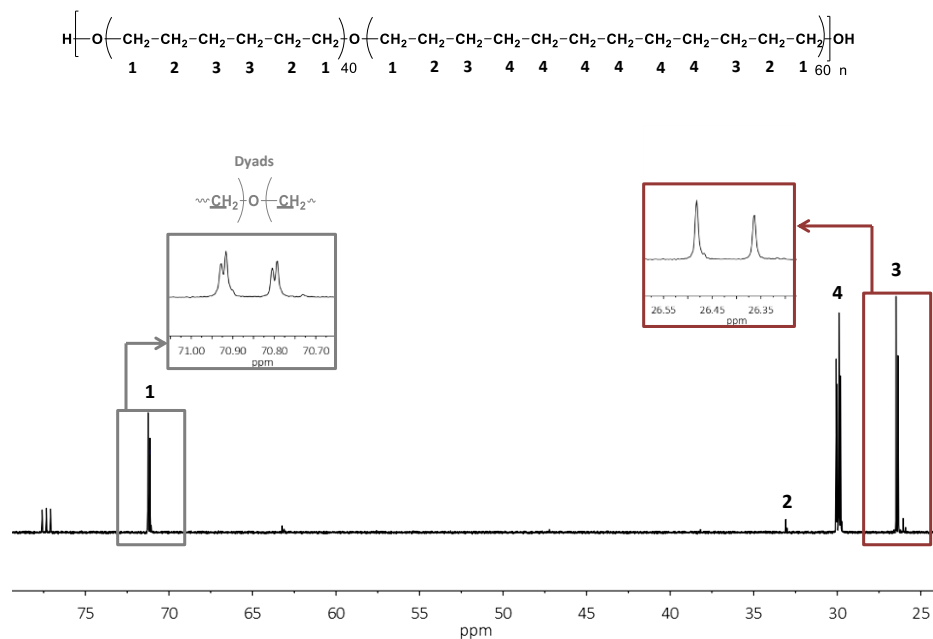
Figure S2.21. ^{13}C NMR spectroscopy of the copolymer 1,6/1,12.
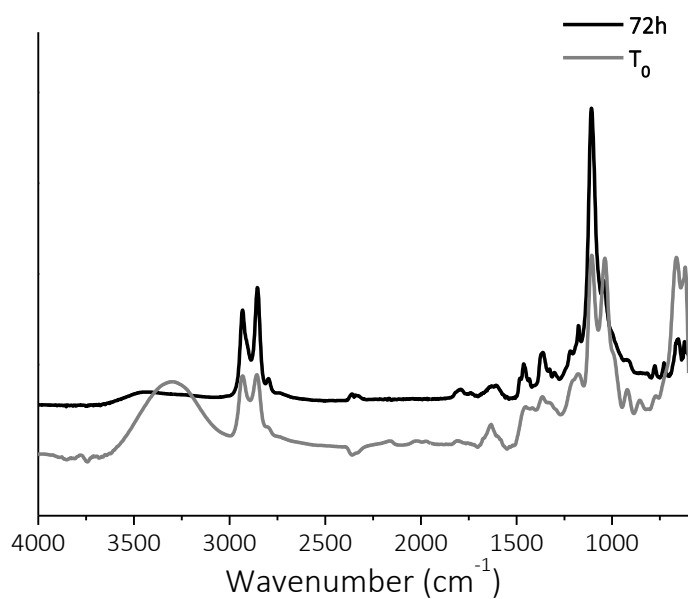
Figure S2.22. FTIR of copolyether 1,6-hexanediol/glycerol at T_0 and after full conversion

Chapter 3.
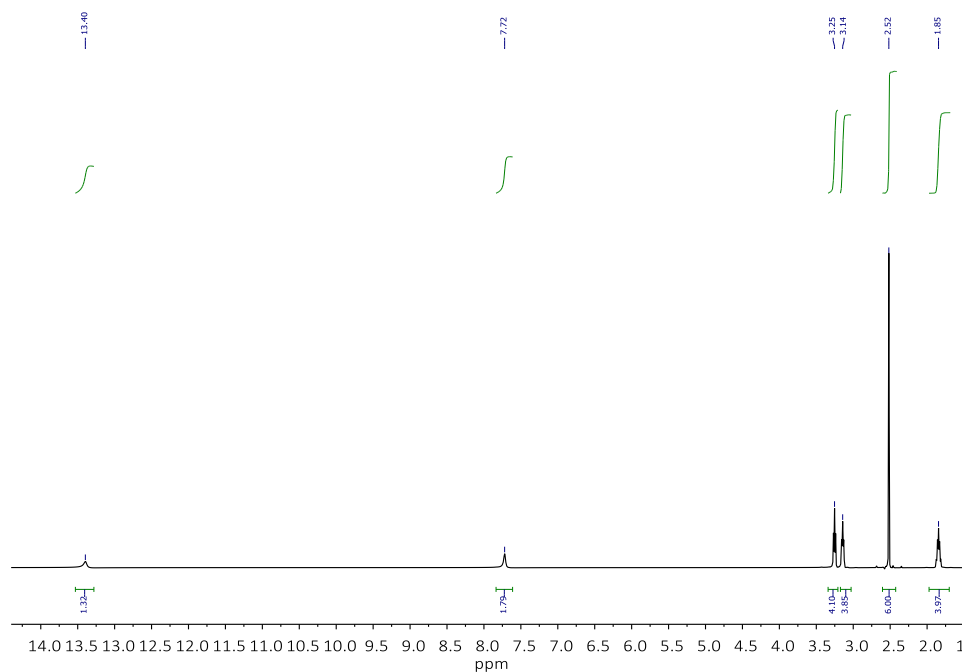
Figure S3.1. ^{1}H NMR spectroscopy in DMSO-d6 of the catalyst MSA:TBD (3:1). δ (ppm) 13.14, (s, 2H, OH, MSA), 7.72, (s, 2H, N-H-O), 3.25 (t, 4H, CH2, TBD), 3.14 (t, 4H, CH2, TBD), 2.52 (s, 9H, CH$_3$, MSA). 1.85 (q, 4H, CH$_2$, TBD).
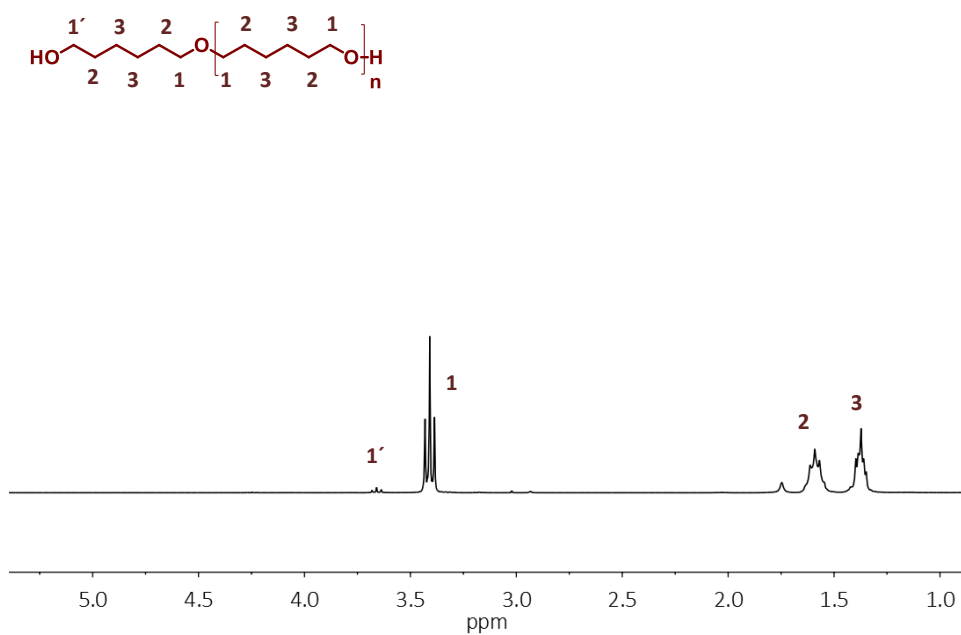
Figure S3.2. ^{1}H NMR spectroscopy in d-CDCl$_3$ of the poly(oxyhexamethylene).
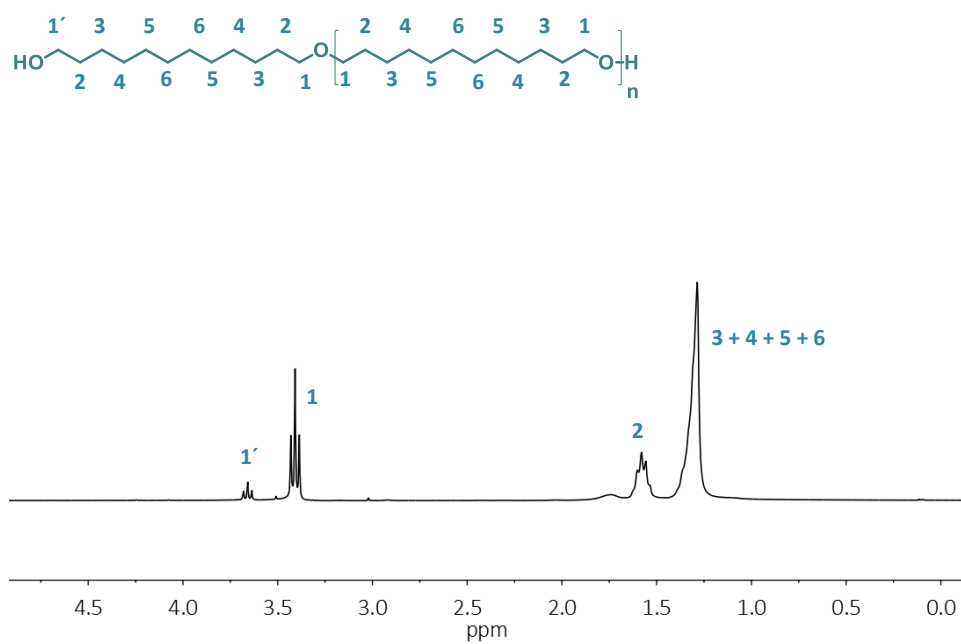
Figure S3.3. ^{1}H NMR spectroscopy in d-CDCl$_3$ of the poly(oxydodecamethylene).
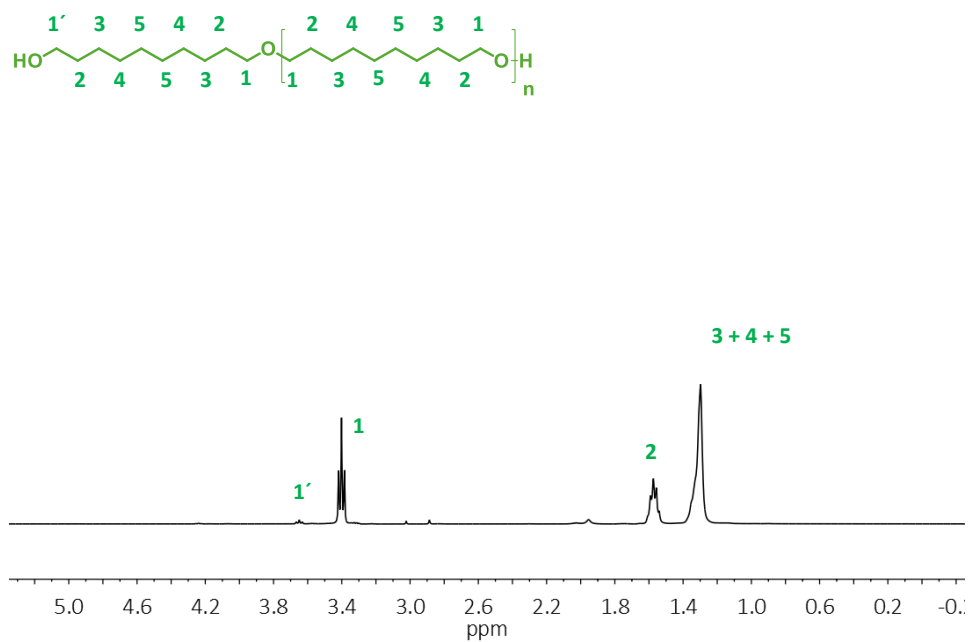
Figure S3.4. ^{1}H NMR spectroscopy in d-CDCl$_3$ of the poly(oxydecamethylene).
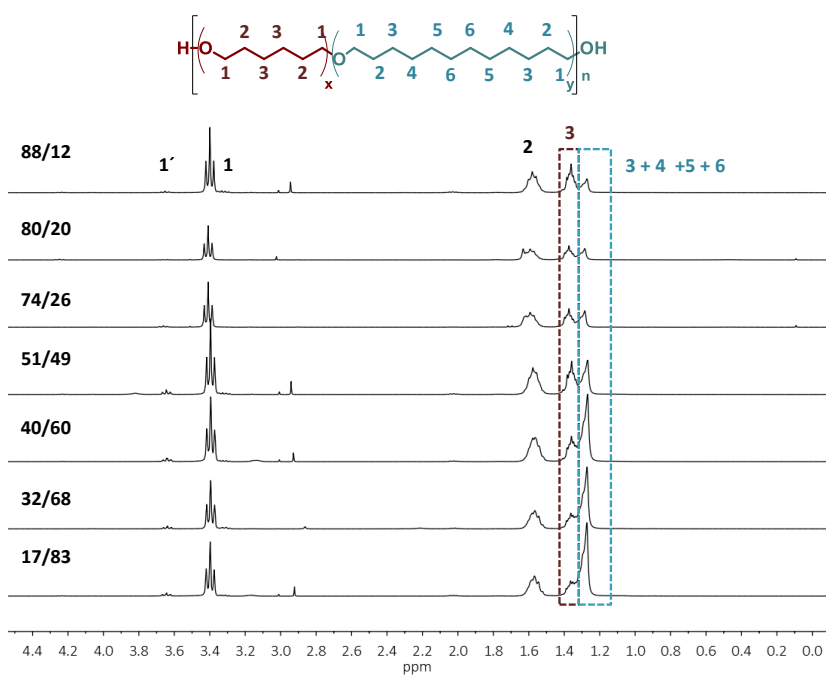
Figure S3.5. ^{1}H NMR spectroscopy in d-CDCl$_3$ of the copolymers
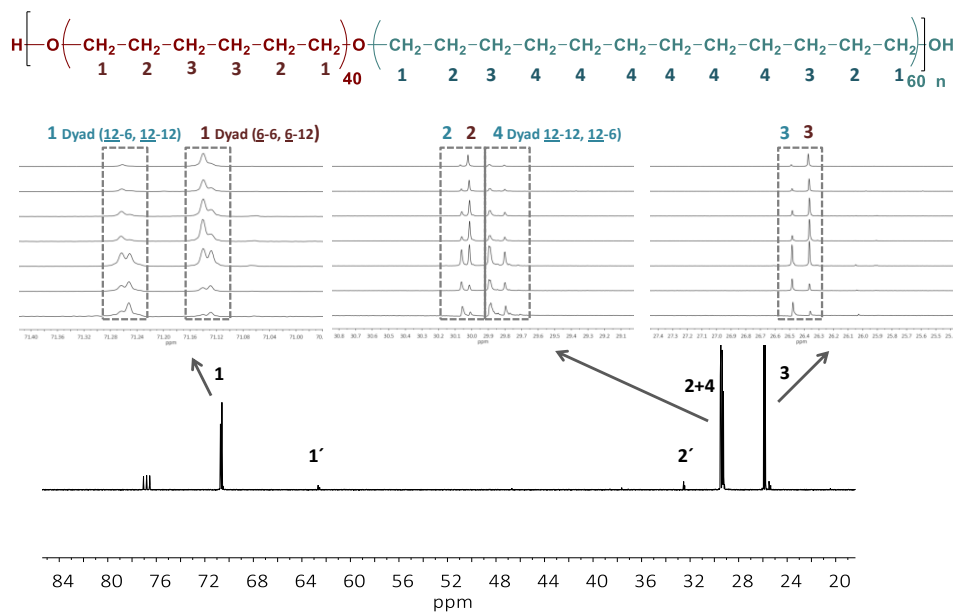
Figure S3.6. ^{13}C NMR spectroscopy in d-CDCl$_3$ of the copolyethers. Signals 1′and 2′make reference to the corresponding carbons of the ending group.
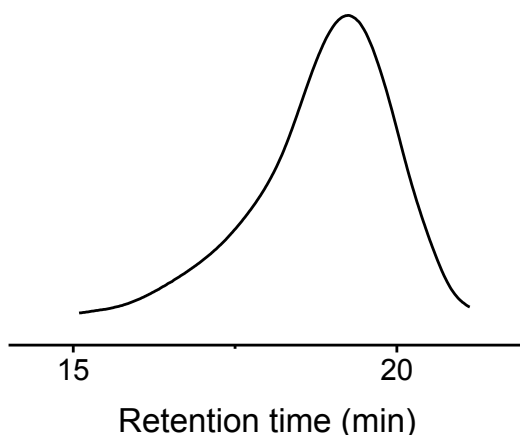
Figure S3.7. SEC trace of the terpolymer.
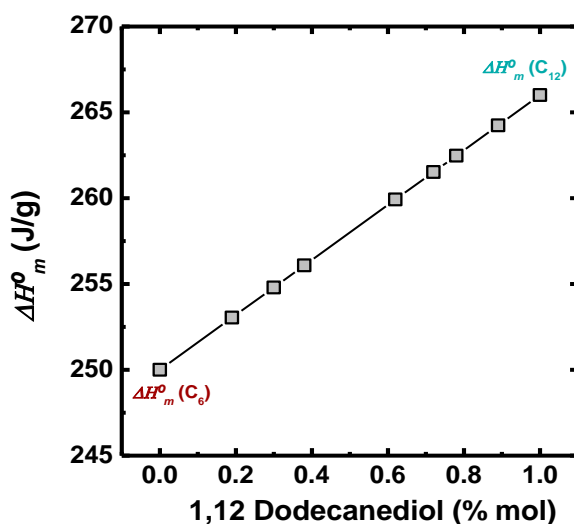
Figure S3.8. Values of $\Delta H_m°$ depending on the composition C6/C12.

$$\Delta H°_{m(C6/C12)} = \Delta H°_{m(C6)} * X_{(C6)} + \Delta H°_{m(C12)} * X_{(C12)} \qquad (1)$$

Where $\Delta H°_{m(C6)}$ and $\Delta H°_{m(C12)}$ is the enthalpy of homopolymers if they were 100% crystalline. $X_{(C6)}$ and $X_{(C12)}$ is the mass fraction of each homopolymer present in the copolymer.

$\Delta H°_{m(C6)}$ and $\Delta H°_{m(C12)}$ were calculated following the procedure reported in the literature.

Chapter 4.
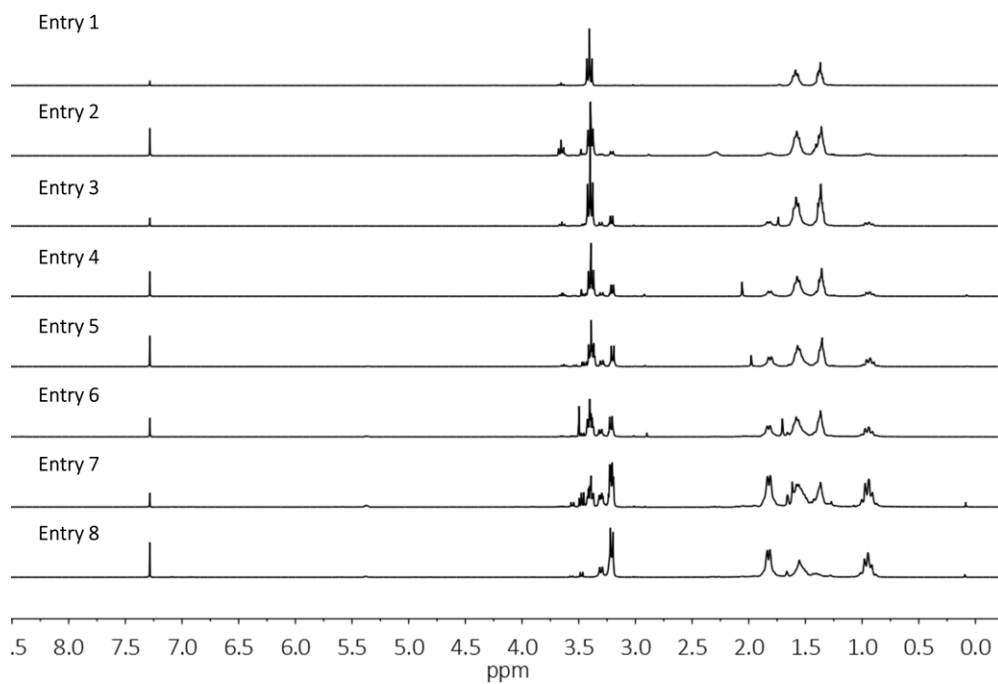
Figure S4.1. ^{1}H NMR spectroscopy in d-CDCl$_3$ of the copolymers
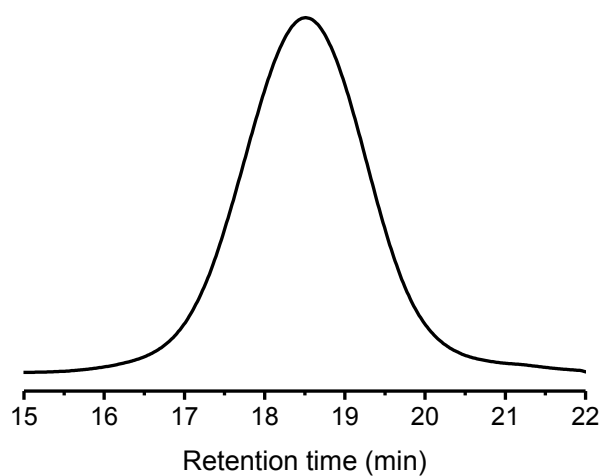
Figure S4.2. SEC trace of the terpolymer.
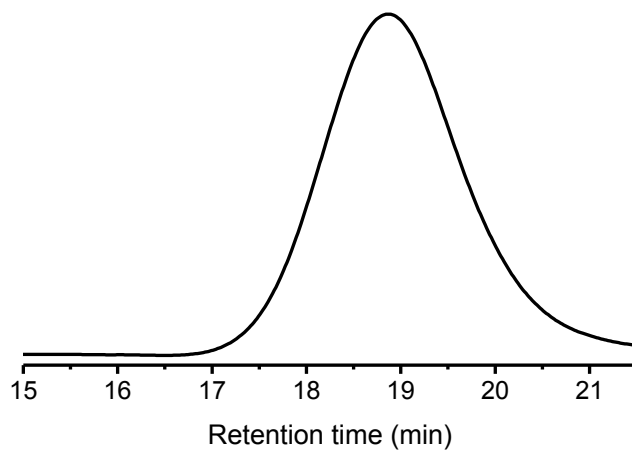
Figure S4.3. SEC trace of the terpolymer.
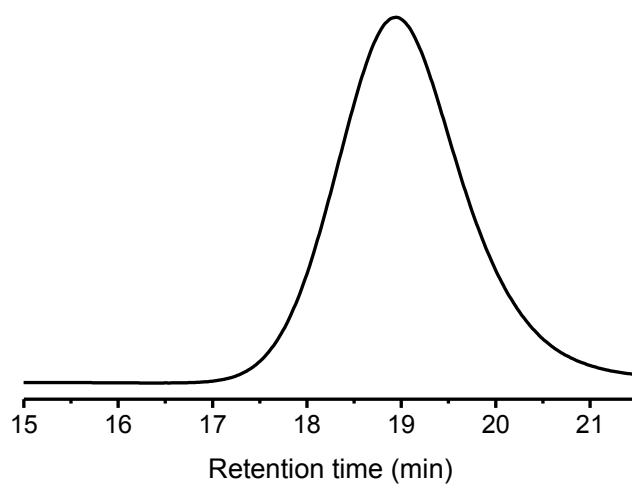
Figure S4.4. SEC trace of the terpolymer.
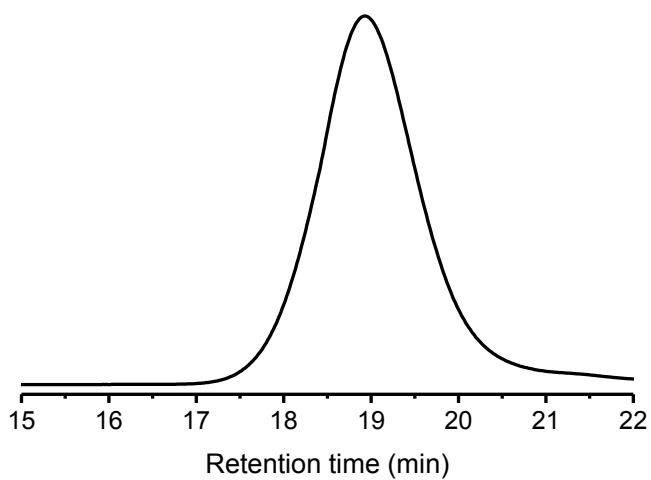
Figure S4.5. SEC trace of the terpolymer.
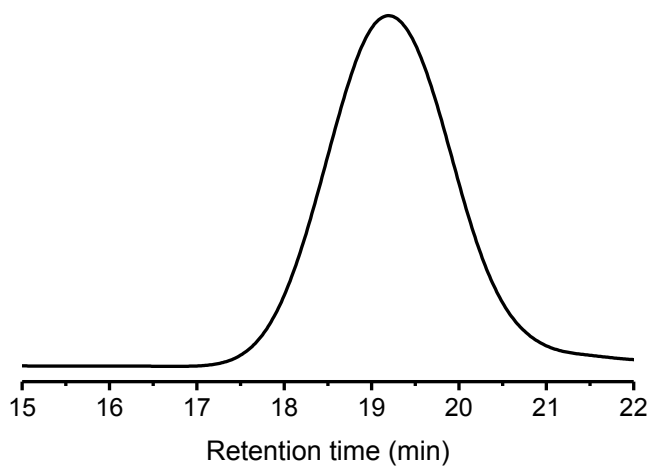
Figure S4.6. SEC trace of the terpolymer.
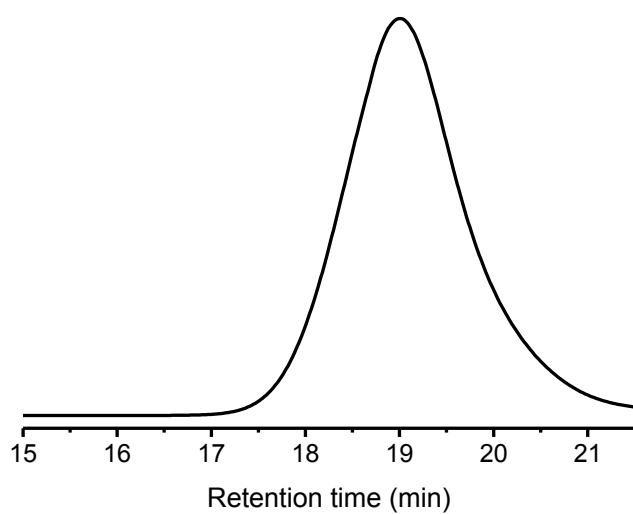
Figure S4.7. SEC trace of the terpolymer.
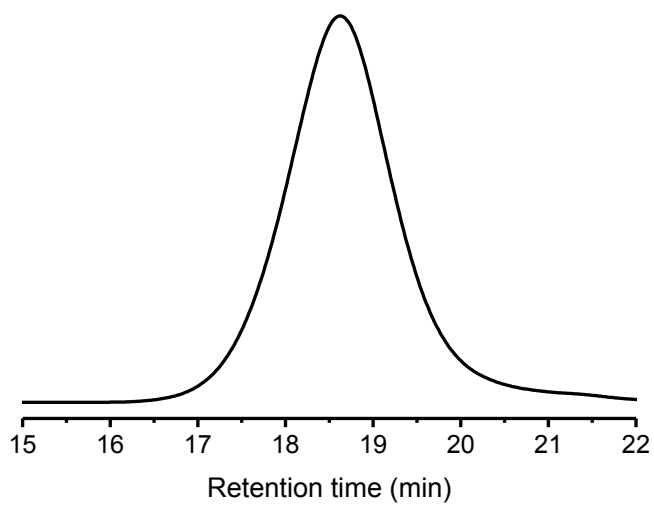
Figure S4.8. SEC trace of the terpolymer.
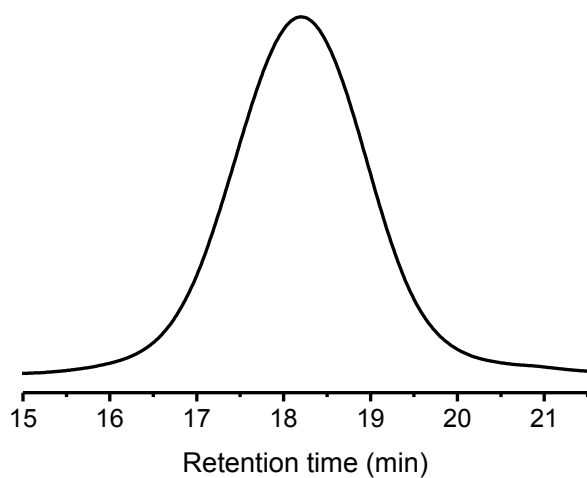
Figure S4.9. SEC trace of the terpolymer.
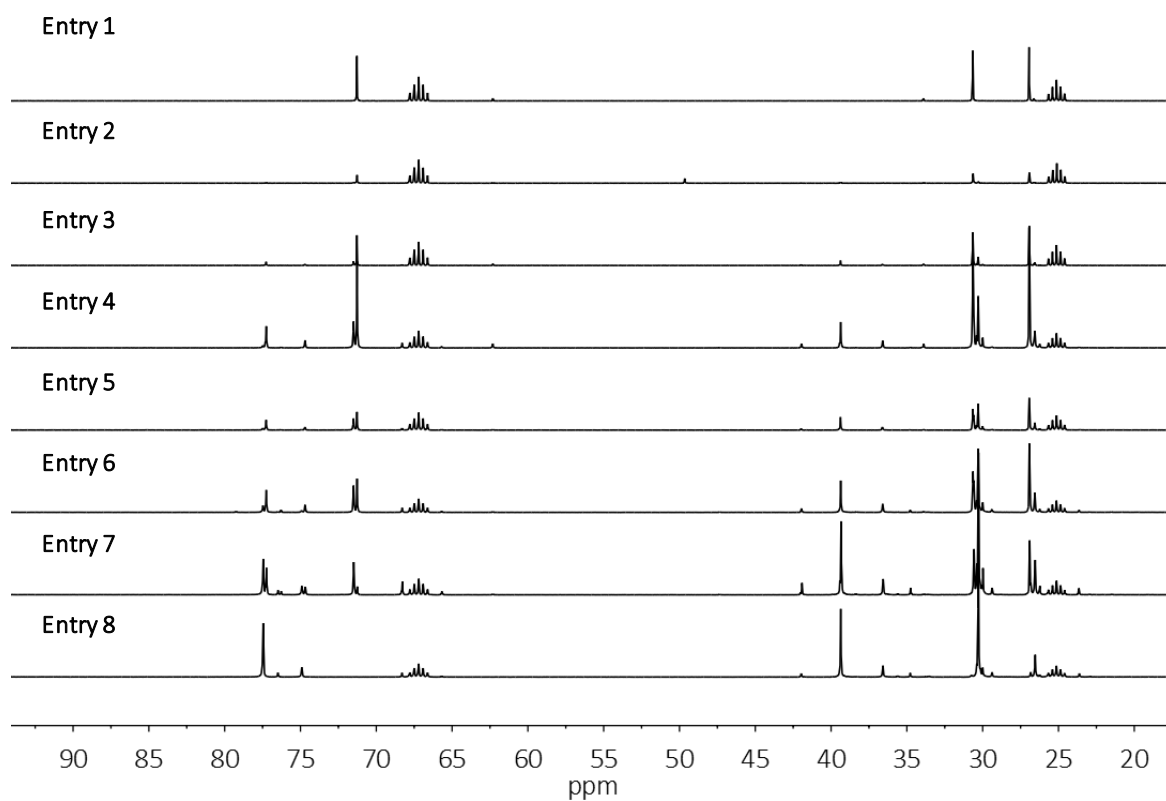
Figure S4.10. ^{13}C NMR spectroscopy in THF of the copolyethers.

Table S4.3. Chemical compositions and molecular characteristics of the copolyethers.

(HDO)/(CHDM) % in the feed	(CHDM) % cis-trans in the feed	(HDO)/(CHDM) % in the polymer [a]	M_n[b] (g/mol)	Đ
0/100	1/99	0/100	9500	2.2
80/20	1/99	81/19	7700	2.1
80/20	90/10	84/16	7100	1.8
50/50	1/99	49/51	8300	2.1
50/50	90/10	56/44	9400	2.2
20/80	1/99	22/78	7000	2.1
20/80	90/10	20/80	6200	1.7

[a]Determined by ^{1}H NMR spectroscopy in CDCl$_3$, [b]Determined by SEC in CHCl$_3$, [c]Determined by ^{13}C NMR spectroscopy in CDCl$_3$
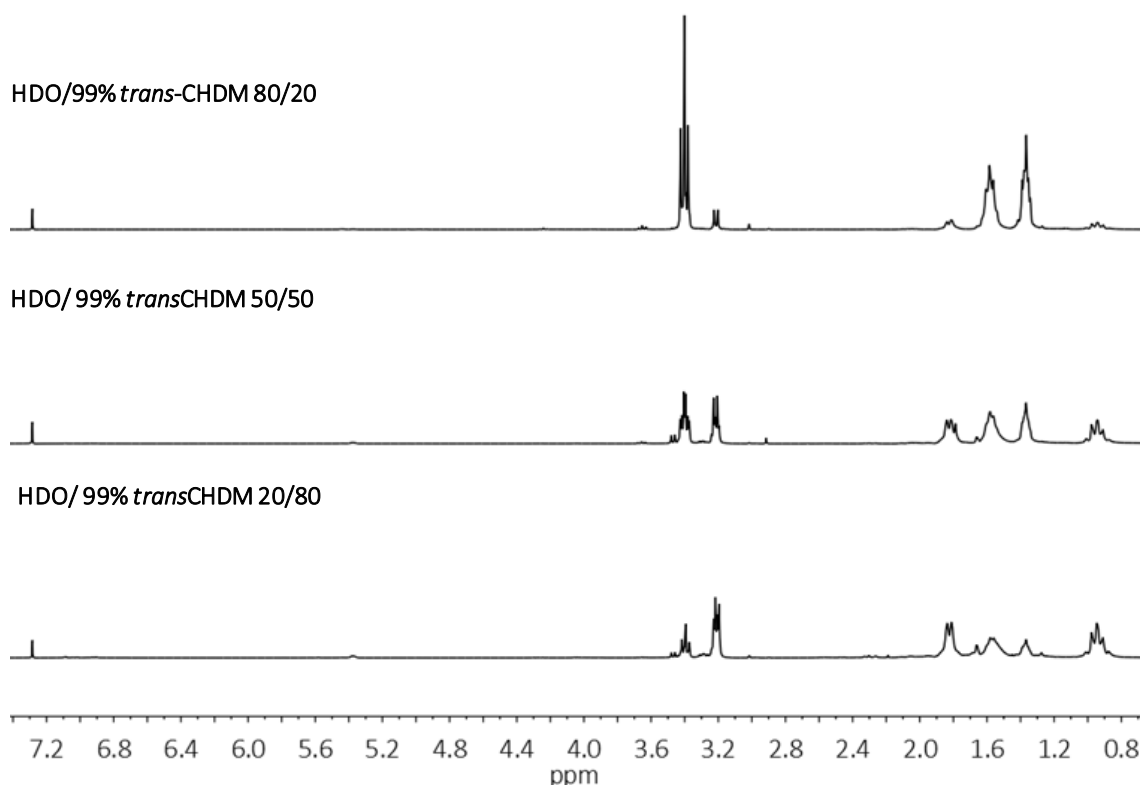
Figure S4.11. ^{1}H NMR spectroscopy in d-CDCl$_3$ of the copolymers synthetized using 01-99% *cis/trans*-CHDM
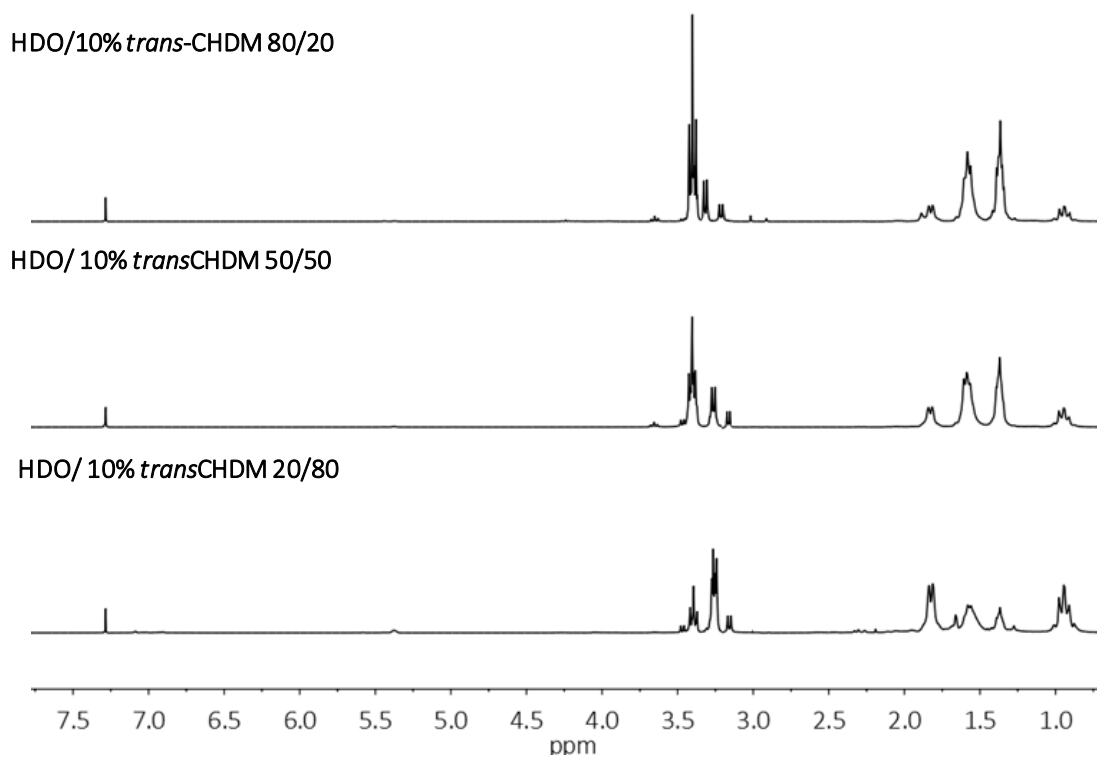
Figure S4.12. ^{1}H NMR spectroscopy in d-CDCl$_3$ of the copolymers synthetized using 90-10% *cis/trans*-CHDM
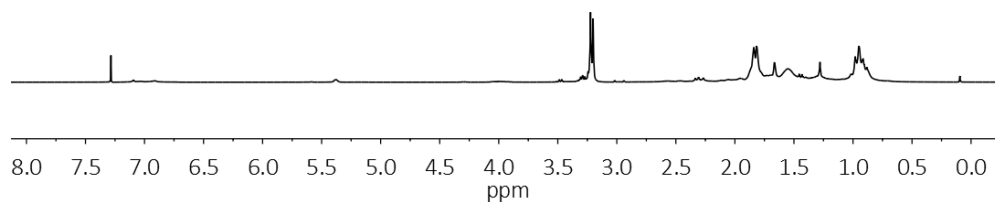
Figure S4.13. ^{1}H NMR spectroscopy in d-CDCl$_3$ of the homopolymer synthetized using 1-99% *cis/trans*-CHDM.
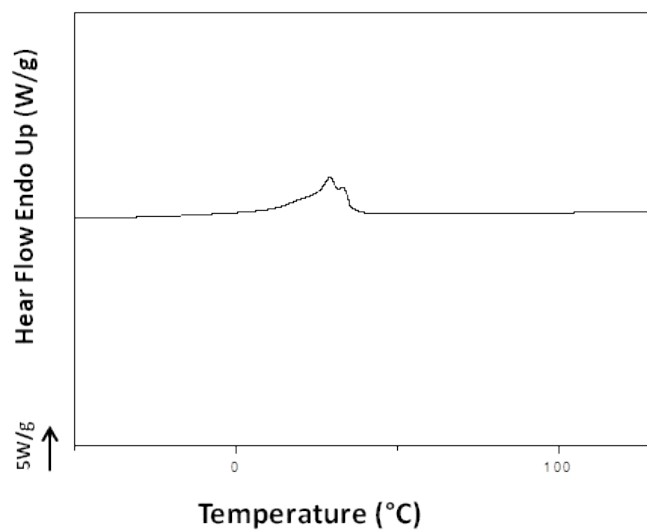
Figure S4.14. DSC heating and cooling scan of the polyether obtained from 99%*trans*-CHDM.

Chapter 5.
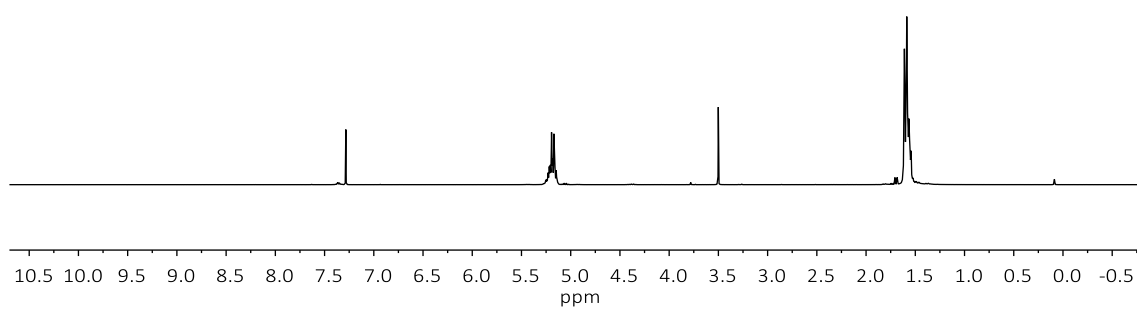
Figure S5.1. ^{1}H NMR spectrum of [BnOH]-[MSA]-[DMAP]-[LLA]=1-0-1-100
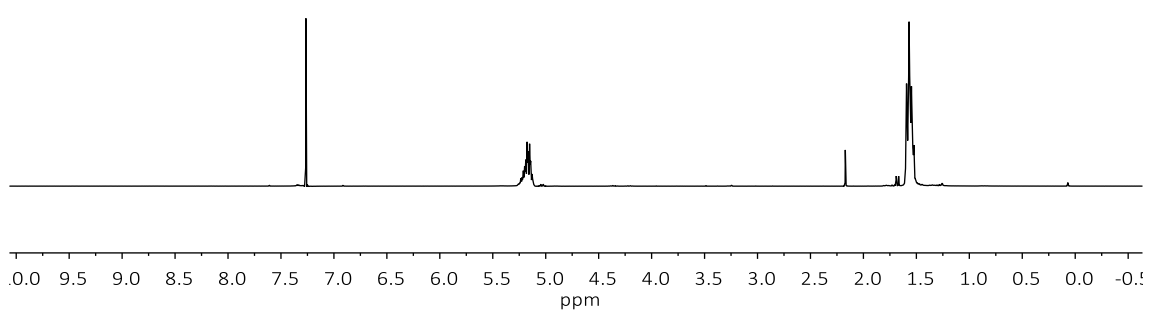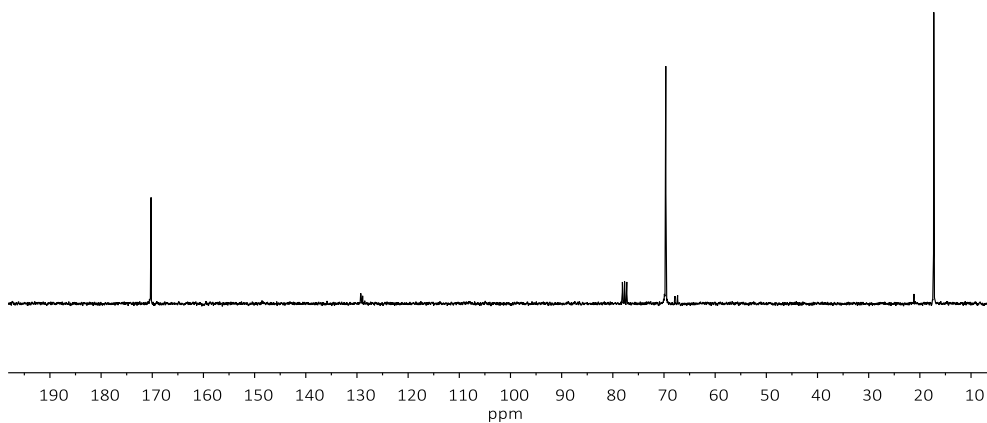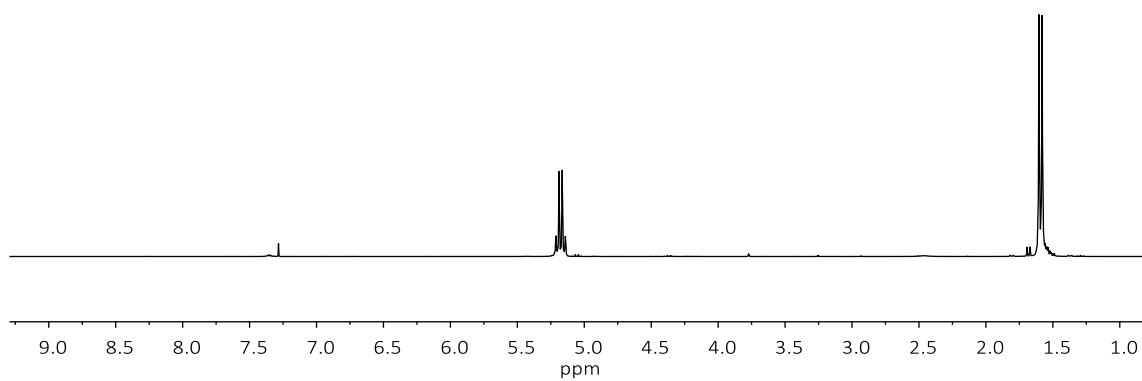
Figure S5.2 . ¹H NMR spectrum of [BnOH]-[MSA]-[DMAP]-[LLA]=1-1-1-100.
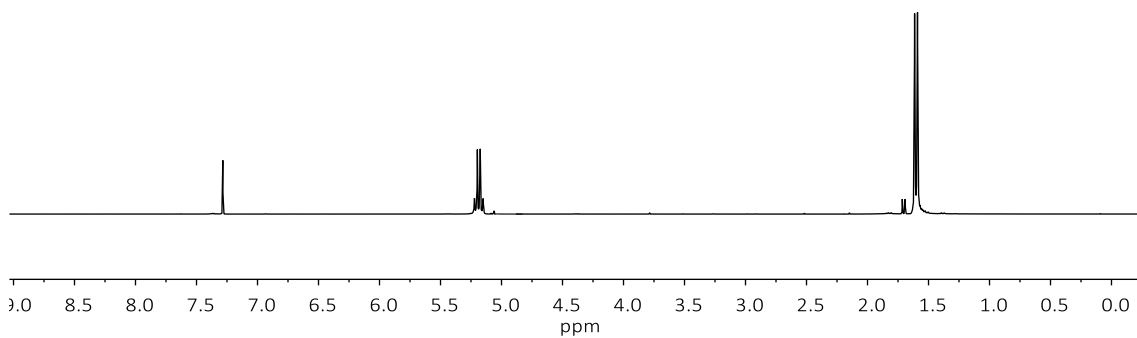
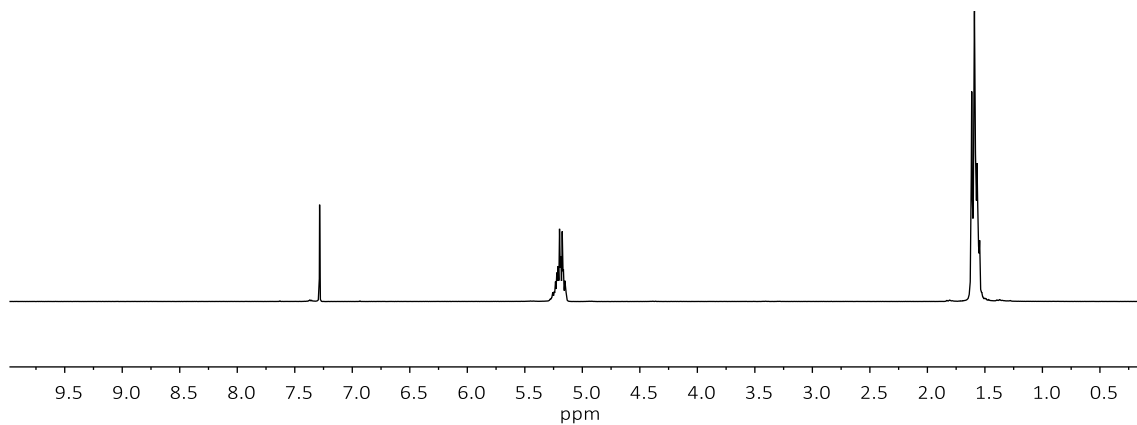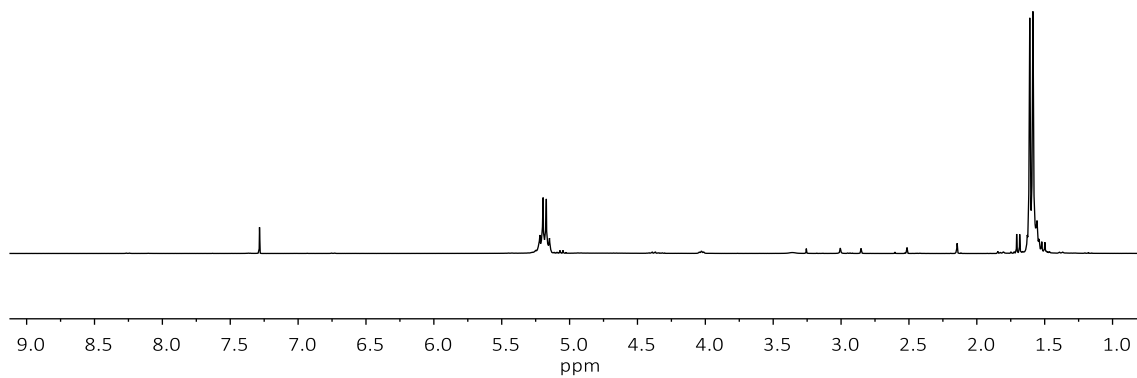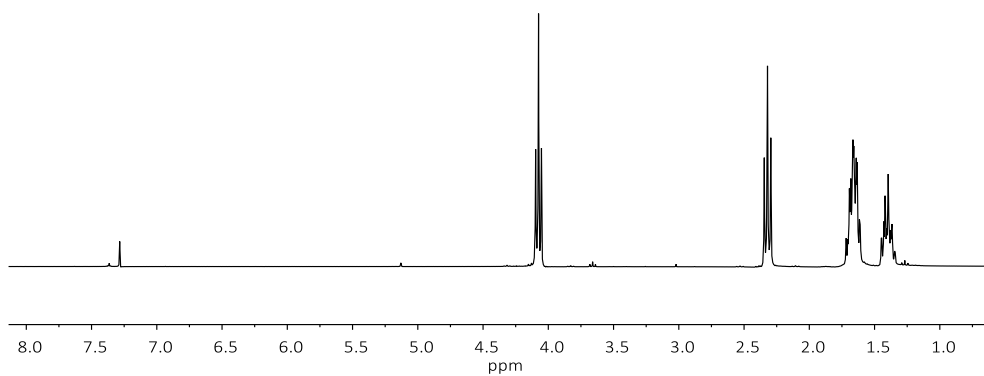Figure S5.3. ¹H NMR spectrum of [BnOH]-[MSA]-[DMAP]-[LLA]=1-2-1-100.
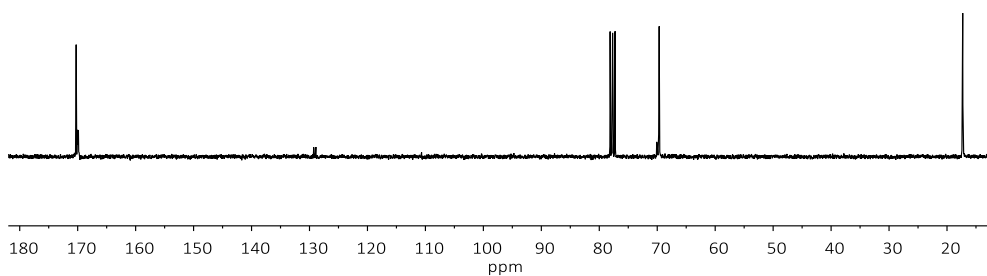
Figure S5.4. ^{13}C NMR spectrum of [BnOH]-[MSA]-[DMAP]-[LLA]=1-1-1-100.

Figure S5.5. ^{13}C NMR spectrum of [BnOH]-[MSA]-[DMAP]-[LLA]=1-2-1-100.
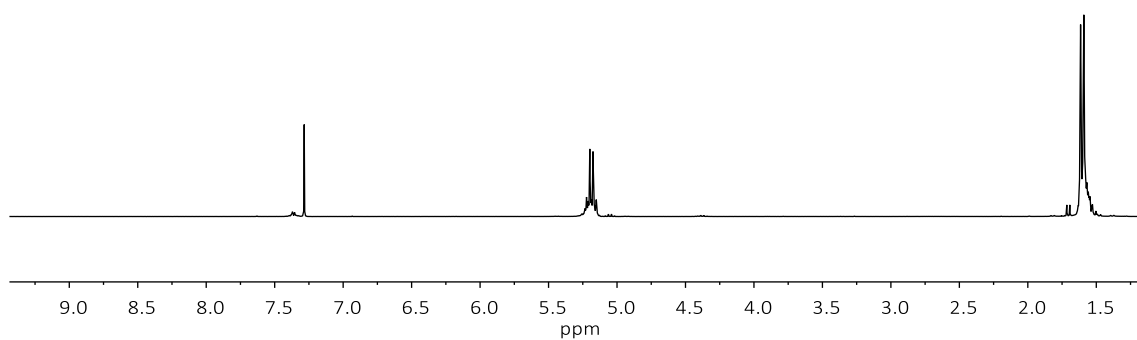
Figure S5.6. ^{1}H NMR spectrum of [BnOH]-[MSA]-[DMAP]-[LLA]=1-1-1-50.

Figure S5.7. ^{1}H NMR spectrum of [BnOH]-[MSA]-[DMAP]-[LLA]=1-2-1-50.

Figure S5.8. ^{1}H NMR spectrum of [BnOH]-[MSA]-[DMAP]-[LLA]=1-4-2-200.

Figure S5.9. ^{1}H NMR spectrum of [BnOH]-[MSA]-[DMAP]-[LLA]=1-4-2-400.

Figure S5.10. ^{1}H NMR spectrum of [BnOH]-[MSA]-[DMAP]-[CLO]=1-4-2-100.
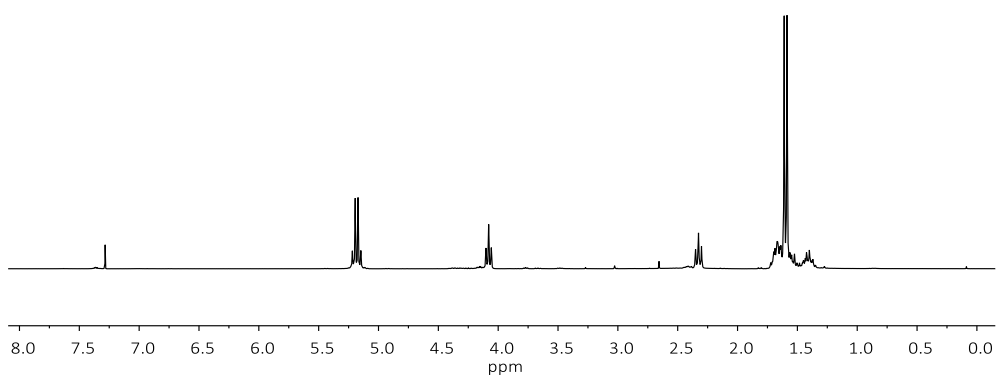

Figure S5.11. ^{1}H NMR spectrum of [BnOH]-[MSA]-[DMAP]-[LLA]-[CLO]=1-4-2-100-100 .

Curriculum Vitae

Andere Basterretxea Gorostiza

Date of birth: 12/11/1988

Nationality: Bilbao, Spain

Phone: +34 626969013

Email: *andere.basterrechea@ehu.eus*

Research Experience

January 2019 | May 2019

Virginia Polytechnic Institute and State University (Virginia Tech), USA.

The Long Research Group – DREAMS lab.

Research focus: UV 3D printing of polyethers

PhD Student

December 2018 (2 weeks)

Corbion N.V

Research focus: Synthesis of PLLA using acid-base mixture organocatalysts

PhD Student

January 2017| September 2019

Mons University

PhD secondment

September 2015 | <u>Present</u>

Universidad del País Vasco (UPV/EHU), POLYMAT, Donostia-San Sebastián, Spain

Research focus: Protic Ionic Liquids/Salts as new generation of organocatalysts for high temperature polymerizations

PhD Student

September 2014 | August 2015

Yamagata University, Department of Polymer Science and Engineering, Yamagata, Japan

Research focus: Study of antimicrobial activity and biocompatibility of polymers.

Research Assistant

February 2012 | August 2012

University of Galway, Department of Ecology, Galway, Ireland

Research focus: Assessment of the impact of a pharmaceutical plant in the water status of the Kinsale Bay

Research Assistant

September 2011 | February 2012

Histocell S.L, Derio, Spain

Research focus: Development of innovative biomaterials based on glycosaminoglycans

Student

Education

September 2015 | Present

PhD Program ``Applied Chemistry and Polymeric Materials´´

Universidad del País Vasco (UPV/EHU), POLYMAT, Spain

September 2016| July 2017

Máster Universitario en Formación del profesorado de Educación Secundaria

Thesis title: "Propuesta de una metodología práctica para el Grado Superior en Educación y Control Ambiental"

Universidad Internacional de la Rioja (UNIR), Spain

September 2012 | July 2014

Erasmus Mundus MSc

Thesis title: "Comparative study on the responsiveness to 17α-ethinyestradiol (EE2) in four teleost fish using molecular biomarkers"

Universidad del País Vasco (UPV/EHU), Spain/ Liége Université, Belgium/ Université de Bordeaux, France

October 2006 | June 2012

Bachelor Degree in Biology

Universidad del País Vasco (UPV/EHU), Spain.

Grants and Fellowships

September 2015| Present

Marie Curie Early Stage Researcher Fellowship

H2020-MSCA-SUSPOL-642671. European Joint Doctorate in ``Organocatalysis and Sustainable Polymers´´

September 2014 | August 2015

Global Training International Fellowship

Basque Government

January 2013 | July 2013

Mediterranean Office of Youth- Mobility Scholarship (Master/Doctorate)

European Commission's Lifelong Learning Program 2007–2013

February 2012 | August 2012

**Leonardo Da Vinci Scholarship**

European Commission's Lifelong Learning Program 2007–2013

Publications

1. Sanchez-Sanchez, A., **Basterretxea, A.**, Mantione, D., Etxeberria, A., Elizetxea, C., Calle, A. de la, García-Arrieta, S., Sardon, H., Mecerreyes, D., n.d. Organic-acid mediated bulk polymerization of ε-caprolactam and its copolymerization with ε-caprolactone. J. Polym. Sci. Part Polym. Chem. 54, 2394–2402.

2. **Basterretxea, A.**, Haga, Y., Sanchez-Sanchez, A., Isik, M., Irusta, L., Tanaka, M., Fukushima, K., Sardon, H., **2016**. Biocompatibility and hemocompatibility evaluation of polyether urethanes synthesized using DBU organocatalyst. Eur. Polym. J. 84, 750–758.
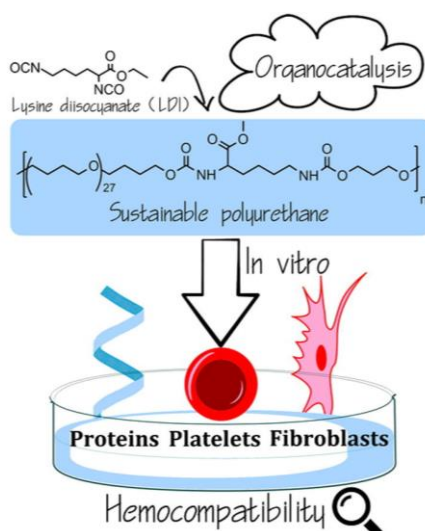
3. Sanchez-Sanchez, A., Rivilla, I., Agirre, M., **Basterretxea, A.,** Etxeberria, A., Veloso, A., Sardon, H., Mecerreyes, D., Cossío, F.P., **2017**. Enantioselective Ring-Opening Polymerization of rac-Lactide Dictated by Densely Substituted Amino Acids. J. Am. Chem. Soc. 139, 4805–4814.

4. **Basterretxea, A**.; Gabirondo, E., Sanchez-Sanchez, A., Etxeberria, A., Coulembier, O., Mecerreyes, D., Sardon, H. Synthesis and Characterization of Poly (ε-Caprolactam-Co-Lactide) Polyesteramides Using Brønsted Acid or Brønsted Base Organocatalyst. Eur. Polym. J. **2017**, 95, 650–659.
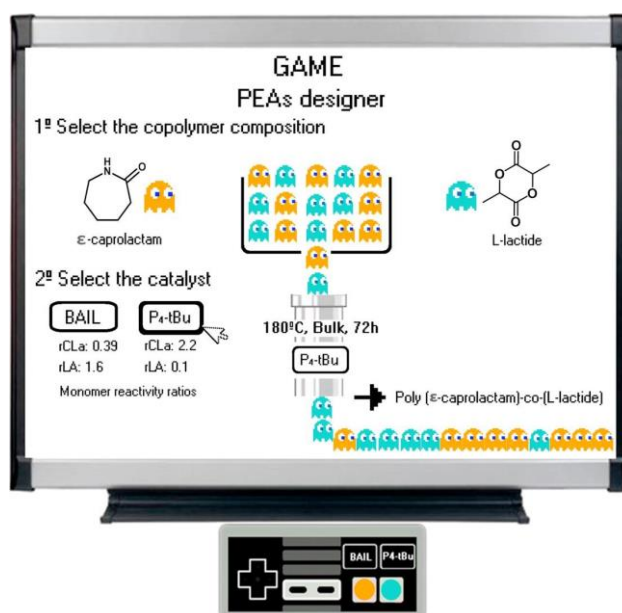
5. Ronco, L.I., **Basterretxea, A.,** Mantione, D., Aguirresarobe, R.H., Minari, R.J., Gugliotta, L.M., Mecerreyes, D., Sardon, H., **2017.** Temperature responsive PEG-based polyurethanes "à la carte." Polymer 122, 117–124.

6. **Patent nº P201830462** as ``Procedimiento para la Síntesis de Poliéteres´´. University of the Basque Country and Basque Center for Macromolecular Desing and Engineering, POLYMAT fundazioa. **(2018)**

7. **Basterretxea, A.**, Gabirondo, E., Jehanno, C., Zhu, H., Flores, I., Müller, A. J., Etxeberria, A., Mecerreyes, D., Coulembier, O., Sardon, H. Polyether Synthesis by Bulk Self-Condensation of Diols Catalyzed by Non-Eutectic Acid–Base Organocatalysts. ACS Sustain. Chem. Eng. 7 (4), 4103–4111 . (March cover assignment).
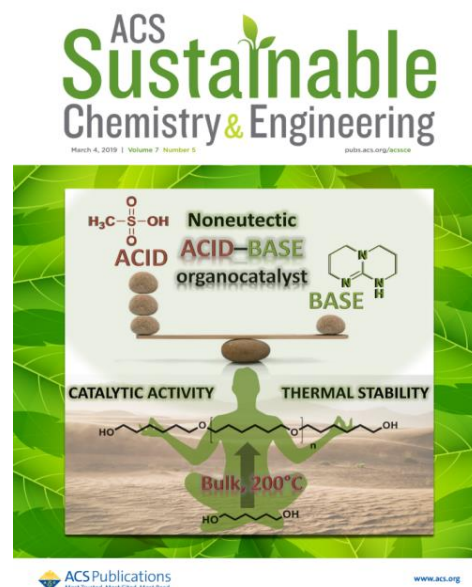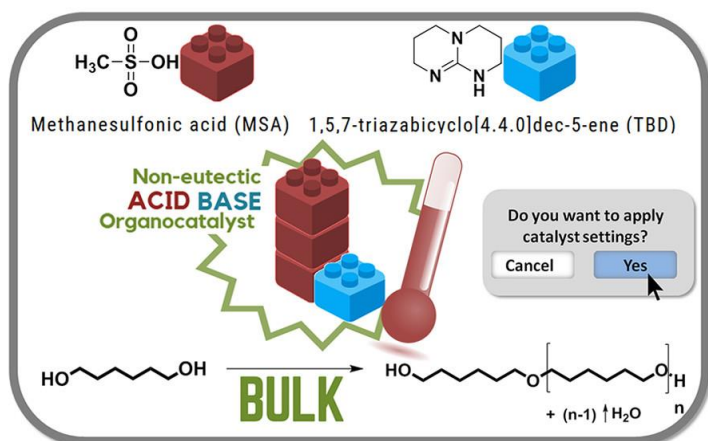

8. Olmedo-Martínez, J. L., Meabe, L., **Basterretxea, A.**, Mecerreyes, D., Müller, A. J. Effect of Chemical Structure and Salt Concentration on the Crystallization and Ionic Conductivity of Aliphatic Polyethers. Polymers, 11 (3), 452.

9. **Basterretxea, A.**, Gabirondo, E., Flores, I., Etxeberria, A., Gonzalez, A., Müller, A. J., Mecerreyes, D., Coulembier, O., Sardon, H. Isomorphic Polyoxyalkylene Copolyethers Obtained by Copolymerization of Aliphatic Diols. Macromolecules, 529, 3506-3515.
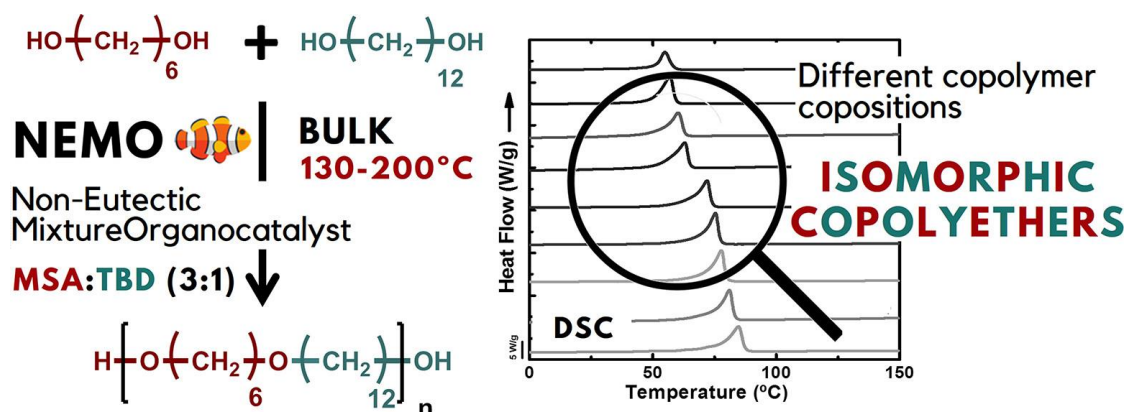
10. Flores, I., **Basterretxea, A**., Etxeberria, A., González, A., Ocando, C., Vega, J., Martinez-Salazar, J., Sardón, H, Müller, A. Organocatalyzed polymerization of PET-mb-poly(oxyhexane) copolymers and their self-assembly into double crystalline superstructures.*Submitted*

11. **Basterretxea, A**., Jehanno, C. Mecerreyes, D., Sardon, H. Dual Organocatalysts Based on Ionic Mixtures of Acids and Bases: a Step Towards High Temperature Polymerizations.*View point*. *Submitted*.
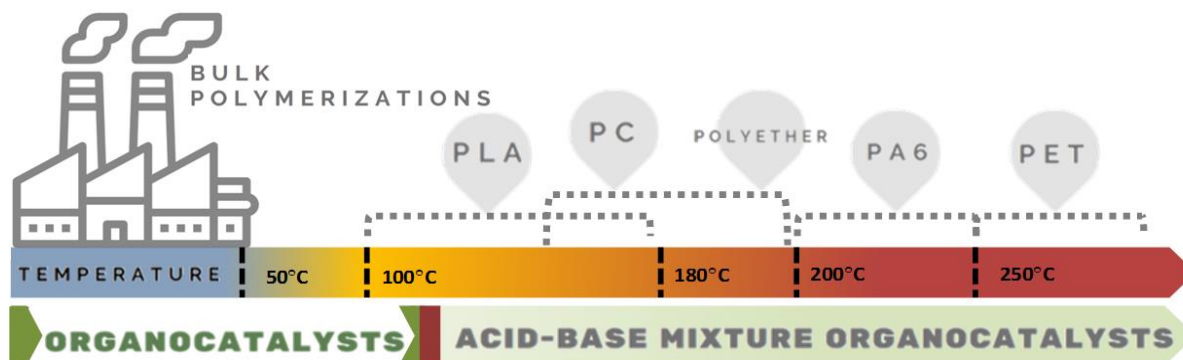
12. **Patent nº P201930629** as ``Polymerización controlada a alta temperatura de polímeros biodegradables utilizando complejos basados en piridina´´. University of the Basque Country and Basque Center for Macromolecular Desing and Engineering, POLYMAT fundazioa. *Submitted* (July 2019)

Contribution to conferences

ORAL PRESENTATION: A. Basterretxea, D. Mecerreyes, O. Coulembier, H. Sardon. *Facile synthesis of medium- and long-chain aliphatic polyethers using organocatalysts*. **ACS Spring 2019 National Meeting**, Orlando, FL, USA, April 2019

ORAL PRESENTATION: A. Basterretxea, D. Mecerreyes, O. Coulembier, H. Sardon. *Facile synthesis of medium- and long-chain aliphatic polyethers using organocatalysts*. **10th ECNP International Conference on Nanostructured Polymers and Nanocomposites.** Donostia-San Sebastián, Spain. October 2018.

POSTER PRESENTATION: A. Sagoniz, A. Basterretxea, M. Iriarte, J. Fernandez, A. Etxeberria. *Copolymers based on L-lactide for potential packaging applications.* **16th EPF European Polymer Congress,** Lyon (France), July 2nd-7th 2017

ORAL PRESENTATION: A. Basterretxea, D. Mecerreyes, O. Coulembier, H. Sardon. *Protic Ionic Liquids as efficient Organocatalysts for High Temperature Polymerizations*. **IX Congreso de Jóvenes Investigadores en Polímeros (JIP-2017)**, Tarragona (Spain). **5th-8th Junio 2017**

POSTER PRESENTATION: A. Basterretxea, D. Mecerreyes, O. Coulembier, H. Sardon. *Preparation of poly (ε-caprolactam)-co-(L-lactide) copolymers using organocatalysis*. International Conference on Advanced Polymers for Science and Tecnology (APST-2016), Vellore, (India), 24th-26th October 2016
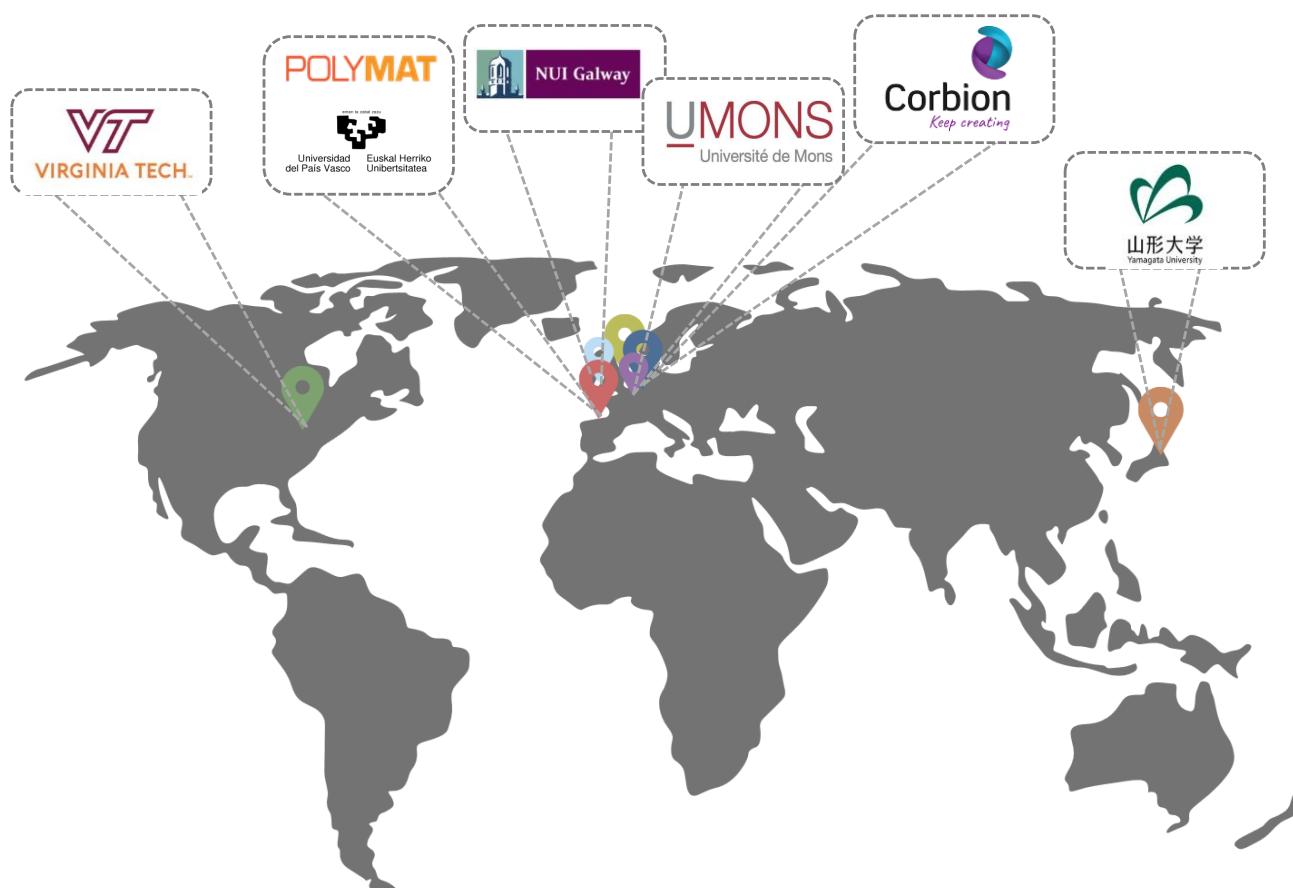
References

Dr. Haritz SARDON

Associate Professor

Polymat, University of the Basque Country, Spain.

E-mail: haritz.sardon@ehu.es

Phone: +34 943015303

Dr. Olivier COULEMBIER

F.N.R.S. Research Associate

Center of Innovation and Research in Materials and Polymers (CIRMAP)

Laboratory of Polymeric and Composite Materials (LPCM)

University of Mons

E-mail : olivier.coulembier@umons.ac.be

Phone :+32-(0)65-373481

Prof. David MECERREYES

Ikerbasque Professor

Polymat, University of the Basque Country, Spain.

E-mail: david.mecerreyes@ehu.es

Phone: +34 943 018018

Prof. Timothy E. LONG

Director of the University's Macromolecules Innovation Institute (MII)

Virginia Tech, Blacksburg, USA.

E-mail: telong@vt.edu

Phone: +1 540-231-6717